

# Prediction of clay minerals and grain-coatings in sandstone reservoirs utilising ancient examples and modern analogue studies



UNIVERSITY OF  
LIVERPOOL

Thesis submitted in accordance with the requirements of the University of

Liverpool for the degree in Doctor of Philosophy by

Patrick James Dowey

November 2012

# Contents

<b>1. INTRODUCTION.....</b>	<b>1</b>
1.1 Background.....	1
1.2 Research objectives.....	3
1.2.1 What factors are common to the formation of chlorite-coated sandstone reservoirs?.....	4
1.2.2 How are clay minerals distributed in modern estuaries, and what processes and factors control their occurrence?.....	9
1.2.3 Do grain-coats occur in modern estuarine environments and how do they form?.....	15
1.3 Methods.....	20
1.3.1 Modern estuarine studies.....	20
1.3.2 Field mapping & sample collection.....	21
1.3.3 Sample preparation & storage.....	22
1.3.4 Grain size analysis.....	23
1.3.5 X-ray Diffraction (XRD).....	24
1.3.6 Infrared Spectroscopy.....	28
1.3.7 Scanning Electron Microscopy (SEM).....	29
1.4 Organisation of the thesis.....	31
<b>2. PRE-REQUISITES, PROCESSES, AND PREDICTION OF CHLORITE GRAIN-COATINGS IN PETROLEUM RESERVOIRS: A REVIEW OF SUBSURFACE EXAMPLES.....</b>	<b>38</b>
2.1 Abstract.....	38
2.2 Introduction.....	39
2.3 Chlorite coat formation: Pre-requisites.....	40
2.3.1 Diagenetic chlorite coats from precursor clay minerals ....	42
2.3.2 Diagenetic chlorite-coats formed from the dissolution of detrital grains.....	45
2.4 Dataset.....	46
2.4.1 Data collection.....	47
2.4.2 Defining depositional environment.....	48
2.4.3 Defining reservoir quality.....	50
2.4.4 Age and depositional latitudes.....	53
2.4.5 Elemental compositions.....	53
2.5 Results.....	54
2.5.1 Depositional environment, reservoir quality and age.....	54
2.5.2 Age and depositional latitude.....	56
2.5.3 Elemental composition, reservoir quality and depositional environment.....	58
2.6 Discussion.....	58
2.6.1 Depositional environment as a control.....	60
2.6.2 Depositional age as a control.....	65
2.6.3 Paleolatitude.....	66
2.6.4 Reservoir quality.....	69

2.6.5	Elemental composition .....	70
2.6.6	Likely and unlikely chlorite-coat sandstone scenarios .....	71
2.7	Conclusions.....	74
<b>3.</b>	<b>CLAY MINERALS IN A COLD CLIMATE: ORIGIN, MINERALOGY AND DISTRIBUTION OF CLAY MINERALS IN THE LEIRÁRVOGUR ESTUARY, SW ICELAND .....</b>	<b>77</b>
3.1	Abstract.....	77
3.2	Introduction: .....	78
3.2.1	Estuarine dynamics.....	79
3.2.2	Geochemical development.....	82
3.3	Study area .....	85
3.3.1	Bedrock geology .....	85
3.3.2	Glacial & sea level context .....	87
3.3.3	Catchment .....	87
3.3.4	Estuary geomorphology .....	89
3.3.5	Clay mineral formation in Icelandic rocks & soils .....	91
3.3.6	Hydrothermal clay mineral alteration.....	92
3.3.7	River water geochemistry .....	93
3.3.8	Offshore clay mineralogy .....	94
3.4	Materials and methods.....	95
3.5	Results .....	102
3.5.1	Sediment texture .....	102
3.5.2	Clay mineral identification in estuary samples.....	105
3.5.3	Bedrock mineralogy .....	112
3.5.4	Glacial mineralogy .....	112
3.5.5	Riverbank soil mineralogy .....	115
3.5.6	Estuary clay mineral distributions .....	116
3.5.7	Estuary non-clay mineral distributions.....	119
3.5.8	Mineral cross-plots & average values.....	123
3.5.9	Worm cast mineralogy.....	128
3.6	Discussion .....	131
3.6.1	Sediment texture .....	131
3.6.2	Detrital & inherited mineralogy.....	134
3.6.3	Non-clay minerals .....	140
3.6.4	Detrital & inherited mineral summary .....	141
3.6.5	Intra-estuarine processes .....	144
3.7	Conclusions:.....	154
<b>4.</b>	<b>CLAY MINERALS IN THE SUN: MINERALOGY AND DISTRIBUTION OF CLAY MINERALS IN THE ANLLÓNS ESTUARY, GALICIA, SPAIN .....</b>	<b>157</b>
4.1	Abstract.....	157
4.2	Introduction .....	158
4.2.1	Estuarine dynamics.....	159
4.2.2	Geochemical development.....	162
4.3	Study area .....	165
4.3.1	Geology and tectonics .....	165
4.3.2	Weathering and soils.....	168
4.3.3	Coastal clay mineralogy .....	169

4.3.4	Relative sea level history .....	171
4.3.5	Anllóns estuary catchment .....	172
4.3.6	Anllóns estuary geomorphology .....	173
4.4	Materials and methods.....	177
4.5	Results .....	181
4.5.1	Clay mineral identification .....	181
4.5.2	Mineralogy of the bedrock .....	185
4.5.3	Mineralogy of riverbank soil sediments .....	186
4.5.4	Estuary sediment texture.....	186
4.5.5	Estuary mineralogy .....	191
4.5.6	Relative estuary mineral data.....	205
4.5.7	Estuary transects .....	214
4.5.8	Mineral indices .....	221
4.5.9	Worm cast distribution & mineralogy.....	222
4.5.10	Average concentrations comparison .....	226
4.6	Discussion .....	228
4.6.1	Sediment texture .....	228
4.6.2	Extra-estuarine controls on mineralogy .....	229
4.6.3	Intra-estuarine controls on mineralogy.....	233
4.6.4	Estuarine dynamics.....	237
4.7	Conclusions.....	245
<b>5.</b>	<b>SPATIAL AND TEMPORAL VARIATION IN MINERALOGY AND TEXTURE OF SAND GRAIN-COATINGS FROM A MODERN ESTUARY: IMPLICATIONS FOR SUBSURFACE INVESTIGATIONS .....</b>	<b>248</b>
5.1	Abstract.....	248
5.2	Introduction .....	249
5.2.1	Ancient clay mineral cements in reservoirs .....	251
5.3	Study area .....	253
5.3.1	Geology and tectonics .....	253
5.3.2	Relative sea level history.....	255
5.3.3	Anllóns estuary catchment .....	257
5.3.4	Anllóns estuary geomorphology .....	257
5.4	Materials and methods.....	259
5.5	Results .....	263
5.5.1	Sedimentary environments .....	263
5.5.2	Estuary cross-sections .....	268
5.5.3	Textural characteristics of grain-coatings .....	270
5.5.4	Mineral identification .....	282
5.6	Discussion .....	288
5.6.1	Core interpretations & transects .....	288
5.6.2	Grain-coat locations & characteristics .....	292
5.6.3	Cause of grain-coatings .....	295
5.6.4	Implications for predicting coat coverings.....	305
5.7	Conclusions.....	313
<b>6.</b>	<b>SUMMARY AND FURTHER WORK.....</b>	<b>316</b>
6.1	Introduction .....	316
6.2	Summary of results and conclusions.....	319

6.2.1	What factors are common to the formation of chlorite-coated sandstone reservoirs? .....	320
6.2.2	How are clay minerals distributed in modern estuaries, and what processes and factors control their occurrence?.....	326
6.2.3	Do grain-coats occur in modern estuarine environments and how do they form? .....	338
6.3	Further Work.....	341
6.3.1	Chlorite coat literature review .....	341
6.3.2	Estuarine surface sediment analysis.....	342
6.3.3	Core coat coverage.....	345
<b>7.</b>	<b>REFERENCES .....</b>	<b>350</b>
<b>8.</b>	<b>APPENDICES (SEE ASSOCIATED DATA) .....</b>	<b>376</b>
8.1	Appendix 1 – Supplementary material to chapter two .....	376
8.1.1	Appendix 1A – USA database table.....	376
8.1.2	Appendix 1B – Europe database table.....	376
8.1.3	Appendix 1C – Rest of world database table .....	376
8.1.4	Appendix 1D – All chlorite compositional data .....	376
8.1.5	Appendix 1E – Average chlorite compositional data .....	376
8.2	Appendix 2 –Supplementary material to chapter three.....	376
8.2.1	Appendix 2A – Sample location co-ordinate table.....	376
8.3	Appendix 3 –Supplementary material to chapter four .....	376
8.3.1	Appendix 3A – Sample location co-ordinate table.....	376
8.4	Appendix 4 –Supplementary material to chapter five.....	376
8.4.1	Appendix 4A – Sample location co-ordinate table.....	376
8.4.2	Appendix 4B – Core logs with all data .....	377
8.5	Appendix 5 –Supplementary material to chapter six .....	377
8.5.1	Appendix 5A - Iceland paleogeography talk (BSRG 2010)	377

## List of Figures

Figure 1.1 - The chemical structure of silica tetrahedra and octahedra	11
Figure 1.2 - Structure of common clay minerals	12
Figure 2.1 - Depositional setting and environment association as defined in Table 2.1	51
Figure 2.2 - Frequency of depositional environments	55
Figure 2.3 - Age and latitude of deposition of examples	57
Figure 2.4 - Elemental ratios from published examples	59
Figure 2.5 - Chlorite examples per millions of years for each time period	67
Figure 2.6 - Schematic representation outlining the likely and unlikely scenarios for the development of chlorite-coated grains in sandstone reservoirs	72
Figure 3.1 – Iceland location maps	85
Figure 3.2 - Photographs of hinterland environments discussed in text	88
Figure 3.3 - Photographs of estuary environments discussed in text	90
Figure 3.4 - Contoured maps of Iceland estuarine sedimentary texture	103 & 104
Figure 3.5 - XRD diffractograms of sample 26 indicating peak positions during various treatments	106
Figure 3.6 - Infrared spectra for representative estuary and hinterland samples	110
Figure 3.7 - Borgarfjörður regional surface environment map with hinterland glacial and riverbank sediment sample locations	114
Figure 3.8 - Contoured maps of relative ratios of clay mineral composition of sediment fine fraction	117 & 118
Figure 3.9 - Contoured maps of relative ratios of non-clay mineral composition of sediment fine fraction	120 & 121
Figure 3.10 - Whole sediment texture and relative clay mineral concentration cross-plots	124
Figure 3.11 - Cross-plots of relative clay mineral	125
Figure 3.12 - Cross-plots of relative non-clay minerals	127
Figure 3.13 - Average clay mineral relative percentages from worm cast, estuary, riverbank soil and glacial sediments	128
Figure 3.14 - Difference maps of clay mineral concentrations in worm cast and surface sediments	129
Figure 3.15 - Difference graph for clay mineral concentrations in worm cast and surface sediments	130
Figure 3.16 - Clay mineral evolution diagram	136
Figure 3.17 - Summary figure outlining the main controls on clay mineral formation and distribution in the Leirárvogur Estuary	155
Figure 4.1 – Spain study area maps	165

Figure 4.2 - Photographs of upstream environments in Anllóns Estuary discussed in text.....	172
Figure 4.3 - Photographs of Anllóns Estuary discussed in text.....	173
Figure 4.4 - Photographs of estuary supratidal and intratidal environments in Anllóns Estuary discussed in text.....	174
Figure 4.5 - Photographs of intertidal environments in Anllóns Estuary discussed in text.....	175
Figure 4.6 - Representative XRD diffractograms of estuary fine fraction sub-sample.....	182
Figure 4.7 - Infrared spectra for representative estuary sample.....	184
Figure 4.8 - Galician regional map with hinterland soil and river sediment sample locations and mineral concentrations.....	187
Figure 4.9 - Contoured maps of estuarine sedimentary texture.....	188 & 189
Figure 4.10 - Plots of whole sediment texture.....	191
Figure 4.11 - Maps of clay mineral concentration in sediment fine fraction.....	194 & 195
Figure 4.12 - Contoured maps of non-clay mineral concentration in sediment fine fraction.....	196, 197, 198 & 199
Figure 4.13 - Sorting versus mineral concentration cross-plots.....	201
Figure 4.14 - Total concentrations of carbonate and clay minerals in sediment fine fraction.....	202
Figure 4.15 - Carbonate versus siliciclastic mineral concentration cross-plots.....	203
Figure 4.16 - Siliciclastic versus siliciclastic mineral concentration cross-plots.....	205 & 206
Figure 4.17 - Contoured maps of relative (carbonate normalised) clay mineral concentration in sediment fine fraction.....	207 & 208
Figure 4.18 - Contoured maps of relative (carbonate normalised) non-clay mineral concentration in sediment fine fraction.....	209, 210 & 211
Figure 4.19 - Relative (carbonate normalised) siliciclastic versus siliclastic mineral concentration cross-plots.....	214 & 215
Figure 4.20 - Estuary mineral transects.....	216
Figure 4.21 - Mineral indices maps.....	218, 219 & 220
Figure 4.22 - Worm cast density map.....	222
Figure 4.23 - Mapped relative (carbonate normalised) mineral concentrations in worm cast and estuary sediments.....	223
Figure 4.24 - Graphed relative (carbonate-normalised) mineral concentrations in worm cast and estuary sediments.....	224
Figure 4.25 - Average relative (carbonate normalised) mineral percentages from worm cast, estuary and hinterland locations.....	226
Figure 4.26 - Models for the distribution of muscovite and kaolinite in estuary sediment.....	240
Figure 5.1 Spanish estuary setting.....	253
Figure 5.2 - Correlation panels along two estuary transects.....	263
Figure 5.3 - Core logs of two representative cores.....	264

Figure 5.4 - Grain-coat images of sand grains using binocular microscope.....	271
Figure 5.5 - SEM image of stub-mounted, grain-coated sands grains.....	272
Figure 5.6 - SEM image of thin section, grain-coated sands.....	273
Figure 5.7 - SEM images and energy dispersive x-ray (EDX) spectra of stub-mounted grain-coat sand grains from core sample.....	275
Figure 5.8 - SEM images and energy dispersive x-ray (EDX) spectra of thin section grain-coat sand grains from core sample.....	276
Figure 5.9 - Cross-plot of grain-coating versus measured particle size characteristics, depth and fine fraction content.....	279
Figure 5.10 - Representative X-ray diffractograms of estuary fine fraction sub-sample.....	280
Figure 5.11 – Mineral Histograms.....	283 & 284
Figure 5.12 - Infrared spectra for representative estuary sample.....	286
Figure 5.13 - Figure of generalised barrier island depositional model	305
Figure 5.14 - Schematic figure of the likely setting for high initial grain-coat coverage.....	308
Figure 6.1 - Outline of the varying physical and temporal scales of the research questions addressed by this thesis and how these aspects are inter-related.....	316
Figure 6.2 - Cross-plot of the key themes of the thesis. The figure outlines the key themes of the thesis: time and scale.....	317
Figure 6.3 - Schematic illustration of concentrations of clay minerals in Icelandic and Spanish estuaries.....	330
Figure 6.4 - Schematic illustration of the controls on clay mineral distribution in Icelandic and Spanish estuaries.....	333
Figure 6.5 - De-glaciation and post-glaciation of the Leirárvogur Estuary.....	345

## List of Tables

Table 2.1 - Depositional environment scheme used to define depositional environments of published chlorite examples.....	49
Table 2.2 - The characteristics of chlorite-coats on sand grains within studied examples.....	52
Table 3.1 - Estuary sediment sample description table.....	96
Table 3.2 - Hinterland sediment sample description table.....	97
Table 3.3 - XRD clay mineral identification table.....	107
Table 3.4 - Mineralogical analyses of lithology and glacial sediments (whole fractions).....	113
Table 3.5 - Clay mineral physical parameters.....	151
Table 4.1 - Mineralogy and formation of the main rock units in Anllóns Basin.....	166
Table 4.2 - Estuary sediment sample description table.....	177
Table 4.3 - Hinterland sediment sample description table.....	178
Table 4.4 - Mineralogical analyses of lithology (whole fractions).....	186
Table 4.5 - Characteristics of 3 main clay minerals in estuary fine fraction.....	241

## Abstract

Understanding how clay minerals affect reservoir quality in sandstone reservoirs is important for improving prediction of recoverable volumes of petroleum. Grain-coating clay minerals may preserve porosity and permeability in sandstones by limiting the development of authigenic minerals such as quartz. Authigenic clay minerals may also reduce porosity and permeability, through mineral growth into pore volumes and ductile deformation during compaction. This thesis draws upon published literature of chlorite-coats in reservoir sandstones and modern analogue studies of estuary sediments, utilising quantitative mineral analysis, microscopy and grain-size analysis. It seeks to address issues concerning clay mineral formation, development and distributions to better enable the prediction of these important minerals.

Authigenic chlorite-coats formed from precursor clay minerals during diagenesis have been reported in varying depositional environments and settings in published literature. Depositional age, paleolatitude of deposition, and chemistry of chlorite are all important factors in the occurrence and impact of chlorite-coats in sandstone reservoirs. Quantitative data compiled from published literature indicate that delta-related environments are the most common host for chlorite-coats, with rivers the second most common. Chlorite-coats are also more common in younger examples although this may be due to a drilling bias. Chlorite-coated examples are not reported in polar regions. Chlorite-coats tend to preserve porosity and are typically an iron-rich variety. The most likely host for chlorite-coated sands are delta settings in proximity to river systems in a warm and wet climate, with sediment supplied from a mixed lithology hinterland.

The surface distribution of clay minerals was studied in two modern estuarine analogues in Iceland and Spain, in order to quantitatively assess their formation, development and distribution. Findings show that the majority of clay minerals were derived directly from hinterland bedrock or associated sediments. Quantitative mineral data indicate that geochemical alteration of some clay mineral species occurs, in Iceland as a result of bioturbation of estuarine sediments and in Spain as a result of reducing conditions within centimetres of the sediment surface. The distribution of clay minerals and siliciclastic minerals appears to be influenced by marine processes; concentrations of these minerals are lower where carbonate minerals are in higher concentrations in the Spanish estuary. Both estuaries show varying concentrations of clay minerals within the estuary surface sediments; this may be related to estuarine transport and depositional processes

that could be partly controlled by the physical characteristics of the clay minerals.

In order to understand early grain-coat formation in a modern estuary analogue, grain-coat textures, mineralogy and average percentage coverage on sand grains were investigated in shallow sediment cores. Results show that grain-coat coverage varies, but is typically low (<25%). Grain-coats consist of mixtures of detrital siliciclastics, bioclastic debris and clay minerals. The average percentage coat coverage is controlled by the concentration of fine fraction within the sediments; less sorted sediments have greater average coat coverage. These sediments occur on the margins of the estuary. Sediments proximal to high-energy marine influence generally have lower average coat coverage. The cause of grain-coating may be varied; co-deposition of fine-grained sediment, bioturbation, and mechanical infiltration/clay illuviation are all potential grain-coating mechanisms. The differences in textures between modern and ancient grain-coats indicate that diagenetic overprinting has an important influence in authigenic coat development.

This thesis draws together diverse approaches to understanding clay minerals and their impact upon reservoir sandstones. It encompasses a variety of geographical, physical and temporal scales in order to better understand this broad research area. The data and interpretations presented are potentially useful in petroleum exploration, and could be implemented in future academic and industry research, at a range of scales, to aid the prediction of clay minerals and grain-coats in sediments.

# Acknowledgements

Firstly, I would like to thank my family for supporting me and my studies over the last decade, I would not have been able to reach this point without the emotional and financial support of Mum, Dad, Rachael and Nigel.

I also want to thank Natasha for her love and support over a difficult, but interesting past twelve months. Thanks for putting up with me (please don't stop doing that).

I would also like to acknowledge and thank my supervisors Richard Worden and Dave Hodgson for their guidance and support, throughout the last four years. They both have challenged and encouraged me to think objectively and systematically about research and how to communicate it. Even if my grammar has not improved, I believe that I am a better scientist for it. Thank you to all the consortium companies (BP, Chevron, ConocoPhillips, Eni, ExxonMobil, Petrobras, Shell and Statoil) and their representatives in the BASIC research project for their support, advice and criticism throughout the last four years. I hope that this work meets with their expectations and that the whole team have been able to build a solid foundation for future projects in this interesting and challenging area.

Special mention has to go to Gemma Byrne, Jummings, Jutely and Johnaldo. Gemma for being an amazing office mate, confidant, fellow rantee, shoulder to cry on and excellent maker of tea; but also for her help and support throughout all stages of the PhD. Thank you to Jummings, my office mate for two years, for the constant supply of half mugs of tea, hilarious food disasters and indiscriminate rants against the world. James for carrying the field equipment, all of the help with the XRD, the in depth and meandering chats about clay minerals (which I will miss a great deal) and for putting up with my wayward driving. Thanks to Johnald, my housemate, for being a great friend and chauffeur, for his interesting meal choices, surprise burps and general shock when it comes to door frames and their locations.

In particular thank you to all the Regional Cids who started in 2008: Tash, Johnaldo, Gem B, Gem K, Vic and Jutely (dishonourable mention to Kirstie), I will miss evenings in the AJ and nights in the Razz and Crazyhouse very much. I want to thank all the postgrads, postdocs and others in the department over the last few years including: Rhodders, Katrien, Kirstie's Ed, Rory, Ludo, Virginie, Tom, Christina, Laura, Ehsan, Ed, Megan, Megan's James, Pete, Holly, Ammo, Laura E, Nicola, Liz, Emma H, Kelly, Emma M, George, Chris, John, Andy and Goz. Writing these acknowledgements has reminded me of the amazing time I have had in Liverpool, and how lucky I have been.

**“I love deadlines. I like the whooshing sound they make as they  
fly by.”**

Douglas Adams  
*The Salmon of Doubt*

**“While there is tea, there is hope.”**

Arthur Pinero  
*Sweet Lavender*

# 1. Introduction

## 1.1 Background

This thesis reports on a series of studies relating to (1) understanding processes of clay mineral formation and distribution in modern estuarine settings, and (2) improving the prediction of grain-coated sandstones in ancient, deeply buried reservoir settings. In deeply buried sandstone reservoirs, quartz overgrowths reduce porosity and permeability severely impeding recoverable volumes (Glennie et al., 1978; Seemann, 1979; Kantorowicz, 1990; King, 1992). Where chlorite cements occur as coats on sand grains they limit the pore space available for the growth of incipient quartz cement (Billault et al., 2003). Although much less common, one occurrence of illite cement has been noted to preserve porosity and permeability in a similar way (Pittman et al., 1992; Storvoll et al., 2002; Taylor et al., 2010). Grain-coating cements can also have a negative impact on reservoir quality with the authigenic development of clay minerals and the deformation of ductile grains resulting in the loss of initial framework porosity and permeability (Imam and Shaw, 1987; Dutton et al., 2012). Although the presence of grain-coating cements can considerably impact the producibility of a reservoir interval, and is therefore commercially significant, the ability to accurately predict positive anomalies due to chlorite coats remains elusive.

Attempts to understand how chlorite-coats may form and to predict their occurrence primarily rely on data from wellbores (Hillier, 1994; Berger et al., 2009), which are then used to deterministically predict likely sedimentary facies that may host chlorite coatings. This approach can be impacted by small or clustered datasets, difficulty in predicting sedimentary facies distributions and limited knowledge of the diagenetic history. Another possible approach is to utilise ancient outcrop studies of clay mineral cements; however this is compromised by the effects of weathering and alteration of minerals by surface water interaction (Retallack and Dilcher, 2012). This present study attempts to improve the understanding of chlorite-coat formation and prediction using two approaches:

- 1) A *meta-analysis*, or quantitative literature review works by collecting together information and data from a number of different studies; these data are then combined with the aim of quantitatively identifying underlying trends and patterns within the whole dataset. This type of study is commonly used in social sciences and medicine, but in geology and related subjects it is generally rare (MacQuarrie and Mayer, 2005; Baas et al., 2007; Cummings et al., 2011), with few quantitative studies (Foley et al., 1987; Davies and Gibling, 2010; Hurst et al., 2011). By collating potentially key characteristics and information from published literature and quantitatively analysing these data, the

common characteristics of chlorite-coated sandstone reservoirs could be elucidated.

2) *Modern sedimentary analogues* to ancient deeply buried sandstones present an excellent opportunity to study the controls and processes that may not be evident in ancient sediments. Modern analogues can enable a better understanding of the stratigraphy (Cairncross et al., 1988) geometry (Hayward, 1985; Foix et al., 2012; Musial et al., 2012) and process sedimentology and facies (Stear, 1985; Eyles and Kocsis, 1988; Esterle and Ferm, 1994) of ancient sediments. This second part of the study aims to assess the types and concentrations of clay minerals in modern estuaries, and to interpret how they formed, developed and were distributed in estuarine sedimentary environments. Similarly the textures of grain-coatings upon sand grains were quantitatively measured in modern analogues to enable a better understanding of the incipient grain-coatings during and after deposition.

## **1.2 Research objectives**

A series of eleven research questions have been developed and investigated during this research. The analysis and interpretation of each of these utilised the methods outlined below. The questions can be divided into three over-arching sections: 1) What factors are common to the formation of chlorite-coated sandstone reservoirs?; 2)

How are clay minerals distributed in modern estuaries, and what processes and factors control their occurrence?; and 3) Do grain-coats occur in modern estuarine environments, and how do they form?

### **1.2.1 What factors are common to the formation of chlorite-coated sandstone reservoirs?**

Rationale: Previous studies have outlined common depositional settings for chlorite-coats, but only dealt with geographically-limited and small datasets (Ehrenberg, 1993; Bloch et al., 2002). However, larger datasets of published studies can provide an opportunity to identify common parameters and pre-requisite controls to help prediction of chlorite-coated sandstones in the subsurface. By collecting a large global dataset of published examples this research will quantitatively assess the typical depositional environments of chlorite-coat formation in published examples. This research will also seek to ascertain how chlorite coats affect reservoir quality, and how the age and latitude of the formation and the chemistry of the chlorite may relate to its occurrence. More accurate predictive models may be developed with a quantitative assessment of the depositional environments that host chlorite-coats and a better understanding of other common factors in reported chlorite-coat formation.

Chlorite-coats on sand grains develop diagenetically from a variety of potential precursor minerals. A very brief outline of these precursor minerals is presented. Ehrenberg (1993) identified bethierine (an iron-rich, 7Å, 1:1 serpentine clay mineral) as potential precursor mineral to chlorite in a study of Norwegian Continental Shelf sandstones. In the Tuscaloosa Formation, Gulf Coast, USA, Ryan and Reynolds (1997) reported that mixed-layer serpentine-chlorite became more chloritic with increasing burial depth. High aluminium chlorite reported in the Wilcox Formation, Texas, USA, are coincident with a decrease in kaolinite relative to chlorite with increasing depth Boles & Franks (1979), suggesting that kaolinite (possibly supplied with iron and magnesium from the illitization of smectite) could develop into an aluminium-rich chlorite. Pore-lining chlorite in sandstones from the Central Graben, UK North Sea was reported to share morphological and chemical characteristics with smectite, and smectite was proposed as the precursor to chlorite (Humphreys et al., 1989). Similarly, in pore-lining chlorites from the Santos Basin, Brazil, evidence for smectite as a precursor is indicated by remnants of corrensite (mixed-layer chlorite-smectite) below pervasive calcite cements and along tight inter-granular contacts (Anjos et al., 2003). Chlorite can also develop from the dissolution of iron- and magnesium-rich detrital grains and volcanic rock fragments (AlDahan and Morad, 1986; Anjos et al., 2000; Blackbourn and Thomson, 2000; Burns and Ethridge, 1979; De Ros et al., 1994; Remy, 1994; Thomson, 1979; Valloni et al., 1991;

Worden and Morad, 2003), and from mud intraclasts (Worden and Morad, 2003).

1.2.1.1 Question one - In which depositional environments did the chlorite-coating sandstone form?

Rationale: Bloch et al. (2002) described widely-cited published examples and grouped them into four classes based on their mode of formation: 1) depositionally-controlled iron-rich chlorites in shallow marine settings, 2) depositionally-controlled chlorite coats in turbidites, 3) provenance-controlled chlorite coats and 4) magnesium-rich chlorite coats associated with saline brines. Bloch et al. (2002) established that chlorite-coats may form through a variety of processes related to climate, depositional environment, sediment mineralogy, interactive fluids and diagenetic conditions. The effect of chlorite-coats on reservoir quality and other factors, which may influence reservoir quality, were also discussed in this published study. Bloch et al. (2002) expanded on earlier research by Ehrenberg (1993), which reported on five Lower Jurassic sandstone reservoirs from the North Sea where iron-rich chlorite coats were noted in coastal settings influenced by rivers. Ehrenberg et al. (2002) linked iron-rich chlorite precursor minerals such as odinite and berthierine, which are noted in modern tropical river-influenced coastal settings (Odin, 1988; Porrenga, 1967). With a detailed and larger quantitative assessment of chlorite-coat occurrence from published literature, the present

study seeks to better establish which depositional environments more commonly host chlorite coats. With this approach the possible controls on chlorite-coat formation can be discussed and predictive models can be refined.

1.2.1.2 Question two - What effect do diagenetic chlorite-coatings have on the reservoir quality of the sandstone?

Rationale: The crystal shape of authigenic chlorite coats on sand grains can have a large impact on the reservoir quality. Coats composed of relatively small chlorite crystals that cover the majority of the pore surface are more likely to preserve porosity and permeability through the prevention of quartz overgrowth (Anjos et al., 2003; Ehrenberg, 1993; Ramm and Ryseth, 1996 Berger et al., 2009; Islam, 2009). Large, pore-filling chlorite crystals reduce porosity and dramatically effect permeability (Islam, 2009; Nadeau, 2000; Pay et al., 2000; Porter and Weimer, 1982 Berger et al., 2009). By quantitatively assessing the reported effect of chlorite-coats in reservoirs examples, it may be possible to understand how common larger chlorite crystal growths are and the overall effect of chlorite on reservoir quality in petroleum reservoirs.

1.2.1.3 Question three - At what age and latitude were the chlorite-coated sandstones deposited?

Rationale: Some chlorite precursor minerals are thought to occur in particular climate zones. For example berthierine has principally been

reported at tropical latitudes (Hornibrook and Longstaffe, 1996; Odin, 1988), and there is a possible link between magnesium-rich chlorite and desert aeolian or playa lake environments (Ajdukiewicz et al., 2010; Hillier et al., 1996), which normally form in restricted latitude ranges. For this reason an attempt was made to relate latitude and the timing of sediment deposition to chlorite-coat occurrence. Using published ages and latitudes of the formations it is possible to begin to understand how climate may affect chlorite-coat development.

1.2.1.4 Question four - What is the range of chemical compositions of chlorite in the published examples?

Rationale: Chemically, the two most common types of chlorite-coat that develop are magnesium-rich and iron-rich chlorite. Bloch et al. (2002) reported that magnesium-rich chlorite coats most commonly develop in environmental and early diagenetic subsurface settings associated with saline brines. This indicates that desert-associated environments and settings are more likely to host magnesium-rich chlorite. Capturing the chemistry of chlorite-coats and relating them to depositional setting may therefore elucidate the processes of formation of chlorite-coats in these types of settings. In this way the chemistry and mineralogy of chlorite-coats could be predicted.

## **1.2.2 How are clay minerals distributed in modern estuaries, and what processes and factors control their occurrence?**

Rationale: Understanding clay mineral distributions in modern estuaries can be applied to understand distributions of buried clays in subsurface reservoirs. Knowledge of clay mineral distributions in modern sediments is important for understanding the sources and controls on sediment types, flow processes and ultimately how and why sediment is deposited (Chamley, 1989; Weaver, 1989; Reading, 1996). Further study of the interplay of different parameters could aid the prediction of clay mineral cements in ancient reservoir sandstones (Ketzer et al., 2003; Worden and Morad, 2003; Worden and Burley, 2003).

This section of the research will identify clay minerals present in two estuaries and quantitatively describe their distribution within the fine fraction of different sediment types. These distributions will then be related to mineral concentration within the estuary river catchment soils, and to processes occurring within the estuary itself. From this the controls on clay mineral types and distribution within two modern estuaries will be characterised.

### 1.2.2.1 Question five - What clay minerals are present and where did they form?

Rationale: To understand how the clay minerals within the two estuaries formed and how their distribution may be controlled by

estuarine and non-estuarine processes the types of clay minerals need to be fully identified. The quantitative identification of clay minerals can allow the location of formation and processes of development to be identified either externally or internally within the estuary system. Differences in concentration between locations may indicate different source areas for clay mineral supply (Feuillet and Fleischer, 1980; Chamley, 1989), or subtle differences in sedimentary flow processes (Whitehouse et al. 1960; Gallenne, 1974; Gibbs 1983; Weaver, 1989) or water geochemistry (Eckert and Sholkovitz, 1976; Sholkovitz et al., 1978; Eisma, 1986) which may control clay mineral distribution. It may also highlight environments and processes (pre-depositional and post-depositional) where the chemistry or structure clay minerals alter (Hover et al., 2002; Wallmann et al., 2008; Michalopoulos and Aller, 2004; Needham et al., 2006; Presti and Michalopoulos, 2008).

Clay minerals are phyllosilicates composed of silicate ( $\text{SiO}_2$ ). As the name implies the silicate in phyllosilicates form sheets. There are two types of sheet: tetrahedra and octahedra. Tetrahedra are composed of a single silicon atom surrounded by four oxygen atoms (fig. 1.1A; Bland and Rolls, 1998), individual tetrahedra may share basal oxygen atoms creating the silicate sheet (fig. 1.1B&C). Octahedral sheets are composed of a series of octahedra laid on a triangular face and are linked by three shared vertices (Fig. 1.2; Meunier, 2005) Composition

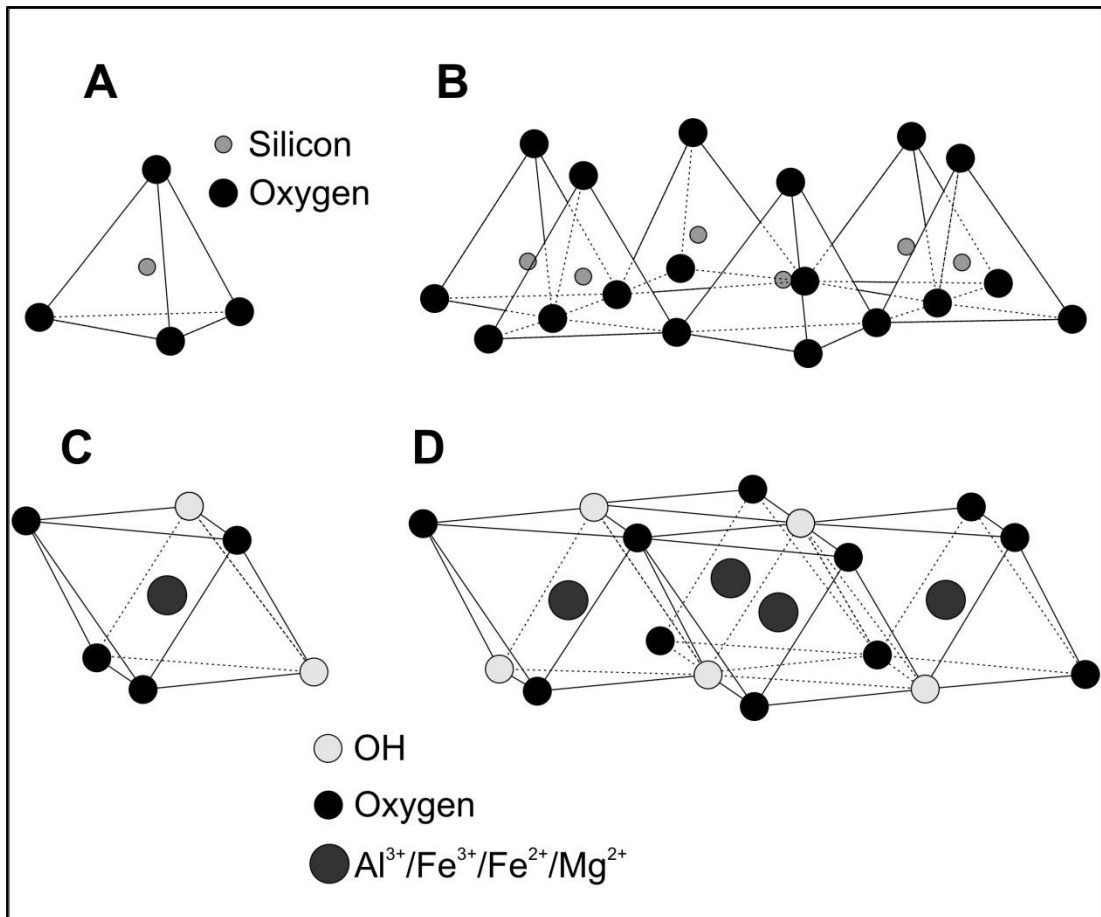


**Figure 1.1. - The chemical structure of silica tetrahedra and octahedra (after Bland & Rolls, 1998). (A) Individual tetrahedra composed of a silicon atom bonded to four oxygen atoms. (B) Side-view of a tetrahedra ring with tetrahedra sharing basal oxygens. (C) Individual octahedra composed of a cation atom at the centre of an array of six oxygens and an OH grouping. (D) Side-view of an octahedral sheet, individual octahedra share three vertices.**

of the octahedral sheet is variable, but each octahedra is composed of one trivalent or divalent cation surrounded by six anions (oxygen or hydroxyl ions).

Clay mineral groups are variations of three principal structural combinations of tetrahedral and octahedral sheets; the connections between sheets occur where the apical oxygens of the tetrahedra become the vertices of the octahedra (Meunier, 2005). The 1:1 layer clay minerals are composed of one tetrahedral sheet (T) and one octahedral sheet (O) and include kaolinite and halloysite (fig 1.2). The

2:1 layer clay minerals are composed of an octahedral sheet sandwiched between two tetrahedral sheets (TOT). The 2:1:1 minerals (Worden and Morad, 2003) are composed of a standard TOT structure, but in the example of chlorite, an octahedral sheet composed of cations and hydroxyls occurs in the inter-layer space (Grim, 1962).

Clay minerals develop in surface conditions via three processes (Millot,

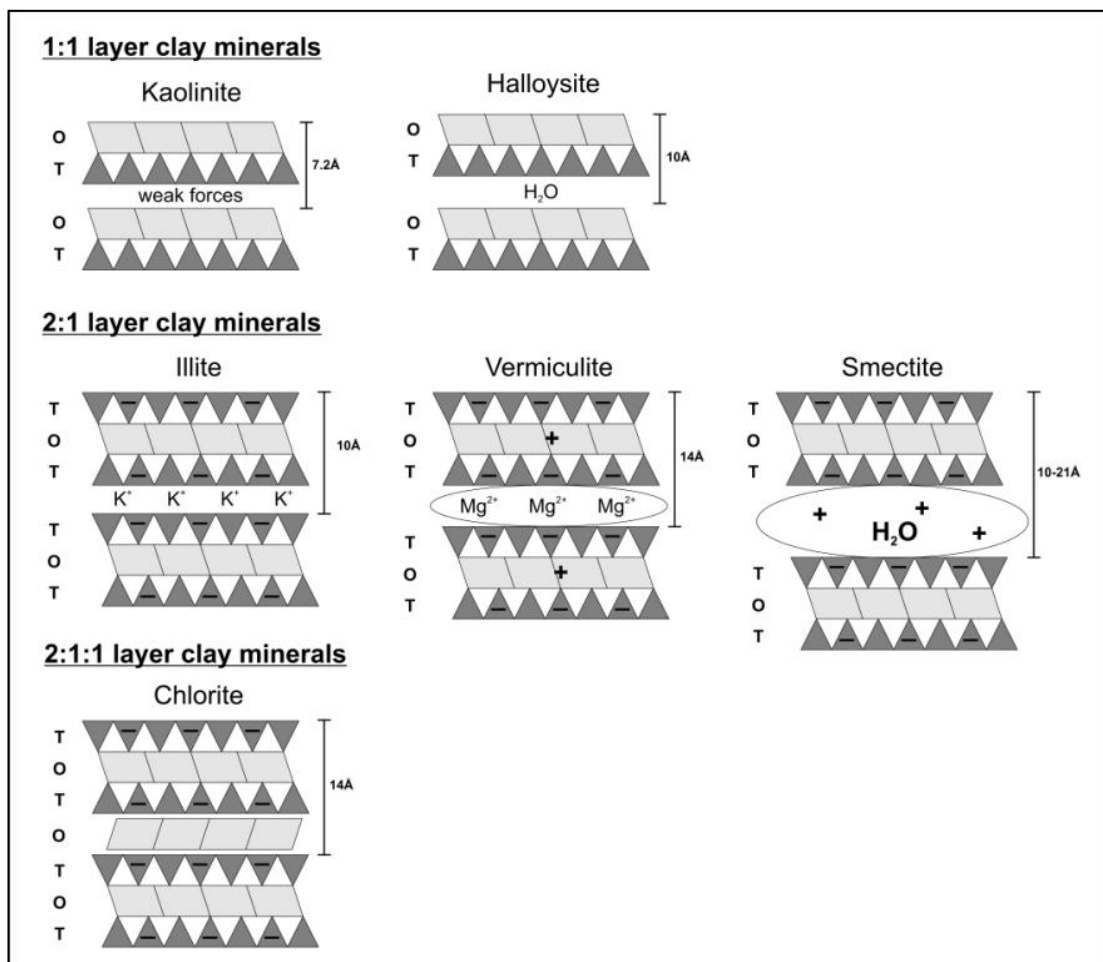


**Figure 1.2. - Structure of common clay minerals.** Clay mineral are composed of two basic building blocks: tetrahedral and octahedral sheets. 1:1 layer clay minerals are composed of one octahedral sheet and one tetrahedral sheet. 2:1 layer clay minerals are composed of a tetrahedra-octahedra-tetrahedra structure, with weakly bonded cations or water in an interlayer position. The 2:1:1 layer clay minerals have a similar structure to a 2:1 layer clay mineral except that in the interlayer spacing there is an octahedral sheet.

1964; Wilson, 1999): 1) detrital inheritance, where clay minerals formed in pre-existing rocks are subsequently weathered and eroded; 2) transformation, whereby the silicate structure of the mineral is maintained, but there are extensive changes within the inter-layer space of the structure, and 3) neoformation where the clay mineral develops from solution, gel or amorphous material.

#### 1.2.2.2 Question six - What is the surface sediment distribution of the clay minerals?

Rationale: There have been few detailed, quantitative studies of clay minerals in modern estuarine and coastal settings. The rare studies that have quantitatively mapped clay mineral distributions generally focused on either the distribution of minerals in surface sediments as controlled by estuarine and coastal dynamics (Feuillet and Fleischer, 1980; Algan et al., 1994; Patchineelam and de Figueiredo, 2000) or seasonal changes (Sarma et al., 1993); or the relationship of estuarine mineralogy to sediment source areas (Allen, 1991; Pandarinath and Narayana, 1992; Prego et al., 2012; Bernárdez et al., 2012). Quantitatively identifying and mapping the clay minerals present in the fine fraction of surface sediments in two modern estuaries allows the processes of clay mineral development and transport and deposition to be determined.

### 1.2.2.3 Question seven - Does bioturbation of sediment have any effect on clay mineral distribution in a modern setting?

Rationale: Previous experimental studies concluded that sediment ingestion by worms can result in the chemical alteration of minerals (McIlroy et al., 2003; Needham et al., 2004; Needham et al., 2005; Worden et al., 2006; Needham et al., 2006). The present research provided an opportunity to ascertain whether these processes also occurred in modern estuarine examples. The composition and concentration of clay minerals and non-clay minerals was assessed in the fine fraction of sediment excreted by estuarine worms. Attempts to relate this to burrowing intensity are also presented.

### 1.2.2.4 Question eight - What are the controls on the types of clay minerals and their distribution pattern?

Rationale: Transport and deposition processes within estuaries may result in the concentration of clay minerals in certain parts of the estuary. Turbidity and salinity are typically cited as potential controls on clay mineral distributions. In estuaries, the point at which marine and fresh waters meet, forming a region of locally-elevated suspended matter content, is termed the turbidity maximum (Postma 1967; Geyer 1993). Its importance in relation to clay minerals is that deposition from suspension can occur in the turbidity maximum zone during the slackwater phases of the tidal cycle. Salinities of marine water are substantially higher than that of river water, and in coastal

environments the components of particle-rich river water including ions, clay minerals and biogenic matter flocculate to form aggregates (Eckert and Sholkovitz, 1976; Sholkovitz et al., 1978; Eisma, 1986). In estuaries, this saline front is located at the front associated with the turbidity maximum. Mapped concentrations of the different clay mineral types present in two separate estuaries enable the possible controls on distribution to be discussed. Bioturbation of lithic grains can also produce clay minerals. Experimental studies have shown that the conditions within annelid worm guts, such as *Arenicola marina*, can result in the generation of clay minerals such as kaolinite, illite and berthierine from un-weathered mafic rock (McIlroy et al., 2003; Needham et al., 2004; Needham et al., 2005; Worden et al., 2006; Needham et al., 2006).

With knowledge of the types and the distribution of clay minerals, the possible causes of the patterns and concentrations can be discussed with respect to the above processes.

### **1.2.3 Do grain-coats occur in modern estuarine environments and how do they form?**

Rationale: Studies of grain-coats in geology are commonly on the basis of ancient sediments relating features noted in sandstones to potential transport and deposition processes at the time of formation. A quantitative study of grain-coat coverage and the mineralogy of coatings, as well as textural descriptions of the coats are essential in

understanding post-depositional and early diagenetic characteristics of authigenic mineral cements. The present study seeks to understand the nature of incipient grain-coating, how they formed and how they may relate to subsurface mineral cements.

Understanding the relationship between modern clay coating and ancient clay coating is still controversial. Buurman et al. (1998) argued that the process of *mechanical infiltration* noted in the geological literature is very similar to the process of *clay illuviation* described in the soil science literature.

Mechanical infiltration is the process of muddy water entering a sandbody and depositing fine clay size particles onto framework grain surfaces. From ancient studies this has generally been inferred to occur in desert and river settings, but it may occur in most sandy environments where waters are prone to carry large suspended loads. An ancient example of this process is reported in the fluvial Sergi Formation, Brazil (Moraes and De Ros, 1990; Moraes and De Ros, 1992). The mechanically-infiltrated clays are reported to have developed in a semi-arid area with a lowered water table, where episodic run-off infiltrated coarse sands, and clays decreased in concentration further away from possible fluid entry points.

Mechanically infiltrated material is also found in the alluvial-fluvial Comodoro Rivadavia Formation, Argentina (Dunn, 1992). River-borne suspended load is reported to have infiltrated through highly sinuous

channels and point-bar deposits. The varying composition of the suspended load appears to be recorded by the composition of the infiltrated material with quartz-rich material interpreted to have been supplied during volcanic episodes within the basin supplying volcanic glass. Other notable examples are reported in the fluvial Sespe Formation, California (Hathon and Houseknecht, 1992), while the aeolian Norphlet Formation, Gulf of Mexico has been subject to several studies discussing the process of mechanical infiltration (Dixon et al., 1989; Thomson and Stancliffe, 1990; Kugler and McHugh, 1990; Ajdukiewicz et al., 2010).

Clay illuviation is a process whereby clay grade sediment is moved from a surface or near surface soil layer down into an underlying soil layer where the sediment accumulates (illuviation – the process of accumulation). Eluviation is defined by Kuhn et al., (2010) as the vertical translocation (the process of transport) of fine clay suspended in percolating soil water. This process occurs through three stages (Kuhn et al., 2010):

1. Dispersion – clay is dispersed into water, this is dependent upon the type of clay mineral, particle size, pH, cations present, organic matter content and electrolyte concentration in fluids.
2. Downward transport – clay particles in suspension percolate with the water through the pores volume and into underlying sediments.

3. Deposition – occurs when i) the flow of water is reduced or stopped, ii) a level with low macroporosity (barrier) is encountered or iii) electrolyte concentrations increase within pore waters resulting in flocculation.

Another potential process which occurs in estuaries may result in the formation of grain-coatings in the bioturbation of sediment by worms. Experimental ingestion of interbedded sands and crushed slate by arenicola worms (McIlroy et al., 2003; Needham et al., 2004; Needham et al., 2005; Worden et al., 2006; Needham et al., 2006) proved that bioturbation leads to the formation of grain-coats. This also has the benefit of adhering the coat to the grain with a sticky mucus membrane generated within the worms gut.

Inherited grain-coatings are another potential method of generating grain-coats. These develop as clay coats that form on framework grains prior to deposition (Wilson, 1992). Two modes of formation have been identified (Wilson, 1992): i) formation in aeolian sands through the infiltration of clay-bearing waters followed by mild re-working, ii) shelf deposits where clay coats form through bioturbation, again with subsequent reworking.

1.2.3.1 Question nine - Do sand grain-coatings vary in character in a modern estuary?

Rationale: Understanding the composition of grain-coats, their texture and coat coverage post-deposition could be instrumental in the

attempt to predict authigenic clay mineral cements in ancient sandstones (Worden and Morad, 2003). The nature and texture of coatings can have a big impact on reservoir quality in ancient sandstones, where incomplete chlorite-coat coverage can result in the development of authigenic quartz overgrowths (Bloch et al., 2002). Differences in grain-coat completeness between different sedimentary environments could be critical to understanding the formation of clay cements and predicting their occurrence in subsurface reservoirs. This research will present a quantitative study of sand grain-coatings in one metre sediment cores and how this relates to facies, sediment texture and position within the Anllóns Estuary, Spain.

#### 1.2.3.2 Question ten - What controls the coat coverage on sand grains in modern settings?

Rationale: As discussed above, processes of sediment transport and deposition in sand bodies may occur through mechanical infiltration (Dixon et al., 1989; Moraes and De Ros, 1990; Thomson and Stancliffe, 1990; Kugler and McHugh, 1990; Moraes and De Ros, 1992; Dunn, 1992; Hathon and Houseknecht, 1992; Ajdukiewicz et al., 2010), clay illuviation Kuhn et al., (2010) or possibly inheritance (Wilson, 1992).

Using quantitative measures of coat coverage and mineral concentrations in one metre core the variation in coat coverage and

types is discussed with respect to research on the formation of grain-coats in both modern and ancient examples.

1.2.3.3 Question eleven - How do modern grain-coatings relate to subsurface coated sand grains in petroleum reservoirs?

Rationale: Ancient sandstones with grain-coatings will have undergone extensive diagenetic alteration during burial to high temperature and pressure and through the interaction of formation fluids (Worden and Burley, 2003). A comparison of how modern grain-coatings differ from ancient grain-coatings is essential if the intervening processes of diagenesis are to be fully understood and to confirm whether the coatings that occur in the modern environments are potential precursors to ancient coatings. Furthermore, the relationships between coat coverage of sand grains and other depositional processes may enable the distribution of mineral cements to be more accurately predicted in subsurface petroleum reservoirs.

## **1.3 Methods**

### **1.3.1 Modern estuarine studies**

Two estuarine field locations were identified for the purposes of this study. The Leirárvogur Estuary in southwest Iceland was chosen due to its location in a simple basalt-dominated catchment, and because lugworms were shown to convert Icelandic basalt into clay minerals (Needham et al., 2005). With a relatively simple mineralogy it was hoped that mapping the concentrations of clay minerals and

understanding the processes of their formation could be better achieved than in a more complex region. The estuary was also large (~7km long, ~4km wide and 4.5m maximum tidal range) allowing sampling of a range of different areas of varying marine and fluvial influence. The Anllóns Estuary, Galicia, northwest Spain (~4km long, ~1km wide and 4.0m maximum tidal range), was chosen as a field site due to its mixed source mineralogy, producing quartzo-feldspathic sediments that are closer to those that might be expected in a sandstone reservoir. Both locations were colonised by intertidal worms enabling a study of sediment ingestion by worms and its effect on mineralogy to be considered.

### **1.3.2 Field mapping & sample collection**

Two field seasons in the Leirárvogur Estuary in July 2009 and May 2010 were undertaken to map the estuary geomorphology and collect surface sediment samples. Sample locations were marked using a standard GPS (UTM WGS84). Fifty-two surface sediment samples were collected from locations within the Leirárvogur Estuary and the surrounding drainage basin. A further three lithology and four glacial diamicton samples, were also collected. Sample sites were selected to provide a wide geographic and environmental spread. Twelve worm cast sediment samples were also collected from within the estuary in close proximity to surface sample locations to enable comparison between worm cast and surface mineralogy.

Two field seasons in the Anllóns Estuary in March 2009 and April 2010 were undertaken to map the estuary geomorphology and collect surface sediment samples. Within the Anllóns Estuary and surrounding drainage basin forty-two sediment surface samples were collected. Sample sites were chosen to give a wide and representative environmental spread. Eight hinterland rock samples were also collected to assess the mineralogical composition of the bedrock in the drainage basin.

Bioturbation intensity was measured in both estuaries in the same fashion. Worm cast density at selected sample sites was measured by counting the number of worm traces in a one metre square quadrat. Multiple counts were undertaken to give an average value for bioturbation intensity.

### **1.3.3 Sample preparation & storage**

Surface samples were collected in screw-top plastic jars during field seasons in both estuaries. Samples were kept in cool dry locations during storage and transport back to Liverpool and then stored in a cold fridge (approximate temperature (2°C) in Liverpool. This was to reduce any reactions which may occur within the stored sediment prior to sub-sampling and analysis.

Twelve sediment cores were collected along the Anllóns estuary to sample the texture and mineral composition of the fine fraction within the sediment. Locations were chosen to cover a range of

environments and to form transects permitting the construction of correlation panels. Cores were collected with a jack-hammer driven window sampler (Van Walt Ltd., 2012). The window sampler drives a 50mm diameter core tube into the sediment, within the cutting head is a 'core-catcher', which keeps the collected core in place and prevents the sediment from being disturbed when the core tube is pulled from the sediment. The sediment core was collected whole within a plastic liner, enabling the core to be sealed within rigid plastic tubing and transported back to the laboratory for logging and sampling. Before logging the core was split into two, with one half re-wrapped in the liner and stored in a cool fridge. The remaining half was logged, split into sections and placed in a sample jar prior to sample preparation. A total of seventy-nine sub-samples were collected from the cores, with sample intervals defined by grain-size, composition, and colour (using a Munsell chart) where possible.

#### **1.3.4 Grain size analysis**

Sediment grain-size and sorting values are based on Laser Granulometry using a Beckman Coulter LS200 (Beckman Coulter Incorporated, 2011). The method involves mixing individual sediment sub-samples and calgon to deflocculate sedimentary components and to generate a slurry. This was then added to the Coulter where the distributions of particles from 0.4  $\mu\text{m}$  to 2000  $\mu\text{m}$  are counted. Grain-size data presented were analysed using Gradistat (version 6)

software (Blott, 2008). All grain-size and sorting values presented use the modified geometric (Folk and Ward, 1957) graphical measures.

### **1.3.5 X-ray Diffraction (XRD)**

X-ray diffraction was performed on the fine fraction of collected samples to determine the types of clay minerals present and to quantitatively measure their concentrations.

#### *1.3.5.1 XRD Sample Preparation*

For (XRD), fine fractions (<2  $\mu\text{m}$ ) and coarse fractions (>2  $\mu\text{m}$ ) of the sediment were separated, with a fine fraction weight percentage (wt %) obtained for each sample location. Sediment sample preparation followed techniques outlined by Jackson (1969) and Moore and Reynolds (1997). Samples were homogenised, sub-sampled, and then air-dried at 60°C for 15-hours. Dry sub-samples were weighed then dispersed in tap water by means of four 5-minute cycles of ultrasonication and stirring. The supernatant liquid was decanted and the clay size fraction (<2 $\mu\text{m}$  e.s.d.) was collected by centrifugation at 3500rpm for 30-minutes. The clay size fraction was then dried at 60°C for 15-hours, ground and then weighed to obtain the clay size fraction percentage. All sediment samples had the majority of organic matter removed (>80%) by NaOCl solution (Kaiser et al., 2002). The solution consisted of 15% NaOCl by volume with distilled water; this solution was bathed samples (0.1g in 200ml of solution) and stirred for 24 hours. A centrifuge was used to settle the fine fraction from the solution.

### 1.3.5.2 *Iceland samples*

Initial identification of minerals present was performed on a subset of the samples collected to define and refine the sample preparation and mineral identification procedure. Due to the large number of Iceland analyses (nine) that needed to be performed on each sample to identify the mineral present and the large number of samples, it was decided at an early stage that the clay mineral identification outlined below would be completed on eight surface sediment samples that were considered to be representative of environments and have a good geographical spread in the estuary. The mineralogy of remaining samples was then identified utilising this information as a guide.

The method used for identification of clay mineral peaks relies upon the saturation of the interlayer spacing with cations such as magnesium and potassium and the sequential heating of samples. Saturation of the interlayer spacing enables the diagnostic peaks for particular clay minerals to be identified, particularly if scans of unsaturated samples are taken prior to the saturation (Moore and Reynolds, 1997). Subsequent sequential heating and scanning of the sample can also enable identification of clay minerals in samples as interlayer spacing's collapse and water is lost from the mineral structure (Tucker, 1988).

Sub-samples of the clay separates were suspended in solutions (0.1g in 200ml of solution) containing one molar KCl or MgCl for twenty minutes using an ultrasonic bath to keep the sample suspended. Both the magnesium- and potassium-saturated sub-samples were oriented on to 0.2µm Ag filter membranes by vacuum suction. Oriented samples were washed to remove salt build-up, and 0.5% PVA solution was added to bind the sub-sample onto the filter membrane. Magnesium-saturated samples were glycolated, then both magnesium- and potassium-saturated sub-samples were heated sequentially to 300°C, 400°C and 550°C in air, for one hour per step. Samples were scanned after each step of treatment, giving a total of nine analyses for each sample within the first batch of eight samples. Potassium-saturation of the inter-layer spacing results in the dehydration of the clay mineral phase at lower temperatures. Potassium-saturation and 550°C heating produces more distinct peaks for the main mineral phases than magnesium-saturation. The remaining forty-four samples were potassium-saturated and heated to 550°C only.

#### 1.3.5.3 *Spain Samples*

Analysis of the fine fraction of Spain samples was comparatively simple as the higher crystallinity of the minerals allowed the software to semi-quantitatively ascertain the types of minerals in each sediment sub-sample. Air dried samples were first scanned and then glycolated

to assess the presence of expandable clay minerals (Moore and Reynolds, 1997).

#### 1.3.5.4 XRD Mineral Identification

Various publications are available on how XRD works (Moore and Reynolds, 1997; Tucker, 1988; Klug and Alexander, 1974; Jenkins and de Vries, 1996). In simple terms, X-ray beams are regularly fired at a sample, the source of the X-ray beam gradually rotates and when the beams interact at a particular angle with a mineral a diagnostic diffraction pattern is generated and measured by a detector (Tucker, 1988; Moore and Reynolds, 1997). All minerals have a unique X-ray diffraction pattern based on crystal structure. XRD can be used to either qualitatively or quantitatively identify minerals in a sediment sample. It is particularly useful when measuring the concentration of clay minerals in samples when used on fine fractions (Tucker, 1988). An X'Celerator detector equipped PANalytical X'Pert PRO diffractometer employed Ni filtered Cu k- $\alpha$  radiation, scanning the range 3.9-70.0°2 $\theta$  with a two hour scan time was utilised to scan fine fraction samples from both field locations. Peaks were identified using data within PANalytical HighScore Plus software from the International Centre for Diffraction Data (The International Centre for Diffraction Data, 2013). For Icelandic samples, the sequences of basal clay mineral peaks in the resultant diffractograms were decomposed using the profile fitting protocol of the PANalytical HighScore Plus

software. For Spanish samples PANalytical HighScore Plus software semi-quantitatively measured the types of minerals in each sediment sample.

Calculations to estimate sample preparation and measurement precision (sample homogenisation, clay separation, sample loading, scanning, and data processing) were undertaken. Sediment samples from a similar location to the Spain case study were run four times using the same techniques outlined above in the same background conditions, from the sample collection stage onward. Mean concentrations, standard deviation and the variance within the four repeated mineral measurements indicate that the precision (or repeatability) for the main mineral types using the outlined sample preparation and measurement is generally within 1%, but for some mineral types is around 0.5%.

### **1.3.6 Infrared Spectroscopy**

In the infrared region of the electromagnetic spectrum, molecules within mineral structures can absorb specific frequencies of the infrared spectrum that are characteristic of their structure; these are also known as resonant frequencies. The varying frequencies that the molecules absorb depend on the type of atomic bonds that are present within the mineral. Within an infrared spectrometer a beam of infrared light is passed through a sample, at specific bands of the infrared spectrum the light matches the vibrational frequency of a

bond and is absorbed. This absorption is measured by a detector within the machine (Farmer, 1974).

An infrared spectral analysis on untreated sub-samples of the fine fraction was also performed on representative samples. 1.5mg of fine fraction sub-sample was mixed with 300mg of potassium bromide; this was hand-ground and then sintered at 10 tonnes in a press to produce a sample pellet of 0.5% concentration. The pellets were heated overnight at 150°C to remove any adsorbed water (Madejova, 2003). FTIR spectra were obtained with a Thermoelectron Nicolet 380 infrared spectrometer with an IR source, a germanium on KBr beamsplitter and a DTGS detector (Thermo Scientific, 2012).

### **1.3.7 Scanning Electron Microscopy (SEM)**

Grain-coat coverage measurements were performed on core sub-samples from the Anllóns Estuary. Each sediment sample was sub-sampled and dried at room temperature in a covered petri dish overnight. Grains were mounted within in a plug of epoxy resin under vacuum to prevent spalling of the coat from the grain surface. The surface of the resin was polished and glued to a glass slide, from which excess material was cut and a final polish applied to reduce the size of the epoxy mounted sediment down to approximately 30 microns thick. The thin section was then covered with a thin veneer of carbon using a vacuum carbon coater. The thin section was then analysed using backscattered electron (BSE) imaging on a Philips XL30

scanning-electron microscope (SEM) with an electron beam generated from a tungsten filament. A 5.5 spot size (diameter of the electron beam) was used with a beam current of 20kv. Elemental analysis on samples was also performed with energy dispersive X-ray (EDX) spectroscopy.

Various publications are available that describe how an SEM works (Welton, 2003; Egerton, 2005; Goldstein et al., 2007). An SEM produces a finely-focused electron beam which interacts with a sample producing a variety of different radiation types (Welton, 2003). Of these, backscatter electrons and secondary electrons are commonly used to image the surface characteristics of samples and these are measured using different detectors which produce a high resolution image of the sample. At the same time, characteristic X-rays produced by all the elements in a sample can be analysed by an energy dispersive X-ray (EDX) system. This allows a rapid determination of all the elements in an area of the sample. Issues arise where samples are particularly thin as the depth of the penetration in the interaction area of the beam can result in the analysis of underlying minerals (Welton, 2003).

For each sample multiple images were taken of the sediment mounted on the thin section, with measurements of coat coverage on individual sand grains performed. The process involves measuring the outer perimeter of the grain that is coated in relation to the perimeter

of the grain that is not coated to give a percentage coat coverage measurement for each grain. This means that coat coverage is independent of grain size. One hundred grains are counted per sample, with a total of 6500 coat coverage measurements performed in this dataset. Precision of the technique through repeated measurement of the same sample during sample run indicates an error of approximately two percent per sample analysed.

Samples were also subject to further BSE textural analysis on stub mounts; this enabled a detailed analysis of the surface texture and extent of sand coatings. Sediment was adhered to an aluminium stub using a carbon-based sticker, and this involved dispersing a subsample of air dried sediment over the stub with the sticker attached. Care was taken to ensure that the subsample was from a representative range of grains within the sediment. The stub-mounted sediment was then covered with a thin veneer of gold-palladium (80%-20% ratio) using a vacuum sputter coater. Tests were also performed on blank stubs and the carbon sticker to reduce the effect of the mounting medium on EDX analysis.

#### **1.4 Organisation of the thesis**

This thesis is presented in a paper-style; the chapters have been written with the intention of submission to high ranking publications, therefore some ideas and discussions are recurrent throughout. The chapters and their publication status are outlined below.

## Chapter Two: Pre-requisites, Processes, and Prediction of Chlorite Grain-coatings in Petroleum Reservoirs: A review of subsurface examples

### Citation:

Patrick J. Dowey, David M. Hodgson, Richard H. Worden, Pre-requisites, processes, and prediction of chlorite grain-coatings in petroleum reservoirs: A review of subsurface examples, *Marine and Petroleum Geology*, Volume 32, Issue 1, April 2012, Pages 63-75, ISSN 0264-8172, 10.1016/j.marpetgeo.2011.11.007.

### Outline:

Chapter two is a literature review (meta-analysis) of chlorite-coated examples in published peer-reviewed journals. Data was collated and analysed to establish common factors in chlorite-coats with a particular focus on depositional environments, age, latitude of sediment deposition and chlorite chemistry.

### Work contributed:

Patrick J. Dowey: Main author. Responsible for data collection, meta-data analysis, drafting, interpretation, and for writing the manuscript.

Hodgson, D. M.: In depth discussions and detailed manuscript review.

Worden, R.H.: Responsible for the initial idea of undertaking a meta-data analysis, responsible for project funding, in depth discussions and detailed manuscript review.

Comments and suggestions from S. Morad, R.H. Lander, L.F De Ros and an anonymous reviewer during submission to Marine and Petroleum Geology.

Chapter Three: Clay minerals in a cold climate: Origin, mineralogy and distribution of clay minerals in the Leirárvogur Estuary, SW Iceland

Publication status:

In preparation for submission to Journal of Sedimentary Research

Outline:

This chapter is a study of surficial sediments in the Leirárvogur Estuary, Iceland. The study assesses the types and concentrations of clay minerals within the estuary and catchment and interprets the likely controls on clay mineral formation and how and what controls their distribution within the estuary.

Work contributed:

Patrick J. Dowey: Responsible for planning and execution of field work, estuary field mapping sediment description and sample collection.

Grain size analysis, mineral identification using XRD and infrared spectroscopy. Development and interpretation of mineralogical and textural maps and cross-plots. Interpretation of mineralogical development and distribution. Primary author of the text and figures.

Hodgson, D. M.: Field assistance, in depth discussions and detailed manuscript review.

Worden, R.H.: Responsible for the project, raising all the funding for the work, identifying the fundamental methodology and approach, defining the field area, field assistance, in depth discussions and detailed manuscript review.

Utely, J.: Field assistance, XRD sample preparation and analysis and in depth discussions.

Byrne, G.M., & Kelly, G.: Field assistance in mapping and sample collection.

Chapter Four: Clay minerals in the sun: Mineralogy and distribution of clay minerals in the Anllóns Estuary, Galicia, Spain

Publication status:

In preparation for submission to Journal of Sedimentary Research

Outline:

This chapter is a study of surficial sediments in the Anllóns Estuary, northwest Spain. The work presented assesses the types and concentrations of clay minerals within the estuary and catchment and interprets the likely controls on clay mineral formation and how and what controls their distribution within the estuary.

Work contributed:

Patrick J. Dowey: Partially responsible for identifying the field area. Responsible for planning and execution of field work, estuary field mapping sediment description and sample collection. Grain size analysis, mineral identification using XRD and infrared spectroscopy. Development and interpretation of mineralogical and textural maps and cross-plots. Interpretation of mineralogical development and distribution. Primary author of the text and figures.

Hodgson, D. M.: Partially responsible for identifying the field area. Field assistance, in depth discussions and detailed manuscript review.

Worden, R.H.: Responsible for the project, raising all the funding for the work, identifying the fundamental methodology and approach, field assistance, in depth discussions and detailed manuscript review.

Utely, J.: Partially responsible for identifying the field area. Field assistance, XRD sample preparation and analysis and in depth discussions.

Byrne, G.M.: Partially responsible for identifying the field area; field assistance in mapping and sample collection.

Daneshvar, E.: Field assistance in mapping and sample collection.

Chapter Five: Spatial and temporal variation in mineralogy and texture of sand grain-coatings from a modern estuary: Implications for subsurface investigations

Publication status:

In preparation for submission to AAPG Bulletin

Outline:

This chapter is a study of sand grain-coatings from sediment cores in the Anllóns Estuary, northwest Spain. The study summarises quantitative analyses of grain-coatings in modern environments, interprets potential processes which may create these grain-coatings and assess how these modern grain-coating may relate to subsurface ancient grain-coatings.

Work contributed:

Patrick J. Dowey: Partially responsible for identifying the field area. Responsible for planning and execution of field work, estuary field mapping sediment description and sample collection. Grain size analysis, mineral identification using XRD and infrared spectroscopy,

grain-coat coverage measurement. Development and interpretation of mineralogical and textural core logs and cross-plots. Interpretation of mineralogical development and distribution. Primary author of the text and figures.

Hodgson, D. M.: Partially responsible for identifying the field area. Field assistance, in depth discussions and detailed manuscript review.

Worden, R.H.: Responsible for the project, raising all the funding for the work, identifying the fundamental methodology and approach field assistance, in depth discussions and detailed manuscript review.

Utely, J.: Field assistance in mapping and sample collection. XRD sample preparation and analysis and in depth discussions.

Byrne, G.M.: Partially responsible for identifying the field area; field assistance in mapping and sample collection.

Daneshvar, E.: Field assistance in mapping and sample collection.

## **2. Pre-requisites, processes, and prediction of chlorite grain-coatings in petroleum reservoirs: A review of subsurface examples**

### **2.1 Abstract**

Deeply buried reservoirs containing chlorite-coated quartz grains commonly have higher than expected porosity and permeability, although prediction of such positive anomalies still remains elusive. A total of 54 published examples based on information and data from 62 scientific papers was collated. Quantification of some of the most common parameters including depositional environment, age and latitude of sand deposition, effect on reservoir quality and chemical composition of chlorite is presented.

The dataset indicates that chlorite-coats are found in sandstones deposited in a range of depositional environments, but most commonly occur in delta-related environments (44%), with fluvial environments the second most common (19%). Age relationships indicate that there is an overall exploration bias in published examples, with chlorite-coats becoming increasingly common through time. The latitude at the time of deposition of sands with chlorite-coats is wide (60°N to 60°S), and indicates that temperate and tropical climates are important for the generation of this clay

mineral. Chlorite can have a variable effect on reservoir quality, but is typically positive. Iron-rich chlorites occur overwhelmingly in coastal environments, while mixed iron-and magnesium-rich chlorites are principally found in marine and terrestrial sandstones.

Analysis of these factors suggests that hinterland geology, basinal soil development and geochemical weathering, and proximity to river systems are essential to the formation of chlorite precursor phases. These characteristics have been combined to define situations where chlorite-coats were more *likely* and more *unlikely* to form. These parameters will provide insights into the formation of chlorite and to further refine predictive models for the presence or absence of chlorite-coated sandstones.

## **2.2 Introduction**

Grain-coating chlorite can help to preserve open pore networks in deeply buried petroleum sandstone reservoirs by moderating the effects of authigenic quartz cement growth on detrital grains (Anjos et al., 2003; Ehrenberg, 1993; Ramm and Ryseth, 1996). Where found as a grain-coating mineral, chlorite can reduce the nucleation area for overgrowths; models of quartz cementation indicate that coat coverage is a key factor in the inhibition of quartz overgrowths (Lander et al., 2008). Pore-filling chlorite can also reduce porosity and permeability by decreasing pore throat diameters (Islam, 2009; Nadeau, 2000; Pay et al., 2000; Porter and Weimer, 1982). Prediction

of chlorite occurrence, whether grain-coating or pore-filling, still remains elusive. Previous attempts to predict the occurrence of chlorite have focused primarily on using depositional environment although it must be noted that chlorite is considered to be the result of burial diagenetic transformation of precursor minerals. This work suggests that river-influenced deltaic and shelf environments and saline-influenced desert environments would lead to iron- and magnesium-rich chlorite respectively (Bloch et al., 2002; Ehrenberg, 1993; Kugler and McHugh, 1990).

A detailed evaluation of the distribution of different chlorite types and their effects on petroleum reservoir sandstones of varying ages and depositional settings has not been published previously, and this work is timely as industry increasingly explores for deeply buried reservoirs. The purpose of this review paper is first to gather data and information from the literature on chlorite-bearing petroleum sandstone reservoirs. The data and information will then be used to establish any patterns in the type, occurrence and effect of chlorite. The ultimate objective is to help improve the prediction of reservoir quality within deeply buried sandstone reservoirs.

### **2.3 Chlorite coat formation: Pre-requisites**

Chlorite (general formula:  $(\text{Mg,Al,Fe})_6 [(\text{Si,Al})_4\text{O}_{10}](\text{OH})_8$ ) is a 2:1:1 clay mineral composed of a tetrahedral-octahedral-tetrahedral structure, inter-layered between these structures is a octahedral sheet

composed of cations and hydroxyls. Chlorite can have a variable chemistry, but the two main types are iron-rich and magnesium-rich chlorite. Identification is normally achieved through X-ray diffraction or ion microprobe analyses (Worden and Morad, 2003).

The concept of open-system burial diagenesis considers mineral cement growth to be the result of large, basin-scale fluxes of water (e.g. Giles et al. 2000), whereas the concept of closed system (isochemical) burial diagenesis considers the generation of mineral cements to be restricted to the components within a sediment volume at the time of deposition with no material lost or gained (e.g. Bjorkum et al., 1998; Ramm and Ryseth, 1996). The extent and scale of open-versus closed-system behaviour depends on the species under consideration. Chlorite, dominated by low solubility  $\text{SiO}_2$  and  $\text{Al}_2\text{O}_3$ , can be considered to be largely isochemical during burial diagenesis (Chuhan et al., 2000). Ferrous iron is somewhat more soluble than  $\text{SiO}_2$  and  $\text{Al}_2\text{O}_3$  and more soluble than ferric iron (Krauskopf and Bird, 1995), but can still be considered to be closed-system on a bed-scale. Therefore the dominant control on the occurrence and type of chlorite is the initial (depositional) mineralogy. As a consequence, precursor (depositional and early diagenetic) mineral sources for chlorite growth need to be considered.

The process of chlorite-coat formation in reservoir sandstones has previously been subject to review (Bloch et al., 2002; Ehrenberg, 1993;

Hillier, 1994; Pittman et al., 1992; Worden and Burley, 2003; Worden and Morad, 2003), and a brief summary of the interpreted pre-requisite conditions is provided below.

### **2.3.1 Diagenetic chlorite coats from precursor clay minerals**

In terms of the number of examples cited, iron-rich chlorite is the most common variety. Over the years, a number of potential precursor minerals and grains have been suggested as the likely candidate for iron-rich chlorite.

#### 2.3.1.1 Berthierine and odinite precursors

A study of iron-rich chlorite-coated quartz grains in reservoirs on the Norwegian Continental Shelf concluded that chlorite developed during diagenesis from an iron-rich clay mineral precursor that formed at the time of deposition (Ehrenberg, 1993). The development of chlorite from a precursor clay mineral was supported by evidence that the shallowest buried chlorites in these areas was mixed layer chlorite-serpentine. Berthierine, an iron-rich, 7Å, 1:1 clay mineral, was identified as the most likely serpentine mineral phase. In deeper sections from the Norwegian Continental Shelf, chlorite, as well as mixed-layer chlorite-serpentine, occurs suggesting a progressive recrystallisation towards chlorite with increasing temperature and depth.

A similar relationship was noted in Tuscaloosa Formation, Gulf Coast, USA (Ryan and Reynolds, 1997). With increasing burial, mixed-layer

serpentine-chlorite became more chloritic. In this study it was concluded that the mixed-layer serpentine-chlorite was an intermediate phase between chlorite and another serpentine mineral, odinite (Fe<sup>3+</sup>- and Mg-rich 1:1 clay mineral between di- and trioctahedral structures, Bailey, 1988).

Other examples of berthierine-coated quartz grains in sandstones come from the Siri Field in the Danish North Sea (Stokkendal et al., 2009), the Clearwater Formation, Alberta, Canada (Hornibrook and Longstaffe, 1996) and shallow sections of the Logan Canyon Formation, Scotian Basin, Canada (Pe-Piper and Weir-Murphy, 2008). Experimental work (Aagaard et al., 2000), using a hydrothermal bomb replicated chlorite coats of a similar morphology and chemistry to naturally occurring chlorites using berthierine-coated sandstones from a shallow Haltenbanken (Norwegian Continental Shelf) sandstone as the starting material.

#### 2.3.1.2 Kaolinite precursor

Boles & Franks (1979) found that chlorite-coats in the Wilcox Formation, Texas, USA, were particularly high in aluminium and noted a decrease in kaolinite relative to chlorite with increasing depth. This suggests that kaolinite (possibly supplied with iron and magnesium from the illitization of smectite) could develop into an aluminium-rich chlorite. Furthermore, Hillier & Velde (1992) reported a mixed-layer chlorite-kaolinite in a sandstone reservoir on the Norwegian Continental Shelf.

This indicates the possible progressive development of chlorite from a kaolinite precursor with increasing diagenetic grade.

#### 2.3.1.3 Smectite precursor

The development of chlorite from a trioctahedral smectite requires either a local source of aluminium or the loss of excess silica (Chang et al., 1986). Pore-lining chlorite in sandstones from the Central Graben, UK North Sea was reported to share morphological and chemical characteristics with smectite, and smectite was proposed as the precursor to chlorite (Humphreys et al., 1989). Similarly, in pore-lining chlorites from the Santos Basin, Brazil, evidence for smectite as a precursor is indicated by remnants of corrensite (mixed-layer chlorite-smectite) below pervasive calcite cements and along tight intergranular contacts (Anjos et al., 2003). During burial diagenesis saline formation waters have been reported to interact with iron-oxide coatings on detrital grains to form smectitic clay coats (Bloch et al., 2002), which progressively develop into magnesium-rich chlorite. The Norphlet Formation is the most widely reported example, and chlorite-smectite precursor coats were concluded to have developed from the interaction of brines and iron-oxide rims either soon after deposition (Ajdukiewicz et al., 2010), or later during deeper burial (Kugler and McHugh, 1990). Chlorite coats in the Hannover and Sclocteren Formations, North German Basin, Germany, were also interpreted to have been partly the result of interaction of brines and

appear to have developed progressively from smectite to corrensite to chlorite (Gaupp et al., 1993; Hillier et al., 1996; Platt, 1994). Another example of chlorite development (via a smectite precursor) from the interaction of saline waters and iron-oxides is the Lower Clair Group, UK (Pay et al., 2000).

### **2.3.2 Diagenetic chlorite-coats formed from the dissolution of detrital grains**

Authigenic chlorite may also develop during diagenesis as a result of the dissolution of iron- and magnesium-rich detrital grains and volcanic rock fragments (AlDahan and Morad, 1986; Anjos et al., 2000; Blackburn and Thomson, 2000; Burns and Ethridge, 1979; De Ros et al., 1994; Remy, 1994; Thomson, 1979; Valloni et al., 1991; Worden and Morad, 2003), and from mud intraclasts (Worden and Morad, 2003), and this can lead to a wide range of chlorite compositions. The development of chlorite-coats in reservoir sands from this range of detrital grains requires at least the partial dissolution of the original grain and the neoformation of a clay mineral. Small et al., (1992) experimentally simulated clay mineral precipitation from solution in sandstones using a hydrothermal bomb. In this closed system experiment, a temperature gradient enabled dissolution of a starting material at one end of the vessel and precipitation of a range of clay minerals on to sand grains at the other end. Although attempts to

generate a 'pure' chlorite proved difficult, the authors were able to generate a magnesium-rich 7Å phase with boxwork morphology.

Thomson (1979) suggested that volcanic rock fragments (VRFs) could be the source of ions for the chlorite coats in the Tuscaloosa Formation, Gulf Coast, USA. The study suggested a positive relationship between chlorite coatings and VRFs. Where VRFs were not co-deposited within sands, chlorite coats did not form and quartz overgrowths were able to develop and fill the pore space. Thomson and Stancliffe (1990) argued that VRFs are the most likely source for magnesium to allow the development of chlorite in the Norphlet Formation. Chlorite in the Central Graben, UK North Sea was interpreted to have developed from a smectite precursor aided by the dissolution of detrital grains (Humphreys et al., 1989). Chlorite-coated grains were reported from the Taranaki Basin, New Zealand, and were interpreted to have developed from the interaction of waters from overlying marine sediments during diagenesis (Martin et al., 1994). However this necessitates the concomitant dissolution of detrital grains. Other examples where the role of detrital grain dissolution may have been important include the Lower Clair Group (Pay et al., 2000) and the Santos Basin, Brazil (Anjos et al., 2003).

## **2.4 Dataset**

To better understand the controls on the formation of chlorite-coatings in sandstone reservoirs, and to assess the effect these factors may

have, a number of question have been defined, that will be discussed by reference to published literature:

- 1) In which depositional environments did the chlorite-bearing sandstone form?
- 2) What effect do diagenetic chlorite-coatings have on the reservoir quality of the sandstone?
- 3) At what age and latitude were the chlorite-coated sandstones deposited?
- 4) What is the range of chemical compositions of chlorite in the published examples?

#### **2.4.1 Data collection**

Online science-literature focused search engines were utilised with the keywords "chlorite" and "petroleum reservoir" to find relevant papers. Further examples were added from citations in these papers and from paper-based searches. A total of 54 examples based on information and data from 62 scientific papers over the past 35 years were used to collate this database (see references). The examples come from a range of geographic locations, ages and depositional environments. A complete listing of the database is available with the appendices for this chapter (appendix 8.1). This dataset represents the majority of easily accessible, widely cited, and relatively recent examples of chlorite-coated sandstone reservoirs. Examples are defined as a particular lithostratigraphic formation where this information is given.

A number of papers and specific examples within some papers were not included because key attributes (principally the depositional environment) were not reported or discussed within the individual paper, these include some papers which may be viewed as seminal in the study of chlorite-coated sandstones (Heald and Larese, 1974; Pittman and Lumsden, 1968). Examples from outcrop localities were not included because of the potential negative effect that weathering may have on present-day mineralogy. The study was predominantly limited to published papers on chlorite-coated grains in sandstone petroleum reservoirs, although some examples are from non-producing subsurface areas. The study included chlorite and chlorite mixed-layer clay minerals (see Appendices 1A-C).

#### **2.4.2 Defining depositional environment**

The varied descriptors applied by many sedimentological studies and the complicated nature of depositional systems make it difficult, in some cases, to compare paleoenvironmental interpretations and the processes operating within that environment. For this study, it was necessary to establish a depositional environment classification scheme based broadly on the type of environments individually described by the various authors in published examples of chlorite-coated sandstone reservoirs (Table 2.1; Fig. 2.1). The scheme is split into three broad settings: 'continental', 'coastal' and 'marine', within

Setting	Environment Association		Description
Continental	1	Desert arid	Sandy aeolian-influenced area composed of dune fields or sand seas
	2	Desert coastal/sabkha/playa	Sandy aeolian-influenced location composed of dune fields or sand seas, with ephemeral to seasonal rivers or lakes, high water tables or proximity to the sea
	3	Alluvial/fluvial/floodplain	Where sediment is deposited within, or in close proximity to, flowing river drainage systems
	4	Lacustrine	Sediment deposited from or into lake waters, includes sediments deposited in mixed fluvial-lacustrine environments
Coastal	5	Delta	Prograding location subject to mixed marine and fluvial processes, where sediment is supplied principally from river systems
	6	Estuary/lagoon	Embayed coastline where river fluvial inputs are diminished and marine processes tend to predominate, sediment is supplied from offshore or erosion of older deposits
	7	Linear clastic shoreline	Linear coastline where river fluvial inputs are diminished and marine processes predominate, sediment is supplied from alongshore transport or erosion of older deposits
Marine	8	Continental shelf	Marine setting where water depths are normally shallow (<200m), located between storm wave base and the shelf edge
	9	Continental slope	Marine location between edge and base of slope. Typically consists of incised canyons with mass wasting deposits, channel fill and associated overbank sediments
	10	Basin plain/fan	Marine location beyond the base of shelf slope; deposition is from sediment gravity flows and pelagic fallout

Table 2.1 - Depositional environment scheme used to define depositional environments of published chlorite examples. Colours used relate to some subsequent figures

which the settings are further divided into 'environmental associations'. Environmental associations describe the features of, and/or processes which operate within, those settings. For example the 'fluvial/floodplain' environment constitutes locations where sediment is deposited within, or in close proximity to, fluvial drainage systems. Using this scheme, a reported example of a chlorite-coated sandstone reservoir can be placed within a gross depositional environment. Where examples are interpreted to have two environmental associations (i.e. fluvial and then estuarine during a rise in relative sea level), assessment of criteria such as: the thickest association and in which sections chlorite-coats were most predominant were used to fit examples in to the scheme. Placing case studies in to the criteria in Table 2.1 depends on the quality and detail of the individual published case studies. Depositional environment is relatively poorly defined in some papers.

### **2.4.3 Defining reservoir quality**

Reservoir quality controls the storage, distribution, and flow of fluids within a reservoir (Slatt, 2006). The effect that chlorite has on reservoir quality can be variable, controls including lithofacies (Morad et al., 2010; Morad et al., 2000) and thermal histories (Bloch et al., 2002; Lander et al., 2008; Taylor et al., 2010) can impact the porosity and permeability of a sandstone reservoir. Some authors (e.g. Pittman et al. 1992) have previously noted that chlorite-coats on detrital sand

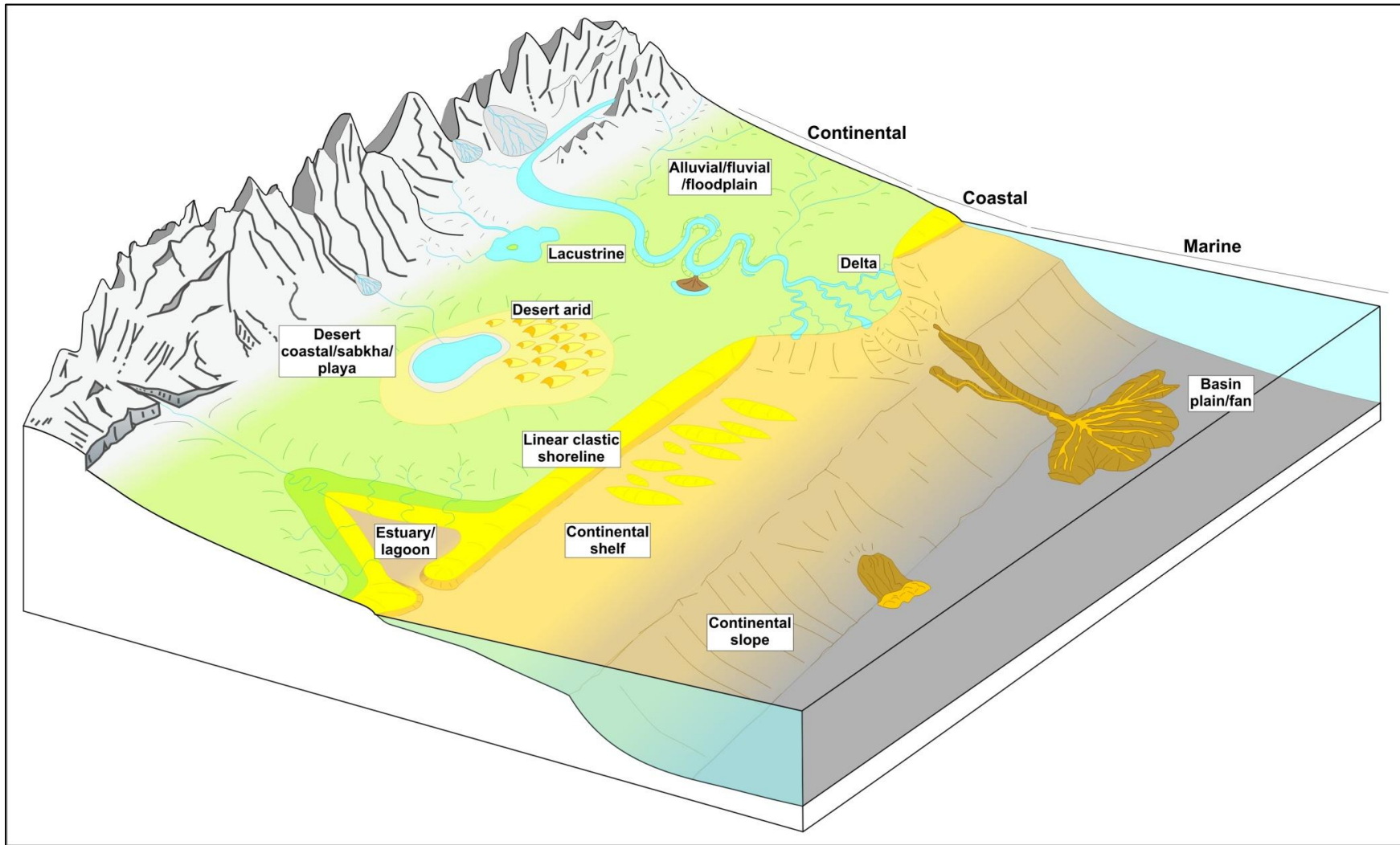


Figure 2.1 - Depositional setting and environment association as defined in Table 2.1.

Effect	Morphology/ occurrence	Impact on reservoir quality
Positive	Pore-lining	Inhibited the growth of authigenic quartz during diagenesis
Mixed	Pore-lining and pore- filling	Inhibited the growth of authigenic quartz during diagenesis and reduced porosity and permeability through micro-porosity formation
Negative	Pore-filling	Reduced porosity and permeability through micro-porosity formation
No effect	N/A	Zero - quartz overgrowth formed despite presence of chlorite
Not discussed	N/A	Not discussed within the example

**Table 2.2 - The characteristics of chlorite-coats on sand grains within studied examples.**

grains can have both a positive and negative effect on reservoir quality. The effect chlorite has on porosity and permeability in relation to other criteria is defined in Table 2.2. Where chlorite was 'pore-lining' or 'grain-coating' and seen to inhibit subsequent quartz overgrowths this was deemed to be 'positive'. Formations where chlorite-coats were described as 'pore-filling' and resulting in the 'generation' of microporosity were classed as 'negative'. 'Mixed' examples are where chlorite was viewed as combining both the pore-lining and pore-filling elements. Examples where authigenic quartz overgrowths were interpreted to develop despite the existence of a chlorite-coat on detrital sand grains and where the role of chlorite-coats was not discussed are defined as 'no effect' and 'not discussed', respectively.

#### **2.4.4 Age and depositional latitudes**

The depositional age of sandstone reservoir units was derived from the published age, epoch or period of a reservoir unit. The latitude at the time of deposition was reported by the authors using the age and relative position of that area at that time, or was identified using published paleogeographic maps (e.g. Habicht, 1979). A range of latitudes is used to express the uncertainty (normally plus or minus 10 degrees) inherent in this interpretation.

#### **2.4.5 Elemental compositions**

Nineteen published examples of chlorite-coated sandstones included analytical data on the composition of chlorite. This study includes examples from a much larger dataset than previous studies comparing elemental composition of chlorites (Ehrenberg, 1993; Kugler and McHugh, 1990). Data collected are principally electron microprobe analyses, but also includes EDX (SEM) and AEM (TEM) analyses. Although attempts were made to use individual analyses, some reported values were already averaged or 'representative' values. Elemental compositions were normalised to 88% because around 12% of the mass of chlorite is in the form of -OH groups (Deer et al., 1992). Elemental compositions were calculated on the basis of ten structural oxygen atoms, plus eight hydroxyls (see appendices 1D & E). Where only tetrahedral occupation of silicon or aluminium was published (alongside Fe/(Mg+Fe) ratios) these values were

recalculated to produce values for silicon tetrahedral occupancy on the basis of four tetrahedral sites per unit cell.

## **2.5 Results**

The dataset is divided into three geographical groupings – “North America”, “Northwest Europe” and the “Rest of the World”, which reflect historical exploration trends as the majority of examples come from mature provinces of North America and Northwest Europe. This approach highlights that more chlorite-coated reservoir sandstones may be discovered during future exploration of frontier areas and deeper targets, making the search for common controls on chlorite distribution pertinent.

### **2.5.1 Depositional environment, reservoir quality and age**

Chlorite-coated sandstone reservoirs are not restricted to any one setting or depositional environment (Fig. 2.2A). However, 54% of all the examples in the database are found in coastal settings, with deltaic depositional environment (as defined by this study) being the most common (44%). A third of all examples occur in terrestrial setting (33%), with fluvial examples accounting for 19% of the overall total. Most other environments individually account for only 2% to 6% of the overall total. Overlain on Figure 2.2A is the effect on reservoir quality for each environment. This indicates that chlorite-coated sandstones overwhelmingly have a positive effect (43%) or have mixed effect (37%). Only three examples (6%) are reported to have a negative

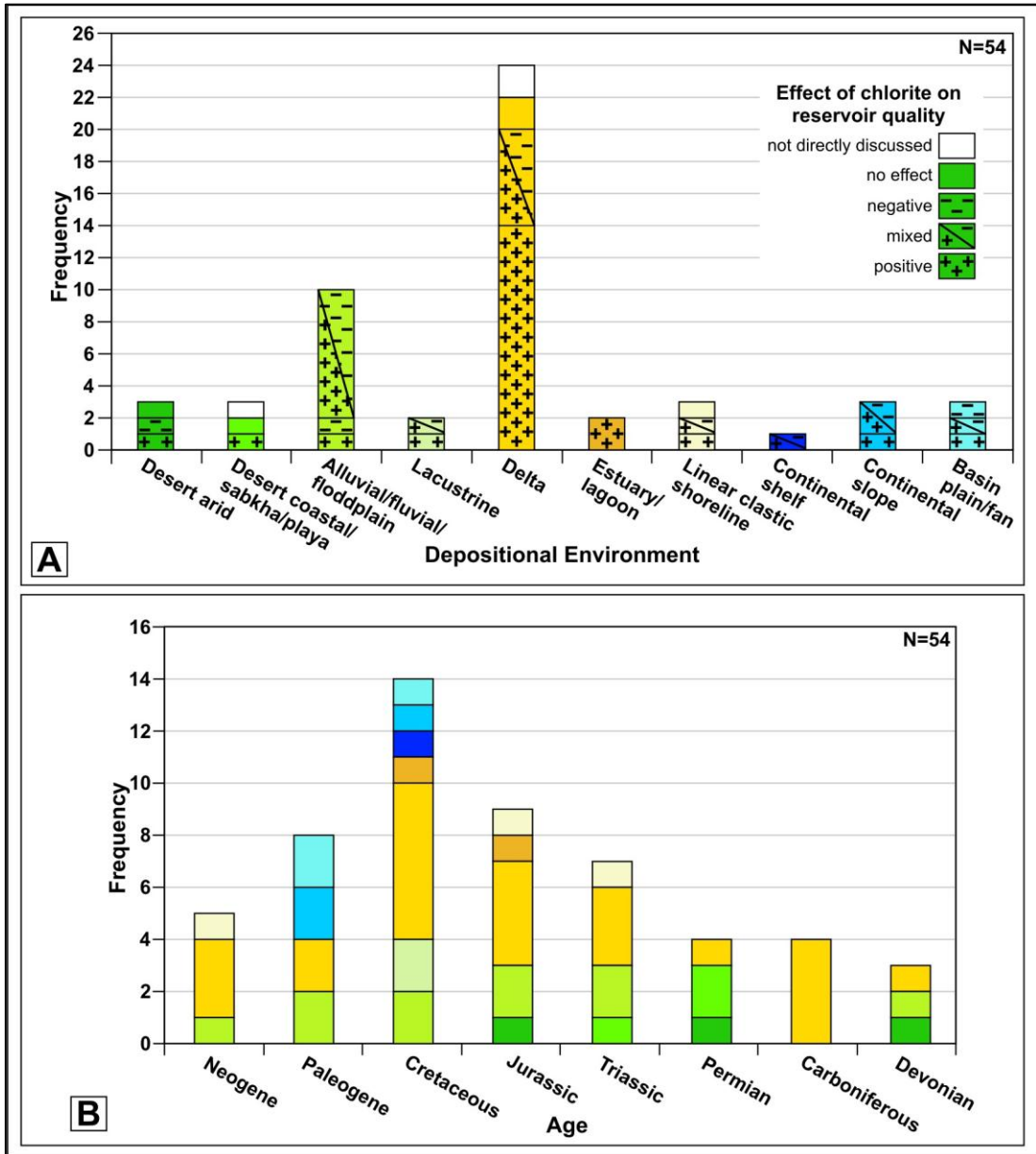


Figure 2.2 - Frequency of depositional environments (colours relate to depositional environment outlined in Table 2.1). A. Reservoir quality assessment for depositional environments. B. Frequency of depositional age and environment.

effect, while 7% have no effect. Most of the depositional environments show an approximate equal split between positive and mixed.

Figure 2.2B is the frequency of depositional age overlain with the frequency of depositional environment for that age. The graph shows that chlorite-coated sandstones within the database are evident throughout the Phanerozoic, but that no examples occur before the Devonian period. The distribution of ages suggests a gradual increase in the number of instances from the Devonian period (6%) through to a peak in the Cretaceous (26%). After the Cretaceous there is a significant decrease in the frequency of examples in the Paleogene (15%) and Neogene (9%). Comparison of age and depositional environment indicate that coastal and deltaic environments occur in all periods, while chlorite-coats in marine (principally deepwater) examples only occur in Paleogene and Cretaceous reservoirs. Fluvial examples also occur in nearly all age groupings (except the Carboniferous and Permian). Desert environments are restricted to the Devonian, Permian, Triassic and Jurassic periods.

### **2.5.2 Age and depositional latitude**

Figure 2.3A is the age and latitudinal range of individual formations during their deposition; beneath this are eustatic sea-level and climate-temperature curves for the Phanerozoic compared to present day conditions (fig. 2.3B). The graph shows an overall northward

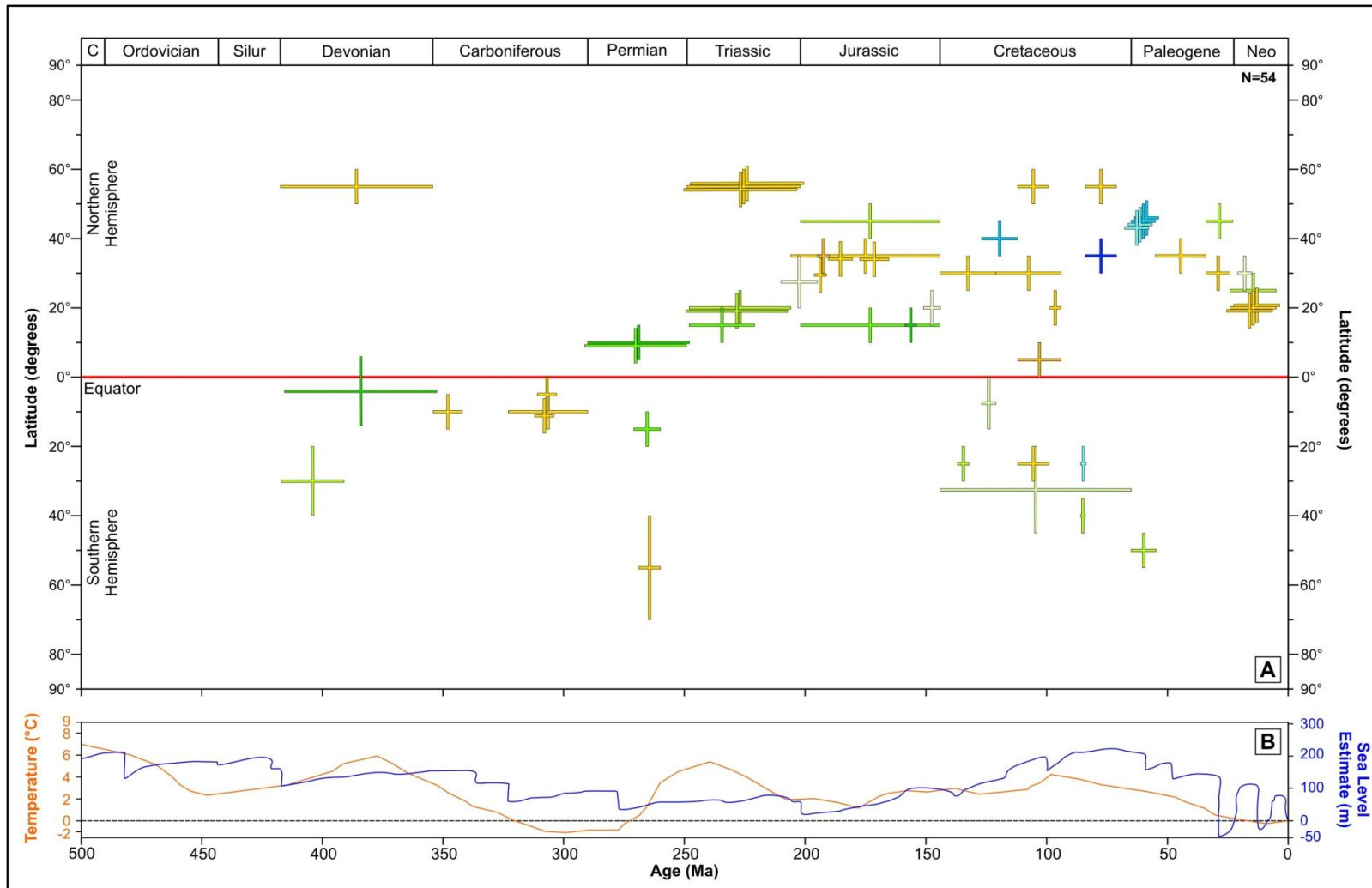


Figure 2.3 - Age and latitude of deposition of examples (colours relate to depositional environment outlined in Table 2.1). A. Latitude range at time of deposition and depositional environment (paleolatitude ranges from Habicht (1979) & Eyles (2008)) C = Cambrian, Silur = Silurian, Neo = Neogene. B. Estimate of sea level (redrawn from Miller et al. (2005)) and temperature (After: Royer et al. (2004)) for Phanerozoic time

occurrence of chlorite-coated sandstones from the Devonian up to the Jurassic, after which there is a large increase in the number and latitudinal range (60°S-60°N) of examples during the Jurassic and Cretaceous (Fig. 2.3B). During the Paleogene and Neogene nearly all examples in the dataset occur at 15°N-50°N.

### **2.5.3 Elemental composition, reservoir quality and depositional environment**

Figure 2.4A is collation of tetrahedral occupancy versus iron-magnesium ratios from published papers. This plot is the standard classification diagram for chlorite (Bayliss, 1975; Foster, 1962). The fill of each data point represents the reservoir quality, while the colour relates to the depositional environment for that particular formation. Figure 2.4B is the average of values for each example in figure 2.4A, the error bars are one standard deviation for these values. Figure 2.4A highlights the variability in the iron-magnesium ratio from all of these examples, with values varying between 0.25 and slightly more than 0.8. Coastal values (yellow) vary over this same range, however, terrestrial (green) and marine (blue) examples are found within the 0.25 to 0.65 range, with exception of two outliers.

## **2.6 Discussion**

Each parameter previously outlined is discussed with respect to its effect on the formation of chlorite and how this may aid the prediction of chlorite in subsurface exploration.

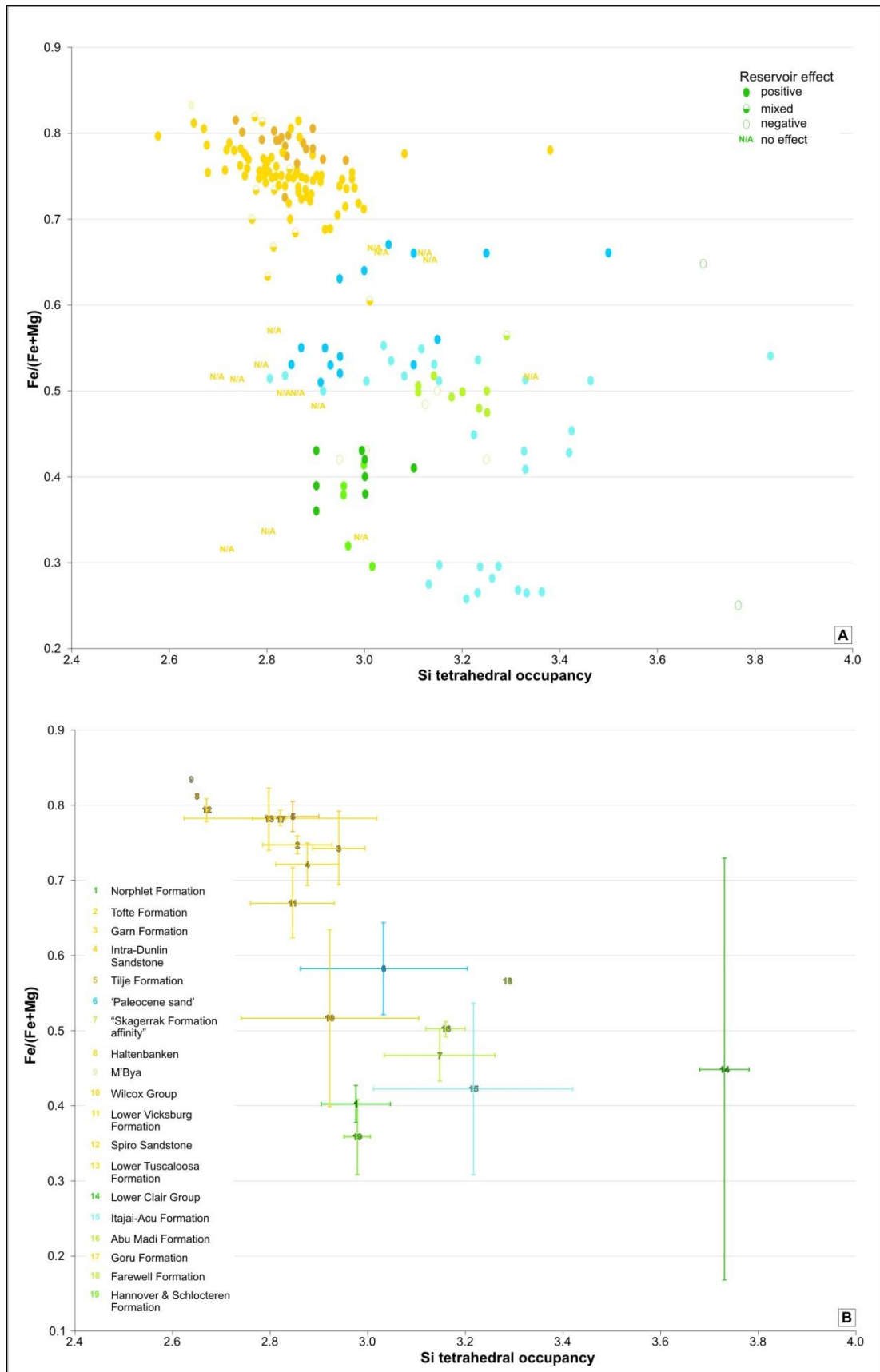


**Figure 2.4 - Elemental ratios from published examples. A. Full dataset with the effect of chlorite on reservoir quality indicated. B. Average values for each formation (with standard deviation error). Colour relate to depositional environment number relates to individual examples.**

### 2.6.1

### **Depositional environment as a control**

In discussion of the relationship between chlorite and depositional environments, it is important to note that chlorite-coats are generated in sandstones during diagenesis through precursor phases (section 2.3), and the link with depositional environment is indirect. In this review a large proportion of the examples in the dataset (fig. 2.2A) occur in coastal environments, and in particular deltaic environments (as defined by this study). The link between deltaic/fluvial-influenced coastal and shelf environments and chlorite-coat formation has been made previously (Bloch et al., 2002; Ehrenberg, 1993). However, sediments deposited in coastal environments account for a considerable number of all petroleum producing reservoirs and hydrocarbon volumes (see figures 62 & 63, Ahlbrandt et al., 2005). Common features of coastal environments, such as high-energy conditions and the repeated reworking of sediment, may be key processes in the formation of reservoir sandstones in general and not just the formation of reservoir sandstones with chlorite-coated grains.

Iron-rich sulphide (pyrite) and carbonate (siderite) are associated with chlorite-coated quartz in sandstones from the Norwegian Continental Shelf (Ehrenberg, 1993). Pyrite is formed in reducing conditions by the reduction of sulphate in the presence of organic matter. (Tucker, 2001). Siderite is precipitated in reducing conditions where carbonate activity (effective concentration) is high and sulphide activity is low.

Sulphide activity is typically low in uncompacted marine sediments flushed with sea water, but it can occur in sediments rich in organics where all  $\text{SO}_4^{2-}$  is removed by bacterial reduction to form sulphides (Tucker, 2001). The close association of siderite, pyrite and Fe-rich clay minerals indicates that iron may be incorporated in to these three minerals as the oxygen conditions and anions vary in the sediment. Another strong association discussed by Ehrenberg (1993) was iron-rich ooids, which are also reported in other examples (Baker et al., 2000; Pe-Piper and Weir-Murphy, 2008). Although the formation of sedimentary iron-ooids is controversial (Van Houten and Bhattacharyya, 1982); it has been proposed that the co-deposition/formation with chlorite precursor minerals indicates that they were formed in nearshore shallow marine environments.

Recent studies report that the chlorite precursor clay minerals berthierine and odinite are found in shallow tropical, prodelta and shelf settings (0-150 m) in close association with river inputs (Odin, 1988; Porrenga, 1967). Examples include the Congo and Niger River prodelta settings as well as the shelf around the Orinoco and Amazon Rivers (Bailey, 1988; Odin, 1988). Berthierine and odinite are reported to develop from iron supplied via river waters. Rivers have the potential to supply large amounts of clay minerals to coastal environments. For example suspended volumes of clay minerals in Amazon River tributaries were found to be high, at between 50% and

98% of solids in suspension (Gibbs, 1967), and this is corroborated by work on large rivers around the world (Fig. 3.7, in Chamley, 1989).

The nature of suspended clay minerals in modern river systems reflects the geology and weathering profiles of soils within the drainage basins (Chamley, 1989; Griffin, 1962), which in turn will be evident in the types, distribution and abundance of clay minerals (Ketzer et al., 2003) deposited within sedimentary basins. River systems supply material and create conditions that are conducive to the formation of the three most common ways in which chlorite (or its precursors) forms: grain-coating Fe-clays, mechanical infiltration of clay mineral (smectite) and alteration of detrital grains. The first two of which are most commonly occur in deltaic and fluvial settings respectively, while the third will can occur in almost any depositional setting during subsequent diagenesis (Morad et al., 2010).

The fluvial/floodplain environmental association has three times as many instances of chlorite-coats reported (ten) as other non-deltaic environments (fig. 2.2A). The relatively high frequency of this environmental association seems to be significant, although this could be a result of combining these diverse environments together in the dataset. One interpretation for this distribution is that fluvial sediments that are associated with arid or semi-arid depositional conditions may have oxy-hydroxide-coatings that help create chlorite during subsequent burial. However, examination of the ten examples in the

fluvial grouping finds that only two discussed evidence of desert influence. The chlorite-coats in sandstones of the Sergei Formation, Brazil, were reported to form from the mechanical infiltration of clays in an arid/semi-arid environment, becoming subsequently chloritized during deeper diagenesis (Moraes and De Ros, 1990). A red bed fluvial unit from the South Viking Graben, UK North Sea (Taylor, 1978), contains chlorite-coats considered to have formed after the near-surface formation of haematite-coatings.

Furthermore, of the ten, one example had Mg-rich chlorite-coats which appear to have been created from a chlorite-smectite precursor and the reaction of unstable detrital silicates and dolomite (Humphreys et al., 1989). In another example (Martin et al., 1994) chlorite-smectite is reported to have developed from the alteration of hornblende due to the interaction of formation waters derived from marine sediments. Chlorite-coats in the fluvial sediments of the Yannan Formation, China, were concluded to have developed from a smectite precursor mechanically infiltrated soon after deposition (Luo et al., 2009). The Abu Madi Formation, Egypt has chlorite-coats that formed from the alteration of precursor clay minerals and from the breakdown of volcanic rock fragments (Salem et al., 2005).

The diverse processes by which chlorite precursor minerals become chlorite grain-coatings in fluvial settings suggests a multi-genetic route of formation. That 63% of cases are deltaic, estuarine, or from the

fluvial/floodplain environmental association indicates that rivers play a key role in supplying chlorite precursor material in suspension to fluvial/floodplain and coastal environments. This interpretation is further reinforced by the wide age-distribution of these examples (fig. 2.2B). Therefore, chlorite precursor material found in fluvial sandstones may have been supplied by the river system itself, either during sedimentation in the case of co-deposition of clay minerals and detrital grains in close proximity to fluvial sands (Humphreys et al., 1989; Salem et al., 2005) or soon after deposition through mechanical infiltration of clay minerals (Matlack et al., 1989).

The frequency of estuarine environments is very low (fig. 2.2A), with only two recorded examples, despite deltaic and estuarine environments both having a combination of tide, wave and fluvial action (Dalrymple et al., 1992). The similar processes operating in these environments may mean that discriminating between estuarine and deltaic environments is challenging (Folkestad et al., 2012; Kitazawa, 2007). Furthermore, a highstand estuarine valley that is incised during a lowstand and then infills to form a delta (as sea level rise begins to slow and ultimately fall), produces a sedimentary succession which may retain both an estuarine and a deltaic signature. There are differences between estuarine and deltaic settings and it may be that estuarine environments are under-represented due to conditions particular to that environment. For example, sediments deposited in

the early infill stage of an estuary may be more poorly sorted (Allen and Posamentier, 1993; Reading and Collinson, 1996) and less likely to become reservoir intervals. As already discussed, river inputs appear to be a key factor in the development of chlorite, estuaries where river inputs are strong may fill quickly ultimately forming deltas. It can therefore be concluded that where fluvial inputs are weak and an estuary infills slowly, an insufficient volume of precursor material may impede the development of chlorite during diagenesis.

Another important aspect is the role of sequence stratigraphy and relative sea level with respect to depositional environment and eodiagenetic development of clay minerals. Relative sea level, along with sediment supply and climate, controls the type, abundance and distribution of clay minerals during eodiagenesis (Ketzer et al., 2003). Chlorite precursor phases berthierine, odinite and smectite form primarily in transgressive systems tract and early high stand systems tract deltaic and estuarine sandstones (Morad et al., 2010). This broadly agrees with observations outlined above, with coastal depositional settings being the predominant location for chlorite-coated quartz grains; however the low incidence of estuarine setting within this dataset may be a result of issues already noted.

### **2.6.2 Depositional age as a control**

There is a preponderance of North American and Northwest European examples in the dataset. The age relationships of chlorite-coated

sandstones are considered here as it may provide an insight into potential biases in the dataset. Figure 2.2B suggests that chlorite is more prevalent in the Cretaceous, a period where more shallow coastal settings were active due to continental fragmentation during the final break-up of Pangaea and high global sea-levels during a greenhouse period (Holdsworth et al., 2000). The Cretaceous was also a period high volcanic activity (Holdsworth et al., 2000) which therefore may have provided more ferro-magnesian-rich lithic and volcanic fragments to sedimentary systems. This appears to be supported, to an extent, by the wide latitudinal range of the examples during this period. But accounting for the length of each period, it can be seen that there is a trend of increasing number of examples per unit time (Fig. 2.5). Although a gross simplification of the tectonic history of many basin histories around the world, a simple assumption, following the law of superposition, is that a greater volume of younger strata is more likely to be shallower than older units, and therefore sandstones with chlorite-coated quartz grains are more likely to be encountered in younger strata than in older. This suggests a possible bias, due to exploration trends.

### **2.6.3 Paleolatitude**

The latitude of formation is assumed to be important in the formation of chlorite-coats. For example berthierine has principally been reported at tropical latitudes (Hornibrook and Longstaffe, 1996; Odin,

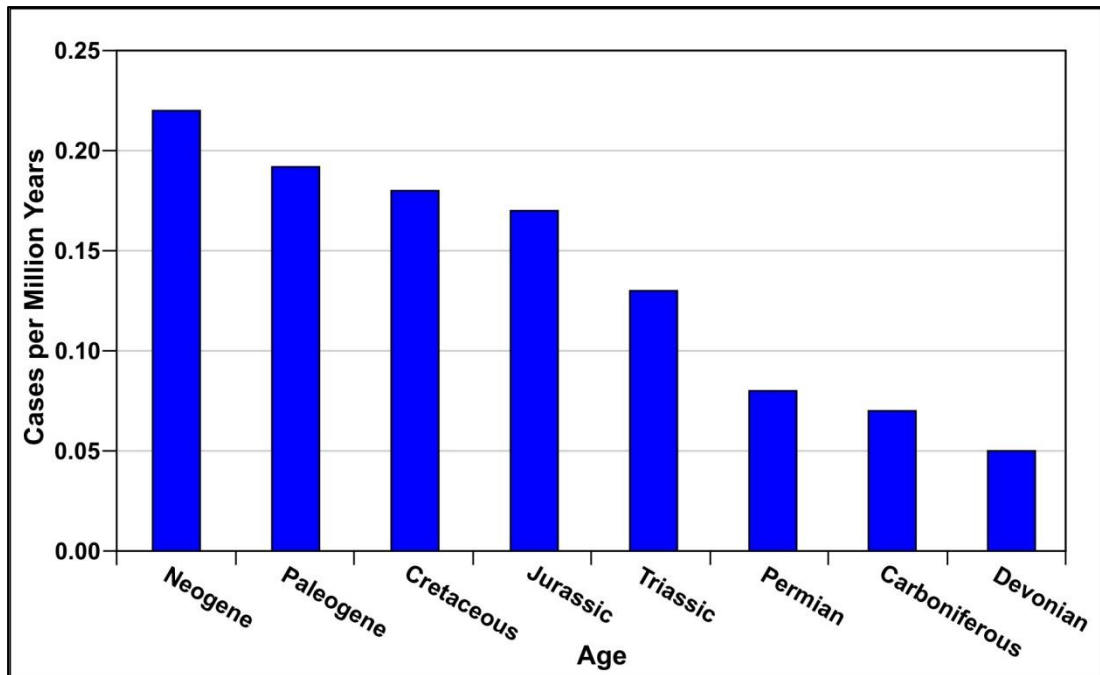


**Figure 2.5 - Chlorite examples per million years for each period. Values on the y-axis are the number of chlorite-coated examples in petroleum reservoirs occurring per million years in each period. Higher values indicate a higher example density for a given period**

1988), and there is a possible link between magnesium-rich chlorite and desert aeolian or playa lake environments (Ajdukiewicz et al., 2010; Hillier et al., 1996), which normally form in restricted latitude ranges. However, an assessment of the latitude at the time of deposition for all chlorite examples has not been made previously.

Figure 2.3 shows that all examples occur between 60°N and 60°S, suggesting that processes at higher latitudes are not conducive to the formation of chlorite-coats. Potential biases within the dataset are minimal as continents have existed at or near the South Pole for much of the Phanerozoic (Habicht, 1979). One of the key processes that occurs between latitudes 60°N and 60°S, but that is retarded at higher latitudes, is chemical weathering (Bland and Rolls, 1998; Chamley, 1989). Weathering involving aluminosilicates creates various

secondary minerals, including clay minerals. Although conditions for weathering reactions are more evident at latitudes nearer the equator (good drainage and high temperatures), it appears that sufficient weathering occurs to provide both ions and detrital grains to sites of deposition at both tropical and temperate latitudes. In areas closer to the poles, free water budgets and temperatures are low and chemical weathering is suppressed.

The second relationship evident from Figure 2.3 is that latitudes of chlorite-occurrence become increasingly northern from the Devonian to the Jurassic, after which most examples occur between around 10°N and 50°N. This reflects the northern drift of most continents, with more recent Cretaceous and Paleogene southern hemisphere outliers occurring on continents with a long residence time in this location (Australian and Indian plates). This further reinforces both role of tectonics and weathering in the generation of material suitable to the formation of chlorite, as there appears to be a strong tie to the continents and lower latitudes where chemical weathering can occur.

As weathering appears to be integral to supplying material for the formation of chlorite-coats, it is worth noting that there are no examples of chlorite-coated sandstone reservoirs prior to the Devonian period. It was during the Devonian that plants became widespread with increasingly deeper root systems, resulting in an

increase in biologically-mediated terrestrial weathering and soil formation (Raven and Edwards, 2001). Although chlorite occurrence is noted in sandstones older than the Devonian (Dapples, 1967; Duffin et al., 1989; Girard and Barnes, 1995; Mens and Pirrus, 1986; Pittman et al., 1997), it would appear from this dataset that conditions most suitable for chlorite-coated sandstone reservoirs are most suitable from the Devonian onwards. A comparison of the stratigraphic distribution of oolitic ironstones (Fig. 1 in Van Houten & Bhattacharyya, 1982) which predominately occur during "greenhouse" conditions, to the occurrence of chlorite examples (figure 2.3), further underlines the multi-genetic modes of chlorite formation. If chlorite-coated grains resulted only from the diagenesis of iron oxides during periods of high weathering intensity, it might be expected that chlorite-coated grains would only be evident from the Ordovician to the Devonian and the Jurassic to the Paleogene, which is not the case (Fig. 2.3).

#### **2.6.4 Reservoir quality**

A detailed study of the literature shows that grain-coating chlorite does not always have a positive effect on the two key aspects of reservoir quality; porosity and permeability. Overall the effect of chlorite on reservoir quality is either positive or mixed (positive and negative), with only 13% of chlorite-coats having either a negative or no effect on porosity and permeability preservation. In mixed examples authigenic chlorite results in a pore-filling as well as a pore-

lining morphology, while the positive designation implies that these sandstones have an optimum amount of clay minerals relative to pore space and grain size. Pittman et al. (1992) suggested that the volume of clay needed to generate pore-lining clay minerals rather than pore-filling clay mineral was between 4% and 13% depending on the sandstone type.

### **2.6.5 Elemental composition**

Published chemical compositions show that chlorite-coated sandstones can have a range of iron-magnesium ratios (fig. 2.4A), varying between 0.25 and 0.85. Coastal examples plot over this full range, but the majority appear to be iron-rich plotting around 0.7 and 0.8. Although there are a couple of outliers (Billault, 2003; Pay et al., 2003), the terrestrial and marine examples plot in the range of 0.25 to 0.55, possibly implying a common factor in formation.

Figure 2.4A illustrates average compositions for each example to avoid skewing the dataset with multiple sets of compositional data from individual analyses. Figure 2.4A shows two broad areas of iron-rich and mixed (iron- and magnesium-rich) chlorites. The iron-rich chlorite zone, with an iron-magnesium ratio of 0.65-0.80 and a silica tetrahedral occupancy of 2.6-2.9, consists primarily of coastal examples. While the mixed zone, with an iron-magnesium ratio of 0.35-0.60 and a slightly higher silica tetrahedral occupancy of 2.9-3.3, consists of terrestrial and marine examples. This relationship may

reflect the importance of iron within fluvial and coastal settings. The predominance of iron-rich chlorite in coastal examples could reflect the flocculation and deposition of iron supplied by river systems on entering seawater; which may then result in clay minerals. This relationship appears to be supported by the majority of iron-rich chlorite coastal examples (Fig. 2.4), with all but one (Goru Formation), reported to have formed through a clay mineral precursor phase(s) rather than from the dissolution of detrital grains (Berger et al., 2009).

#### **2.6.6 Likely and unlikely chlorite-coat sandstone scenarios**

This is the first time that a large dataset reviewing chlorite-coated examples from a variety of locations, reservoirs and depositional settings has been compiled. Using the trends and controls identified in the previous discussion, situations where chlorite-coatings are likely and unlikely to form are outlined in Figure 2.6 and described below. It is hoped that the scenarios may provide insights into both the formation of chlorite and facilitate predictive and testable models for the presence or absence of chlorite in sedimentary basins.

The provenance of sediment is often crucial for the formation of sandstones with good reservoir quality (Primmer et al., 1997). Material derived from the hinterland (the provenance) is crucial for supplying all the key ingredients for chlorite precursor minerals. In the likely scenario for the formation of chlorite (fig 2.6), an ideal hinterland might be composed primarily of granite with a considerable volume

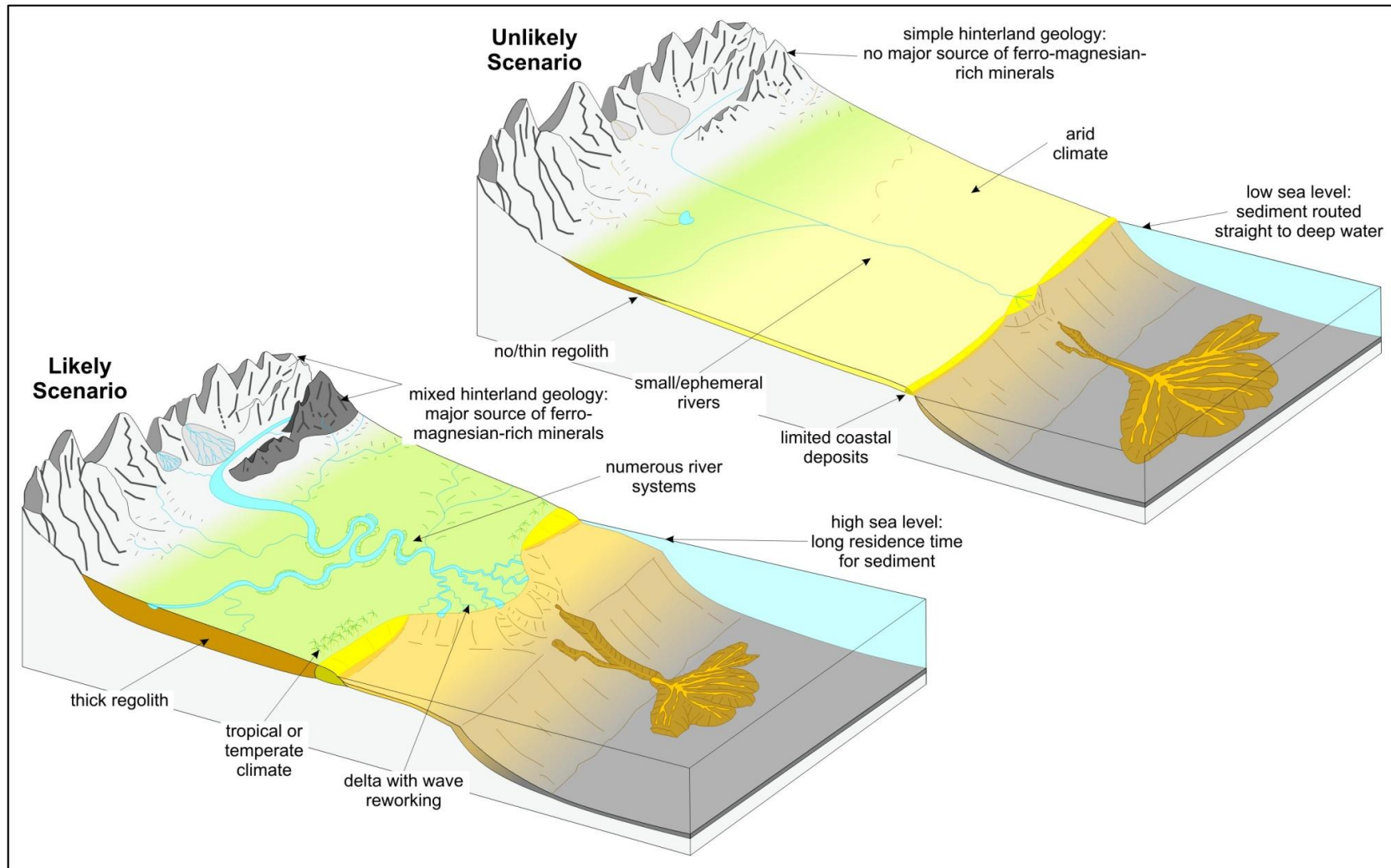


Figure 2.6 - Schematic representation outlining the likely and unlikely scenarios for the development of chlorite-coated grains in sandstone reservoirs.

of basalt. This rock suite would provide a mix of coarse-grained quartzo-feldspathic sediment potentially creating coarse-grained reservoir sandstones, but also ferro-magnesian-rich minerals which when deposited as clay minerals, flocculated iron and/or detrital grains may develop into chlorite during subsequent diagenesis. Whilst in the unlikely scenario, the hinterland geology would be simple with no major source of ferro-magnesian-rich minerals, which although it may provide ideal sediment to form reservoir sandstones, is unlikely to lead to the development of chlorite-coats upon sand grains.

The type of regolith is partly a function of the hinterland geology of a drainage basin. At temperate and tropical latitudes elevated weathering rates produce thick soil profiles which may then supply sediment to river systems (Bland and Rolls, 1998; Chamley, 1989). In the likely scenario in Figure 2.6, a thick regolith in a tropical or temperate climate has enabled weathering processes operating in soils to generate clay minerals, such as kaolinite and smectite, plus iron oxides and hydroxides which may form chlorite during diagenesis. In the unlikely scenario in Figure 2.6, a thin and areally-limited regolith formed due to an arid climate that suppresses the breakdown of ferro-magnesian-rich minerals and limits the supply of clay minerals and iron oxides and hydroxides.

The dominance of deltaic environments and the high proportion of fluvial examples already noted appear to suggest that proximity to

permanent river systems is integral to chlorite formation. Numerous rivers in the likely scenario provide a transport path for material generated upstream by the regolith. Although chlorite precursor material supplied by the river could be deposited in a diverse range of fluvial related environments, the river terminus at a coastal delta provides the most favourable environment for chlorite precursor formation.

Initial reservoir quality would be improved during periods of relatively high sea level as sediment would be subject to reworking. Furthermore, grain-coating chlorite on quartz grains is noted to be more prevalent in deltaic deposits during transgressive and early highstand systems tracts (Morad et al., 2010). In the unlikely scenario, rivers are small and ephemeral supplying a low volume of sediment to the coast, sea level is low so that most sediment passes directly out to deepwater marine environments. Coastal depositional environments remain narrow and largely do not become reworked.

## **2.7 Conclusions**

1. Chlorite-coats have formed in a range of depositional environments but are most commonly found in coastal settings and particularly in deltaic environments. Fluvial environments are the second most common setting for chlorite-coats. The role of rivers is crucial to the development of chlorite as these

arteries provide the supply of precursor material that proceeds to form chlorite during mesodiagenesis.

2. Latitude at the time of deposition indicates a wider range (60°N and 60°S) than predicted for some precursor minerals, and indicates that wet temperate and tropical climates are important in generating clay minerals, through the process of chemical weathering, which is greatly reduced at higher latitudes.
3. Although Cretaceous sandstones are the most common hosts for chlorite-coats, accounting for the length of this period, the number of examples decreases back through time to the Devonian. This may be a consequence of less petroleum exploration being undertaken in older rocks. While it appears that conditions suitable to the formation of chlorite-coats are most prevalent from the Devonian onwards, which may be related to the development of land plants, and an increase in biologically-mediated terrestrial weathering and soil formation.
4. Chlorite-coats can have a variable effect on reservoir quality, but is normally positive.
5. Elemental compositions of coastal and marine composition show a wide range of similar  $Fe/(Mg+Fe)$  values (0.25-0.82). Coastal examples are overwhelmingly iron-rich, which could be a result of the flocculation of riverine iron which is then subsequently incorporated in clay minerals.

6. Hinterland geology, soil development and river systems are all key parts in the generation and supply of detrital grains, precursor clay minerals and iron which, given favourable depositional and diagenetic circumstances, can go on to develop in to chlorite-coated sandstones.

### **3. Clay minerals in a cold climate: Origin, mineralogy and distribution of clay minerals in the Leirárvogur Estuary, SW Iceland**

#### **3.1 Abstract**

Detailed analysis of clay minerals and non-clay mineral concentrations within the fine fraction of estuarine sediments in the Leirárvogur Estuary, southwest Iceland, was determined utilising X-ray diffraction (XRD) and infrared spectroscopy. This enabled the origin, development and distribution of the clay minerals within a high latitude estuarine environment to be constrained.

The dominant rock-type in the drainage basin has a strong control on the clay minerals produced, with dioctahedral chlorite, inter-layered vermiculite and nontronitic smectite all developed from a basalt parent material. The suite of clay minerals vary in concentration by environment, but are generally present within all estuarine, riverbank soil and glacial sediments within the basin. Data presented indicate that inter-layer spacing in smectite and inter-layer vermiculite are being filled or partially filled to produce inter-layer vermiculite or chlorite in sediment ingested and excreted by arenicola worms. This may suggest that chemical alteration of clay minerals within the estuary may be occurring through this process. Distribution maps and

mineral concentration cross-plots indicate that smectite is the most dominant clay mineral and is found in highest concentration in areas of lowest energy around the margin of the estuary and close to small stream inputs. Conversely, inter-layer vermiculite and chlorite tend to be concentrated in areas of higher energy closer to marine-dominated influence. Differential concentration of clay minerals in estuary sediments may be related to the hydrodynamic properties of the clay minerals. In the following order: inter-layer vermiculite, chlorite and then smectite maybe more easily suspended.

### **3.2 Introduction:**

Clay minerals found in soils and sedimentary environments originate via three processes (Millot, 1964; Wilson, 1999): 1) detrital inheritance, where clay minerals formed in pre-existing rocks are subsequently weathered and eroded, for example detrital chlorite weathering from a schist; 2) transformation, whereby the silicate structure of the mineral is maintained, but there are extensive changes within the inter-layer space of the structure, for example mica weathering to vermiculite due to the loss of  $K^+$ ; and 3) neof ormation where the clay mineral develops from solution, gel or amorphous material, for example the development of kaolinite in tropical settings. In each of these processes the parent materials and local environmental (physical, geochemical and biological) conditions play a major role in controlling the types and proportions of clay minerals generated.

Although the underlying processes of clay mineral formation outlined above are broadly known and accepted, the relationship between the formation and deposition of clay mineral, and the locations and processes whereby they develop is still not well understood despite being the subject of a body of literature (see reviews in: Chamley, 1989; Weaver, 1989; Wilson, 1999). Studies have shown that sediment source lithologies and soils within river catchments, as well as offshore sediments moved onshore, play a key role in controlling the range and distribution of clay minerals in coastal settings (Taggart and Kaiser, 1960; Hirst, 1962; Schubel, 1972; Feuillet and Fleischer, 1980; Allen, 1991; Pandarinath and Narayana, 1992; Sarma et al., 1993; Patchineelam and de Figueiredo, 2000; Belzunce-Segarra et al., 2002; Sionneau et al., 2008; Bernárdez et al., 2012).

### **3.2.1 Estuarine dynamics**

The nature of the physico-chemical interaction between river and marine water bodies can have an important impact on where clay minerals are deposited.

#### **3.2.1.1 Turbidity maximum**

Within estuaries, the turbidity maximum is the point at which marine and fresh waters meet forming a region of locally-elevated suspended matter content (Postma 1967; Geyer 1993); its position within an estuary can vary seasonally with flood and storm events (Schubel, 1972; Sarma et al., 1993) as well as with the tidal cycle (Allen et al.,

1980). Deposition from suspension can occur in the turbidity maximum zone during the slackwater phases of the tidal cycle, with sediment being eroded and re-suspended from the sediment surface during the rising and falling stages (e.g. Meade, 1972; Park, 1999). Depending on the nature of the estuary this may result in preferential deposition of suspended matter in areas up to the limit of the tide, and around the margins of the estuary where flow velocities are lowest. Sediment deposited in sub-aqueous estuarine channels at low tide may be more likely to become re-suspended during the rising tide (Allen, 2000). In a field study from the Loire Estuary (Gallenne, 1974), montmorillonite was reported to be concentrated relative to illite in suspended material moving up and down the estuary with the tide. Montmorillonite was interpreted to remain suspended while other clay minerals were deposited, with montmorillonite only falling from suspension during slackwater phases. This supports the contention of Whitehouse et al. (1960) and Gibbs (1983) whereby montmorillonite (the dioctahedral variety of smectite) remains suspended due to a much lower settling velocity.

In the James River Estuary (Feuillet and Fleischer, 1980; Chamley, 1989), concentrations of two suites of clay minerals, marine- and river-supplied, show distinct relative changes in concentration. River supplied clay minerals were reported as kaolinite, illite and vermiculite, while marine clay minerals were illite, chlorite and montmorillonite. An

increase in the suite of marine-sourced clay minerals occurs from the tidal limit (turbidity maximum) down to the marine end of the estuary, with a concurrent decrease in the river-supplied suite of clay minerals over the same section. The reverse relationship occurs from the tidal limit, up the estuary. This indicates that clay minerals in the James River Estuary are equally diluted, with internal mixing at the interface between river and marine waters within the estuary being the main control on concentrations.

#### 3.2.1.2 Saline waters

In coastal environments, ions, clay minerals and biogenic matter flocculate to form aggregates (Eckert and Sholkovitz, 1976; Sholkovitz et al., 1978; Eisma, 1986). Marine water has a higher salinity than that of particle-rich river water. In rivers, suspended particles are kept apart by a positively charged layer of ions surrounding the particle. On mixing with sea water, this charged layer is compressed enabling particle attraction to occur (Gibbs, 1983). Aggregation of material develops from particle collision through Brownian motion processes, differential settling velocity of particles or turbulence (Weaver, 1989). In estuaries, this saline front is normally located at the front associated with the turbidity maximum.

Experimental work on static differential flocculation using a large number of clay mineral mixtures from modern sedimentary environments (Whitehouse et al., 1960) indicated that, with increasing

salinity, illite and vermiculite, then kaolinite and chlorite, and lastly montmorillonite (dioctahedral smectite) settle out of a static water column. Two further studies using standards of illite, kaolinite and montmorillonite (but note a different montmorillonite standard used in each study) simulated flocculation in a turbulent coastal setting and reported contrasting orders of deposition. Edzwald and O'Mella, (1975) found first montmorillonite, then kaolinite and illite were deposited, whereas (Gibbs, 1983) found the reverse: illite then kaolinite and lastly montmorillonite. These conflicting findings are probably due to different experimental set-ups, and further hindered by the difficulty in recreating complex and dynamic environments in the laboratory.

### **3.2.2 Geochemical development**

While the majority of the literature on clay minerals in estuaries has focused on the depositional controls, a few studies have also looked at the geochemical development of clay minerals within coastal settings and their formation in adjacent marine shelf waters.

#### 3.2.2.1 Geochemical alteration

Large scale chemical transformation of clay minerals can occur in coastal environments, with cation exchange within clay mineral inter-layer zones normally resulting in the adsorption of Na, K and Mg at the expense of Ca. Typically, it has been suggested that there is limited mineral structural change of the T-O-T layer and that cation incorporation is generally considered to be reversible (Russell, 1970;

Chamley, 1989). A study of 'estuarine' Mississippi Delta sediments reported the rapid uptake of  $K^+$  by smectite in brackish waters (Hover et al., 2002) and a similar loss of  $K^+$  is noted in marine sediments from Rio Ameca, Mexico (Russell, 1970). Further studies on core sediments, show that plagioclase feldspar, pyroxene, olivine, and volcanic ash, in marine slope sediments north of Sakhalin Island, become progressively transformed with sediment depth (down to 25m) into smectite through chemical alteration (Wallmann et al., 2008). Neof ormation of clay minerals from biogenic silica also commonly occurs on marine shelves (Michalopoulos and Aller, 2004; Presti and Michalopoulos, 2008) and this has been repeated experimentally (Michalopoulos and Aller, 1995; Michalopoulos et al., 2000).

#### 3.2.2.2 Biological alteration

One possibly important factor in understanding the genesis, alteration and distribution of clay minerals in modern estuarine environments is the role of bioturbation in the production of clay minerals. Experimental studies have shown that the conditions within annelid worm guts, such as *Arenicola marina*, can result in the generation of clay minerals such as kaolinite, illite and berthierine from unweathered mafic rock (McIlroy et al., 2003; Needham et al., 2004; Needham et al., 2005; Worden et al., 2006; Needham et al., 2006). The rate of clay mineral formation in biologically-digested sands can be 2-3 orders of magnitude higher than that of un-ingested sediment

(Needham et al., 2006); similarly the large numbers of these organisms in intertidal environments can lead to the rapid turnover of sediment.

Within estuaries, clay mineral distribution patterns and the controls on them are still relatively poorly understood and may vary depending on local factors such as the size and shape of the estuary, water body mixing regime, sediment source regions, seasonal effects and large storm and flood events. Issues with the recreation of marine and partially marine environmental conditions also appear to limit the utilisation of experimental studies. The opportunity to study the types of clay minerals and their spatial distribution in a small estuary with simple hinterland mineralogy may enable a better understanding of the interplay of controls on both formation processes and dispersal patterns.

The Leirárvogur Estuary in southwest Iceland (fig. 3.1A) was chosen because it is supplied with the products of weathering from a predominately basalt-rich parent material (fig. 3.1B; After: Jóhannesson and Sæmundsson, 1999). The aim of this paper, therefore, is to distinguish the types and distribution of clay minerals present in the Leirárvogur Estuary and to understand the underlying controls on their distribution:

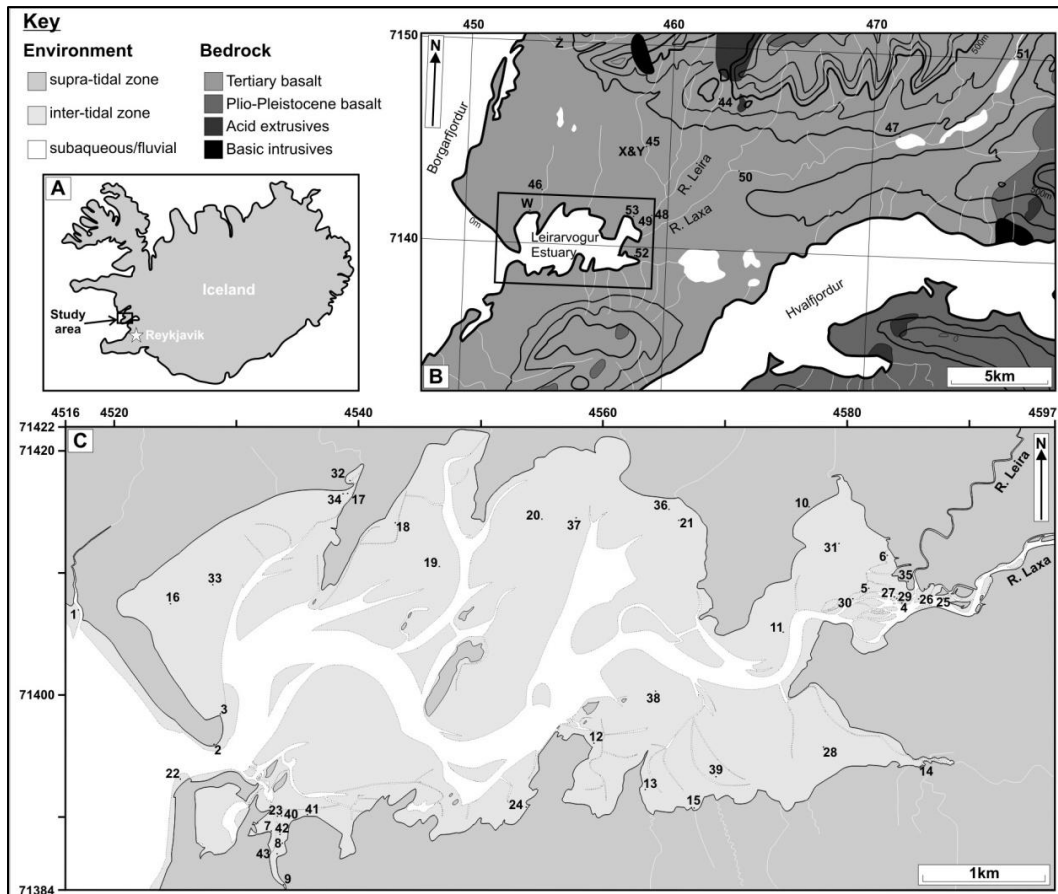


**Figure 3.1 – Iceland location maps. (A) Study area. (B) Borgarfjörður local geology map with lithology, glacial and hinterland sediment sample locations (After Jóhannesson and Sæmundsson, 1999). (C) Leirárvogur Estuary with estuarine sample locations.**

1. What clay minerals are present and where did they form?
2. What is the surface sediment distribution of the clay minerals?
3. What are the controls on the types of clay minerals and their distribution pattern?
4. Does bioturbation of sediment have any effect on clay mineral distribution in a modern setting?

### 3.3 Study area

#### 3.3.1 Bedrock geology

Tectonically, Iceland (fig. 3.1A) lies at the junction between the Reykjanes and Kolbeinsey Ridges (Sigmundsson, 2006) forming two

segments of the Mid-Atlantic Ridge (Thordarson and Hoskuldsson, 2002). Interaction between the ridge system and an underlying mantle plume (Sigmundsson, 2006), plus the isostatic effects of recent glaciations, have created a highly geodynamic setting. Located on the Mid-Atlantic Ridge, the island is dominated by tholeiitic olivine basalt, composed of plagioclase feldspar, pyroxene and olivine phenocrysts, plus interstitial glass (Mattsson and Oskarsson, 2005). Rhyolitic volcanic rocks are relatively rare (~10%) and tend to be glassy or very fine-grained. Where phenocrysts do occur they tend to be plagioclase feldspar (Jónasson, 2007).

The geology of the Leirárvogur Estuary catchment (Fig. 3.1B) is principally composed of basic and intermediate extrusive rocks (Jóhannesson and Sæmundsson, 1999). These are mainly Upper Tertiary in age (>3.1 m.y.). Only the upper eastern reaches of one of the two main input rivers drain rocks of Pliocene-Pleistocene age (0.7-3.1 m.y.). Rare acidic extrusive rocks, closely associated with volcanoes (Piper, 1971), are composed of rhyolitic lavas and tuffs, and these occur in the northern reaches of the study area. The rocks in the area dip 5-8° to the southeast and form the southern limb of the Borgarfjörður anticline, which developed due to loading as repeated eruptions generated a dense lava pile (Thordarson and Hoskuldsson, 2002).

### **3.3.2 Glacial & sea level context**

Le Breton et al. (2010) utilised palaeo-shoreline mapping to propose a synthesis of the vertical motions of Iceland driven by post-glacial rebound following Weichselian glaciations (after 18 ka). The main conclusion was that since the end of the Last Glacial Maximum the coastline of Iceland has been in a net regressive state (relative sea-level fall). Locally, this contention is supported by marine notches and exposed beach terraces to the north of the Leirárvogur Estuary marking a former higher sea level (Ingólfsson, 1988). However, regional sea level estimates (Le Breton et al., 2010), extensive erosion of cliffs to the north of the estuary and submerged peats dated at 6.3-6.0ka (Ingólfsson, 1988), indicate that regional relative sea level has been much lower than it is at present. Therefore, unlike many mid-latitude marine marginal settings, the Leirárvogur Estuary is presently undergoing an transgressive period after a long-term regression.

### **3.3.3 Catchment**

The Leirárvogur Estuary (fig. 3.1C) is fed by two rivers: the Leirá and Laxá, both of which are direct run-off river systems with no feed from inland glaciers (fig 3.1B). The larger of the two is the Laxá River with a drainage length of approximately 25 km. The Laxá River drains a series of upland lakes (fig. 3.2A). The Leirá River drains mountains approximately 10 km north of the estuary. The upper reaches of the both rivers drain exposed bedrock (fig. 3.2B) and alluvial sediments

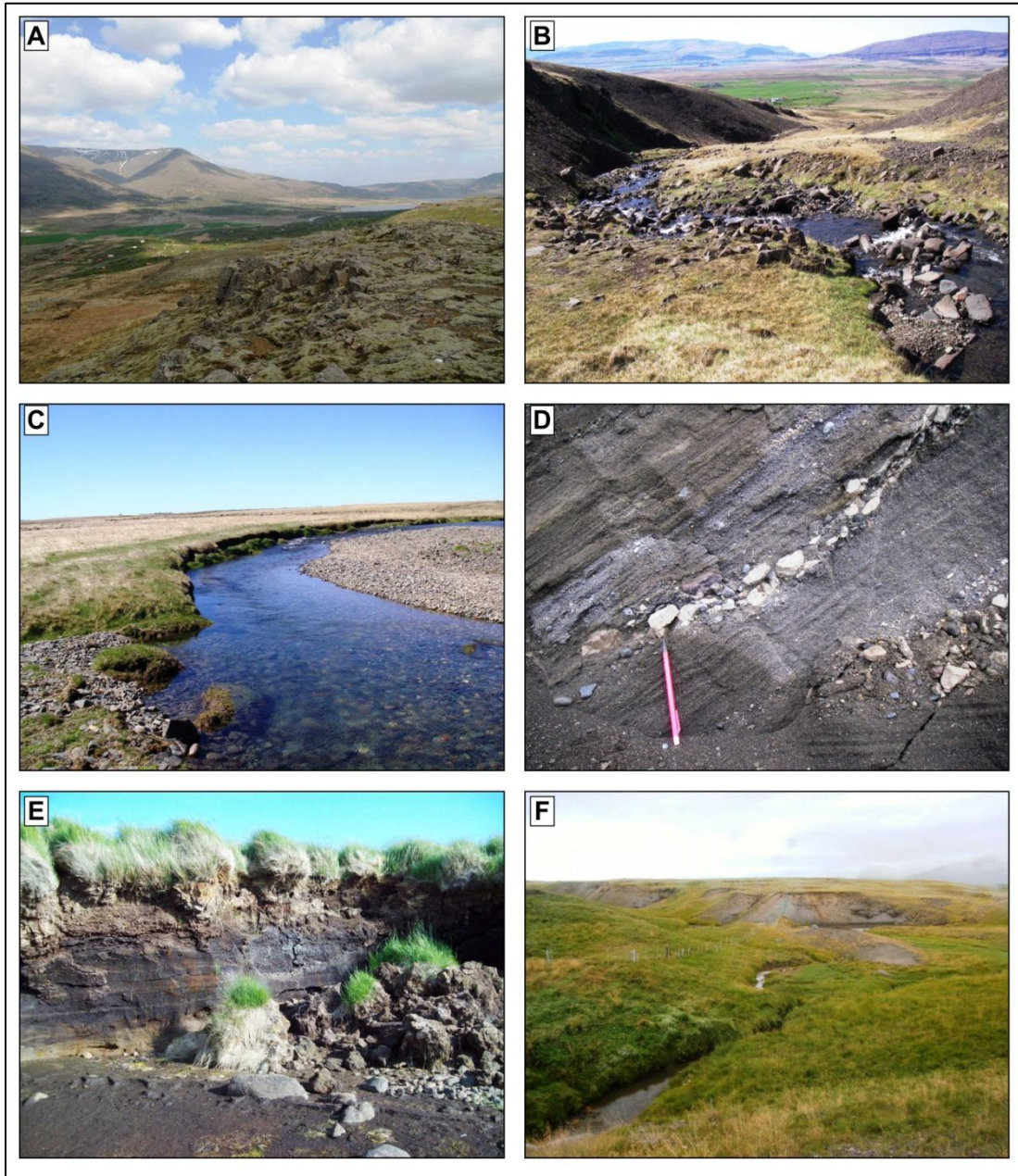
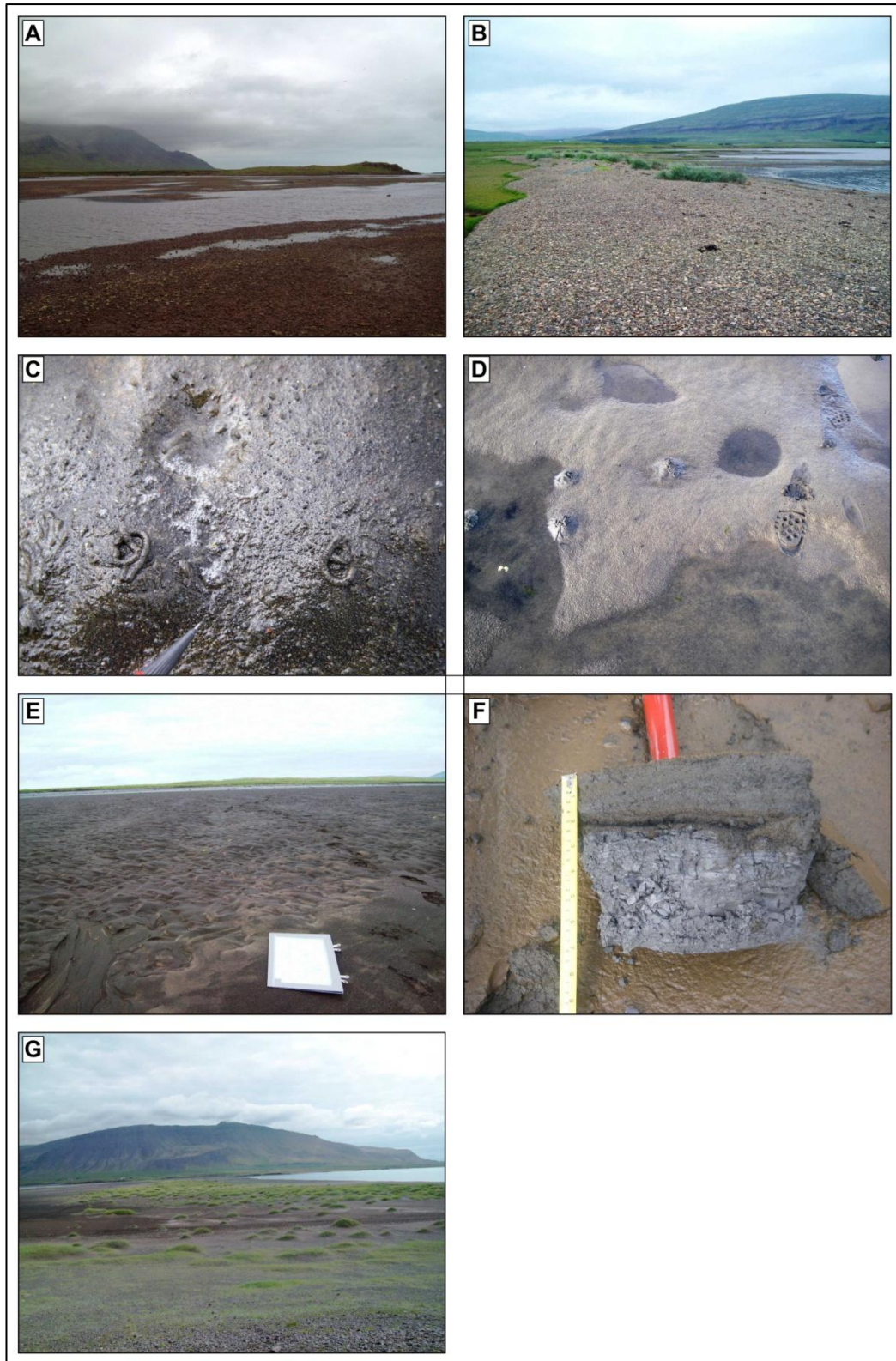


Figure 3.2 - Photographs of hinterland environments discussed in text. (A) Upland lake on the Laxá river. (B) Upland Leirá river. (C) Downstream Leirá river. (D) Glacial sediments. (E) Peat deposits on the edge of estuary. (F) Small incised stream on north side of estuary.

(fig. 3.2C), in lowland areas they drain exposed glacial sediments (fig. 3.2D), peats (fig. 3.2E) and farmland. A study of basalt weathering utilising elemental river water analyses in south-western Iceland (Gíslason et al., 1996) collected discharge data on the larger Laxá river drainage system. The measured catchment area of the Laxá River is 142 km<sup>2</sup>, and has an average discharge rate of 7.8 m<sup>3</sup>/s (measured period: July 1973-December 1974). Total dissolved solids (TDS) are primarily composed of inorganic species with small amounts of organic matter (De Zuane, 1997). In the Laxá River, this TDS value is 58 mg/l, which is slightly below average for all rivers in southwest Iceland (74 mg/l). Smaller river systems also drain into the estuary over peat land and farmland on both the northern and southern sides of the estuary (fig. 3.2F).

### **3.3.4 Estuary geomorphology**

**The** Leirárvogur Estuary is **~7km long, ~4km wide and has 4.5m maximum tidal range**. At low tide the confluence of the Leirá and Laxá Rivers at the eastern end of the estuary is exposed, forming a poorly-sorted, gravel-rich bayhead delta with a braided network of shallow channels (fig. 3.3A). The area to the north of the bayhead delta is covered by saltmarsh, with a dendritic network of tidal creeks. On top of this, a gravel-rich washover deposit has developed (fig. 3.3B) with sediment possibly sourced from the bayhead delta. Downstream of the bayhead delta area, a broad sinuous tidal



**Figure 3.3 - Photographs of estuary environments discussed in text. (A) Gravelly bayhead delta. (B) Large gravel washover onto saltmarsh. (C & D) Intertidal sediments showing bioturbation. (E) Large expanse of intertidal sands. (F) Glacial sediment, occurring just below the surface (6.5cm) of the intertidal flat. (G) Large frontal spit on the north-side of the estuary.**

channel of varying width extends out towards the marine end of the estuary. Several NNE-SSW bedrock islands within the estuary reflect the structural grain of a local dyke swarm. The central inter-tidal portion of the estuary is composed of moderately- to poorly-sorted medium sands, which exhibit variable intensities of bioturbation (fig 3.3C&D). The margins of the inter-tidal area are slightly finer-grained (medium to fine sand) than those in more open areas (fig. 3.3E). Beneath the surface of the intertidal flat, particularly at the margins of the estuary and in the eastern portions, glacial sediments (fig. 3.3F) are found at shallow depths (<5cm). The marine western portion of the estuary is partially fronted by a sandy frontal spit attached to the north (fig. 3.3G); on the south side is a smaller spit, underlain by bedrock.

### **3.3.5 Clay mineral formation in Icelandic rocks & soils**

Soils in Iceland are of volcanic origin and the majority are andosols, reportedly dominated by glass with smaller amounts of the amorphous minerals allophone and ferrihydrite (Wada et al., 1992; Arnalds, 2004; Sigfusson et al., 2006; Sigfusson et al., 2008). Secondary minerals are also produced from the surface weathering of rocks, and these are typically found in joints and cracks. Douglas (1987) identified an undefined smectite plus other poorly crystalline, undifferentiated and unidentified clay minerals associated with manganese-rich coatings on the surface of weathered basalts.

### **3.3.6 Hydrothermal clay mineral alteration**

In a heavily glaciated terrain it is worth considering the types of clay minerals developed through hydrothermal and low grade metamorphic processes on basalt, which may have been exposed through deep incision and erosion during the most recent glaciation (White, 1972; White, 1988). Typically, low temperature metamorphism and hydrothermal alteration of basalt results in the replacement of glass, olivine, pyroxene, and the partial replacement of plagioclase feldspar (Kristmannsdottir, 1979). The sequence of alteration of parent material to form clay minerals progresses with increasing temperature and depth, and is typically coincident with a range of zeolite minerals. Studies from Icelandic hydrothermal boreholes (Kristmannsdottir, 1979; Schiffman and Friedleifsson, 1991; Sveinbjörnsdóttir, 1992) reported smectite developing at relatively low temperatures (<200°C) primarily through weathering; with progressive heating at depth, the smectite becomes increasingly more iron-rich. Between 200°C and 240°C an inter-layer smectite-chlorite develops, with Fe-rich chlorite becoming dominant above 240°C temperature (Kristmannsdottir, 1979). Highly variable geothermal water compositions and temperature are reported to result in a high degree of variability in the chemistry and mineralogy of the clay minerals developed at depth (Sveinbjörnsdóttir, 1992). Smectite and chlorite clay minerals are evident in surface outcrops in the vicinity of the Leirárvogur catchment. A study of Pliocene-Pleistocene rock cropping out in the

Hvalfjörður area (Weisenberger and Selbeckk, 2009) described the development of chlorite/smectite in basalt pores becoming progressively more chlorite-rich with depth and temperature.

### **3.3.7 River water geochemistry**

Studies of Icelandic river waters provide insight into the development of secondary minerals in Iceland. Dissolved solids in water samples of the Laxá river in Kjós (a different river to this study), reported a link between weathering state, clay mineral formation and major element concentrations in river and ground waters (Stefánsson and Gíslason, 2001). Fe and Al were reported to have very low mobilities compared to Na, because of their incorporation into amorphous minerals such as ferric hydroxides like goethite and lepidocrocite, and hydrous aluminosilicates like allophone and imogolite found in the catchment soils. With increasing alteration of the basalt source rock, smectite begins to develop, incorporating Ca, Fe, Mg, Si, and Al, limiting mobility of these elements in the river and ground waters. A similar study on a number of major rivers in Iceland (Louvati et al., 2008) found a similar relationship with TDS concentrations highest in spring-fed rivers draining relatively younger rocks; lowest concentrations were in direct run-off rivers from relatively older rocks. Gíslason et al. (1996) used river water element data to link the total denudation rate from a range of different river catchments in southwest Iceland to the setting and age of the rocks within the catchment. They found that the total

denudation rate is higher in younger catchments with basalts erupted beneath glaciers. At the present day, these rock types tend to have higher basaltic glass content than older areas erupted in non-glacial settings, where more reactive phases may already have been lost. In relatively younger catchments, Na and K are more mobile than Ca, Mg, and Si due to the relative stability of plagioclase and pyroxene compared to glass, furthermore mobile elements become readily incorporated into clay minerals and zeolites. In relatively older areas, Sr, Ca, Mg and Si are relatively more mobile than in relatively younger areas as there is less unaltered glass available. Plagioclase may also have begun to dissolve resulting in the instability of first stage alteration minerals containing Ca, Mg and Si.

### **3.3.8 Offshore clay mineralogy**

Offshore investigations of clay mineral contents in modern day sediments and glacially-derived sediments indicate the presence of a suite of clay minerals derived from onshore Iceland and submarine ridge processes, mixed with inputs from more exotic North American terranes. Clay minerals in oceanic sediments to the north and west of Iceland are dominated by smectite with minor amounts of illite, chlorite and kaolinite (Lackschewitz and Wallrabe-Adams, 1991; Andrews and Eberl, 2007). A similar suite of minerals was found in sediment cores on the mid-Atlantic ridge between Iceland and Greenland (Fagel et al., 1996; Gehrke et al., 1996; Fagel et al., 2001).

Gehrke et al. (1996) suggested that poorly crystalline smectite has been derived from Icelandic ice rafting, while increases in kaolinite, chlorite and illite and more crystalline smectite concentrations in cores correspond with Heinrich ice rafting events from the North American Laurentide ice sheet. Although this interpretation appears credible, chlorite may also be derived from Icelandic ice rafted sediments.

### **3.4 Materials and methods**

Two field seasons in July 2009 and May 2010 were undertaken to map the estuary and collect surface sediment samples. Sample locations were marked using a standard GPS (UTM WGS84). Fifty-one surface sediment samples were collected from locations within the Leirárvogur Estuary and the surrounding drainage basin. Sample sites were selected to provide a wide geographic and environmental spread. Twelve worm cast sediment samples were also collected from within the estuary in close proximity to surface sample locations to enable comparison between worm cast and surface mineralogy.

Bioturbation intensity was measured in areas around selected sample sites by counting the number of worm traces in a one metre square quadrat. Multiple counts were undertaken to give an average value for bioturbation intensity.

A further three lithology and four glacial diamicton samples, were also collected. Sediment sample locations are shown in figure 3.1,

Map Location	Depositional setting	Environment description	Sediment description
1	Marine	Shoreface	Moderately sorted medium sand
2	Estuary/Marine	Shoreface - mouth of estuary	Poorly sorted gravel
3	Estuary	Intertidal flat behind northern spit	Moderately sorted coarse sand
4	Estuary/River	Gravel bar on bayhead delta intertidal zone	Very poorly sorted gravel
5	Estuary/River	Gravel bar on bayhead delta intertidal zone	Poorly sorted gravel
6	Estuary/River	Gravel bar on bayhead delta intertidal zone	Very poorly sorted silt
7	Estuary	Intertidal flat proximal to intertidal creek	Moderately sorted medium sand
8	Estuary	Intertidal flat proximal to intertidal creek	Poorly sorted medium sand
9	Estuary	Intertidal flat proximal to intertidal creek	Poorly sorted Fine sand
10	Estuary/River	Intertidal gravel outwash	Very poorly sorted coarse sand
11	Estuary	Intertidal flat proximal to main channel	Poorly sorted medium sand
12	Estuary	Intertidal flat proximal to shore	Poorly sorted medium sand
13	Estuary	Intertidal flat proximal to shore	Poorly sorted Coarse sand
14	Estuary	Intertidal flat proximal to shore and river draining small lake	Very poorly sorted silt
15	Estuary	Intertidal flat proximal to shore	Poorly sorted very fine sand
16	Estuary	Intertidal flat behind northern spit	Poorly sorted medium sand
17	Estuary	Intertidal flat proximal to creek	Poorly sorted medium sand
18	Estuary	Intertidal flat proximal to shore	Moderately well sorted medium sand
19	Estuary	Intertidal flat	Moderately well sorted medium sand
20	Estuary	Intertidal flat	Poorly sorted fine sand
21	Estuary	Intertidal sand-mud flat	Very poorly sorted very fine sand
22	Marine	Shoreface - mouth of estuary	Moderately well sorted coarse sand
23	Estuary	Intertidal flat proximal to intertidal creek	Very poorly sorted medium sand
24	Estuary	Intertidal flat proximal to shore	Very poorly sorted silt
25	Estuary/River	Gravel bar on bayhead delta intertidal zone	Very poorly sorted coarse sand
26	Estuary/River	Gravel bar on bayhead delta intertidal zone	Very poorly sorted gravel
27	Estuary/River	Gravel bar on bayhead delta intertidal zone	Poorly sorted gravel
28	Estuary	Intertidal flat	Moderately sorted fine sand
29	Estuary/River	Gravel bar on bayhead delta intertidal zone	Very poorly sorted gravel
30	Estuary/River	Gravel bar on bayhead delta intertidal zone	Poorly sorted fine sand
31	Estuary	Intertidal flat	Poorly sorted fine sand
32	Estuary/River	Tidal bay	Poorly sorted silt
33	Estuary	Intertidal flat	Moderately well sorted medium sand
34	Estuary	Intertidal flat proximal to creek	Poorly sorted fine sand
35	Estuary	Saltmarsh soil on bayhead delta intertidal zone	Poorly sorted coarse sand
36	Estuary	Intertidal sand-mud flat	Poorly sorted fine sand
37	Estuary	Intertidal flat	Moderately sorted fine sand
38	Estuary	Intertidal sand flat	Very well sorted medium sand
39	Estuary	Intertidal flat proximal to shore	Poorly sorted fine sand
40	Estuary	Intertidal flat proximal to intertidal creek	Moderately sorted medium sand
41	Estuary	Intertidal flat proximal to shore	Very poorly sorted sand
42	Estuary	Intertidal flat proximal to intertidal creek	Moderately sorted medium sand
43	Estuary	Intertidal flat proximal to intertidal creek	Poorly sorted medium sand

**Table 3.1 - Estuary sediment sample description table.**

Map Location	Depositional setting	Environment description	Sediment description
44	Riverbank	Upstream, gravelly bank	Very poorly sorted gravel
45	Riverbank	Upstream river bank	Very poorly sorted gravel
46	Riverbank	Soil sample on small creek	Very poorly sorted very fine sand
47	Riverbank	Small river draining alluvial sediment	Very poorly sorted gravel
48	Riverbank	Upstream river bed	Poorly sorted medium sand
49	Riverbank	Soil on small creek	Very poorly sorted gravel
50	Riverbank	Upstream riverbank	Very poorly sorted very fine sand
51	Riverbank	Small delta at head of lake	Poorly sorted coarse sand

**Table 3.2 - Hinterland sediment sample description table.**

environmental and sedimentological descriptions are given in Table 3.1 and 3.2.

Sediment grain-size and sorting values (Tables 3.1 & 3.2) are based on Laser Granulometry using a Beckman Coulter LS200 (Beckman Coulter Incorporated, 2011). The method involves mixing individual sediment sub-samples and calgon to deflocculate sedimentary components and to generate a slurry. This is then added to the Coulter where the distributions of particles from 0.4  $\mu\text{m}$  to 2000  $\mu\text{m}$  are counted. Where sediment samples were greater than 2000  $\mu\text{m}$  visual estimates using grain-size descriptors were used. Grain-size data presented were analysed using Gradistat (version 6) software (Blott, 2008). All grain-size and sorting values presented use the modified geometric (Folk and Ward, 1957) graphical measures.

For x-ray diffraction (XRD) analysis, fine fractions (<2  $\mu\text{m}$ ) and coarse fractions (>2  $\mu\text{m}$ ) of the sediment were separated, with a fine fraction weight percentage (wt%) obtained for each sample location. Sediment sample preparation followed techniques outlined by Jackson (1969) and Moore and Reynolds (1997). Samples were homogenised, sub-sampled, and then air-dried at 60°C for 15-hours.

Dry sub-samples were weighed then dispersed in tap water by means of four 5-minute cycles of ultrasonication and stirring. The supernatant liquid was decanted and the suspended clay-size fraction (<2 $\mu$ m e.s.d.) was collected by centrifugation at 3500rpm for 30-minutes. The clay-size fraction was then dried at 60°C for 15-hours, ground and then weighed to obtain the clay-size fraction percentage. All sediment samples had the majority of organic matter removed (>80%) by NaOCl (Kaiser et al., 2002). The solution consisted of 15% NaOCl by volume with distilled water; this solution was bathed samples (0.1g in 200ml of solution) and stirred for 24 hours. A centrifuge was used to settle the fine fraction from the solution.

Initial identification of minerals present was performed on a subset of the samples collected to define and refine the sample preparation and mineral identification procedure. Due to the large number of Iceland analyses (nine) that needed to be performed on each sample to identify the mineral present and the large number of samples, it was decided at an early stage that the clay mineral identification outlined below would be completed on eight surface sediment samples that were considered to be representative of environments and have a good geographical spread in the estuary. The mineralogy of remaining samples was then identified utilising this information as a guide.

The method used for identification of clay mineral peaks relies upon the saturation of the interlayer spacing with cations such as magnesium and potassium and the sequential heating of samples. Saturation of the interlayer spacing enables the diagnostic peaks for particular clay minerals to be identified, particularly if scans of unsaturated samples are taken prior to the saturation (Moore and Reynolds, 1997). Subsequent sequential heating and scanning of the sample can also enable identification of clay minerals in samples as interlayer spacing's collapse and water is lost from the mineral structure (Tucker, 1988).

Sub-samples of the clay separates were suspended in solutions (0.1g in 200ml of solution) containing one molar KCl or MgCl for twenty minutes using an ultrasonic bath to keep the sample suspended. Both the magnesium- and potassium-saturated sub-samples were oriented on to 0.2µm Ag filter membranes by vacuum suction. Oriented samples were washed to remove salt build-up, and 0.5% PVA solution was added to bind the sub-sample onto the filter membrane. Magnesium-saturated samples were glycolated, then both magnesium- and potassium-saturated sub-samples were heated sequentially to 300°C, 400°C and 550°C in air, for one hour per step. Samples were scanned after each step of treatment, giving a total of nine analyses for each sample within the first batch of eight samples. Potassium-saturation of the inter-layer spacing results in the

dehydration of the clay mineral phase at lower temperatures. Potassium-saturation and 550°C heating produces more distinct peaks for the main mineral phases than magnesium-saturation. The remaining forty-four samples were potassium-saturated and heated to 550°C only.

Using the following preparation techniques, eight sediment samples were selected for treatment with magnesium and potassium saturation and sequential heating steps to fully define the suite of clay minerals present. The remaining forty-four samples were potassium-saturated and heated to 550°C only.

After organic removal, two further subsamples were taken; one for saturation with potassium and one for saturation with magnesium (Moore and Reynolds, 1997). The subsamples were suspended in solutions containing an excess of either magnesium or potassium for 15 hours, then washed with distilled water to remove excess salts. Both the magnesium- and potassium-saturated sub-samples were oriented onto 0.2µm Ag filter membranes by vacuum suction. The oriented samples were washed with distilled water to remove salts, and 0.5% PVA solution was added to bind the sub-sample onto the filter membrane.

Magnesium-saturated samples were glycolated, then both magnesium- and potassium-saturated sub-samples were heated sequentially to 300°C, 400°C and 550°C in air, for one hour per step.

Samples were scanned after each step of treatment, giving a total of nine analyses for each sample within the first batch of eight samples. The X'Celerator detector equipped PANalytical X'Pert PRO diffractometer employed Ni filtered Cu k- $\alpha$  radiation, scanning the range 3.9-70.0°2 $\theta$  with a two hour scan time. The sequences of basal clay mineral peaks in the resultant diffractograms were decomposed using the profile fitting protocol of the PANalytical HighScore Plus software. The software package was also used to obtain semi-quantitative non-clay mineral proportions for the clay size fraction based on mineral reference intensities and the quantitative analyses of the total mineralogy of lithology samples (Moore and Reynolds, 1997).

An infrared spectral analysis on untreated sub-samples of the fine fraction was also performed on representative samples. 1.5mg of the fine fraction sub-samples was mixed with 300mg of potassium bromide; this was hand-ground and then sintered at 10 tonnes in a press to produce a sample pellet of 0.5% concentration. The pellets were heated overnight at 150°C to remove any adsorbed water (Madejova, 2003). FTIR spectra were obtained with a Thermoelectron Nicolet 380 infrared spectrometer with an IR source, a germanium on KBr beamsplitter and a DTGS detector (Thermo Scientific, 2012).

Distribution maps of the modal grain-size, sorting, fine fraction, bioturbation intensity, relative clay mineral and relative non-clay

mineral content within the fine fraction of estuary samples were generated, utilising the software package Surfer 7 (Golden Software, 2012). Using GPS co-ordinates collected in the field, sample values and concentrations are mapped. Interpolation between points was performed with a kriging algorithm (Journel, 1989; Cressie, 1990). A relative smectite to inter-layer vermiculite index was also plotted by dividing the concentration of the inter-layer vermiculite by the sum of the smectite and inter-layer vermiculite concentrations.

## **3.5 Results**

### **3.5.1 Sediment texture**

The estuary sediments are composed primarily of fine to coarse sands (Fig 3.4A), with the coarsest sediment (granule and pebble grade) occurring in the eastern section of the estuary on the bayhead delta. Coarse and very coarse sands are also located at the front of the estuary, particularly around the estuary mouth. Highest concentrations of clay and silt tend to occur in sheltered areas near to the estuary edge, and towards the upper reaches of the estuary. Estuary sediment is poorly to very poorly sorted (fig. 3.4B), with better sorted sediments (at best poorly sorted) principally occurring in open

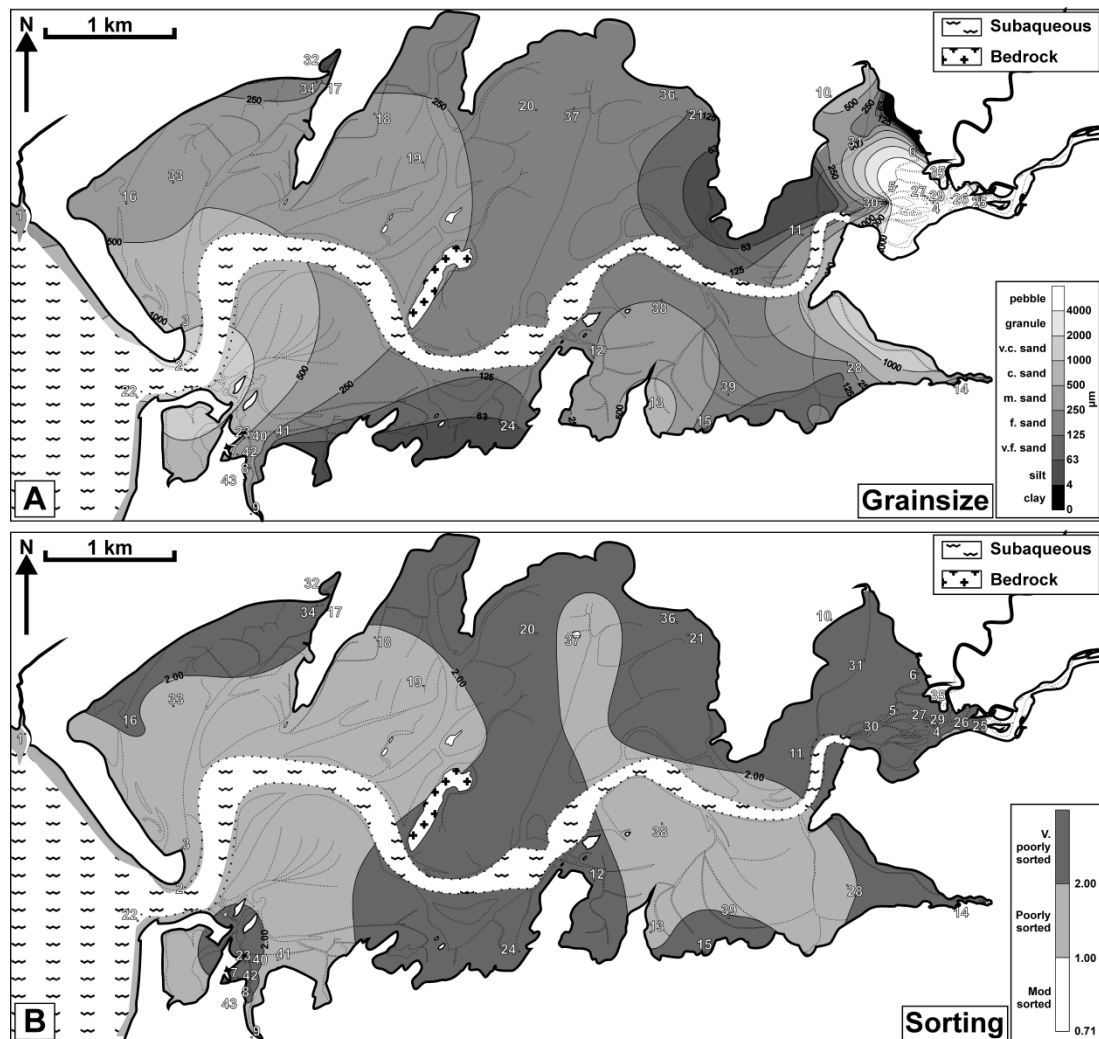


**Figure 3.4 - Contoured maps of Iceland estuarine sedimentary texture. (A) Modal grainsize. (B) Sorting.**

estuary areas close to the main channel and at the front of the estuary. Figure 3.4C is a map of the fine fraction weight percentage (wt %) within individual sediment samples. Fine fraction concentrations in estuary sediments are typically low (2-10 wt %), but higher concentrations (10-35 wt %) occur near the edge of the estuary and at input points of small rivers and tidal creeks into the estuary. The lowest fine fraction content (0-2 wt %) occurs at the front of the estuary and in open, sandflat areas. There is a large degree of local variation in the fine fraction content in the bayhead delta region and

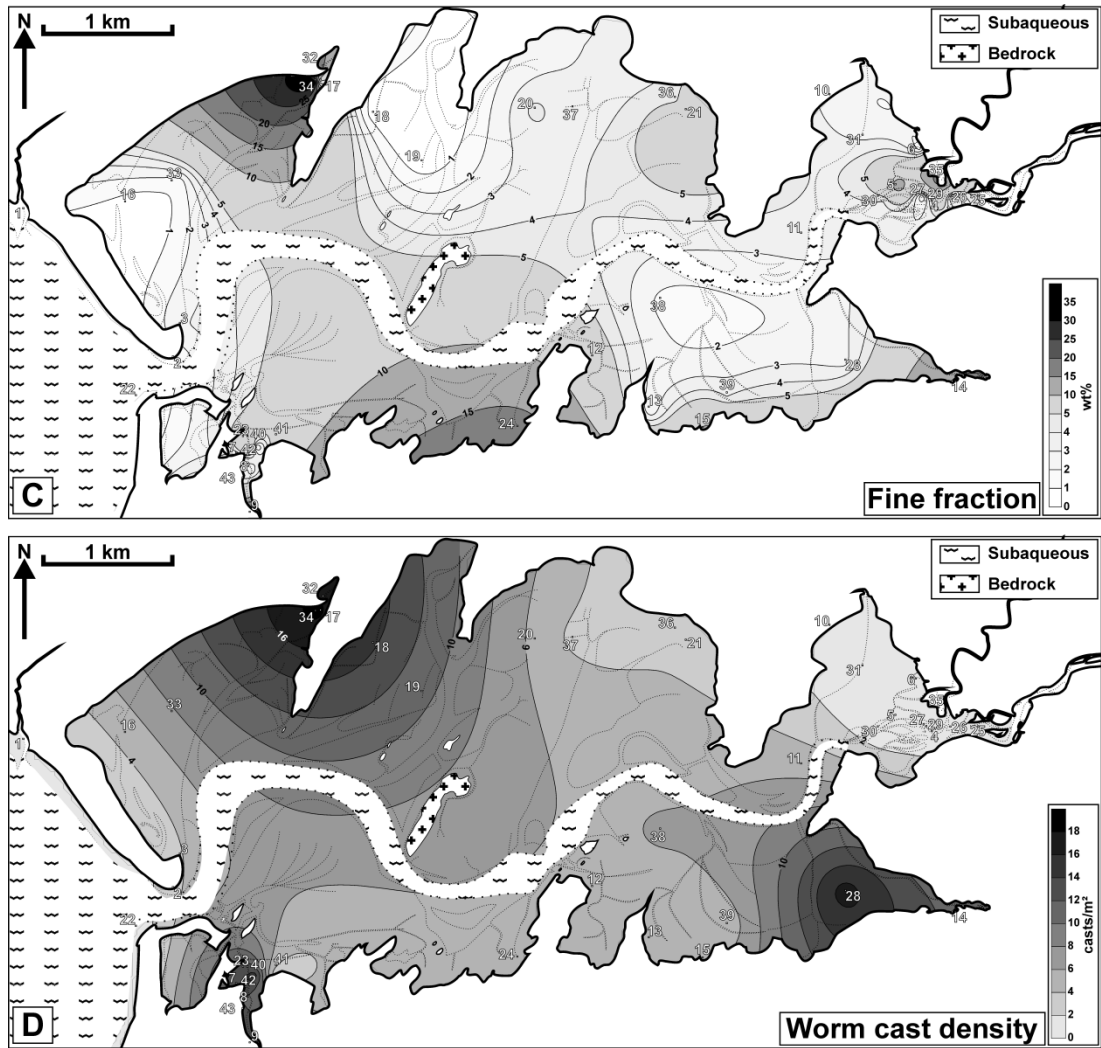


**Figure 3.4 - Contoured maps of Iceland estuarine sedimentary texture. (C) Fine fraction (weight percentage) of whole sediment sample. (D) Bioturbation intensity** in the tidal creek behind the southern spit at the front of the estuary (fig 3.4C). Bioturbation intensity (fig. 3.4D) is highest in locations proximal to small river inputs on the northwest, southwest and southeast corners of the estuary (up to 14-18 casts/m<sup>2</sup>). Lowest values are apparent on the bayhead delta (<2 casts/m<sup>2</sup>), with intermediate values on the open inter-tidal sand areas.

### 3.5.2 Clay mineral identification in estuary samples

Clay minerals within the fine fraction (<2 µm) from surface sediment and worm cast samples were identified using X-ray diffraction techniques, supplemented with information from FTIR spectroscopy.

#### 3.5.2.1 X-ray diffraction

Due to the large number of samples analysed, the clay mineral identification described below was completed on eight surface sediment samples that were considered to be representative of environments and have a good geographical spread in the estuary. This was done to confirm the identities of clay minerals present; the mineralogy of remaining samples was then identified utilising this information as a guide.

XRD scans were performed on subsamples after each procedure: potassium saturation (air-dry), glycolation, 300, 400, and 550 °C heating, then on a separate subsample: magnesium saturation (air-dry), 300, 400, and 550 °C heating (fig 3.5 A&B; Table 3.3). Glycolation is commonly used as an indicator of expandable phases such as smectite or vermiculite; during this procedure ethylene glycol is adsorbed onto inter-layer cations between tetrahedral-octahedral-tetrahedral (TOT) sheets resulting in the swelling of the mineral and the development of a peak around 16-17 Å (Harward and Brindley, 1965; Mosser-Ruck et al., 2005). Progressive heating is another technique commonly used to identify clay minerals, where dehydration and

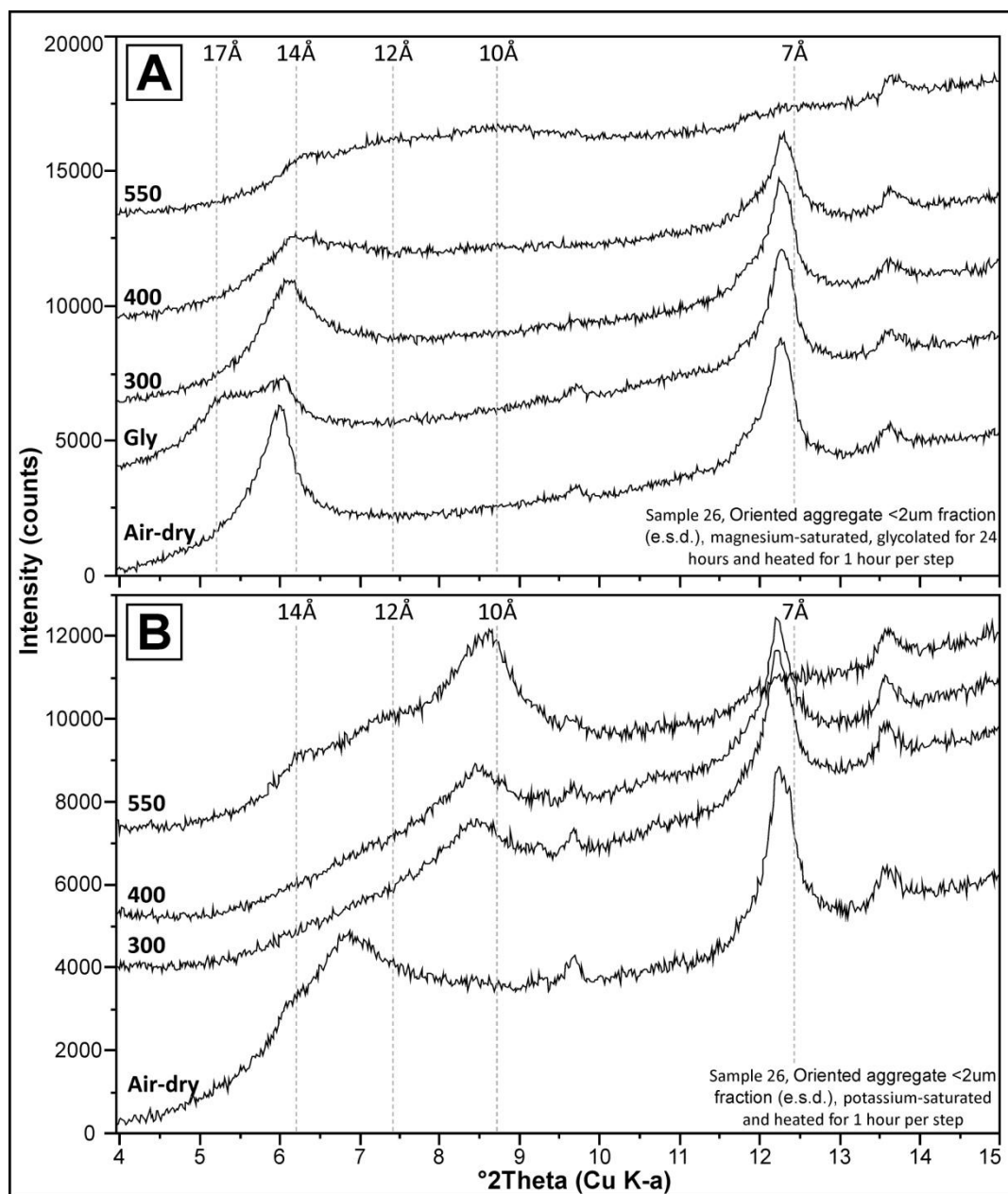


**Figure 3.5 - XRD diffractograms of sample 26 indicating peak positions during various treatments (see Table 3.3 for reference). (A) Magnesium-saturated sample. (B) Potassium-saturated sample. See text and table 3.3 for full outline of treatments. In both A & B the three peaks that are measured are evident at ~14Å (chlorite), ~12Å (inter-layer vermiculite) and 10Å (smectite).**

Magnesium saturation			
Procedure	Chlorite	Inter-layer vermiculite	Smectite
air dry	14.4Å & 7.2Å	14.4Å	14.4Å
glycolation	14.4Å & 7.2Å	14Å-17Å	17Å
heating to 300	14.4Å & 7.2Å	14Å	14Å
heating to 400	14.4Å partial collapse & 7.2Å	14Å-12Å	14Å-10Å
heating to 550	13.8Å reduction, and 7.2Å collapse	12Å	10Å
Potassium saturation			
Procedure	Chlorite	Inter-layer vermiculite	Smectite
air dry	14.4Å & 7.2Å	14.4Å	14.4Å
heating to 300	14.4Å & 7.2Å	14Å	14Å
heating to 400	14.4Å partial collapse & 7.2Å	14Å-12Å	14Å-10Å
heating to 550	13.8Å reduction, and 7.2Å collapse	12Å	10Å

**Table 3.3 - XRD clay mineral identification table. Table shows position of each clay mineral identified on the basis of sequential treatments**

migration of inter-layer cations results in the progressive collapse of inter-layer zones at different temperatures (Starkey et al., 1984; van Groos and Guggenheim, 1986; Tucker, 1988; Kloprogge et al., 1992). In this study, magnesium-saturated, air-dry samples (fig. 3.5A) have two distinct peaks at 14.4 Å and 7.2 Å. Upon glycolation, a component of the 14.4 Å phase, shifts to 16.5Å; this indicates the presence of two phases within the initial 14.4 Å peak. The shifted peak at 16.5 Å is an expandable phase, such as smectite or vermiculite (Moore and Reynolds, 1997).

At the 300°C heating step, the expandable clay mineral has collapsed back toward the 14 Å region. The 400°C heating step results in the partial collapse of the peak around 14 Å, and there also appears to be a broad shoulder between 14 Å and 10 Å. The final 550°C stage produces three broad humps at 14.4 Å, 12 Å and 10 Å; these three

humps indicate that there are three component clay minerals. Complete collapse of expandable clay minerals at 550°C produces a peak at 10 Å (Starkey et al., 1984; van Groos and Guggenheim, 1986; Kloprogge et al., 1992). The broad 12 Å hump is indicative of a partially inter-layered 2:1 clay mineral such as hydroxy inter-layered vermiculite (Meunier, 2007). The last clay mineral is identified by the behaviour of the 7.2 Å peak. The first two heating steps only result in the partial degradation of this peak. At 550°C the residual peak at 14Å peak drops in intensity, and there is a coincident collapse of the 7Å peak; this is behaviour diagnostic of chlorite (Starkey et al., 1984; Tucker, 1988; Moore and Reynolds, 1997). Well-ordered interstratified clay minerals would potentially yield super-order peaks in the 24-32Å in air-dried or glycolated samples (Moore and Reynolds, 1997), but a check on this region and the poorly crystalline nature of the traces indicated that this type of clay mineral is not present in the Leirárvogur Estuary.

The potassium-saturated air-dry sample (fig. 3.5B) shows a similar progression to the magnesium-saturated sample. Potassium-saturation of the inter-layer spacing results in the dehydration of the clay mineral phase at lower temperatures. Potassium-saturation and 550°C heating produces more distinct peaks for the main mineral phases than magnesium-saturation and was therefore performed on the remaining fifty-six samples.

In summary (Table 3.3), clay minerals identified in the Leirárvogur Estuary are: (i) 14 Å chlorite phase; (ii) a phase that expands on glycolation and collapses to 10 Å at heating to 550°C; (iii) hydroxy inter-layered 2:1 structure vermiculite (Meunier, 2007).

Clay mineral nomenclature can be unwieldy and complicated. For simplicity and ease of reading in the remainder of the text the 'expandable' clay mineral will be referred to as 'smectite', and the 'hydroxy-inter-layer vermiculite' as 'inter-layered vermiculite'. The 14 Å-type phase will continue to be referred to as chlorite.

#### 3.5.2.2 Infrared spectroscopy

The OH-stretching region (3800-2400 cm<sup>-1</sup>) of representative sample locations is shown in figure 3.6. The broad band centred at 3425cm<sup>-1</sup> is attributed to the stretching mode of adsorbed water. The bands at 2850-3000 cm<sup>-1</sup> and 2300-2400 cm<sup>-1</sup> are due to organics in the sediment and gas phase and carbon dioxide in the infrared spectrometer chamber respectively. The broad nature of the bands indicates that the clay minerals probably have a disordered structure (Farmer, 1974; Hornibrook and Longstaffe, 1996). The dominance of the water peak even after heating suggests the presence of adsorbed water in inter-layer spacings (Madejova, 2003).

Sample 44 has a distinct band at 3619 cm<sup>-1</sup>, this relates to an Al-OH bond and is common in smectites that have a high proportion of Al in the octahedral sites (Farmer, 1974; Madejova, 2003). The band

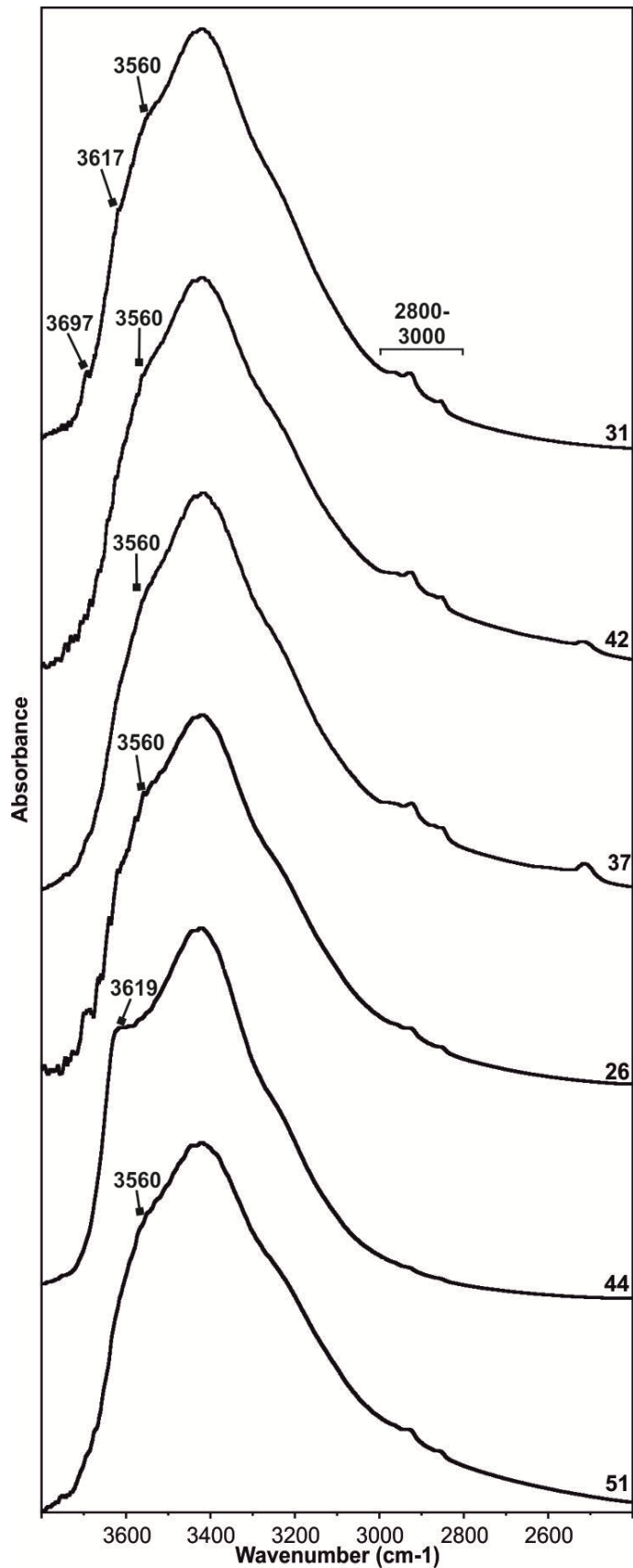


Figure 3.6 - Infrared spectra for representative estuary and hinterland samples. The broad nature of the bands after heat treatment may indicate that the clay minerals present are poorly crystalline (Farmer, 1974; Hornibrook & Longstaffe, 1996). The band at approximately 3560  $\text{cm}^{-1}$  is indicative of an iron-rich smectite such as nontronite. Bands at 3617 and 3697  $\text{cm}^{-1}$  in sample 31 suggests that low concentrations of kaolinite may be present

located around  $3560\text{ cm}^{-1}$  in all but one of the samples (sample 44) is at the approximate position for the FeFeOH where this grouping dominates the octahedral sheets in the smectite clay mineral nontronite (Madejova, 2003). Nontronite is an Fe-rich dioctahedral smectite and is known to be a weathering product of pyroxene in basalt (Eggleton, 1975); this supports the evidence for a dioctahedral expandable phase identified using XRD. For vermiculite, an OH stretching band of  $\text{Mg}_3\text{OH}$  unit would be expected at  $3677\text{ cm}^{-1}$  (Farmer, 1974), although there are small peaks evident in this region, it is not distinct enough to confirm its presence, thus supporting the interpretation of the presence of nontronite smectite. Sample 31 (fig. 3.6), has very small peaks at  $3617$  and  $3697\text{ cm}^{-1}$  and this may indicate the presence of a kaolinite. The size of these peaks indicates that kaolinite is present at trace concentrations; such low concentrations are unlikely to be solely responsible for the significant  $7\text{\AA}$  peak seen, as XRD data indicate that chlorite is also present.

In summary, infrared spectroscopy data indicate that the smectite mineral within the fine fraction is likely to be an Fe-rich smectite such as nontronite; there is no evidence for the expandable phase being a vermiculite clay mineral. There is a suggestion that kaolinite is present only in trace quantities within the fine fraction.

### **3.5.3 Bedrock mineralogy**

XRD analysis of bedrock samples (Table 3.4) indicates that the Tertiary basalt is composed of plagioclase feldspar (63%) and pyroxene (30%), with minor amounts of quartz (2%), ilmenite (2%) and magnetite (2%). Younger Pliocene-Pleistocene basalt is composed of plagioclase (68%), pyroxene (21%), with minor amounts of olivine (7%) and ilmenite (4%). Small exposures of acid extrusives occur in the upper reaches of the Leirárvogur drainage basin (fig 3.1B), and this is composed of a high proportion of quartz (46%) and its high temperature polymorphs, tridymite (13%) and cristobalite (8%) as well as plagioclase (33%).

Trace quantities of chlorite, smectite and inter-layer vermiculite identified above are also evident in two of the basalts analysed (Table 3.4).

### **3.5.4 Glacial mineralogy**

The same suite of clay minerals are found in glacial sediment, riverbank soil and estuary samples, and have broadly similar quantities in three of the four samples (fig 3.7A). Smectite comprises around 50-65% of the clay minerals in the fine fraction, while the inter-layer vermiculite comprises 20-25%. Chlorite accounts for 10-40% of the clay minerals.

Glacial non-clay minerals (Fig. 3.7B), also contain the same suite of minerals as in riverbank soil and estuary samples. Plagioclase concentrations are high, accounting for the majority of the minerals in

Map Location	Description	Plagioclase	Quartz	Tridymite	Cristobalite	Pyroxene	Olivine	Ilmenite	Magnetite	Pyrite	Smectite	Inter-layer vermiculite	Chlorite
Whole lithology samples													
A	Basic lava (Tertiary)	63	2	-	-	30	-	2	2	-	trace	trace	trace
B	Weathered acid extrusive	33	46	13	8	-	-	-	-	trace	trace	trace	trace
C	Basic lava (Pliocene-Pleistocene)	68		-	-	21	7	4	-	-	-	-	-

**Table 3.4 - Mineralogical analyses of lithology and glacial sediments (whole fractions).**

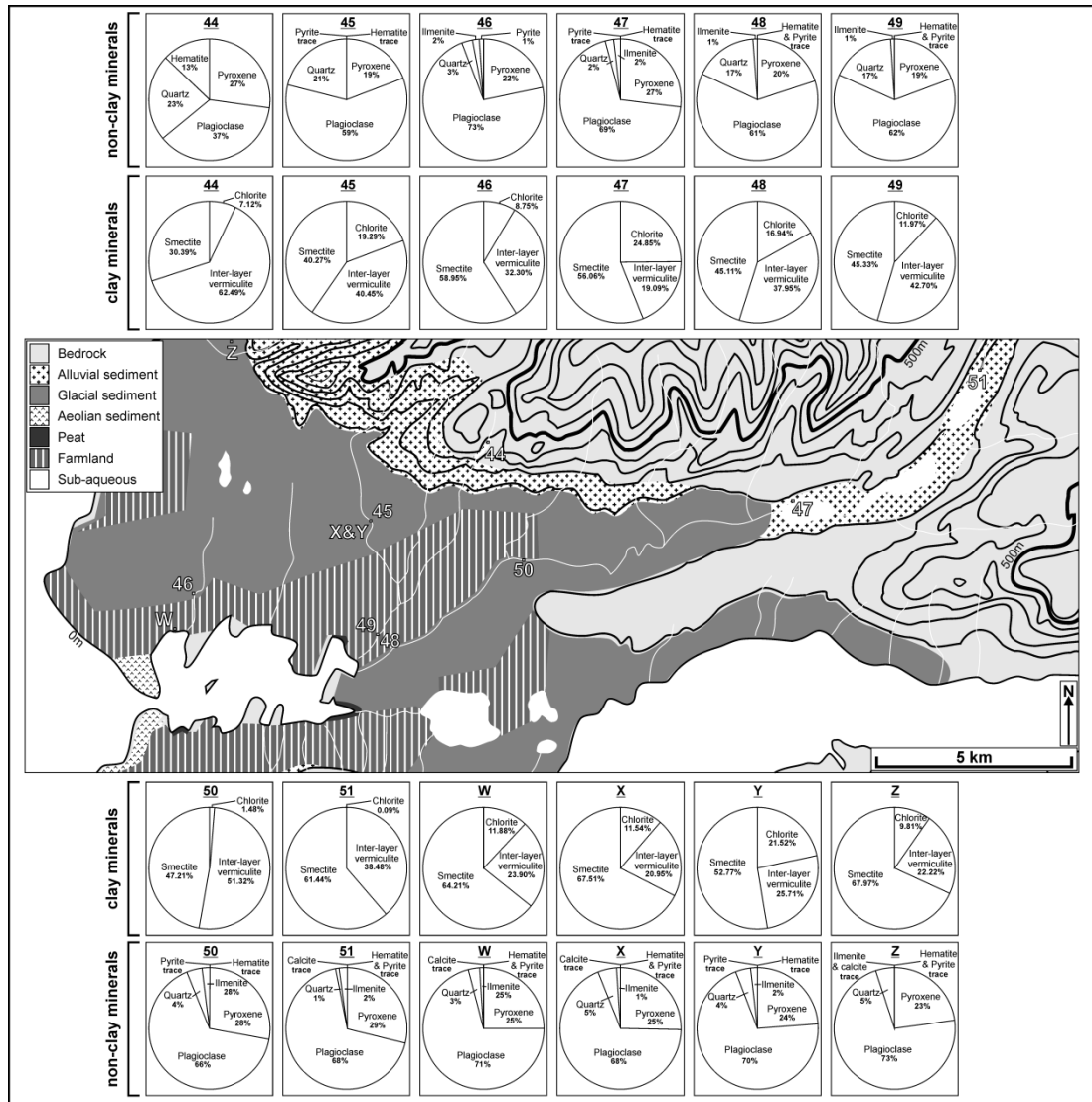


Figure 3.7 - Borgarfjörður surface environment map with hinterland glacial and riverbank sediment sample locations. Numbered samples are riverbank soils, lettered samples are glacial sediments. Pie charts with clay mineral and non-clay mineral concentrations in fine fraction from sample sites. Fine fractions samples from both glacial and riverbank samples contain the same suite of clay minerals, with varying concentrations. Plagioclase, quartz and pyroxene are the most common constituents.

the fine fraction (68-73%). The remainder is composed of pyroxene (23-25%) and quartz (3-5%). Other minerals: calcite pyrite, hematite and ilmenite are present at maximum 2% but are generally present in trace amounts.

### **3.5.5 Riverbank soil mineralogy**

Figure 3.7A displays distributions of riverbank soil samples from around the estuary and in the drainage basin. Different riverbank soil samples generally contain the same suite of clay minerals in varying concentrations: chlorite, inter-layer vermiculite and smectite.

Low chlorite concentrations occur in two Laxá riverbank samples (50 & 51) and generally varies between 5 and 25%. Inter-layer vermiculite concentrations are relatively variable at between 19 and 80%, with smectite within a narrower range of between 30 and 58%.

The non-clay minerals in the riverbank samples (Fig. 3.7B) have variable mineralogies. Samples 46, 47, 50 and 51 are similar to the glacial sediments as they have the same suite of non-clay minerals in similar concentrations, with plagioclase the dominant mineral (66-73%), pyroxene (22-29%) and quartz (1-3%) in lesser concentrations, and very low concentrations or only trace quantities of calcite, pyrite, hematite and ilmenite. In samples 44, 45, 48 and 49, the same suite of minerals is present in each sample, but quartz has a higher concentration (17-23%) with respect to the other minerals in the samples. Pyroxene (19-27%) and plagioclase (37-62%) have lower

concentrations; hematite, pyrite and ilmenite are generally present in trace amounts or are very low in concentration. One exception is sample 44 which has an exceptionally high hematite concentration (14%).

### **3.5.6 Estuary clay mineral distributions**

Relative clay mineral distributions are based on the deconvolution of the peak areas in the fine fraction of samples which have been potassium-saturated and heated to 550°C.

Relative chlorite concentrations (fig. 3.8A) within the estuary are primarily in the range of 6% and 12%. Highest relative concentrations of chlorite (12-20%) occur at the front of the estuary, at the bayhead delta, and at points in the central part of the estuary. Relative inter-layer vermiculite concentrations (fig. 3.8B) vary between 20% and 30%. Higher concentrations occur at the front of the estuary and at certain points on the northern side and the upper reaches of the estuary. There is also some variability in the area around the creek behind the southern spit. The relative smectite concentrations within the fine fraction (fig. 3.8C), are primarily within a range between 55% and 70%. Lower concentrations of smectite occur at the front of the estuary and on the northern side of the estuary, while higher concentration occur close to river inputs and close to the washover north of the bayhead delta. There is significant variability in smectite concentrations in sediment in a tidal creek behind the southern spit.

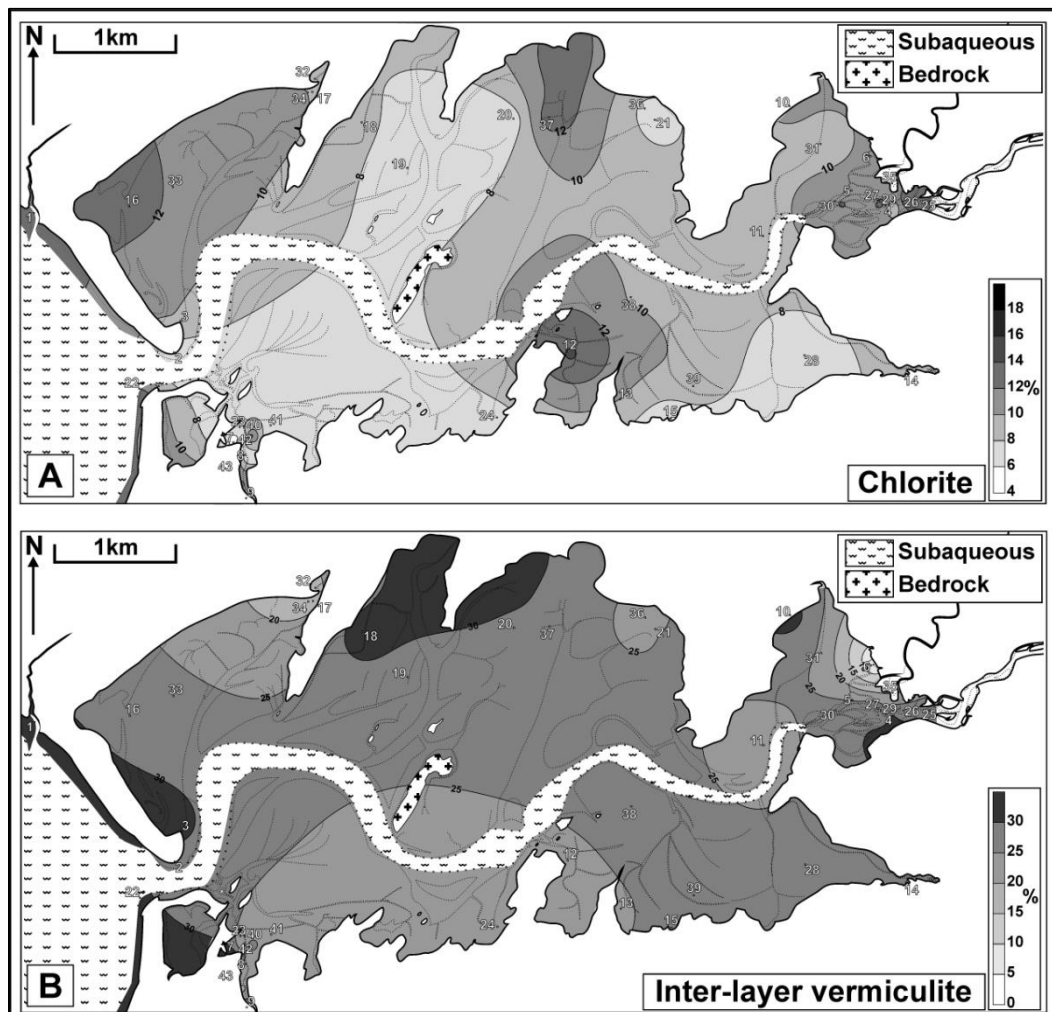


Figure 3.8 - Contoured maps of relative ratios of clay mineral composition of sediment fine fraction. (A) Chlorite. (B) inter-layer vermiculite. The chlorite map has higher concentrations closest to the bayhead delta, and towards the margins of the estuary. Inter-layer vermiculite has lower concentrations around the margins of the estuary.

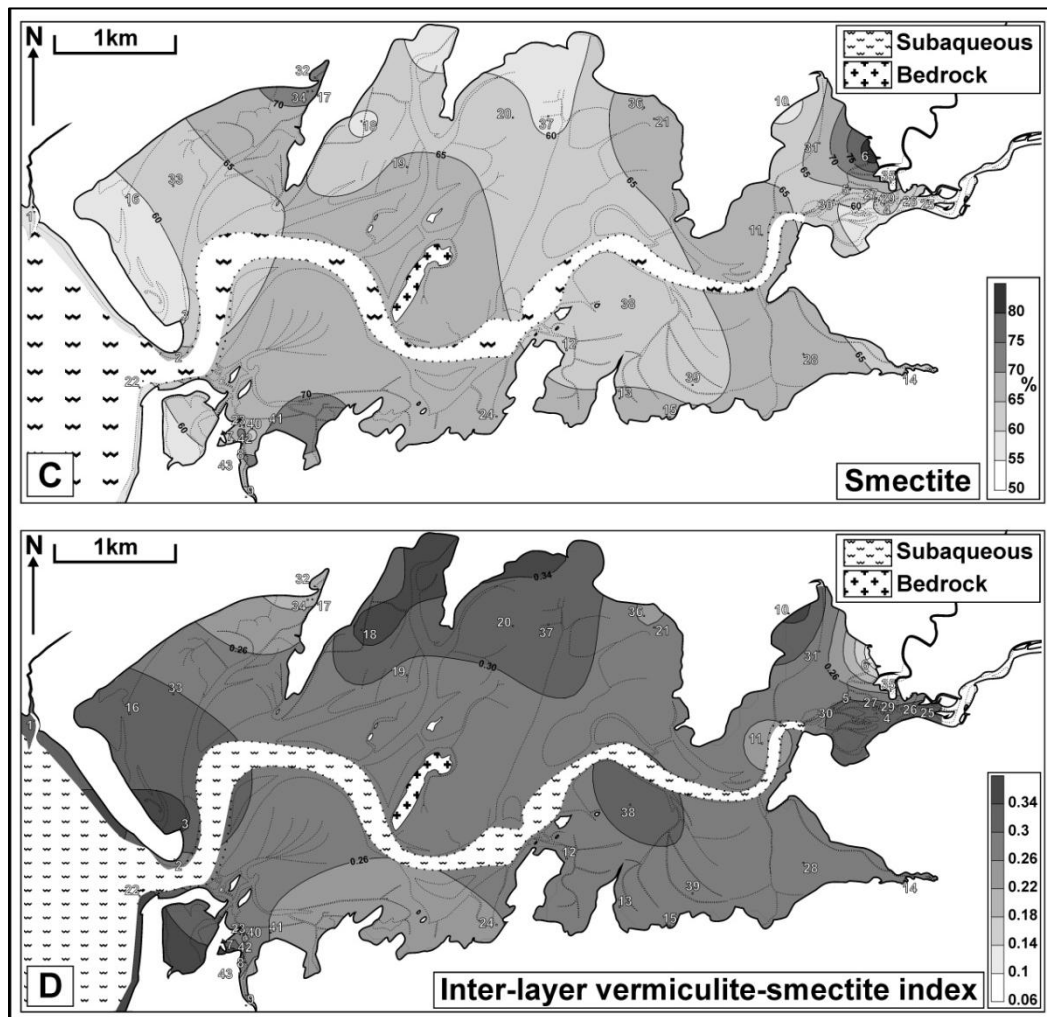


Figure 3.8 - Contoured maps of relative ratios of clay mineral composition of sediment fine fraction. (C) Smectite. (D) Inter-layer-vermiculite - smectite index. Smectite concentrations are highest close to the margins and stream input of the estuary, with lowest concentrations in the marine and central portions of the estuary. The inter-layer vermiculite-smectite map has a broadly similar distribution to inter-layer vermiculite.

The inter-layer vermiculite-smectite index is the concentration of inter-layer vermiculite divided by the sum of the smectite and inter-layer vermiculite concentrations. Using this method allows an assessment of the concentrations of the smectite and inter-layer vermiculite, without the effect of chlorite concentrations. Figure 3.8D shows a broadly similar pattern to that of the inter-layer vermiculite (fig. 3.8B) with high values on the north-central portion and marine mouth sections of the estuary. Lowest values occur close to the river input on the north-side and in sediments close to the large washover on the saltmarsh.

### **3.5.7 Estuary non-clay mineral distributions**

The concentrations of calcite and aragonite correlate closely with each other (fig. 3.9A&B), with calcite ranging from 0% to 14% and aragonite from 0% to 25%. Highest concentrations occur in areas closest to the marine end of the estuary and in open areas proximal to the channel and on a beach washover to the north of the bayhead delta.

Ilmenite concentrations are generally low (fig. 3.9C), with most estuary surface sediments containing concentrations between 0.5% and 1.5%. Lower concentrations occur in open areas proximal to channels, whilst the highest concentrations tend to occur nearer the front of the estuary, at the edges and in protected locations proximal to river and creek inputs.

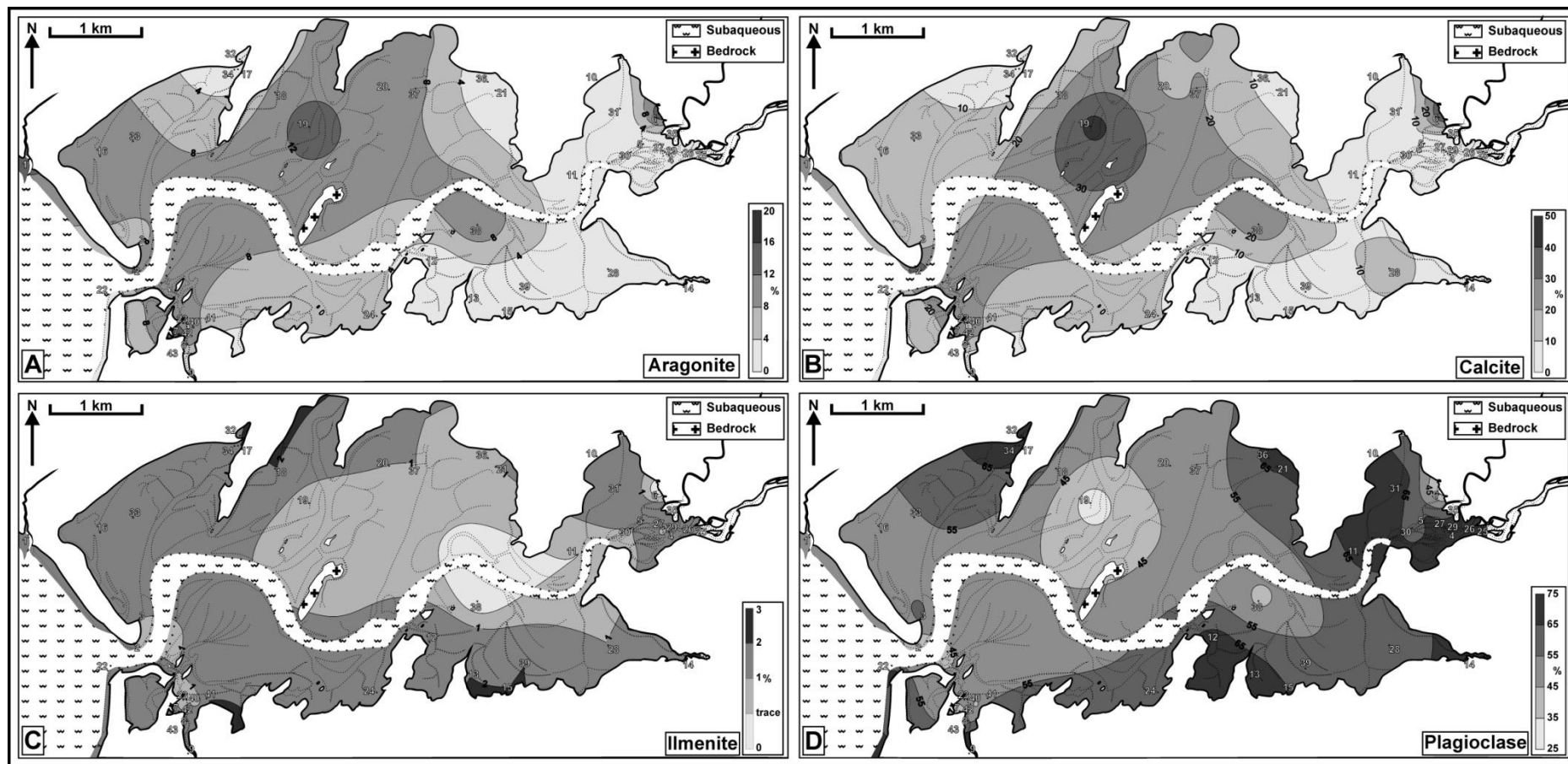


Figure 3.9 - Contoured maps of relative non-clay mineral composition of sediment fine fraction. (A) Aragonite. (B) Calcite. (C) Ilmenite. (D) Plagioclase.

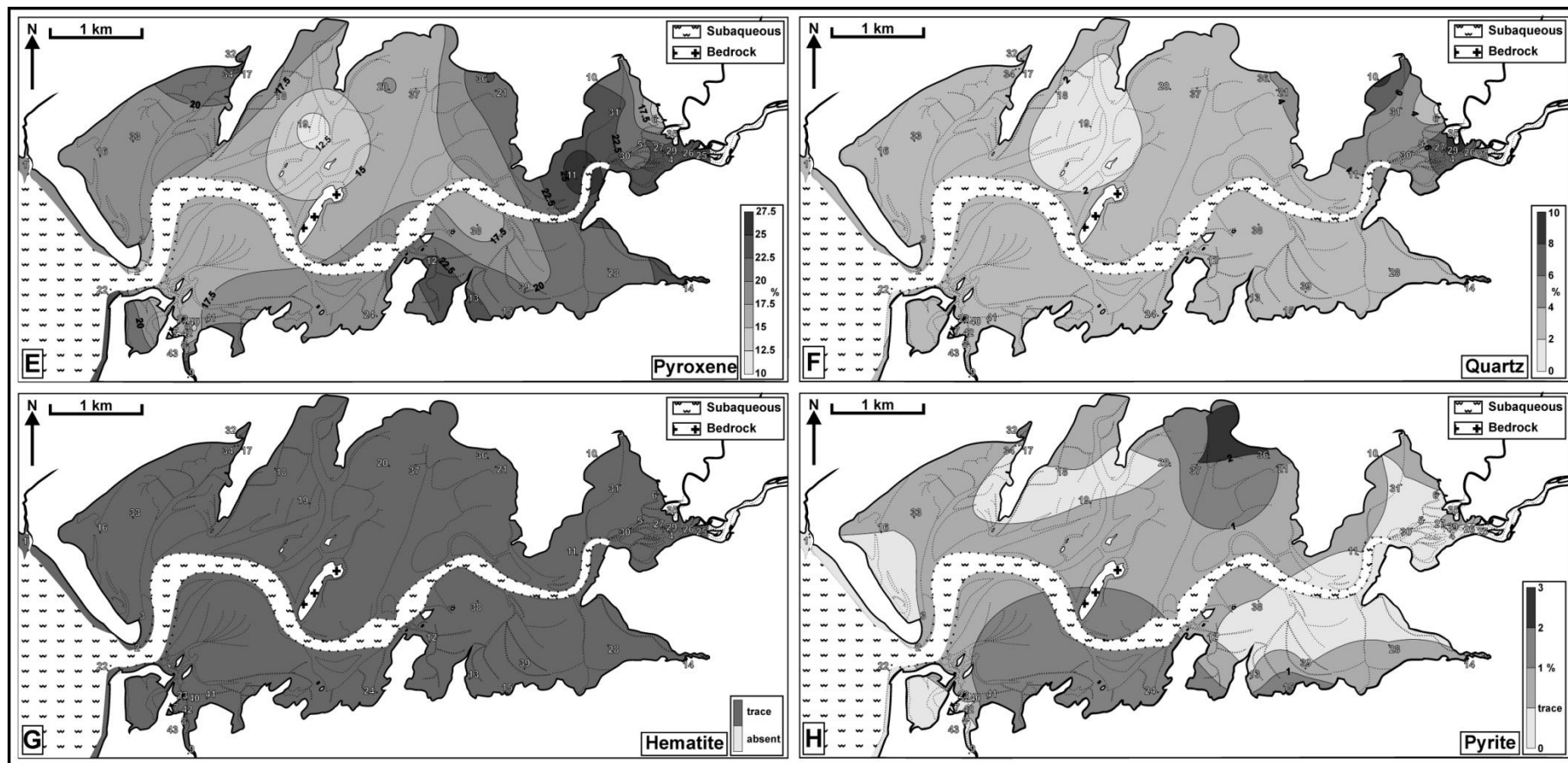


Figure 3.9 - Contoured maps of relative non-clay mineral composition of sediment fine fraction. (E) Pyroxene. (F) Quartz. (G) Hematite. (H) Pyrite.

Plagioclase feldspar is the dominant mineral within the fine fraction (fig. 3.9D), and typically ranges from 35% to 70% in most samples. Highest concentrations (55-70%) are close to river and stream inputs, protected bays, and in the upper part of the estuary. Lowest concentrations (25-45%) primarily occur in open and exposed areas close to the channel. Relative pyroxene content (fig. 3.9E) within the estuary generally ranges from 12.5% to 25%, with highest concentrations occurring on the south-side of the shoreface, the upper reaches of the creek behind the southern spit, the protected bay on the south-central side and in the upper reaches of the estuary. Lower pyroxene concentrations tend to occur in open and exposed areas of the estuary close to the channel.

Quartz concentrations are generally low (fig. 3.9F), and range from 2% to 5% over the majority of the estuary. The highest concentrations (5-10%) occur on the bayhead delta and in the upper reaches of the estuary; conversely the lowest concentrations (0-2%) occur in open exposed areas and in shoreface sediments.

Pyrite concentrations in surface sediments are low in the estuary (fig. 3.9H) with no values above 3%. The lower limit of detection of pyrite is ~1%, but individual XRD diffractograms were assessed for pyrite peaks, where the pyrite could not be quantified a trace value was assigned to the map. Zero percent concentrations occur at the front of the estuary, on the north-side of the estuary close to a stream input,

around the bayhead delta, and downstream of this site. Highest values occur on the north central area of the estuary (1-3%), and on the south central area of the estuary (1-2%).

Hematite was present below quantifiable detection limits, but was present in trace quantities in every sample. (Fig. 3.9F)

### **3.5.8 Mineral cross-plots & average values**

Mineral cross-plots of selected minerals and textural characteristics were plotted to further develop trends noted in the mineral concentration maps. Visual assessment of relationships between two variables was supplemented with r-value calculations (Townend, 2003) and comparison to p-values ( $p=0.05$ ) for the sample number minus two degrees of freedom (Siegle, 2009). This gives a 95 percent confidence limit for correlations noted below. Figure 3.10 is a cross-plot of smectite and inter-layer vermiculite versus fine fraction weight percentage and sorting. Smectite shows a increase in concentration with an increase in fine fraction content and as sorting becomes poorer (fig. 3.10A&B), while inter-layer vermiculite displays a decrease in concentration with increasing fine fraction content and as sorting becomes poorer (fig. 3.10C&D). Confidence values for these relationships are close to the p-values, but indicate that relationships are evident. Cross-plots of clay mineral concentrations show variable trends (fig. 3.11). Smectite versus chlorite (fig. 3.11A), displays a negative relationship, with chlorite concentrations lower where

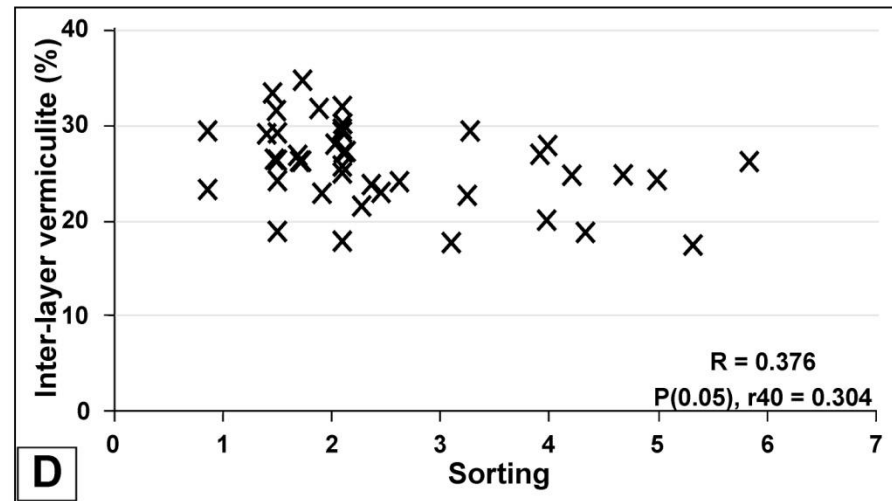
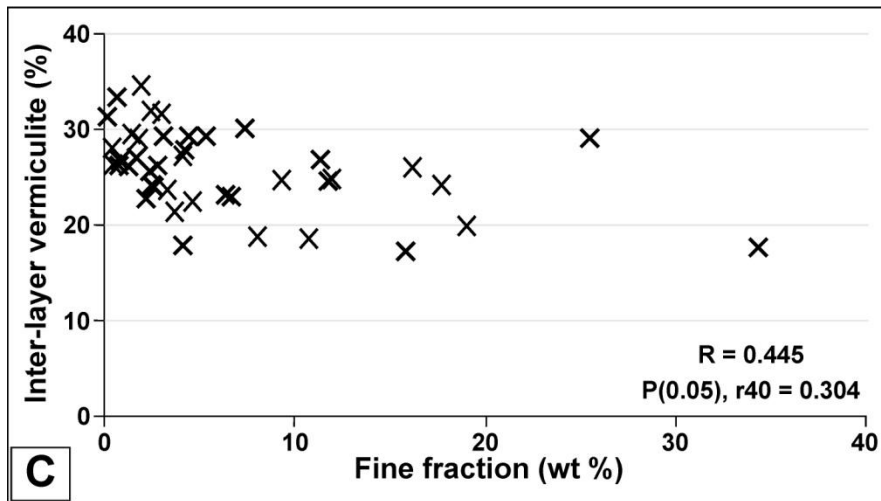
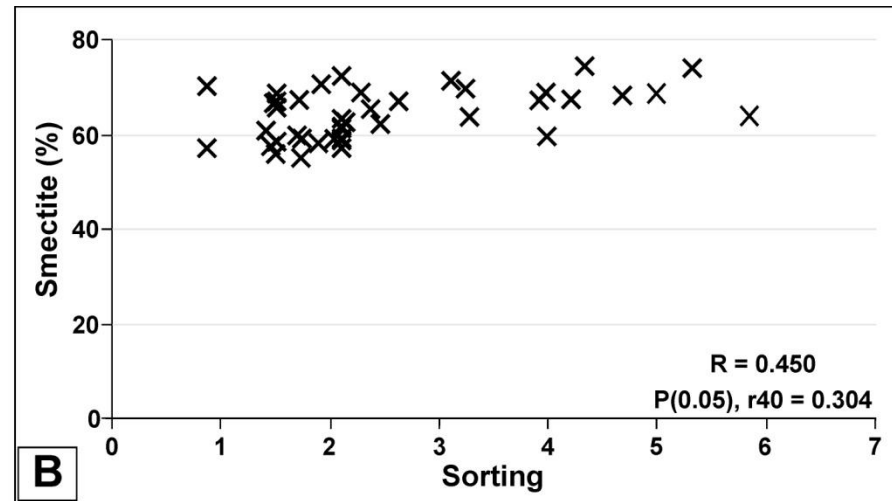
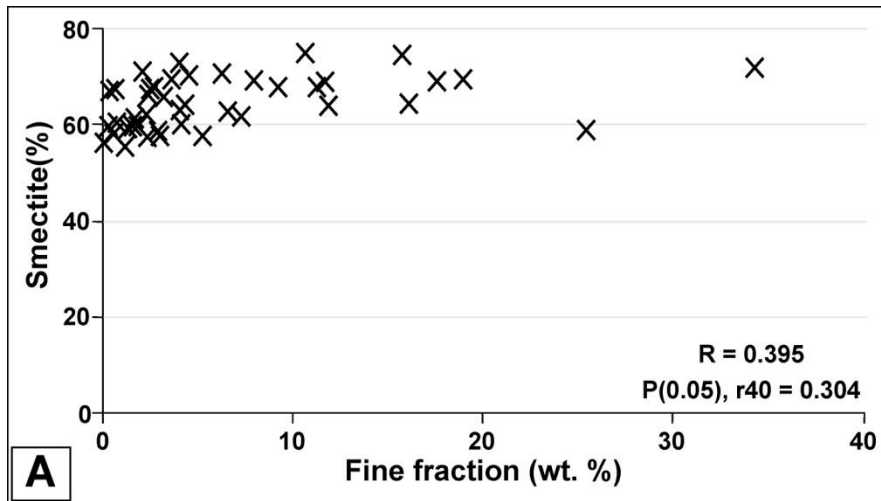


Figure 3.10 - Whole sediment texture and relative clay mineral concentration cross-plots. (A) Fine fraction versus smectite. (B) Sorting versus smectite. (C) Fine fraction versus inter-layer vermiculite. (D) Sorting versus inter-layer vermiculite.

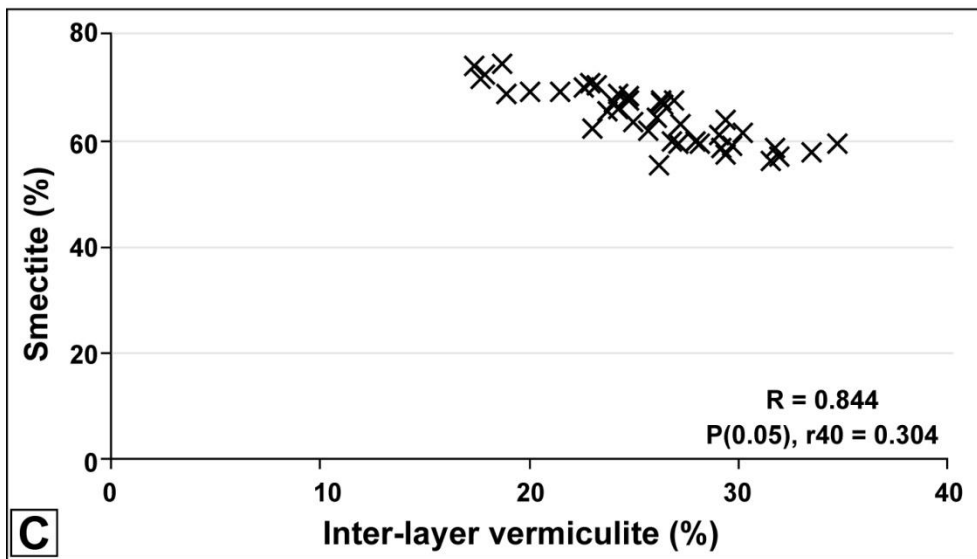
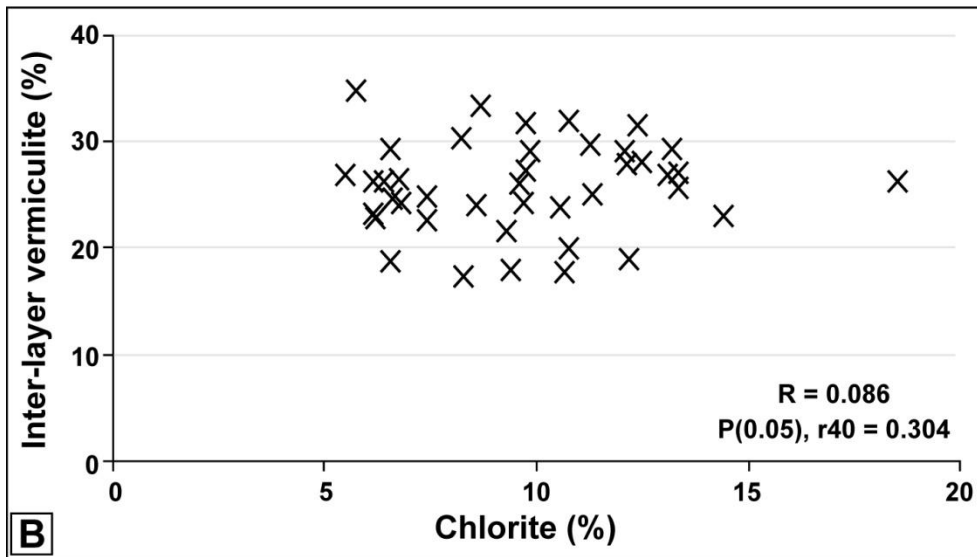
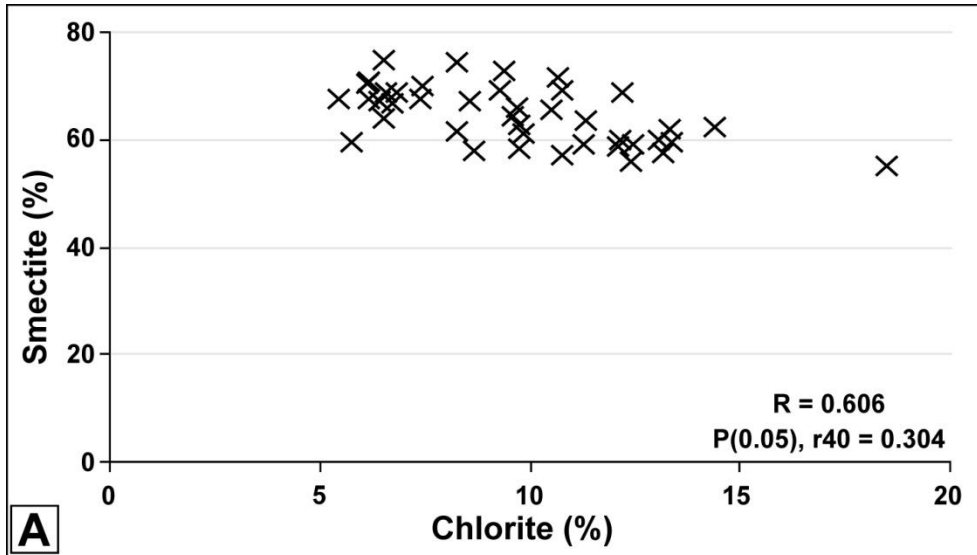


Figure 3.11 - Cross-plots of relative clay mineral. (A) Chlorite versus smectite. (B) Chlorite versus inter-layer vermiculite. (C) Smectite versus inter-layer vermiculite.

smectite is increased in concentration. Inter-layer vermiculite versus chlorite (fig. 3.11B) displays no relationship. Inter-layer vermiculite versus smectite concentrations shows a strongly negative trend (fig. 3.11C); where smectite concentrations are increased, inter-layer vermiculite concentrations are lower.

Cross-plots of non-clay minerals also have some trends (fig. 3.12). Calcite and aragonite have a positive relationship (fig. 3.12A), while cross-plots of plagioclase, pyroxene and quartz all display a positive relationship (fig. 3.12 B, C & D).

Figure 3.13 represents the average clay mineral relative percentage in the fine fraction of sediments from worm cast, estuary hinterland and glacial sediments. The figure shows that average chlorite concentrations are similar for all four classes of sediment. Average inter-layer vermiculite and smectite concentrations are very similar in worm cast glacial and estuary samples, but have nearly 20% difference in hinterland sediments. Although standard deviations are high for hinterland sediments, the difference compared to glacial, worm cast and estuary surface sediment concentrations appears to be large enough to indicate that this is not a sampling issue. Similarly, the relatively small number of glacial and hinterland sediments in the dataset may reduce the statistical significance of the data. However, the similarity in concentration of clay minerals still produces a low standard deviation; the broad geographical distribution of glacial

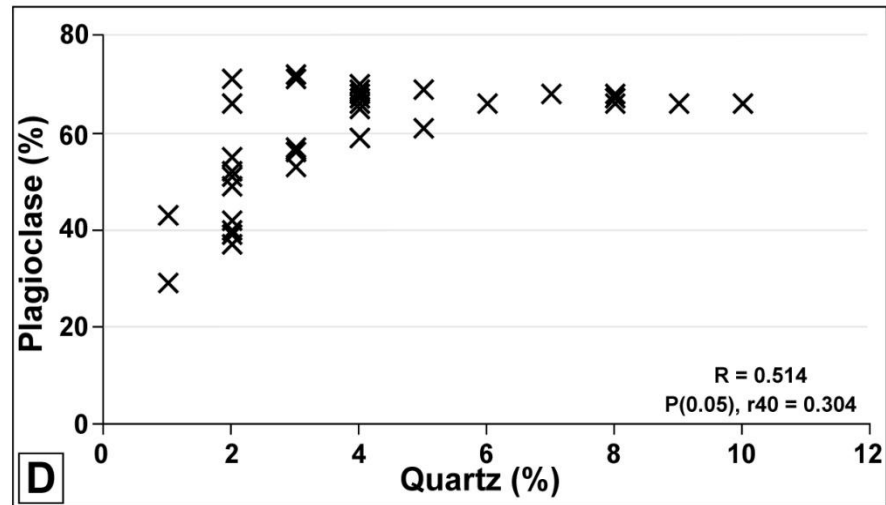
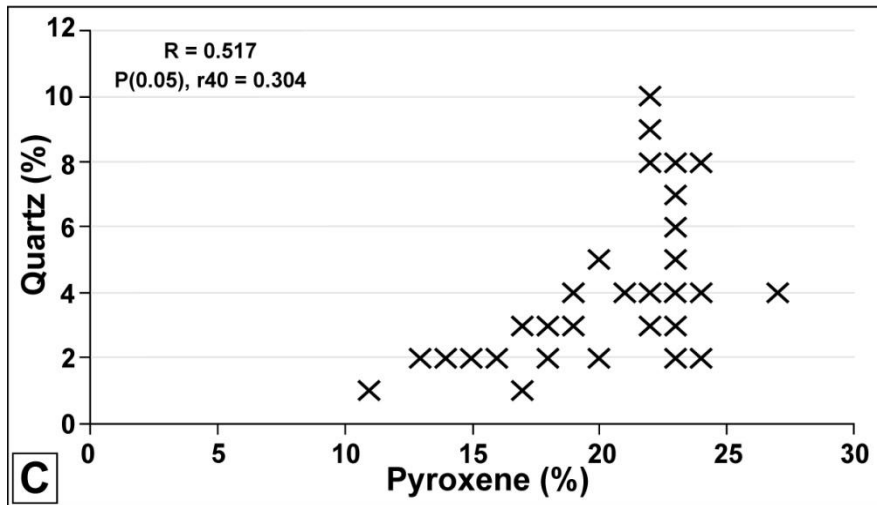
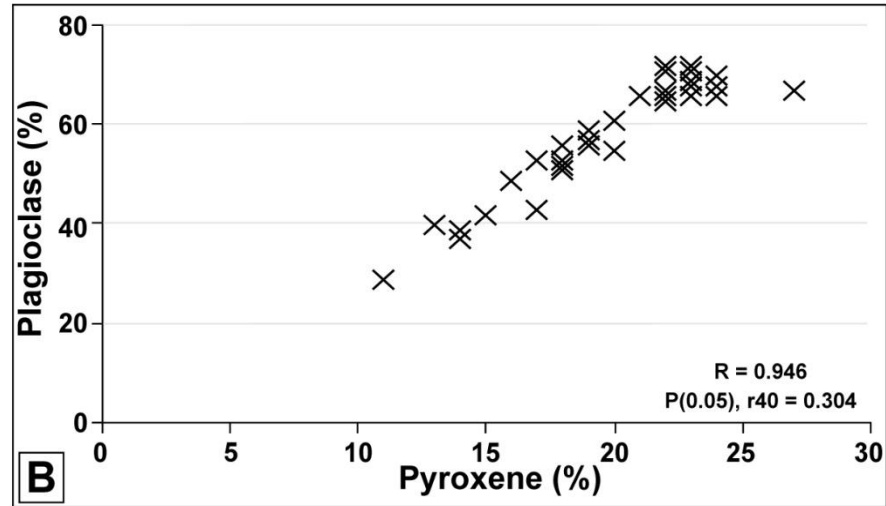
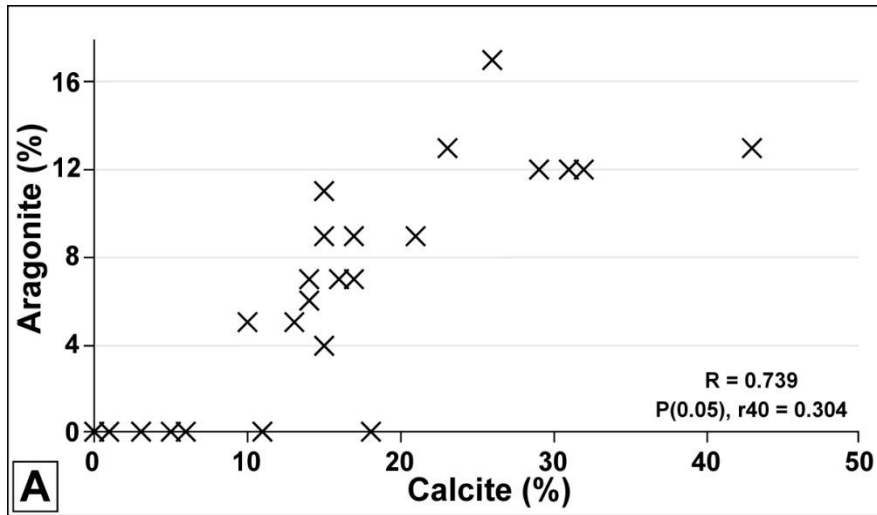


Figure 3.12 - Cross-plots of relative non-clay minerals. (A) Calcite versus aragonite. (B) Pyroxene versus plagioclase. (C) Pyroxene versus quartz. (D) Quartz versus plagioclase.

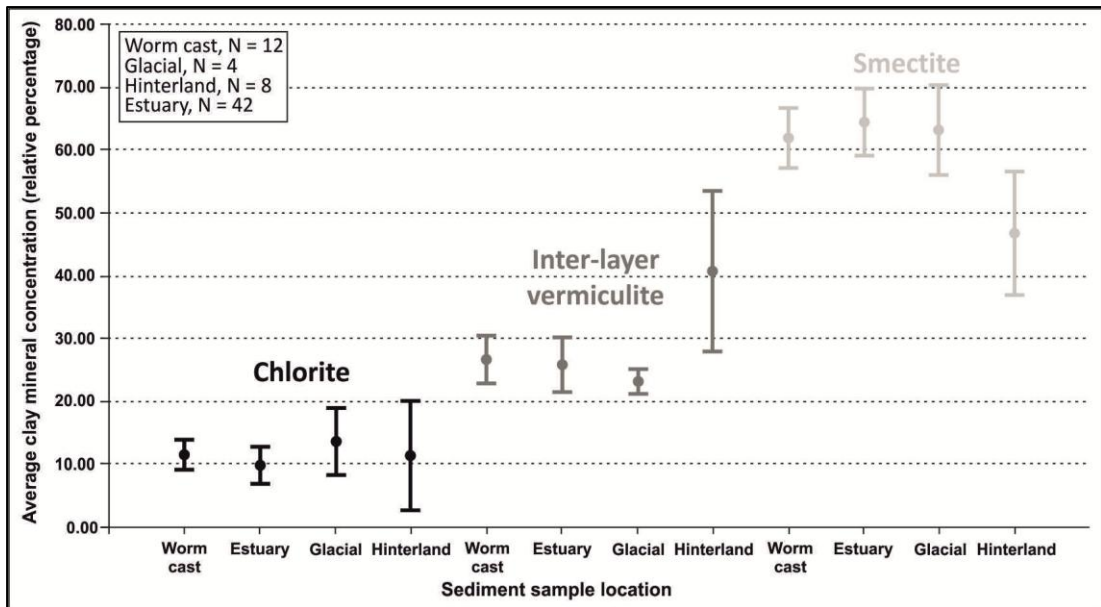


Figure 3.13 - Average clay mineral relative percentages from worm cast, estuary, riverbank soil and glacial sediments. Error bars are one standard deviation. Average concentrations are calculated by averaging the concentrations (relative, carbonate-normalised, concentrations in estuary samples) in samples from a particular environment.

sediments (fig. 3.1) should mean that any compositional variability in these sediments has been sampled.

### 3.5.9 Worm cast mineralogy

Plotting difference maps for each clay mineral (worm cast value minus surface value) allows comparison of the concentrations between each location (Fig. 3.14). In all but two of the twelve samples smectite has a negative value with positive values predominating for both chlorite and inter-layer vermiculite. The worm casts appear to have less smectite than the estuary sediments, while inter-layer vermiculite and chlorite have higher concentrations in the worm cast samples. A comparison of the values for each location

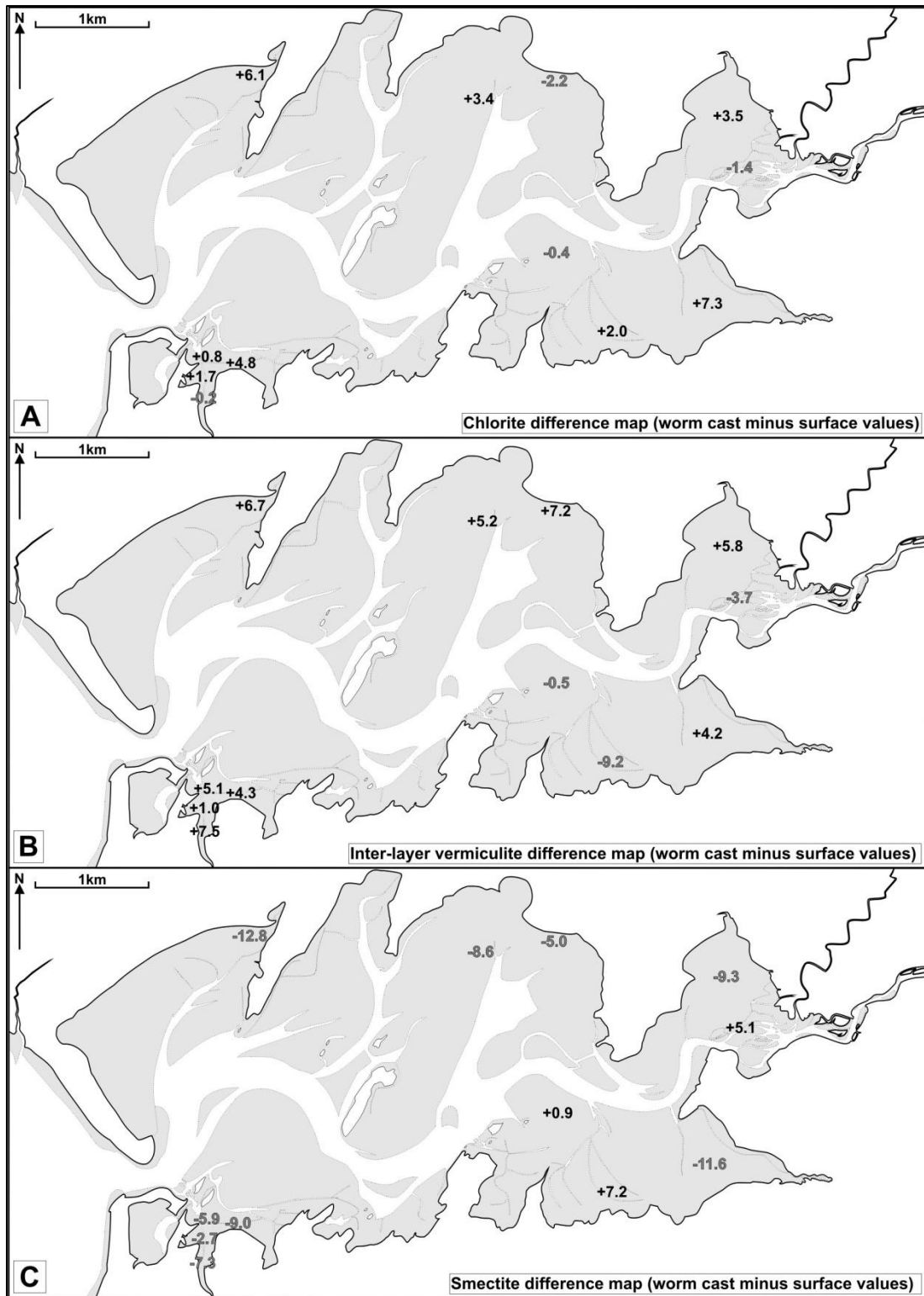


Figure 3.14 - Difference maps of clay mineral concentrations in worm cast and surface sediments. (A) Difference in chlorite concentrations between worm cast and surface sample value. (B) Difference in inter-layer vermiculite concentration between worm cast and surface sample value. (C) Difference in smectite concentrations between worm cast and surface sample value. Negative smectite values and positive chlorite and inter-layer vermiculite values indicate that generally smectite and inter-layer vermiculite may be altering to inter-layer vermiculite and chlorite.

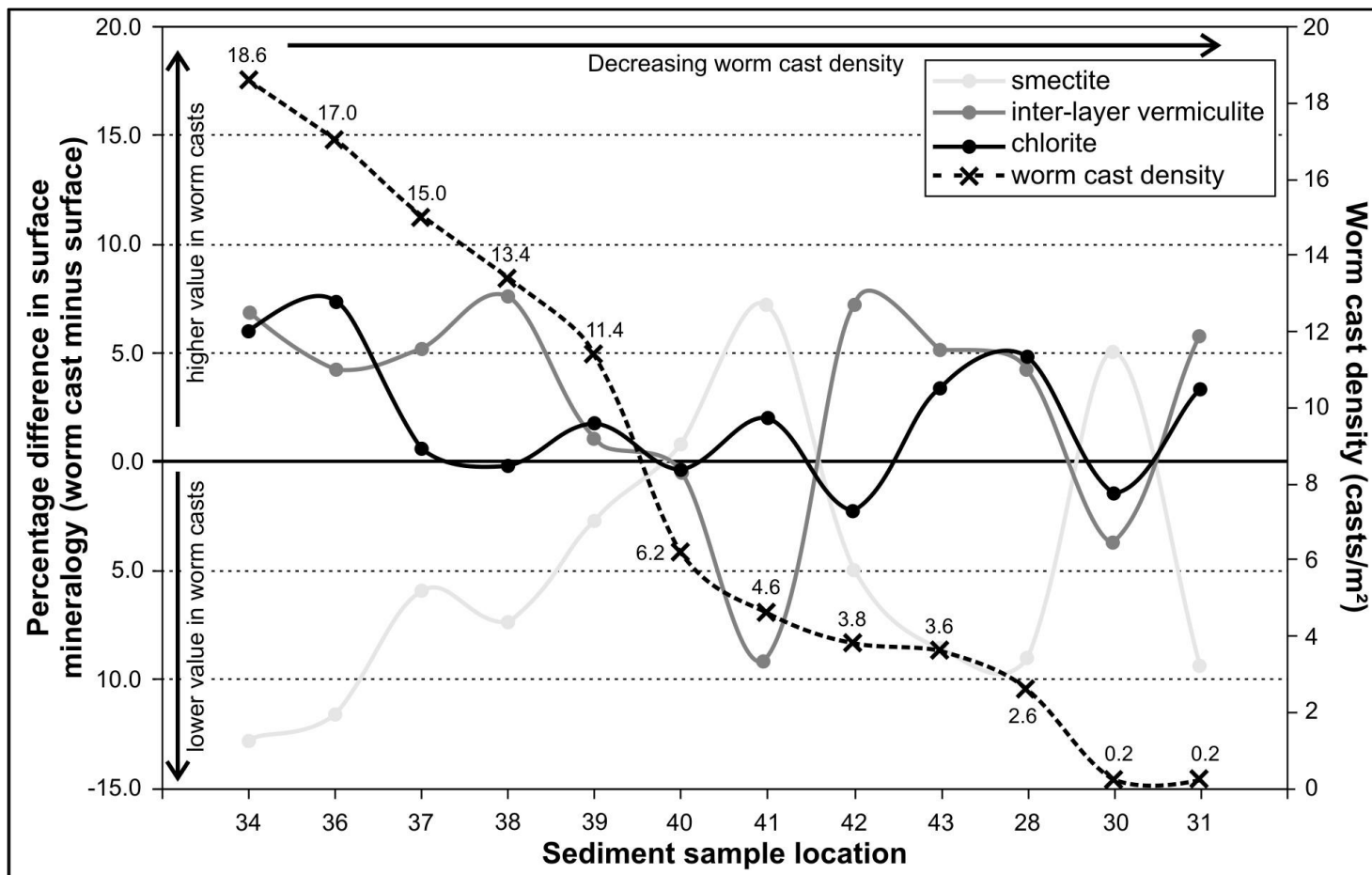


Figure 3.15 - Difference graph for clay mineral concentrations in worm cast and surface sediments. Smectite concentrations appear generally lower in sample locations where bioturbation is more intense, conversely inter-layer vermiculite is also more concentrated in these areas.

alongside worm cast density (Fig. 3.15) shows a more pronounced pattern with a relatively lower (or negative) value for smectite in the worm casts and there is a relatively higher (or positive) concentration of chlorite and inter-layer vermiculite.

## **3.6 Discussion**

### **3.6.1 Sediment texture**

Sediment in the Leirárvogur Estuary is texturally immature. Sorting is generally poor or very poor (fig. 3.4B) and this supports the interpretation that the transgression and filling of the estuary was initiated relatively recently (Ingólfsson, 1988; Le Breton et al., 2010). This may be compounded by the short transport length of river-supplied sediment, which would limit the degree of sorting. Modal sediment grain-size is well segregated and conforms to the coarse-fine-coarse tripartite facies model found in most modern estuaries (Dalrymple et al., 1992); with a fine to medium sand central portion, a coarse to very coarse marine end, and a pebble dominated bayhead delta. This division of grain-size confirms that sediment dispersal is controlled by both marine and fluvial processes.

Sediments at the marine end of the estuary have a coarser modal grain-size with lower fine fraction content and slightly better sorting (fig. 3.4); this reflects marine reworking. The bayhead delta, at the confluence of the Leirá and Laxá rivers, has the coarsest sediment (fig. 3.4A). The coarseness requires the majority of fluvially derived

sediment present to have been carried as bedload, and this is most likely to occur during infrequent, high discharge events during storms or spring freshets (floods). Visual inspection of river waters during field sampling in low rainfall conditions during mid-summer showed very little suspended material in both the Leirá and Laxá Rivers. However, this observation is unlikely to be representative of river-borne concentrations during infrequent high discharge events. This contention is supported by published sample average discharge rates for rivers in the southwest of Iceland (Gíslason et al., 1996). Over a period of three years the larger of the two Leirárvogur Estuary rivers average discharge was found to be low (7.8 m<sup>3</sup>/s) compared to the total average for other rivers in southwest Iceland (83.9 m<sup>3</sup>/s). This may reflect the length and area of the Laxá River catchment compared to other rivers in the area, and because the river is not glacially-fed it may have a lower base stream flow and less glacially derived sediment. Similarly TDS content of the river is also low compared to local rivers and may reflect low denudation rates in a relatively old catchment (Gíslason et al., 1996).

The observation that the Leirárvogur Estuary Rivers may not, ordinarily, supply a large volume of suspended sediment to the estuary, and the indication that the estuary has only recently developed (Ingólfsson, 1988), may suggest that a proportion of the sediment in the estuary is entrained and reworked from local glacial sediments. Glacial

sediment is actively being eroded on the northern and southern margins of the estuary, as well as in the vicinity of the bayhead delta and the frontal spit at the present day (fig. 3.1C & 3.2D). Glacial sediments found a few centimetres below surface sediments in portions of the present day inter-tidal flat (fig. 3.3F); also indicate extensive glacial sediment under parts of the estuary. Another potential source of glacially-derived sediment is from offshore, with sediment brought onshore through tides and storms. Similarly, active coastal erosion of glacial sediments are significant in the area (Ingólfsson, 1988), with eroded sediment suspended and possibly drawn into the estuary with flood tides.

A large, poorly-sorted, shingle washover beach on the grassy top of the bayhead delta (fig. 3.3B) is composed of smooth, flat, blade-shaped clasts and is characteristic of glacially-entrained sediment (Menzies, 2002). Potential sources for the sediment are from high discharge river events eroding glacial sediment within the catchment, or equally from the erosion and transport of glacial deposits surrounding and underlying the estuary. The presence of the washover indicates the importance of storm events and tides in controlling local grain-size in the upstream, eastern half of the estuary, while also underscoring the role of glacial sediment in supplying, either river-supplied or locally supplied sediment to the estuary.

The finest modal grain-sizes and the largest fine fraction concentrations sampled were in sheltered areas close to some river inputs, and in the upper reaches at the eastern end of the estuary (fig. 3.4A&C). Fine grained sediment transported in suspension in rivers is likely to encounter a rapid decrease in flow velocity on encountering the estuarine water body. Flocculation of fine particles may also be induced due to the mixing of saline and fresh waters close to the turbidity maximum. Flocculation of sediment to form larger particles increases the settling velocity required for deposition of the particles and may result in deposition close to the river input points. This appears to be evidenced by the high fine fraction content in sediments proximal to river systems on the north-west and south-east sides of the estuary (fig. 3.4C).

The local variability in fine fraction weight percentage in areas of high sampling density, such as on the bayhead delta, and in the small creek behind the southern spit, suggests that there is the potential for a large degree of lateral and stratigraphic variation between proximal sample sites. Other areas, like the intertidal sandflat, display low fine fraction variability even where great distances separate sample sites (fig.3.4C).

### **3.6.2 Detrital & inherited mineralogy**

Smectite, inter-layer vermiculite and chlorite are found in the bedrock, glacial sediments (that may underlie a large part of the estuary) and

in most surface sediment samples (figs. 3.7& 3.8), and are also noted in offshore sediments (Fagel et al., 1996; Gehrke et al., 1996; Fagel et al., 2001). The ubiquity of these minerals may indicate early generation of clay minerals, or that they are largely detrital or inherited from bedrock, glacial sediment and/or riverbank soils. A consideration of the three clay minerals and the non-clay minerals, and how they may have developed externally to the estuary is presented below.

#### 3.6.2.1 Smectite

An expandable 2:1 layer clay mineral identified by XRD is generally the most abundant clay mineral (fig. 3.5); FTIR suggests that this is possibly a nontronite-type smectite (Madejova, 2003; fig. 3.6). All smectites are expandable and retain an open inter-layer zone between TOT sheets that can gain and lose ions depending on local chemical conditions. Smectite is noted in bedrock samples in trace quantities, as well as in the fine fraction of glacial and riverbank soil samples.

Smectite is a common clay mineral and can form from a variety of parent minerals including volcanic glass, feldspars and pyroxenes (fig.3.16; Eggleton, 1975; Eggleton et al., 1987). Typically, at surface conditions, it forms in areas of low temperatures and precipitation, subject to low levels of weathering intensity (Weaver, 1989; Wilson, 1999).

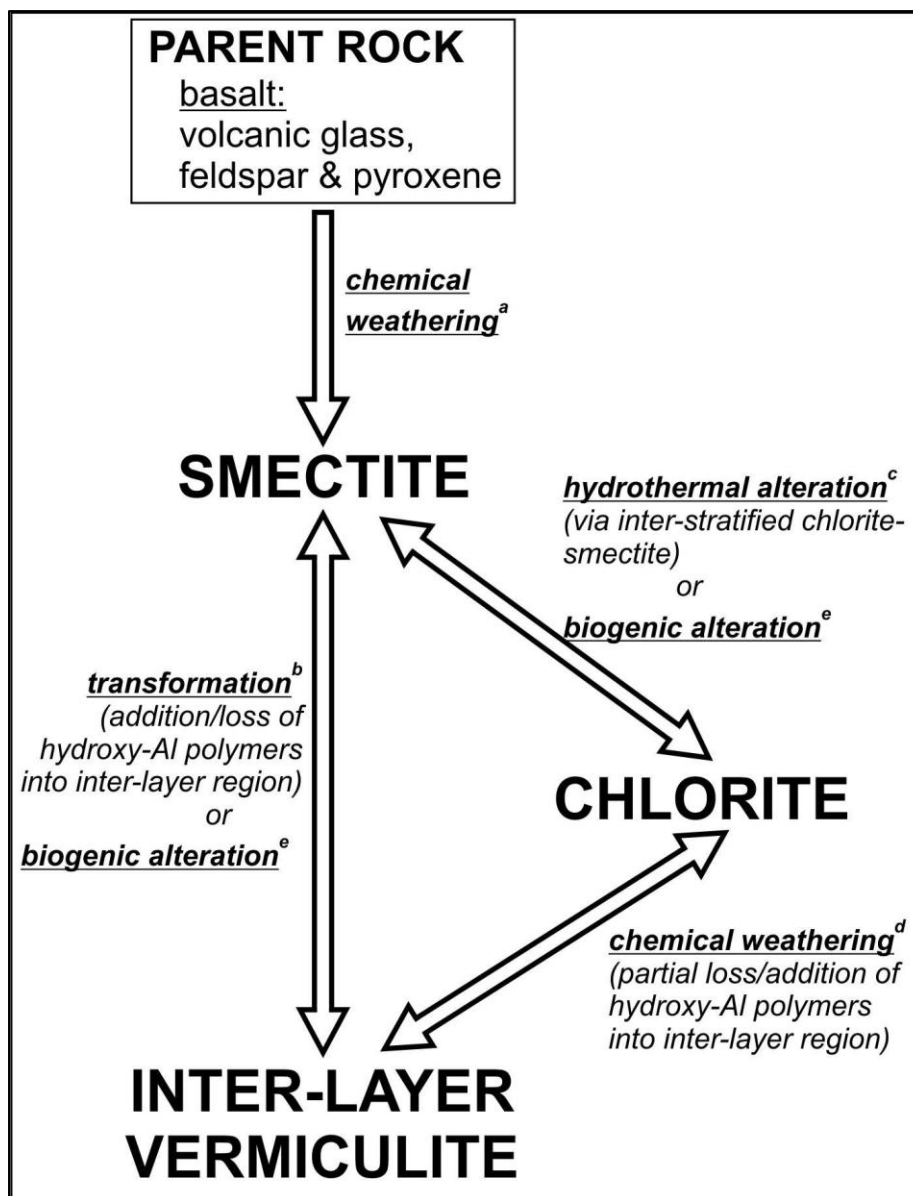


Figure 3.16 - Clay mineral evolution diagram (a) (Eggleton et al., 1987; Eggleton, 1975; Weaver, 1989; Wilson, 1999; Ramussen et al., 2010): (b) (Meunier, 2007; Wilson, 1999; Brown and Newman, 1973): (c) (Kristmannsdóttir, 1979; Schiffman and Friedleifsson, 1991; Sveinbjörnsdóttir, 1992): (d) (Proust et al., 1986): (e) this study.

The high concentration of smectite in the Leirárvogur Estuary and catchment is likely to be due the widespread predominance of volcanic basalt in the basin (fig. 3.1). Low intensity chemical weathering of bedrock, saprolites and soils (Ramussen et al., 2010) is likely to generate smectite in the catchment. The indication of an iron-rich nontronitic smectite indicates that smectite probably formed from pyroxene (Eggleton, 1975).

#### 3.6.2.2 Inter-layer vermiculite

Inter-layer vermiculite is generally the second most common clay mineral in the fine fraction of the sediments (fig. 3.5). Partial collapse of inter-layer vermiculite on heating during XRD analysis indicates that the inter-layer zone is partially filled with hydroxyl-Al polymers adsorbed on to the surface of TOT sheets (Meunier, 2007). In smectites, this inter-layer spacing is unfilled and completely collapses on heating to 550°C. Inter-layer vermiculite is noted in bedrock samples in trace quantities, as well as in the fine fraction of glacial and riverbank soil samples.

Inter-layer vermiculite can develop through either the partial depletion of hydroxides from 2:1:1 structure clay minerals, such as chlorite, or through the addition of hydroxyl-Al polymers between the sheets of 2:1 clay minerals, such as vermiculite and smectite (fig. 3.16; Wilson, 1999; Meunier, 2007). Field studies (Proust et al., 1986) show that vermiculite can develop from chlorite through an ordered inter-

stratified chlorite/vermiculite with Mg and Fe<sup>2+</sup> preferentially lost, resulting in a mineral relatively enriched in Si, Al and Fe<sup>3+</sup>. This process has been proven experimentally and has shown that regularly interstratified chlorite-vermiculite and vermiculite can develop from chlorite through chemical oxidation (Ross and Kodama, 1976). Conversely, hydroxy inter-layer clay minerals have been produced experimentally from an expandable clay mineral, such as smectite through the adsorption of Al complexes (Brown and Newman, 1973; Wilson, 1999).

Geochemical alteration of chlorite and smectite within soils is known to occur and the addition or loss of Al-hydroxyls in the inter-layer spacing of these 2:1 layer minerals seems likely but is probably dependent on local geochemical conditions. This may be true in the Leirárvogur catchment, given the contention that both riverbank soils and estuary sediments appear to be derived from broadly similar glacial sediments (fig. 3.7). If correct, the increase in inter-layer vermiculite and decrease in smectite average concentrations becomes important (fig. 3.13). Factors that promote the development of hydroxy inter-layer clays in soils are low organic content, oxidising conditions and frequent wetting and drying cycles (Wilson, 1999). The progressive stages of inter-layer development may be variable depending on environmental conditions. An issue with this interpretation is that regional soil maps indicate that the drainage

basin is composed primarily of andosols, which are typically high in organic content (up to 20%), poorly drained and often have reducing conditions (Arnalds, 2004). However, the data presented do show (fig. 3.13) that there is a distinct difference in both inter-layer vermiculite and smectite concentrations in hinterland sediments compared to other sediments sampled.

### 3.6.2.3 Chlorite

Chlorite is present in the majority of sediment samples in low concentrations (fig. 3.5B). Structurally a chlorite is a 2:1:1 clay mineral with a rigid inter-layer octahedral sheet composed of cations and hydroxyls between TOT sheets (Worden and Morad, 2003). The broad nature of the chlorite peak (fig. 5) may indicate that it is not fully developed and may not have a well-ordered structure (Weaver, 1960; Hinckley, 1963; Guggenheim et al., 2002). Chlorite is noted in bedrock samples in trace quantities, as well as in the fine fraction of glacial and riverbank soil samples.

Chlorite can form in a variety of settings, including soils, through the addition of hydroxyl-Al polymers filling the inter-layer zone between TOT sheets of smectite 2:1 layer clay minerals (Meunier, 2007). Transformation of expandable clay minerals such as vermiculite and smectite to form 'pedogenic chlorite' occurs through the introduction of hydroxyl-Al polymers into inter-layer spacing and can be sourced from organic acids breakdown of tetrahedral and octahedral sheets

in the mineral, or indirectly from soil solution following the weathering of aluminous minerals (Wilson, 1999). Chlorite can also form hydrothermally through the alteration of precursor clay minerals such as smectite.

Evidence from hydrothermal studies in Iceland (Kristmannsdóttir, 1979; Schiffman and Friedleifsson, 1991; Sveinbjörnsdóttir, 1992) indicates that chlorite is likely to develop hydrothermally in the Leirárvogur catchment (fig.3,16). Chlorite is in very low concentrations within samples 50 and 51 on the Laxá River, and such low values may reflect differences in the source areas or that chlorite in these areas is preferentially altering to other clay minerals in the riverbank soils, possibly inter-layer vermiculite.

### **3.6.3 Non-clay minerals**

All the glacial sediments, and some of the riverbank soil samples (samples 46, 47, 50 and 51), have similar non-clay mineralogies, with plagioclase feldspar the dominant mineral, and with lesser amounts of pyroxene and quartz. The similarities of these samples suggest that at least some of the glacial samples are broadly related. The higher quartz concentrations in some of the samples (44, 45, 48 and 49) could be related to a greater supply of sediment (either glacially derived or from upstream river sources) from acid extrusives in the northern part of the study area. The high hematite content in one of the riverbank soils (sample 44) may reflect intense weathering (Wilson, 2004) or

alteration (Markusson and Stefánsson, 2011) of iron-bearing minerals, or could be the result of the accumulation of fluviably-transported iron complexes (Matsunaga et al., 1984). The riverbank soil with the high hematite content is located at the head of the Leirá River; it receives direct runoff from basaltic bedrock, which suggests the most likely source for hematite is the weathering of recently eroded iron-rich basaltic fragments.

#### **3.6.4 Detrital & inherited mineral summary**

The similarity in the suite of minerals between glacial, riverbank and estuary sediments reflects the basalt bedrock in the drainage basin and overall lack of fractionation during sediment transport and deposition. All of the minerals in riverbank sediments are present in glacial sediments suggesting that they were formed prior to soil development. However, concentrations in the estuary vary suggesting that clay minerals continue to develop and that other factors control relative concentrations.

The similarity in composition and concentration of glacial sediments (fig. 3.7 A&B) indicates similar genesis, transport and depositional process for these sediments. This is likely to be due to glacial erosion of generally homogeneous bedrock, with the scale and intensity of glacial erosion acting to mix any heterogeneity in original source mineral concentrations. The sample with the slightly different clay mineralogy (Y; fig. 3.7) is from a fine-grained clay lens within a coarser

diamicton (X; fig. 3.7). This difference in concentration within one glacial outcrop probably represents mineral size sorting effects during transport and deposition. This small difference in local mineral concentrations could produce variations in mineral concentration in both riverbank and estuary sediments, when these sediments are supplied from extensive areas of particularly fine-grained glacial sediments.

Riverbank soils sediments have the same suite of clay minerals as both glacial and estuary sediments, but display much more internal variability in both clay mineral and non-clay mineral concentrations than glacial sediments (fig. 3.7). The riverbank sediments are soils and it is here assumed that these are derived from a combination of glacial sediment, which underlies a significant proportion of the drainage basin, upstream sediments and tephra deposits (Wada et al., 1992).

The similarity of chlorite concentrations across all sedimentary environments and glacial sediments probably reflects the fact that, although chlorite is not stable at surface conditions, the reactivity and cation exchange capacity of chlorite may be less than that of either smectite or inter-layer vermiculite.

There are two possible causes for the distinct difference between average hinterland smectite and inter-layer vermiculite average

concentrations, compared to glacial, estuary and worm cast concentrations (fig. 3.13).

The first is that average values of hinterland smectite and inter-layer vermiculite are broadly similar and upon entering the estuary cations are lost from the inter-layer spacing of the inter-layer vermiculite resulting in an increase in smectite. The similarity of the glacial sediment to other in-estuary sediment samples could be coincidental and due to an analogous evolution of clay minerals in very different time-temperature conditions. However, experimental loss of interlayer material typically requires high pH conditions or heating, and naturally occurring inter-layers are harder to remove than those artificially produced (Rich, 1968). Also, this would require that the majority of the sediment within the estuary was supplied from either the rivers or streams, which based on field observations, is not the case in the Leirárvogur estuary.

The second potential cause of the difference in smectite and inter-layer vermiculite concentrations is that the majority of the sediment within the estuary and the wider region are glacially-derived. In this case, estuary (plus worm cast) sediments are derived primarily from glacial sediments, with glacially-derived soils in the hinterland undergoing transformation from smectite to inter-layer vermiculite. This interpretation suggests that geochemical conditions in riverbank soil sediments are leading to partial infilling of the inter-layer spacing

between TOT sheets in the smectite with hydroxyl-Al polymers producing an increase in inter-layer vermiculite, which has been shown to occur experimentally (Brown and Newman, 1973; Wilson, 1999). This second explanation appears more likely and is supported by the strong similarity between glacial and estuary clay mineralogy, and the low suspended matter content in the Leirá (Gíslason et al., 1996) and Laxá river systems. The active erosion of glacial sediments on estuary margins and the possible marine supply of eroded glacial material from the coast to the north of the estuary (Ingólfsson, 1988), strongly implies that this is the source for most of the sediment in the estuary.

### **3.6.5 Intra-estuarine processes**

Mineral concentrations within the Leirárvogur Estuary sediments display a non-uniform distribution (figs. 3.8, 3.9 & 3.14). This variability suggests that estuarine distributions are controlled by internal processes within the estuary. A discussion of the possible causes of the differences in mineral concentration is presented below.

#### **3.6.5.1 Geochemical alteration**

The overall suite of clay minerals within estuary sediments is the same as both glacial and riverbank soil sediments. This suggests that there is limited generation of neoformed minerals within the estuary waters or sediments as noted in some coastal environments elsewhere (Michalopoulos and Aller, 2004; Presti and Michalopoulos, 2008).

However the differential concentration of minerals within estuary sediments may indicate that geochemical alteration of minerals could be occurring. This is particularly possible with respect to smectite, inter-layer vermiculite and chlorite, where addition or loss of Al-hydroxyls in inter-layer positions within the structure of clay minerals could change the concentration of these clay minerals within the sediments.

Relative smectite and inter-layer vermiculite display broadly inverse concentrations (fig. 3.8), which is particularly evident when the concentrations of these two minerals are cross-plotted (fig. 3.11). It indicates that in areas where one has a relatively higher concentration the geochemical conditions may be enough to alter the composition of the inter-layer spacing. Inter-layer vermiculite could be produced through the adsorption of Al complexes by smectite (fig. 3.16; Brown and Newman, 1973; Wilson, 1999), or particularly intense weathering of inter-layer vermiculite could result in the loss of Al complexes producing smectite. This would require a particular set of geochemical circumstances within surface sediment in the estuary, however based on the data and evidence presented in this work it seems unlikely that this has happened, and other factors such as estuarine hydrodynamics may account for the differential concentrations.

Hematite is present in trace amounts in all the samples indicating that it is a relatively rare weathering product. As already noted it is present in significant quantities in one riverbank soil sample. Its presence may be due to supply from upstream or equally from intense weathering (Wilson, 2004) or alteration (Markusson and Stefánsson, 2011) of iron-bearing minerals in the estuary itself.

#### 3.6.5.2 Bioturbation

Bioturbation intensity (fig. 3.4D) appears highest in locations proximal to river inputs and lowest on the bayhead delta-top and at the marine end of the estuary. It is assumed that lugworm cast density is proportional to the number of lugworms living in a given area. The distribution may be due to the local environmental factors in the estuary. Negative impacts on lugworm cast density are stressful or unstable environments that do not lend themselves to burrowing such as i) gravelly or poorly sorted sediment as in the bayhead delta gravels; ii) very high energy environment such as those behind the spit. Conversely, a positive impact on lugworm cast density is the supply of fluvially-transported organic matter down rivers and creeks.

The distribution of mineral concentrations in worm cast sediment compared to surface locations (fig. 3.14 & 3.15) suggests that there is a subtle enrichment in inter-layer vermiculite and possibly chlorite relative to smectite in the sediment ingested by the worms. The cause of this difference may be the acidic environment in an *Arenicola*

worm gut, causing the partial infilling of the inter-layer spacing within smectite and/or inter-layer vermiculite (fig. 3.16). This seems likely given previous experimental work (Worden et al., 2006) indicating that the worm gut can weather minerals in fresh bedrock samples more intensely than undigested sediment.

Pyrite has variable concentrations across the estuary (fig. 3.9H), but highest concentrations in surface sediments are located in areas of lowest bioturbation intensity (fig. 3.4D). Pyrite in sediments forms in reducing conditions through the reaction of detrital iron bearing minerals with  $H_2S$ , which is formed through the reduction of dissolved sulphate in pore waters by bacteria (Berner, 1984). Un-compacted marine sediments flushed with sea water typically have low sulphide activity and pyrite tends to occur in anoxic offshore sediments. However pyrite can occur in organic-rich sediments where all  $SO_4^{2-}$  is removed by bacterial reduction to form sulphides (Tucker, 2001). Pyrite is generally absent in terrestrial settings due to the low concentrations of dissolved sulphate in sediments in these environments and the high oxidation state (Berner, 1984), and this probably explains its paucity in hinterland samples.

Field observations indicate that reducing conditions occur at a shallow depth under large parts of the estuary. The locations where high concentrations of pyrite are found in estuary sediments could indicate that only these locations have particularly reducing

conditions. The high concentration of pyrite in relatively unbioturbated sediment may reflect the impact of bioturbation on the oxidation state of sediments. Where sediment has been bioturbated it might be expected that oxygen levels are higher, where oxidation levels are raised the iron-bearing minerals within the sediment are less prone to react with H<sub>2</sub>S and form pyrite.

#### 3.6.5.3 Physical processes

The interaction of fluvial and marine waters is augmented by the cyclicity of a tidal prism moving up and down an estuary twice daily producing a complicated series of transport and deposition processes within estuaries. With increasing salinity, flocculation processes result in the deposition of clay minerals and other flocculated material (Gibbs, 1967; Gibbs, 1985). The increasing salinity is coincident with higher flow velocities at the turbidity maximum (Geyer, 1993; Park, 1999), potentially re-suspending and breaking apart deposited flocculated material. The balance between these two competing processes will vary considerably in space and through time. Factors which will have a bearing on the deposition of sediment are likely to include: estuary geometry and geomorphology, tidal range, position in the lunar and diurnal tidal cycles, local weather conditions, river discharge rate, concentration of biological matter, clay minerals types and their source (fluvial or marine) and concentration, clay mineral particle size and geometry, clay mineral specific gravity and clay mineral

chemical composition and relative charges (Meade, 1972; Feuillet and Fleischer, 1980; Chamley, 1989; Geyer, 1993; Crump et al., 1998; Park, 1999; Allen, 2000; Shi and Zhou, 2004; Mitchell and Soga, 2005; Manning et al., 2006; Baugh and Manning, 2007; Galler and Allison, 2008; Wu et al., 2012;).

The effects of geochemical alteration and biological alteration has been considered and it is useful to discuss physical processes which could produce the mineral concentration trends noted. The focus of this work is concerned principally with the distribution of clay minerals and for this reason, relative clay mineral concentrations are treated separately to relative non-clay mineral concentrations.

#### *Estuary clay minerals*

Mapped relative clay mineral distributions in the estuary show that smectite tends to dominate, with lesser amounts of inter-layer vermiculite and chlorite (fig. 3.8). Smectite concentrations tend to be highest close to the stream input on the northern side of the estuary (fig. 3.8C), and in an area of the estuary north of the bayhead delta. These areas are characterised by relatively low modal grain-size and high fine fraction content and are also generally very poorly sorted. Smectite concentrations plotted against sorting and fine fraction content (fig. 3.10 A&B) show that an increase in fine fraction content and a decrease in sorting results in a slight increase in smectite content of sediments. This is supported, in part, by the relative

decrease in inter-layer vermiculite in the same areas (fig. 3.8B), and an inverse distribution when inter-layer vermiculite is plotted against fine fraction content and sorting (fig. 3.8 C&D). Cross-plots of relative clay mineral concentrations show that where the smectite is concentrated in estuary sediments it is at the expense of both inter-layer vermiculite and chlorite (figs. 3.11A, B&C).

Relating mineral concentrations to physical parameters (table 3.5) may be important when considering the settling velocity of smectite and inter-layer vermiculite. The size, shape, specific gravity and specific surface area can all have an impact on how a suspended clay mineral behaves in a moving water body. Comparison of smectite and inter-layer vermiculite indicates that smectite is generally finer-grained, can have a lower specific gravity (although there is overlap in these values) and that due to the expansion of the inter-layer zone, can have a very high specific surface area when compared to inter-layer vermiculite (Mitchell and Soga, 2005). In simple terms, this may mean that the smectite is more easily suspended than inter-layer vermiculite and is therefore more likely to be concentrated in less-well sorted and finer grained sediments than in better sorted coarse grained sediments. The shape of smectite may also play a part, with the mineral often forming very thin sheets (Mitchell and Soga, 2005), which are very likely to remain suspended in water. This is supported experimentally where smectite is known to



Mineral	Shape	Size	Specific Gravity	Specific surface m <sup>2</sup> /g	Notes
Smectite	laths or films	long axis: <1-2µm, max; short axis: 1/100 of width	2.2-2.7	50-120, expansion of inter-layer can create spec surface gravity of 840	
Chlorite	flakes (similar to illite)	1µm	2.6-2.96	65-100	similar to mica
Inter-layer vermiculite	flakes	long axis: up to 10µm; short axis: 0.003-0.1µm	2.60-3.0	65-100	similar to mica

**Table 3.5 - Clay mineral physical parameters, based on Mitchell & Soga, (2005)**

where increased smectite concentrations in areas proximal to river and stream inputs has been noted (Sarma et al., 1993).

Chlorite may be regarded as somewhere between these two end members with a similar specific gravity and specific surface characteristics to inter-layer vermiculite, but are typically smaller in size (Table 3.5; Mitchell and Soga, 2005).

If smectite is considered to be more easily suspended than inter-layer vermiculite, the high energy environments toward the front of the estuary may either suspend or re-suspend smectite leaving a relatively high concentration of inter-layer vermiculite towards the marine end of the estuary. This may occur particularly during the middle stages of the flood and ebb tides when sediment velocities peak. During the slackwater phase of flood and ebb tides, flow velocities are low, giving smectite an opportunity to deposit. The primary issue is that smectite is found in all of the fine fraction sediments in significant quantities, and this interpretation would only account for a certain fraction of the fine fraction (possibly the smallest, lightest most easily

suspended fraction). Furthermore, the data presented only account for the fine fraction of the sediment ( $<0.2 \mu\text{m}$ ), the coarsest clay mineral aggregates may be greater than  $0.2 \mu\text{m}$  (Table 3.5). The concentrations of chlorite in the estuary fine fractions (Figs. 3.8A & 3.11) exhibit less systematic variations than smectite or inter-layer vermiculite. However there is a subtle increase in chlorite where smectite concentrations are lower and there is no observed variation trend in chlorite and inter-layer vermiculite concentration. This may suggest that chlorite is less affected by estuarine dynamics.

In summary, distinguishing the processes which may control clay mineral concentrations within estuary sediments is a challenge. It appears that smectite and inter-layer vermiculite (and possibly chlorite) may be controlled by the movement of the tidal prism. Identifying if salinity or turbidity within the wedge controls deposition within the estuary is presently not possible.

#### *Estuary non-clay minerals*

Relative calcite and aragonite content show a similar distribution pattern (figs. 3.9 A&B), and this is confirmed when the concentration of these minerals are cross-plotted (fig. 3.12A). Carbonate mineral concentrations are highest in the west of the estuary closest to the marine influence, and decrease towards the east, which indicates a marine source for carbonate material. Carbonate mineral concentrations in estuary sediments north of the bayhead delta, close

to the washover beach are also high, and this may support the suggestion that this area receives sediment transported during storm events at high tide.

Distribution maps of the relative quantities of quartz, plagioclase and pyroxene in the fine fraction are broadly similar (figs. 3.9 D, E&F). This similarity of distribution is supported by mineral cross-plots (figs. 3.12B, C&D), with a positive correlation between all three minerals suggesting that there is no differential alteration during weathering. Concentrations of these three minerals are lowest in areas of high carbonate content, probably reflecting dilution relative to the marine sediment source.

### **3.7 Conclusions:**

1. XRD and FTIR analysis indicate that the three main mineral phases within all surface sediments analysed are a dioctahedral chlorite, inter-layered vermiculite and a nontronitic smectite.
2. The basalt parent material of the weathering products sampled in glacial, riverbank soil, estuary and worm cast sediments has a strong control on the eventual clay minerals developed (fig. 3.17). This produces a suite of clay minerals that vary in concentrations, but are present within all sediment types.
3. Distribution maps and mineral concentration cross-plots indicate that smectite is the most dominant clay mineral and is found in highest concentration in areas of lowest energy around the margin

of the estuary and close to stream inputs. Conversely, inter-layer vermiculite and chlorite tend to be concentrated in areas of higher energy closer to marine-dominated influence.

4. Differential concentration of clay minerals in estuary sediments may be related to the hydrodynamic properties of the clay minerals. In the following order: inter-layer vermiculite, chlorite and then smectite maybe more easily suspended and transported out of the estuary (fig. 3.17).
5. Chemical alteration of clay minerals within the estuary through ingestion by arenicola worms (fig. 3.17) appears to confirm previous experimental work, with indications that the worms create conditions where inter-layer spacing in smectite and inter-layer vermiculite are being filled or partially filled to produce inter-layer vermiculite or chlorite.

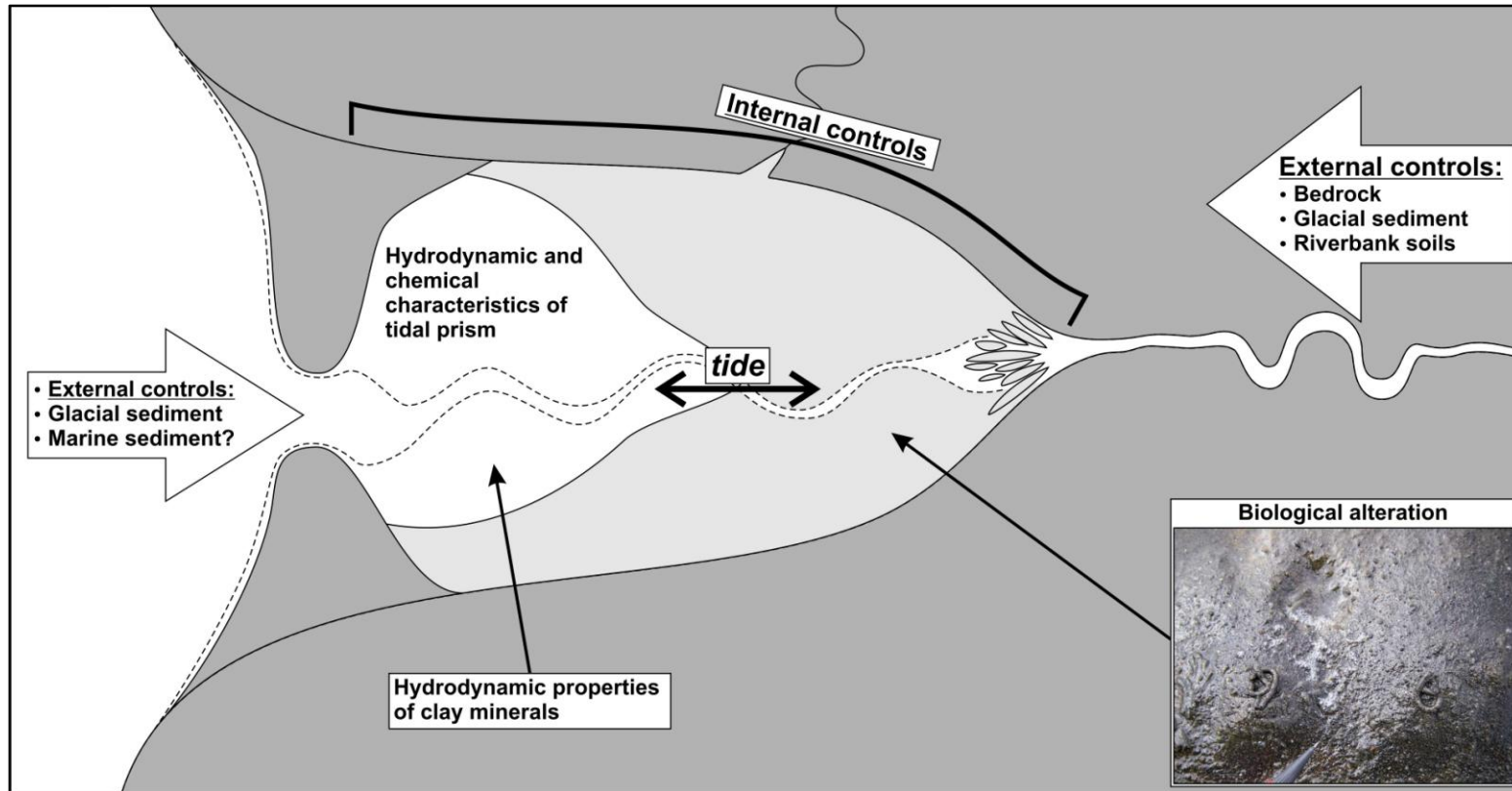


Figure 3,17 Summary figure outlining the main controls on clay mineral formation and distribution in the Leirárvogur Estuary. Controls on estuarine clay minerals external to the estuary include: bedrock type, glacial sediment, riverbank soils and marine sediments. These factors control the types of minerals present. Internal controls on estuarine clay minerals include: hydrodynamic and chemical characteristics of the tidal prism (partially controlled by relative sea level and estuary morphology), bioturbation and the hydrodynamic properties of the clay minerals. These factors affect the concentration of the clay minerals present through chemical alteration of the clay minerals and the concentration of the minerals within parts of the estuary intertidal zone.

## **4. Clay minerals in the sun: Mineralogy and distribution of clay minerals in the Anllóns Estuary, Galicia, Spain**

### **4.1 Abstract**

Detailed analysis of clay minerals and non-clay mineral concentrations within the fine fraction of estuarine sediments in the Anllóns Estuary, Galicia, northwest Spain, was determined utilising X-ray diffraction and infrared spectroscopy. This enables the origin, development and distribution of the clay minerals within a mid-latitude estuarine environment to be constrained.

Chlorite, muscovite and kaolinite are present in variable concentrations throughout the estuary. Chlorite and muscovite are likely to be detritally derived, while kaolinite is a result of weathering within the drainage basin. Marine reworking of sediment appears to reduce the concentration of clay minerals and increase carbonate mineral concentration in the marine-dominated sections of the estuary. In lower energy and fluvial-dominated sections clay mineral concentrations increase and carbonate concentrations decrease. Relative clay mineral (carbonate-normalised) distributions show that kaolinite and muscovite have an inverse concentration pattern, which may be related to the hydrodynamic behaviour of these different clay

minerals. Pyrite has higher concentrations where chlorite is deficient, which indicates the alteration of chlorite to pyrite under reducing conditions. Mineral alteration through bioturbation of sediments does not appear to occur and may be related to the unreactive nature of pre-weathered sediments.

## **4.2 Introduction**

The study of clay minerals and their distribution in modern estuaries can be a useful tool for understanding sediment provenance, transport pathways and depositional controls in coastal settings (Chamley, 1989; Weaver, 1989; Algan et al., 1994). Estuaries are particularly dynamic coastal settings where the interplay between fluvial and marine processes can be examined (Dalrymple et al., 1992). An understanding of clay minerals evident in a modern estuary, and some of the early post-depositional effects of geochemical and biological interaction in these settings, may provide valuable insight to both modern systems and ancient, deeply-buried sediments.

Clay minerals found in soils and sedimentary environments occur through three processes (Millot, 1964; Wilson, 1999): 1) *detrital inheritance*, where clay minerals form in pre-existing rocks which are subsequently weathered and eroded, for example detrital chlorite weathering from a schist; 2) *transformation*, whereby the silicate structure of the mineral is maintained, but there is extensive changes within the inter-layer space of the structure, for example mica

weathering to vermiculite due to the loss of  $K^+$ ; 3) *neof ormation* where the clay mineral develops from solution, gels or amorphous material, for example the development of kaolinite in tropical settings. In each of these processes the parent materials and local environmental conditions (physical, geochemical, biological and microbiological) play a major role in controlling the types of clay minerals generated.

Although the underlying processes of clay mineral formation outlined above are broadly known and accepted, the relationship between site of formation and the site of deposition of clay minerals is still not well constrained despite being the subject of a growing body of literature (see reviews in: Chamley, 1989; Weaver, 1989; Wilson, 1999). Studies have shown that sediment source rock-type and soils within river drainage catchments, as well as offshore sediments moved onshore, play a key role in controlling the range and distribution of clay minerals in coastal settings (e.g. Taggart and Kaiser, 1960; Hirst, 1962; Schubel, 1972; Feuillet and Fleischer, 1980; Allen, 1991; Pandarinath and Narayana, 1992; Sarma et al., 1993; Patchineelam and de Figueiredo, 2000; Belzunce-Segarra et al., 2002; Sionneau et al., 2008; Bernárdez et al., 2012).

#### **4.2.1 Estuarine dynamics**

The nature of the physico-chemical interaction between river and marine water bodies can have an important impact on where clay minerals are deposited.

#### 4.2.1.1 Turbidity maximum

Within estuaries, the turbidity maximum is the point at which marine and fresh waters meet forming a surface. This is a region of locally-elevated suspended matter content ( Postma, 1967; Geyer, 1993) and its position within an estuary can vary seasonally with river flood events ( Schubel, 1972; Sarma et al., 1993) and with a much higher frequency during the tidal cycle and spring-neap-spring tidal cycle (Allen et al., 1980). Deposition from suspension tends to occur at this point during the slackwater phases of the tidal cycle, with sediment being eroded and re-suspended during the rising and falling stages (Meade, 1972; Park, 1999). Depending on the nature of the estuary this may result in preferential deposition of suspended matter in the areas of the upper tidal limit and around the margins of the estuary, whereas sediment deposited at low tide also becomes re-suspended during the next rising tide (Allen, 2000). In a field study from the Loire estuary (Gallenne, 1974), montmorillonite was reported to be concentrated relative to illite in suspended material moving up and down the estuary with the tide. Montmorillonite was interpreted to remain suspended while other clay minerals were deposited, with montmorillonite only falling from suspension during slackwater phases.

In the James River Estuary (Feuillet and Fleischer, 1980; Chamley, 1989), concentrations of two suites of clay minerals, marine- and river-supplied, show distinct relative changes in concentration. River

supplied clay minerals were reported as kaolinite, illite and vermiculite, while marine clay minerals were illite, chlorite and montmorillonite. An increase in the suite of marine-sourced clay minerals occurs from the tidal limit (turbidity maximum) down to the marine end of the estuary, with a concurrent decrease in the river-supplied suite of clay minerals over the same section. The reverse relationship occurs from the tidal limit, up the estuary. This indicates that clay minerals in the James River Estuary are equally diluted, with internal mixing at the interface between river and marine waters within the estuary being the main control.

#### 4.2.1.2 Saline waters

In coastal environments, ions, clay minerals and biogenic matter flocculate to form aggregates (Eckert and Sholkovitz, 1976; Sholkovitz et al., 1978; Eisma, 1986). By definition, saline marine water has higher ion content than that of particle-rich river water. In rivers, suspended particles are kept apart by a positively charged layer of ions around the particle, on mixing with sea water this charged layer is compressed enabling particle attraction to occur (Gibbs, 1983). Aggregation of material develops from particle collision through Brownian motion processes, differential settling velocity of particles or turbulence (Weaver, 1989). In estuaries, the saline front is often associated with the turbidity maximum.

Experimental work on static differential flocculation using a large number of clay mineral mixtures from modern sedimentary environments (Whitehouse et al., 1960) indicated that with increasing salinity illite and vermiculite, then kaolinite and chlorite, and lastly montmorillonite (dioctahedral smectite) settle out of a still water column. Two further studies using standards of illite, kaolinite and montmorillonite (but note a different montmorillonite standard used in each study) simulated flocculation in a turbulent coastal setting and reported different and contrasting orders of deposition. Edzwald and O'Mella, (1975) found first montmorillonite, then kaolinite and illite were deposited, whereas (Gibbs, 1983) found the reverse: illite then kaolinite and lastly montmorillonite. These conflicting findings are probably due to different experimental protocols, and further hindered by the difficulty in recreating complex and dynamic environments in the laboratory. In summary, there is no consensus about the relative order of clay mineral flocculation and settling.

#### **4.2.2 Geochemical development**

While the majority of the literature on clay minerals in estuaries has focused on the depositional controls, a few studies have also looked at the geochemical development of clay minerals within coastal settings and their formation in adjacent marine shelf waters.

#### 4.2.2.1 Geochemical alteration

Large scale chemical transformation of clay minerals can occur in coastal environments, with cation exchange within clay mineral inter-layer zones normally resulting in the adsorption of Na, K and Mg at the expense of Ca. Typically, it has been suggested that there is no mineral-structural change and the cation incorporation is generally considered to be reversible (Russell, 1970; Chamley, 1989). A study of reportedly estuarine Mississippi Delta sediments reported the rapid uptake of K<sup>+</sup> by smectite in brackish waters (Hover et al., 2002) and a similar loss of K<sup>+</sup> is noted in marine sediments from Rio Ameca, Mexico (Russell, 1970). Further studies on core sediments, show that plagioclase feldspar, pyroxene, olivine, and volcanic ash, in marine slope sediments north of Sakhalin Island, become progressively transformed with depth (down to 25m) into smectite through chemical alteration (Wallmann et al., 2008). Neof ormation of clay minerals from biogenic silica also commonly occurs on marine shelves (Michalopoulos and Aller, 2004; Presti and Michalopoulos, 2008) and this has been repeated experimentally (Michalopoulos and Aller, 1995; Michalopoulos et al., 2000).

#### 4.2.2.2 Biological alteration

An important factor in understanding the genesis alteration and distribution of clay minerals in modern estuarine environments is the role of bioturbation in the production of clay minerals. Experimental

studies have shown that the conditions within annelid worm guts, such as *Arenicola marina*, can result in the generation of clay minerals such as kaolinite, illite and berthierine from un-weathered mafic rock (McIlroy et al., 2003; Needham et al., 2004; Needham et al., 2005; Worden et al., 2006; Needham et al., 2006). The rate of clay mineral formation in biologically-digested sands can be 2-3 orders of magnitude higher than that of un-ingested sediment (Needham et al., 2006). Similarly, the large numbers of these organisms in intertidal environments can lead to the rapid turnover of sediment.

The distribution of clay minerals is typically influenced by a variety of factors, including hinterland source rock, salinity variations, tidal sediment dynamics, geochemical alteration and potential biological interactions. A quantitative understanding of the types and distribution of clay minerals in modern coastal settings could provide important insights into the physical controls on clay mineral distribution, and enable the development of models for the prediction of clay mineral evolution during burial and diagenesis. The aim of this paper is to distinguish the types and distribution of clay minerals present in the Anllóns Estuary, Galicia, Spain; and to understand the underlying controls on formation and distribution:

1. What minerals are present within the fine fraction of the Anllóns Estuary and where did they form?

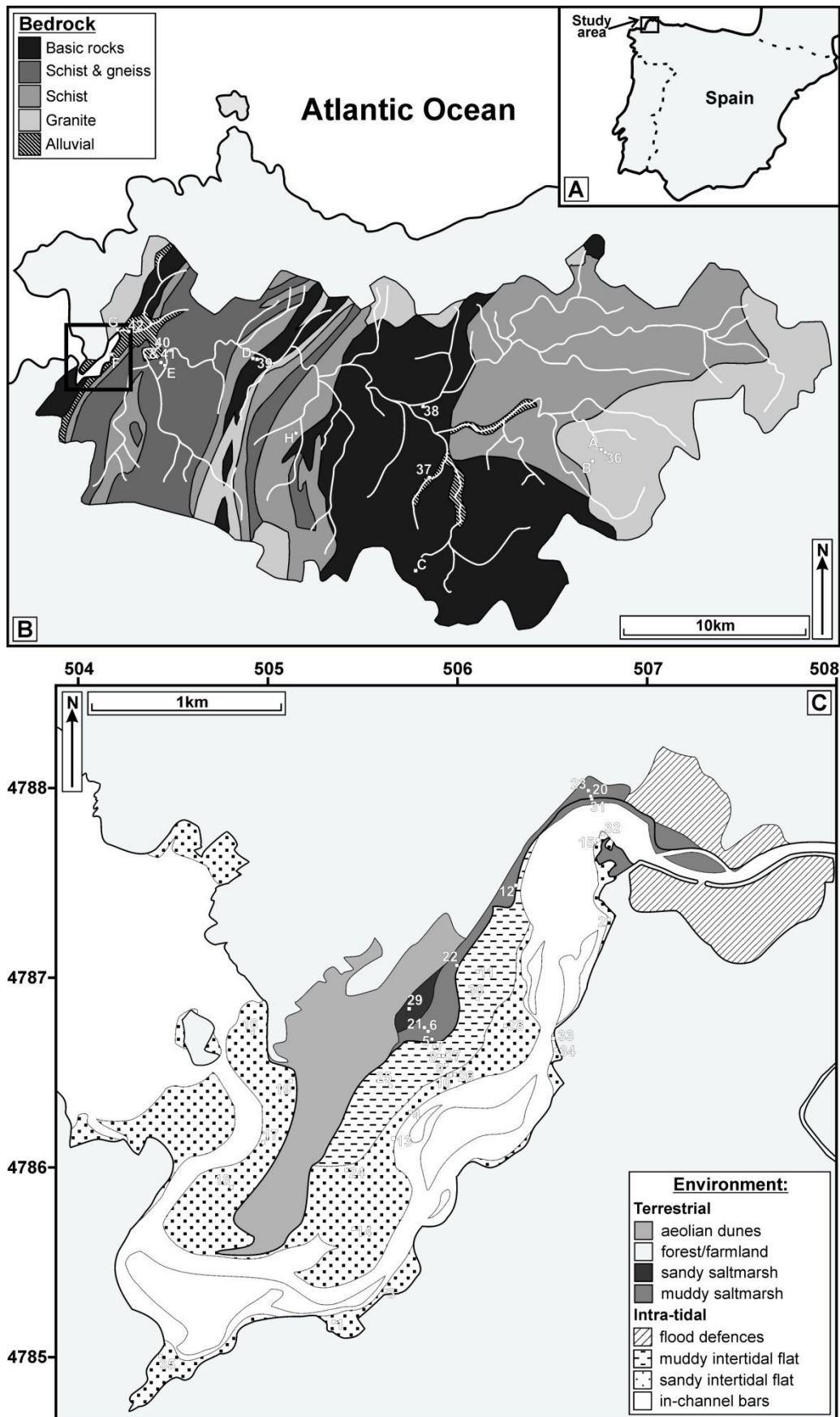
2. What is the distribution of the clay minerals in the surface sediment and what are the controls on this distribution pattern?
3. What effect does biological interaction with sediment have on clay minerals and their distribution?

### **4.3 Study area**

The Anllóns Estuary and surrounding study area are located in Galicia on the northwest coast of Spain (fig. 4.1A). A summary of the geological history, geomorphology and mineralogy of the study area is presented below.

#### **4.3.1 Geology and tectonics**

The geology of the study area is dominated by a north-south structural trend resulting from the Late Devonian to Late Carboniferous Variscan Orogen, which overthrust a series of allochthonous complexes onto the Gondwanan margin (fig. 4.1B). Two regional metamorphic events are associated with the Variscan orogen. The first during the early Variscan was a high pressure Barrovian-style metamorphic event related to Nappe emplacement, the grade of metamorphism and the types of minerals are variable and dependent on position within the rock pile. The second high temperature metamorphic episode is strongly associated with granite intrusions, these produced inverted metamorphic gradient with underlying cold rocks (Dallmeyer et al., 1997).



Outcropping footwall units are primarily schistose meta-sediments and granites. Hanging-wall rocks are more variable and include gabbroic and ultramafic ophiolitic and lower continental crust units plus basalt alkaline granitoids and low grade metamorphosed terrigenous sequences (Dallmeyer et al., 1997; Llana-Fúnez and Marcos, 2001). The mineralogy of bedrock in the Galician region is complex due to the juxtaposition of various terranes associated with the Variscan event, and the related phases of metamorphism. A list of the primary accessory minerals in the Anllóns River catchment are outlined in Table 4.1 (Gil Ibarguchi and Ortega Gironés, 1985). The phyllosilicate minerals chlorite and muscovite occur as primary minerals within the rocks sourcing the estuary and its catchment, and are therefore considered to be detrital.

<b>Unit</b>	<b>Main minerals</b>	<b>Accessory minerals</b>	<b>Formation</b>
Mica schist	Quartz, plagioclase, phengite (high Si:Al ratio muscovite), rutile	Biotite, chloritoid, kyanite, garnet	Semi-pelitic sedimentary sequence
Gneiss	Quartz, biotite, plagioclase, phengite, garnet	Apatite, rutile, tourmaline, allanite (epidote)	Semi-pelitic sedimentary sequence
Calc-alkaline orthogneiss	Quartz, microcline, oligoclase, biotite, garnet, phengite	Zircon, apatite, allanite, rutile, tourmaline, fluorite	Metamorphosed volcanic/sub-volcanic origin
Felsic gneiss	Quartz, albite, zoisite/clinozoisite (epidote), garnet, phengite	Amphibole, biotite	Metamorphosed volcanic/sub-volcanic origin
Eclogite	Garnet, amphibole, barroisite (Na-Ca amphibole)/glaucophane	Phengite, quartz, kyanite, rutile, zoisite	Deformed basic dykes
Amphibolite	Plagioclase, (An <sub>25-50</sub> ), ferro-tschermakitic hornblende (Al subs for Si)	Biotite, garnet, opaques, rutile, sphene, epidote	Igneous origin

**Table 4.1 - Mineralogy and formation of the main rock units in Anllons Basin (Information from: Gil Ibarguchi and Ortega Gironés, 1985).**

### 4.3.2 Weathering and soils

Galician granites can weather to generate large, deposits of kaolinite (Wilson, 1998; Fernández-Caliani et al., 2010). A stable isotope study on the origin and evolution of a kaolinite deposit at Nuevo Montecastelo in Galicia (Fernández-Caliani et al., 2010) reported that the deposit developed through a large scale supergene event leaching soluble elements during the Tertiary. Na, Ca and minor Mn, Sr, P & U first leached from plagioclase and apatite, and then during a later stage the partial dissolution of K-feldspar and muscovite released K, Rb, Cs and Ba. A weathering study of granite outcrops in Galicia (Calvo et al., 1983), reported the development of gibbsite (along with kaolinite and beidelite) from the alteration of plagioclase. Gibbsite was also noted in soils and saprolites in Galicia (Macias Vazquez, 1981) formed during the earliest stages of low temperature weathering from feldspar, particularly in well-drained, unsaturated settings.

Smectite is a rare secondary mineral in Galicia, but it has been reported to form from the weathering of muscovite inclusions in feldspar crystals in granite-derived saprolites (Taboada and García, 1999). Also noted in that study was the weathering of the edges of biotite grains to Fe-oxyhydroxides and interstratified biotite-vermiculite. Fernandez Sanjurjo et al. (2001) also reported undated soil profiles (developed on gabbro) consisting of inter-layered kaolinite-smectite, gibbsite and goethite, beneath modern soils containing hydroxyl inter-

layered vermiculite, kaolinite, gibbsite and maghemite within the Anllóns River basin. That study suggests that the inter-layered kaolinite-smectite formed initially as smectite under less intense leaching conditions, before subsequently becoming Al-enriched under stronger leaching conditions associated with a wetter climate. This was then covered by alluvium, forming a soil, subsequently reducing the effects of further weathering in the older profile.

### **4.3.3 Coastal clay mineralogy**

A number of studies have reported the range and concentration of clay minerals in bays, rias and estuaries around the north western Iberian coastline. Mineralogical analysis of sediments from Ria de Vigo (Southern Galicia), reported dioctahedral mica (illite or muscovite), kaolinite, plus minor gibbsite, chlorite and Fe-rich smectite; with a similar clay mineral suite offshore on the Galician Platform and in deeper waters of the Celtic Sea (Belzunce-Segarra et al., 2002). The authors of that study suggest the suite is generally consistent with a terrigenous source from the Galician hinterland, excepting smectite, which is reported as potentially forming authigenically in deep sea sediments due to its paucity in terrestrial soils. Transmission electron microscopy confirms the iron-rich chemistry of the smectite, and invokes possible alteration of volcanic material or low temperature reactions of hydroxides and biogenic silica in its formation. This is supported by another survey (Oliviera et al., 2002), which indicated

that the proportion of smectite in the clay fraction of Iberian Shelf sediments increases towards the open shelf, away from ria and estuary sediment supply. Chlorite was also noted, with highest concentrations closest to the rias, indicating supply from sediment that was derived from onshore. The study also found changes in crystallinity (based on the height and half-height width of the 7Å peak using XRD) in illite and kaolinite from river to marine environments. This is reported to be controlled by the variability in geochemical conditions from the nearshore across the shelf. Illite crystallinity increased, in shelf sediments compared to river sediment, possibly due to the tendency of magnesium and iron to replace potassium and aluminium in seawater. While kaolinite decreased in crystallinity in the outer shelf sediments compared to inner and middle shelf sediments, possibly due to chemical degradation.

On the northern Galician coast, studies of sediment supplied to three rias (Bernárdez et al., 2012; Prego et al., 2012) reported a strong hinterland control on mineralogy. The study described discrete differences in ria mineralogy at the termination of northerly draining river catchments which follow the regional north-south lithological grain (fig. 4.1). An increase in muscovite in the Viveiro Ria reflects a drainage basin dominated principally by granite; whilst in the Ortigueira Ria, serpentine (chrysolite) and amphibole (riebeckite)

concentrations are higher due to a mafic and ultra-mafic complex in close proximity.

#### **4.3.4 Relative sea level history**

A study of Late Pleistocene raised marine and continental deposits preserved in embayments and rias along the north-west Galician coast (Alonso and Pages, 2007) provide insight into the relative sea level history of the area. Gravels and sands dated at 100-54 ka deposited on a polycyclic abrasion surface 2-3 metres above present day sea level mark the previous inter-glacial period. Overlying this, soils, debrites and solifluction features are indicative of a terrestrial, periglacial environment during the earliest glacial stages and the beginning of relative sea level fall. As base level continued to fall, swamps developed depositing muds and peats. The final unit dated at 25-15 ka (contemporaneous with the last glacial maximum) is composed of breccias, gravels and conglomerates forming both river channel-fills and debrites.

In the upper reaches of Ria de Vigo, the San Simón Bay forms an estuary at the confluence of three rivers. Sediment cores from this estuary indicate an aggradational development from estuary channels to abandonment and tidal flat development dated at 3.4-3.1 ka (Pérez-Arlucea et al., 2007). This is followed by incision, and then another phase of channel development and tidal flat development dated at 0.98-0.78 ka. Pérez-Arlucea et al. (2007)

interpreted this with respect to North Atlantic climatic oscillations controlling sediment supply rates to the basin. A colder (wetter) climate period supplied increased volumes of sediment resulting in the infilling of channels and tidal flat development; with incision representing relative sediment starvation during warmer (drier) periods (Pérez-Arlucea et al., 2007).

#### **4.3.5 Anllóns estuary catchment**

The Anllóns Estuary, Galicia (fig. 4.1C) is a relatively deeply incised, partially-filled valley with one large river, the 60 km long Anllóns that drains a 516 km<sup>2</sup> catchment (Varela et al., 2005) comprised principally of soils developed from granite and schist (fig. 4.1B). One small stream drains into the south side of the estuary southwest of the spit (fig. 4.2A). The area has an oceanic climate with a mean annual rainfall of 1000 to 2000 mm/yr (Arribas et al., 2010).

Anthropogenic effects on river and estuary environmental conditions are low due to the lack of heavy industry in the area and along the catchment. Sections of the river downstream of the town of Ponteceso contain flood defences (fig. 4.2B), which permit flooding during high tide. The northern flood defence is an enclosed marshland partially filling through a network of channels (fig. 4.2C). The southern flood defence is open to the river and estuary channel and becomes completely covered at high tide (fig. 4.2D).

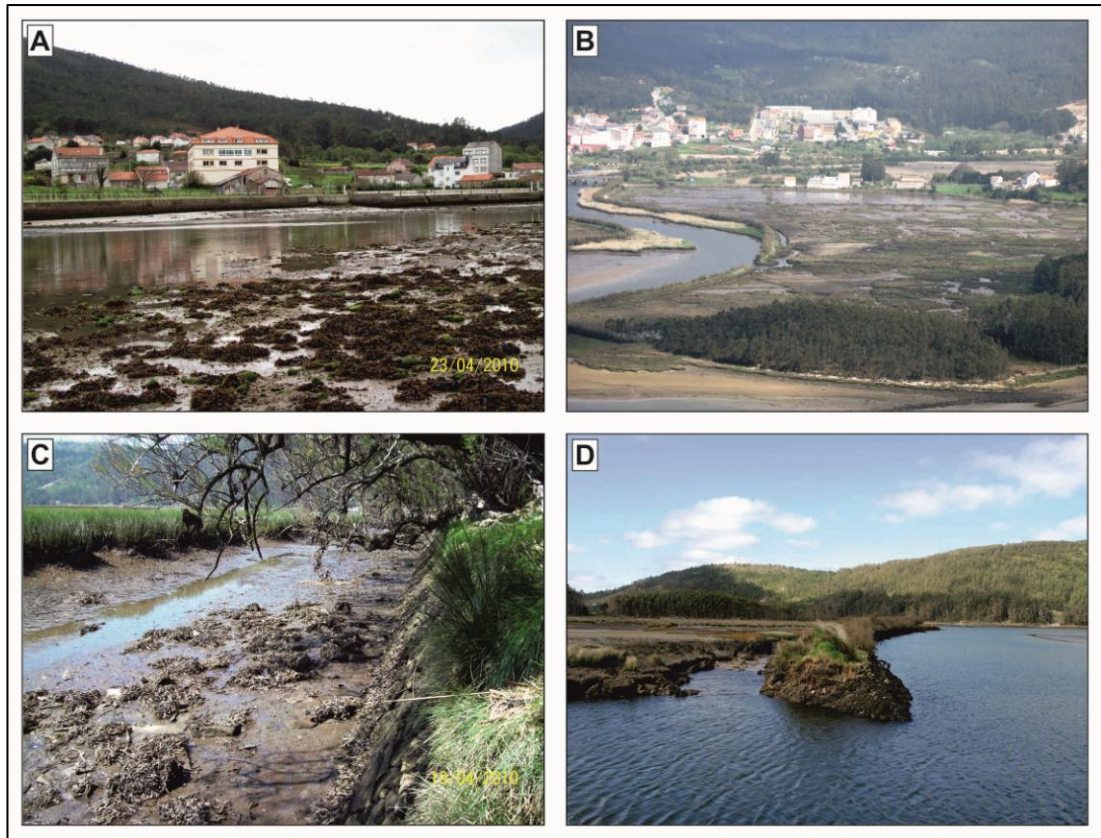


**Figure 4.2 - Photographs of upstream environments in Anllóns Estuary discussed in text. (A) Small river draining into south side of the estuary. (B) Managed flood defence. (C) Photograph of northern managed flood defence taken from retaining wall. (D) Southern managed flood defence with channel open to river.**

### **4.3.6 Anllóns estuary geomorphology**

The Anllóns Estuary is ~4km long, ~1km wide and has 4.0m maximum tidal range. Downstream of the managed flood defences the estuary channel turns 90 degrees toward the south-west (fig. 4.3A), seeming to follow the grain of the regional geological trend. The estuary channel has a variable width with a series of in-channel bars (fig. 4.3B) splitting its course. A large frontal sandy spit (fig. 4.3C) attached to the north side of the estuary protects the inner portion of the estuary and forces the main estuary channel around its tip. The spit is mantled by an extensive aeolian dune system (fig. 4.3D).

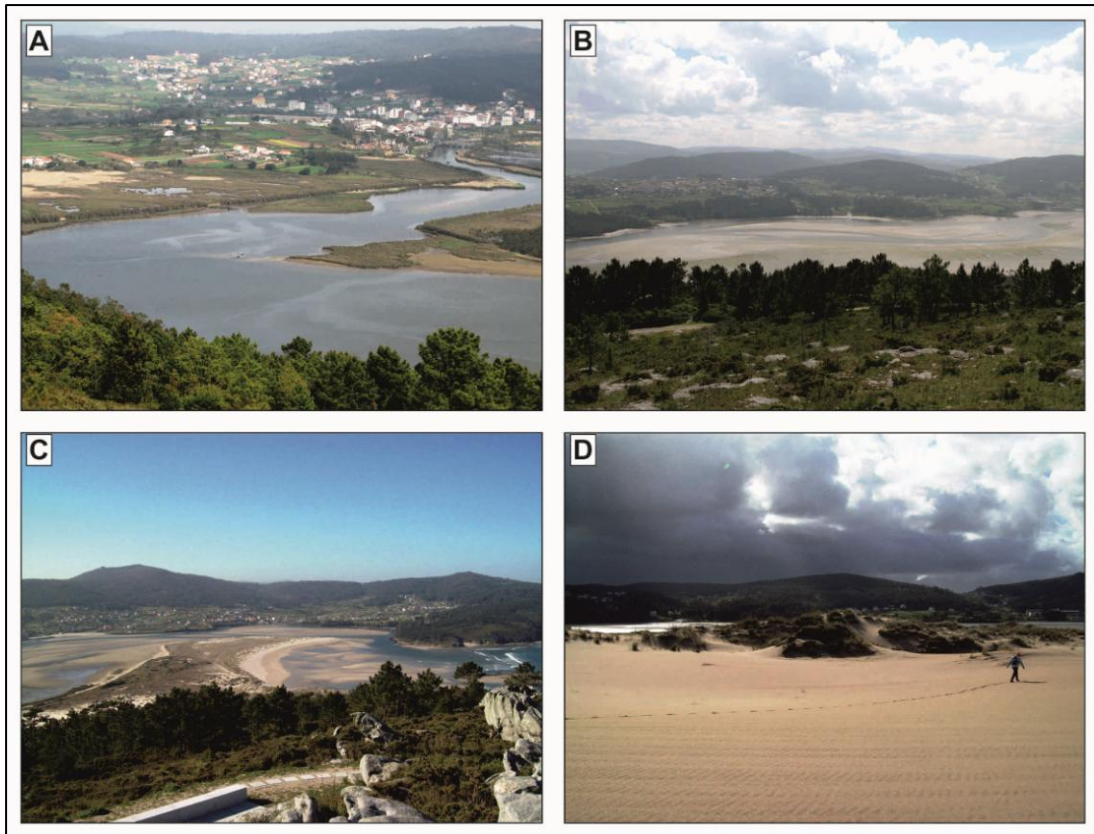


**Figure 4.3 - Photographs of Anllóns Estuary discussed in text. (A) ninety degree turn in main channel. (B) In-channel bars. (C) Frontal spit at estuary mouth. (D) Aeolian dune system mantling the frontal spit.**

The exposed tidally-influenced portions of the estuary have three components: intertidal to supra-tidal saltmarsh, intertidal mudflat and intertidal sand flat. The saltmarshes are principally developed in the middle and upper reaches of the estuary, with a large expanse on the northern western side of the estuary channel (fig. 4.4 A); the saltmarsh has a terraced edge of a variable height above the sandflat (fig. 4.4 A). Surface sediment underlying the saltmarsh is composed of sand close to the dune system, and becomes increasingly mud-rich up the estuary; the saltmarsh is cut by small creeks and channels which fill with water during high-tide (fig. 4.4 B&C). From the saltmarsh towards the centre of the estuary the muddy intertidal flat is flat-lying and

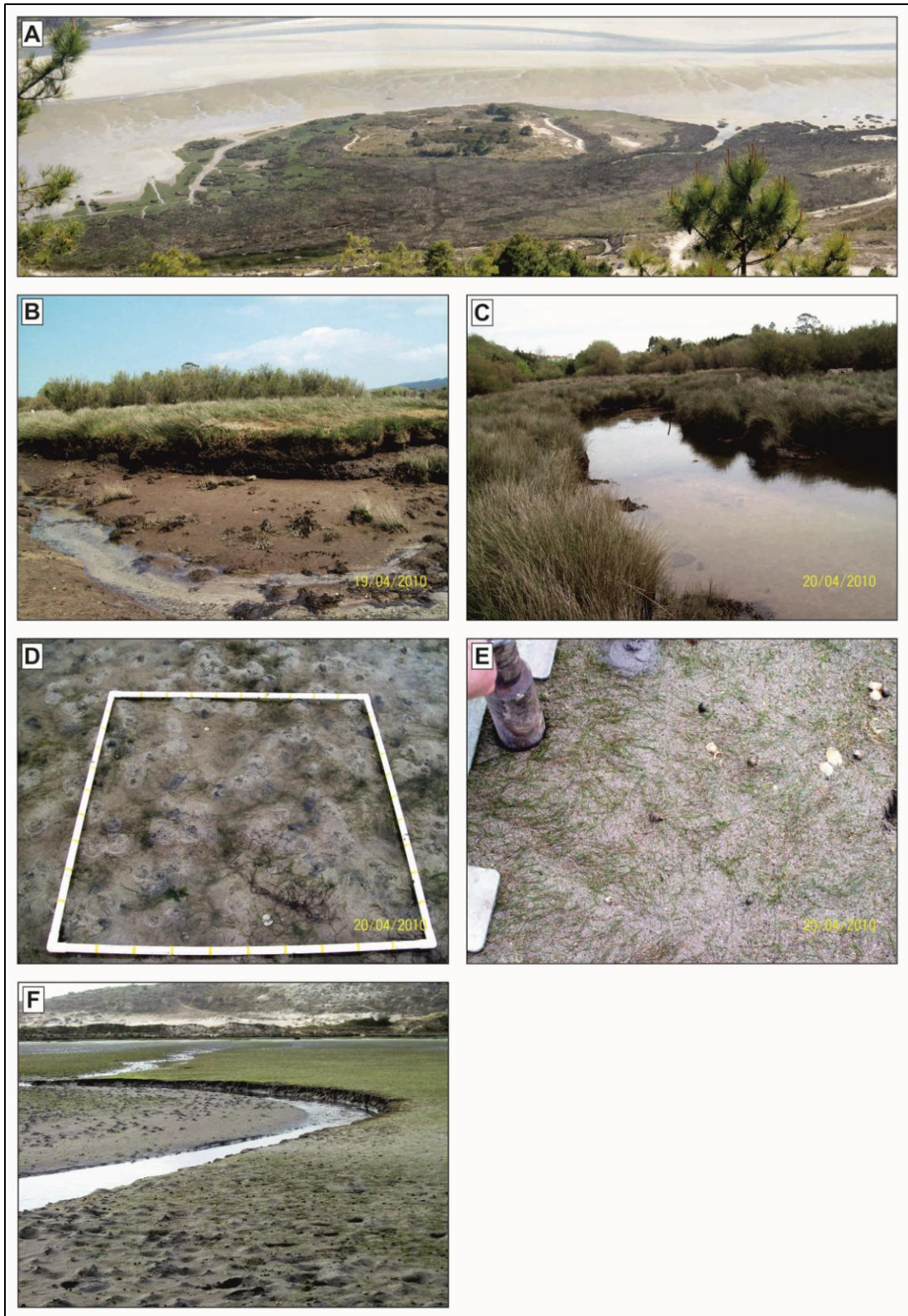


**Figure 4.4 - Photographs of estuary supratidal and intratidal environments in Anllóns Estuary discussed in text. (A) Saltmarsh on the northern side of the estuary. (B) Estuary terrace. (C) Saltmarsh creeks. (D) Muddy inter-tidal flat. (E) Heavily vegetated sandflat. (F) Meandering creek on muddy sand flat.**

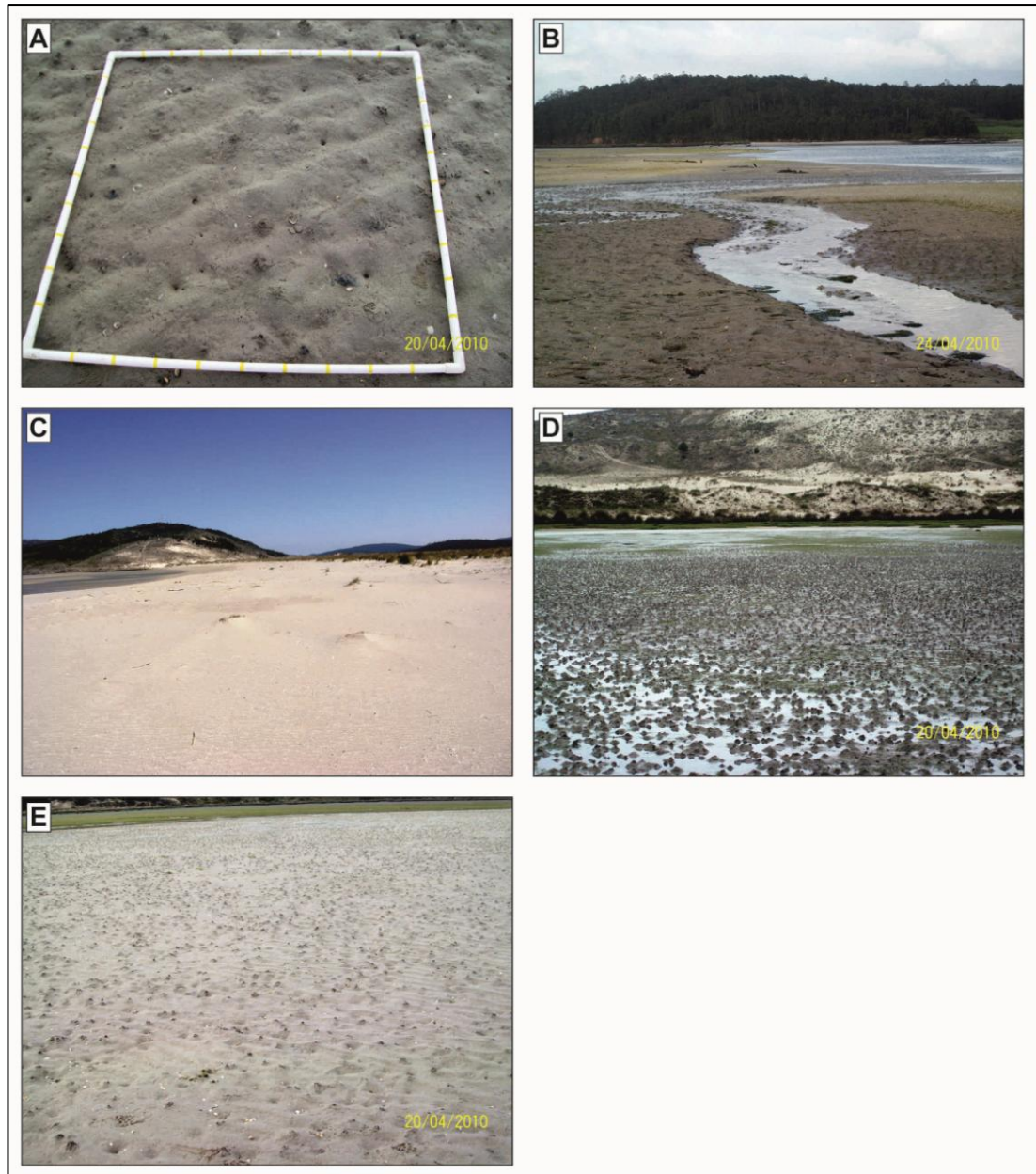


**Figure 4.5 - Photographs of intertidal environments in Anllóns Estuary discussed in text. (A) Sandy inter-tidal flat. (B) Inter-tidal flat creeks. (C) Shoreface at the front of the spit. (D) Excreted traces from annelid worms on the surface of the muddy sandflat. (E) Excreted traces from annelid worms on the surface of the sandflat.**

capped by a thin veneer (1-5 cm) of muddy sand (fig. 4.4D) that overlies relatively clean sand beneath. Plants such as sea grass also occur on the sediment surface (fig. 4.4E); with small, meandering tidal streams that drain the saltmarsh also crossing the flat (fig. 4.4F). Further towards the estuary channel, the sandy intertidal flat has very low

relief and is composed primarily of relatively clean sand with low silt and mud concentrations (fig. 4.5A). The sandy intertidal flat also has tidal creeks but these are straighter and drain into the main estuary channel at high tide (fig. 4.5B). The sandy intertidal flat continues around the headland created by the spit and connects with the shoreface at the estuary mouth (fig. 4.5C). The sandy and muddy intertidal portion of the estuary exhibit variable intensities of bioturbation by annelid worms (fig. 4.5D&E).

#### **4.4 Materials and methods**

Within the Anllóns Estuary and surrounding drainage basin forty-two sediment surface samples were collected (Table 4.2 & 4.3). Sample sites were chosen to give a wide and representative environmental spread. Eight hinterland rock samples were also collected to assess the mineralogical composition of the bedrock in the drainage basin (Table 4.4). Sample locations are shown in Figure 4.1, and environmental and sedimentological descriptions are given in Table 4.2 and 4.3.

Sediment grain size and sorting data (Tables 4.1 & 4.2) are based on laser granulometry using a Beckman Coulter LS200 (Beckman Coulter Incorporated, 2011). Slurry is made from a sediment sub-sample by adding calgon to de-flocculate sediment components. This is then added to the Coulter where the distributions of particles from 0.4  $\mu\text{m}$  to 2000  $\mu\text{m}$  are counted. Grainsize data presented were analysed

Map location	Setting	Estuary environment	Sediment description
1	Estuary	Intertidal sand flat	Moderately sorted medium sand
2	Estuary	Intertidal sand flat	Poorly sorted medium sand
3	Estuary	Intertidal sand flat	Moderately well sorted medium sand
4	Estuary	Intertidal sand flat	Very poorly sorted fine sand
5	Estuary	Supratidal saltmarsh	Very poorly sorted medium sand
6	Estuary	Supratidal saltmarsh	Poorly sorted medium sand
7	Estuary	Intertidal sand flat	Poorly sorted medium sand
8	Estuary	Intertidal sand flat	Poorly sorted medium sand
9	Estuary	Intertidal sand flat	Poorly sorted medium sand
10	Estuary	Intertidal sand flat	Poorly sorted medium sand
11	Estuary	Intertidal sand flat	Poorly sorted medium sand
12	Estuary	Supratidal saltmarsh	Moderately sorted medium sand
13	Estuary	Intertidal sand flat	Moderately sorted medium sand
14	Estuary	Intertidal sand flat	Moderately sorted medium sand
15	Estuary	Intertidal sand flat	Very poorly sorted medium sand
16	Estuary	Shoreface	Moderately sorted medium sand
17	Estuary	Shoreface	Moderately sorted medium sand
18	Estuary	Shoreface	Moderately sorted coarse sand
19	Estuary	Shoreface	Moderately sorted coarse sand
20	Estuary	Intertidal sand flat	Moderately well sorted medium sand
21	Estuary	Supratidal saltmarsh	Moderately sorted medium sand
22	Estuary	Supratidal saltmarsh	Very poorly sorted very fine sand
23	Estuary	Supratidal saltmarsh	Very poorly sorted fine sand
24	Estuary	Intertidal sand flat	Moderately sorted medium sand
25	Estuary	Intertidal sand flat	Poorly sorted medium sand
26	Estuary	Intertidal sand flat	Poorly sorted medium sand
27	Estuary	Intertidal sand flat	Poorly sorted medium sand
28	Estuary	Intertidal sand flat	Moderately well sorted medium sand
29	Estuary	Supratidal saltmarsh	Poorly sorted medium sand
30	Estuary	Intertidal sand flat	Poorly sorted medium sand
31	Estuary	Intertidal sand flat	Poorly sorted medium sand
32	Estuary	Intertidal sand flat	Poorly sorted medium sand
33	Estuary	Intertidal sand flat	Moderately well sorted medium sand
34	Estuary	Intertidal sand flat	Moderately sorted medium sand
35	Estuary	Intertidal sand flat	Poorly sorted medium sand

**Table 4.2 - Estuary sediment sample description table**

Map location	Depositional setting	Environment description	Sediment description
36	Terrestrial	Soil	Very poorly sorted very fine sand
37	River	River sediment	Poorly sorted medium sand
38	River	River sediment	Moderately sorted medium sand
39	River	River sediment	Poorly sorted medium sand
40	River	River sediment	Very poorly sorted fine sand
41	River	River sediment	Poorly sorted fine sand
42	River	River sediment	Poorly sorted fine sand

**Table 4.3 - Hinterland sediment sample description table.**

using Gradistat (version 6) software (Blott, 2008). All grain size and sorting values presented use the modified geometric (Folk and Ward, 1957) graphical measures.

Fine fractions (<2  $\mu\text{m}$ ) and coarse fractions (>2  $\mu\text{m}$ ) of the sediment were separated, with a fine fraction weight percentage (wt %) obtained for each sample location. Sediment sample preparation followed techniques outlined by Moore and Reynolds (1997) and Jackson (1969). Samples were homogenised, sub-sampled, and then air-dried at 60°C for 15-hours. Dry sub-samples were weighed then dispersed in tap water by means of four 5-minute cycles of ultrasonication and stirring. The supernatant liquid was decanted and the clay size fraction (<2 $\mu\text{m}$  e.s.d.) collected by centrifugation at 3500rpm for 30-minutes. The clay size fraction was then dried at 60°C for 15-hours, ground and then weighed to obtain the clay size fraction percentage.

Random powders of each fine fraction sub-sample were scanned using a PANalytical X'Pert PRO X-ray diffractometer employing Ni

filtered Cu k- $\alpha$  radiation, with a scanning range of 3.9-70.0°2 $\theta$  and using extended count times. PANalytical HighScore Plus software was used to semi-quantitatively ascertain the types of minerals in each sediment sub-sample from estuary and hinterland locations, as well as whole rock lithology samples. The XRD detection limits vary from mineral to mineral but for most well crystalline minerals concentrations down to approximately 0.5% were obtainable. Issues arose where minerals appeared poorly crystalline, in very low concentrations or where peaks overlapped. The semi-quantitative analysis produces whole number reports so reporting accuracy is  $\pm 0.5\%$ .

Samples were then glycolated for twenty-four hours and re-scanned over a range of 3.9 to 13.0 °2 $\theta$ , to assess the presence of expandable clay minerals (Moore and Reynolds, 1997).

An infrared spectral analysis on untreated sub-samples of the fine fraction was also performed on representative samples. 1.5mg of fine fraction sub-sample was mixed with 300mg of potassium bromide; this was hand-ground and then sintered at 10 tonnes in a press to produce a sample pellet of 0.5% concentration. The pellets were heated overnight at 150°C to remove any adsorbed water (Madejova, 2003). FTIR spectra were obtained with a Thermoelectron Nicolet 380 infrared spectrometer with an IR source, a germanium on KBr beamsplitter and a DTGS detector (Thermo Scientific, 2012).

Distribution maps of the modal grain-size, sorting, fine fraction and mineral concentration content within the fine fraction of estuary samples were generated, utilising the software package Surfer 7 (Golden Software, 2012). Using GPS co-ordinates collected in the field, individual point analyses were mapped. Interpolation between points was performed with a kriging algorithm (Journel, 1989; Cressie, 1990). Relative mineral concentrations were obtained by recalculating the concentrations of non-carbonate minerals to discount the presence of marine carbonate minerals (aragonite plus calcite). Indices of a range of minerals were also plotted utilising the quantitative measurement of mineral content within the relative fine fraction of the sediment samples. For example, the chlorite index was derived by dividing the concentration of chlorite by the sum of chlorite plus the other clay minerals present within the fine fraction. This enabled the relationship between the chlorite and the other clay mineral to be expressed without the effects of other minerals present within the fine fraction.

## **4.5 Results**

### **4.5.1 Clay mineral identification**

Clay minerals within the fine fraction (<2 µm) from surface sediment and worm cast samples were identified using X-Ray diffraction techniques, supplemented with information from FTIR spectroscopy.

#### 4.5.1.1 X-ray diffraction

Non-clay minerals of a quantifiable concentration identified in the fine fraction are gibbsite, quartz, plagioclase, K-feldspar, pyrite, gibbsite, calcite and aragonite, and peaks for most of these minerals are evident in figure 4.6.

Clay minerals are evident in the low angle inset (fig. 4.6B): broad peak at  $\sim 14.1 \text{ \AA}$ , a sharp peak at  $9.9 \text{ \AA}$ , a sharp peak at  $7.1 \text{ \AA}$  and a broad peak at  $\sim 7.2 \text{ \AA}$ . The  $9.9 \text{ \AA}$  peak corresponds to a mica (001) peak. The sharp nature of this peak indicates that it has a well-ordered structure and is likely to be detrital muscovite. The two peaks at  $7.1 \text{ \AA}$  and  $7.2 \text{ \AA}$  indicate that there are two discrete clay mineral phases, and these correspond to a kaolinite (001) and a chlorite (002) peak (Moore and Reynolds, 1997). Chlorite is confirmed by the presence of the  $14 \text{ \AA}$  peak (001). The sharp chlorite (002) peak also suggests that this is detrital rather than formed at surface conditions (Guggenheim et al., 2002). Similarly, the broad nature of the kaolinite (001) peak is indicative of an authigenic mineral possibly formed from the weathering of other pre-existing minerals such as feldspar (Wilson, 2004).

Glycolation of samples is commonly used to indicate the presence of expandable phases such as smectite or vermiculite. During this procedure glycol is adsorbed onto inter-layer cations between tetrahedral-octahedral-tetrahedral (TOT) sheets resulting in the

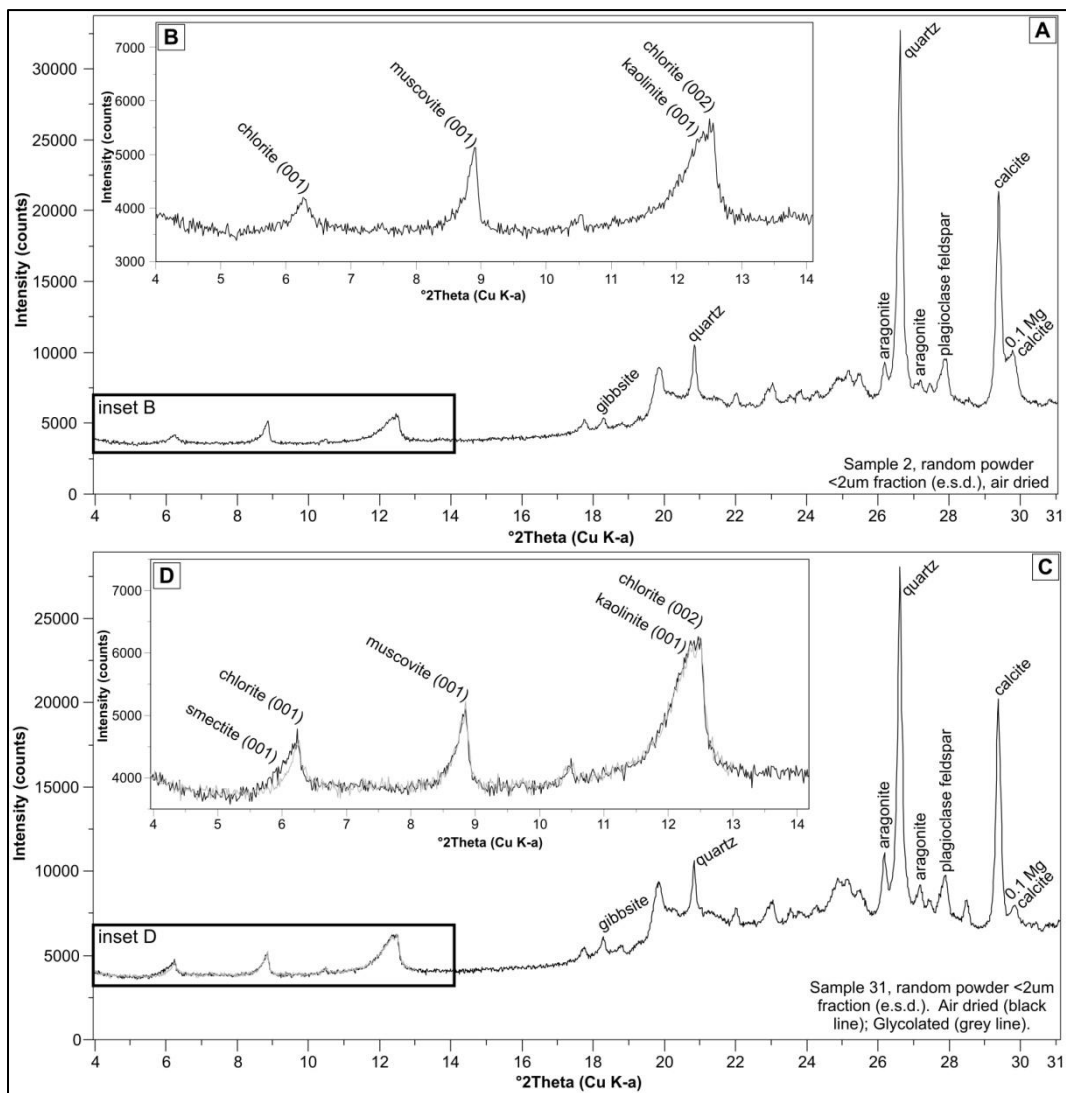


**Figure 4.6 - Representative XRD diffractograms of estuary fine fraction sub-sample. (A) Sample 2, low angle diffractograms with main peaks noted. (Inset B) close-up of (A), clay minerals in sample. (C) Sample 31, low angle diffractograms with main peaks noted. (Inset D) close-up of (C), clay minerals in sample, indicating the presence of smectite. Amphibole peak is present at  $\sim 10^{\circ}2\theta$ , but is in a low concentration as to be unquantifiable in the samples analysed.**

swelling of the mineral and the development of a peak around  $\sim 16-17 \text{ \AA}$  (Harward and Brindley, 1965; Mosser-Ruck et al., 2005). Figure 4.6C is composed of a glycolated and un-glycolated trace from a representative sample. In the inset figure (fig. 4.6D) the small drop in the shoulder region of the chlorite 001 peak upon glycolation suggests that a smectite mineral may be present in very small quantities, but

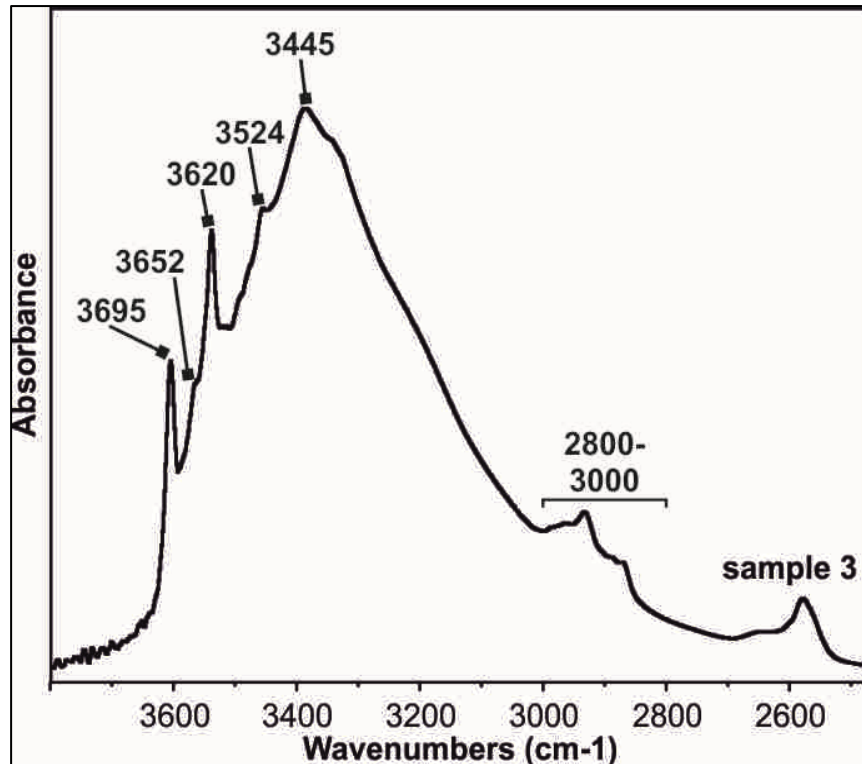


**Figure 4.7 - Infrared spectra for representative estuary sample (location 3). Bands at 3695, 3652 and 3620  $\text{cm}^{-1}$  indicate the presence of kaolinite. The larger 3620  $\text{cm}^{-1}$  band over the 3695  $\text{cm}^{-1}$  band indicates the presence of muscovite- or illite-type mica. The band at 3524  $\text{cm}^{-1}$  indicates that a magnesium-rich chlorite is present.**

quantification of the amount of smectite concentrations was not possible.

In summary, clay minerals identified in quantifiable concentrations within the Anllóns Estuary are: (i) kaolinite, (ii) chlorite, (iii) muscovite, and there is also evidence for the presence of a small quantity of smectite in some locations.

#### 4.5.1.2 Infrared spectroscopy

Infrared spectroscopy was performed on a selection of fine fraction samples and a representative trace is presented (fig. 4.7). In the OH-stretching region (3800-2500  $\text{cm}^{-1}$ ) there are several identifiable bands:

3695, 3652, 3620, 3524, and 3445  $\text{cm}^{-1}$ . The band at 2850-3000  $\text{cm}^{-1}$  is likely to be due to simple organic molecules (e.g.  $-\text{CH}_3$ ,  $-\text{CH}_2-$ ); the 3445  $\text{cm}^{-1}$  band is indicative of adsorbed water. Kaolinite is evidenced in the spectra by the distinct bands at 3695, 3652, and 3620  $\text{cm}^{-1}$ . The 3620  $\text{cm}^{-1}$  band represents hydroxyls between tetrahedral and hydroxyl sheets, while the remaining bands represent OH groups at the octahedral surface forming weak hydrogen bonds with oxygens in the next tetrahedral sheet (Madejova, 2003). Where the 3620  $\text{cm}^{-1}$  band is larger than the 3695  $\text{cm}^{-1}$  band, this indicates the presence of a muscovite- or illite-type mica (Farmer, 1974) and this is present in the spectra (fig. 4.7). The band at 3524  $\text{cm}^{-1}$  indicates that a magnesium-rich chlorite is present (Farmer, 1974).

In summary, infrared spectroscopy analysis supports the presence of all the clay minerals identified using X-ray diffraction (chlorite, muscovite and kaolinite) with the exception of smectite, which may have bands obscured by the other clay minerals (specifically kaolinite and muscovite at 3620  $\text{cm}^{-1}$ ). It also confirms that the mica is muscovite or illite (as opposed to biotite), and that the chlorite is a magnesium-rich variety.

#### **4.5.2 Mineralogy of the bedrock**

Mineralogical analyses of bedrock samples are outlined in Table 4.4. The rock types sampled consist primarily of granite, but a hornblende diorite, a paragneiss and hornblende schist were also sampled.

Quartz, plagioclase, muscovite mica, and lesser amounts of chlorite and K-feldspar, are the primary rock-forming minerals. High concentrations of hornblende are evident in diorite and schist samples. Accessory minerals include diopside, clinozoisite, ilmenite, biotite, kaolinite and gibbsite, although these are not ubiquitous.

#### **4.5.3 Mineralogy of riverbank soil sediments**

Individual riverbank soil samples from the Anllóns river catchment (fig. 4.8) have a broadly similar suite of minerals in the sediment fine fraction. Quartz, plagioclase, chlorite, kaolinite and gibbsite are present in every sample, with broadly similar concentrations. K-feldspar is also present in all samples except samples 37 and 42. Muscovite is present in every sample except sample 37. Smectite is also present in trace quantities in sample 36, 38, 39, 40, 41 and 42. Pyrite is present in trace quantities (<1%) in samples 37, 39, 40, 41 and 42.

#### **4.5.4 Estuary sediment texture**

Estuary surface sediment samples from zero to five centimetre depth were collected and analysed for grain size and sorting. The estuary is composed primarily of medium sand (fig. 4.9A), with coarser sediment on the shoreface at the front of the spit composed of coarse and medium sand. Finer grain sizes are noted on the saltmarsh where

Map location	Rock type	Quartz	K- feldspar	Plagioclase feldspar	Hornblende	Diopside	Clinozoisite	Ilmenite	Biotite	Muscovite	Chlorite	Kaolinite	Gibbsite
A	Granite	22	19	18	-	-	-	-	9	30	1	-	-
B	Granite	31	25	22	-	-	-	-	-	19	3	-	-
C	Hornblende diorite	5	-	23	50	-	-	3	-	-	14	-	5
D	Granite	29	11	27	-	-	-	-	-	34	-	-	-
E	Granite	35	22	20	-	-	-	-	-	16	3	3	-
F	Paragneiss	44	-	17	-	-	-	-	-	32	7	-	-
G	Granite	36	23	30	-	4	-	-	-	-	7	-	-
H	Hornblende schist	-	-	6	70	8	16	-	-	-	-	-	-

**Table 4.4 - Mineralogical analyses of lithology (whole fractions).**

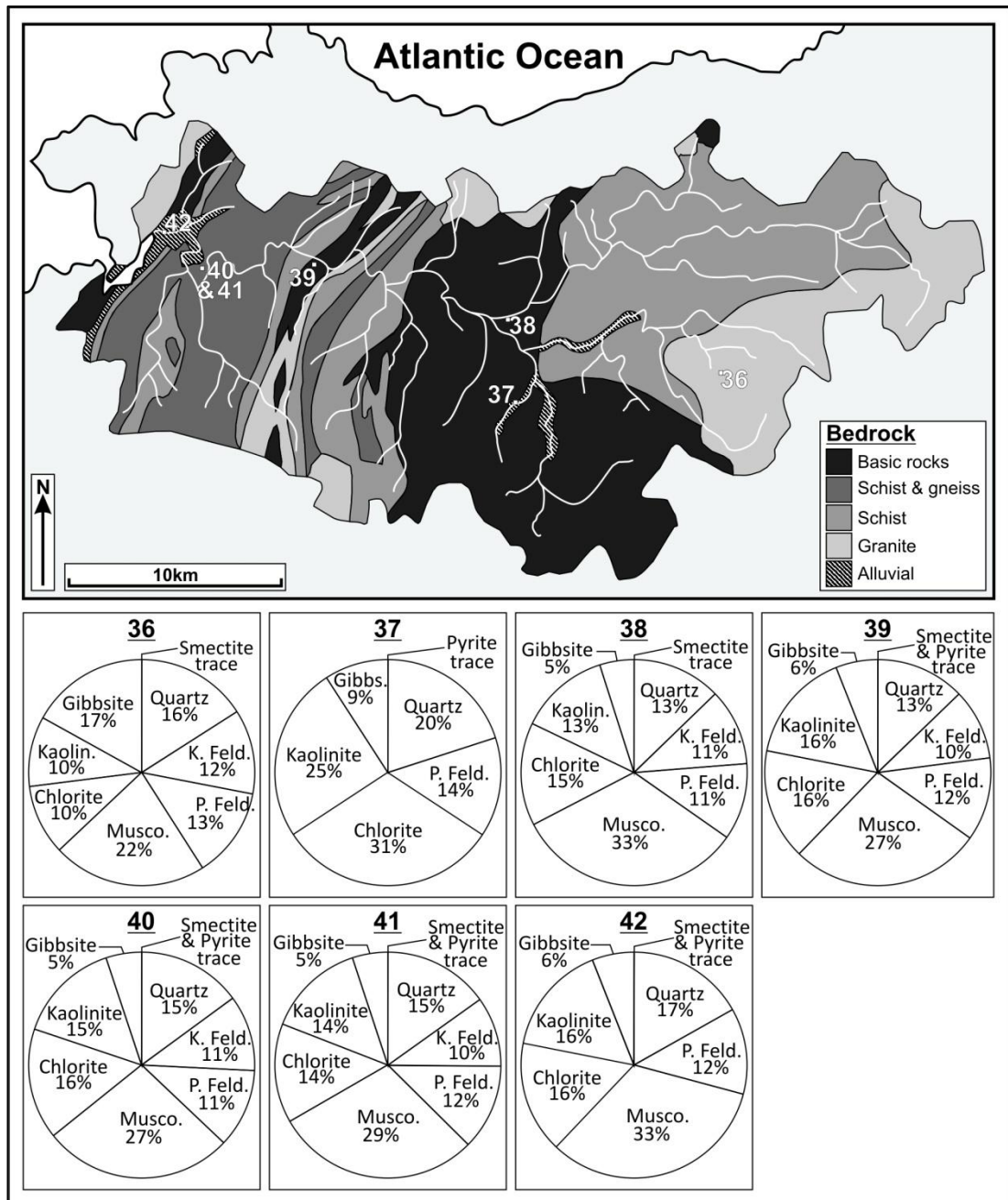


Figure 4.8 - Galician regional map (After: Devesa-Rey et al., 2008) with hinterland soil and river sediment sample locations and mineral concentrations. Quartz, plagioclase, chlorite, kaolinite and gibbsite are present in every sample, K-feldspar and muscovite is found in nearly every sample. The minerals present tend to reflect the underlying lithologies within the basin.

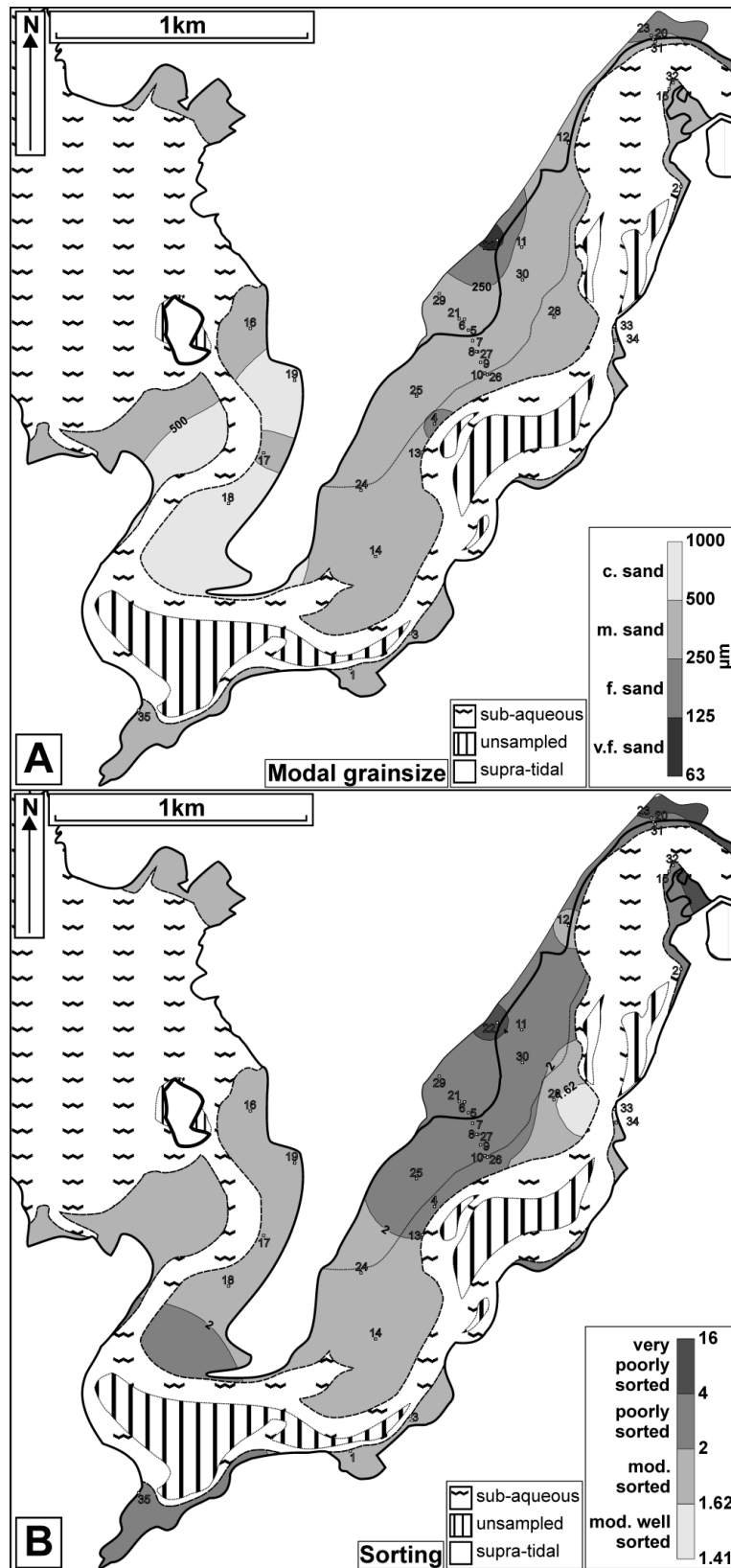


Figure 4.9 - Contoured maps of estuarine sedimentary texture. (A) Modal grain size. (B) Sorting. Grain size broadly increases and sorting is generally better towards the marine-dominated end of the estuary.



**Figure 4.9 - Contoured maps of estuarine sedimentary texture. (C) Fine fraction (weight percentage) of whole sediment sample. fine fraction contents are lower towards the marine-dominated end of the estuary.**

sediment becomes slightly finer (fine and very fine sand) landward. Estuary surface sediment has variable sorting (fig. 4.9B), with moderately to moderately well-sorted sediment on the shoreface and on the open sandflat areas. Poorly sorted surface sediment appears to correspond with muddy intertidal flat and saltmarsh locations, as well as upstream on the channel bend (fig. 4.3A) and where the small stream drains into the estuary in the south of the estuary (fig. 4.2A). Very poorly sorted sediments occur primarily in saltmarsh sediments, particularly in the upper estuary areas. Fine fraction contents (fig. 4.9C) are low (<2 wt %) over most of the surface area of the estuary,

particularly on the shoreface and open sandy intertidal flat areas. On the muddy intertidal areas concentrations are approximately 2-4 wt%, higher concentrations occur on saltmarsh sediments (6-14 wt %), with higher concentrations moving away from the axis of the estuary.

Cross-plots of estuary sediment particle size measures and fine fraction weight percentage are plotted (fig. 4.10A-C) enabling a comparison of these characteristics. Grain size appears to have no relationship with either fine fraction content or sorting (fig. 4.10A & C); however there appears to be a broad trend between the fine fraction content within the sediment and sorting of the sample (fig.4.10B). An increase of fine fraction concentration within the sample appears to correspond to a decrease in sorting.

#### **4.5.5 Estuary mineralogy**

The quantitative XRD mineral data collected from the forty-six estuary sediment samples have been visualised using a variety of techniques. The X-ray diffraction mineral data have been mapped and cross-plotted alongside sediment texture information to assess the distributions and relationships between sediment texture and mineralogy (section 4.5.5.1). To assess the concentrations of detrital or authigenic minerals, without the effects of marine-derived carbonate (calcite and aragonite), raw XRD mineral concentrations have been normalised to remove the carbonate component and then mapped

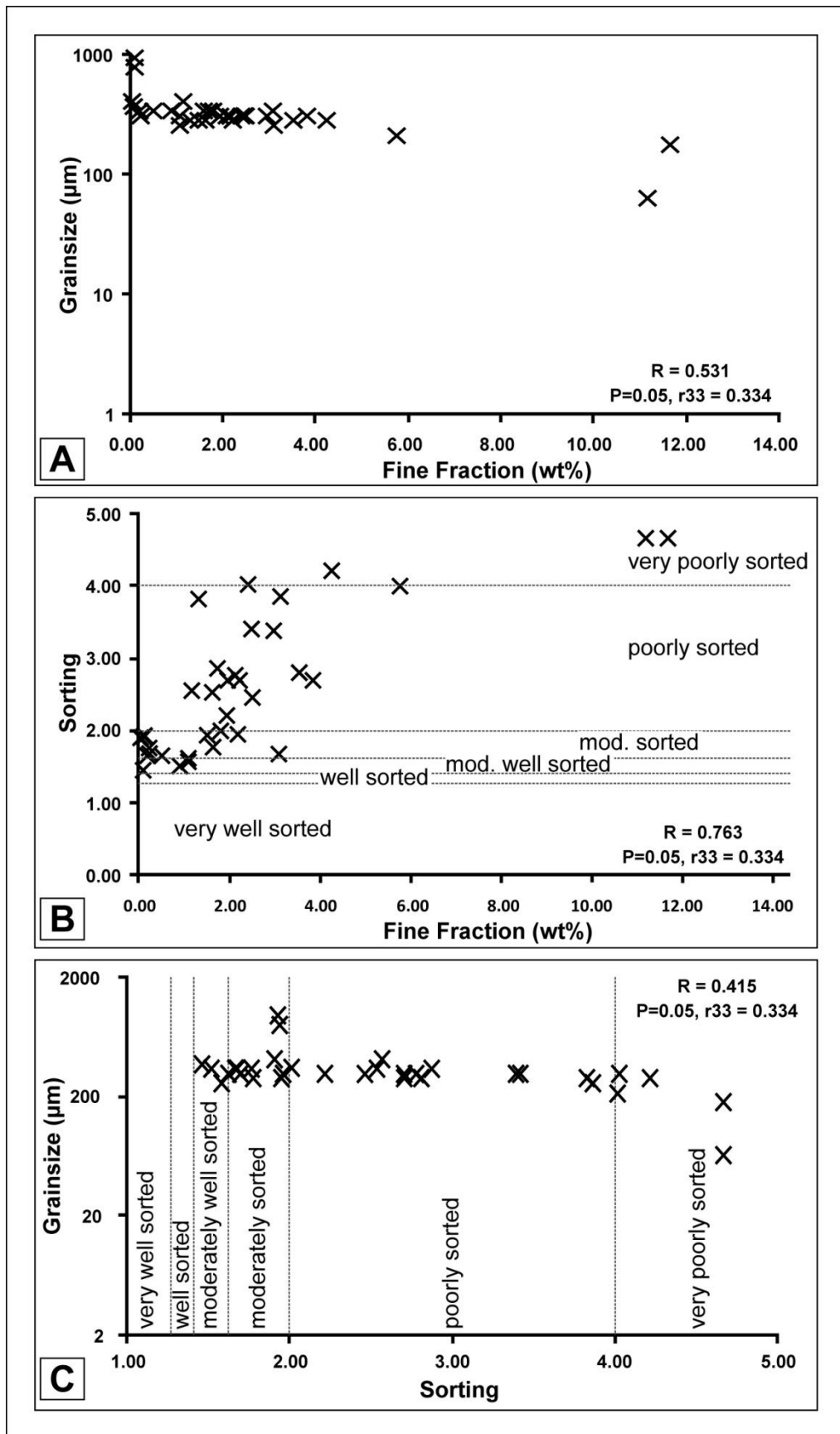


Figure 4.10 - Plots of whole sediment texture. (A) Fine fraction vs. grain size. (B) Fine fraction vs. sorting. (C) Sorting vs. grain size. Sorting decreases where the fine fraction content is higher. Grain size appears to be unrelated to fine fraction or sorting.

and cross-plotted (section 4.5.5.2). Also, to understand the mineral development across and down the estuary, transects have been generated using both the original XRD mineral data and the relative mineral data (section 4.5.5.3). Mineral indices were also plotted for a variety of mineral groupings to assess relationships between particular sub-sets of minerals (section 4.5.5.4).

#### 4.5.5.1 Estuary mineral data

X-ray diffractograms of clay minerals present in the Anllóns estuary (fig. 4.6) show that chlorite, kaolinite and muscovite are present in measureable concentrations and that trace quantities of smectite are also present within the fine fraction of estuary sediments. Mapped chlorite concentrations (fig. 4.11A) vary from between 2% to 14%, but lowest values (2-6%) appear to occur in sediments on the shoreface, and in open intertidal sandflat areas. Intermediate concentrations (6-8%) are evident on the muddy intertidal flat, with much higher concentrations in saltmarsh sediments.

Kaolinite concentrations (fig. 4.11B) and muscovite concentrations (fig. 4.11C), follow a broadly similar pattern to chlorite concentrations, with lowest concentrations (5-9% and 5-15% respectively) in the open marine-influenced shoreface and sandflat areas of the estuary, with elevated concentrations in the muddy intertidal flat areas (9-11% and 15-25% respectively) up through to the highest concentrations in saltmarsh sediments (>11% and 25-35% respectively).

Smectite was only evident in trace quantities within the sediments analysed (fig. 4.11B), but was principally recognized where concentrations of the other clay minerals were highest (fig. 4.11A-C).

Maps of non-clay minerals present within the Anllóns estuary (fig. 4.12) show that plagioclase, K-feldspar, quartz, gibbsite, calcite, aragonite and pyrite are present. Calcite occurs throughout the estuary (fig. 4.12A), with lowest concentrations (0-10%) in saltmarsh sediments and in the upper reaches of the estuary. Concentrations increase towards the main channel (10-30%), with highest concentrations occurring on the shoreface (30-50%). The same relationship is noted with aragonite concentrations (fig. 4.12B), where lower concentrations occur in saltmarsh sediments (0-5%), increasing in muddy intertidal areas (5-15%), and with highest concentrations on the shoreface (15-30%).

Quartz is present throughout the estuary (fig. 4.12C), with lowest concentrations (4-8%) in open areas on the shoreface and on the sandy intertidal areas. Higher concentrations of quartz are evident in the muddy intertidal areas (8-12%), with still higher concentrations on the saltmarsh and in the intertidal portions of the estuary (12-20%). Plagioclase is present in all areas sampled, (fig. 4.12D), at around 6-10% in shoreface and sandy intertidal flat areas. Higher concentrations (10-16%) are evident in saltmarsh areas particularly in the upstream portion of the estuary.

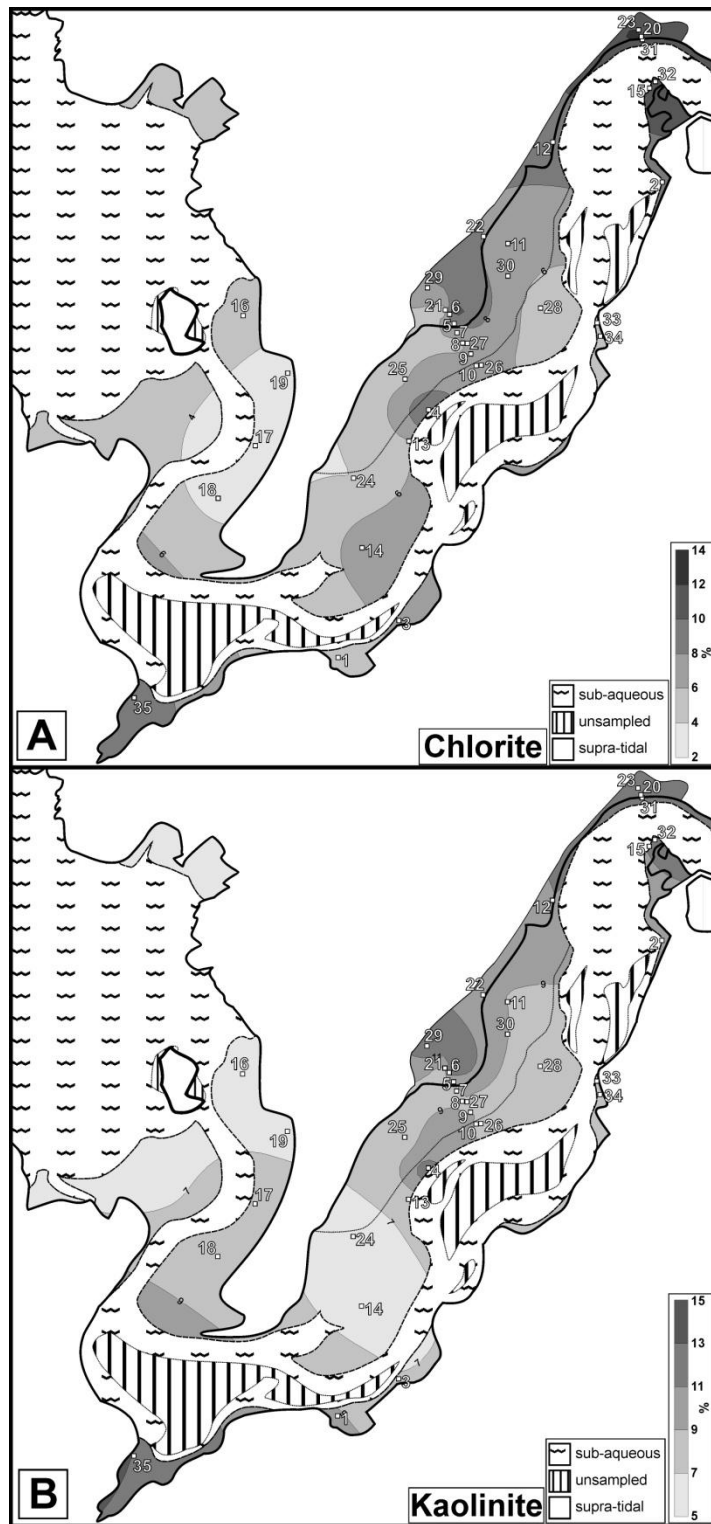


Figure 4.11 - Maps of clay mineral concentration in sediment fine fraction. (A) Chlorite. (B) Kaolinite. Chlorite and kaolinite are in higher concentrations towards the low energy and fluvial-dominated parts of the estuary.

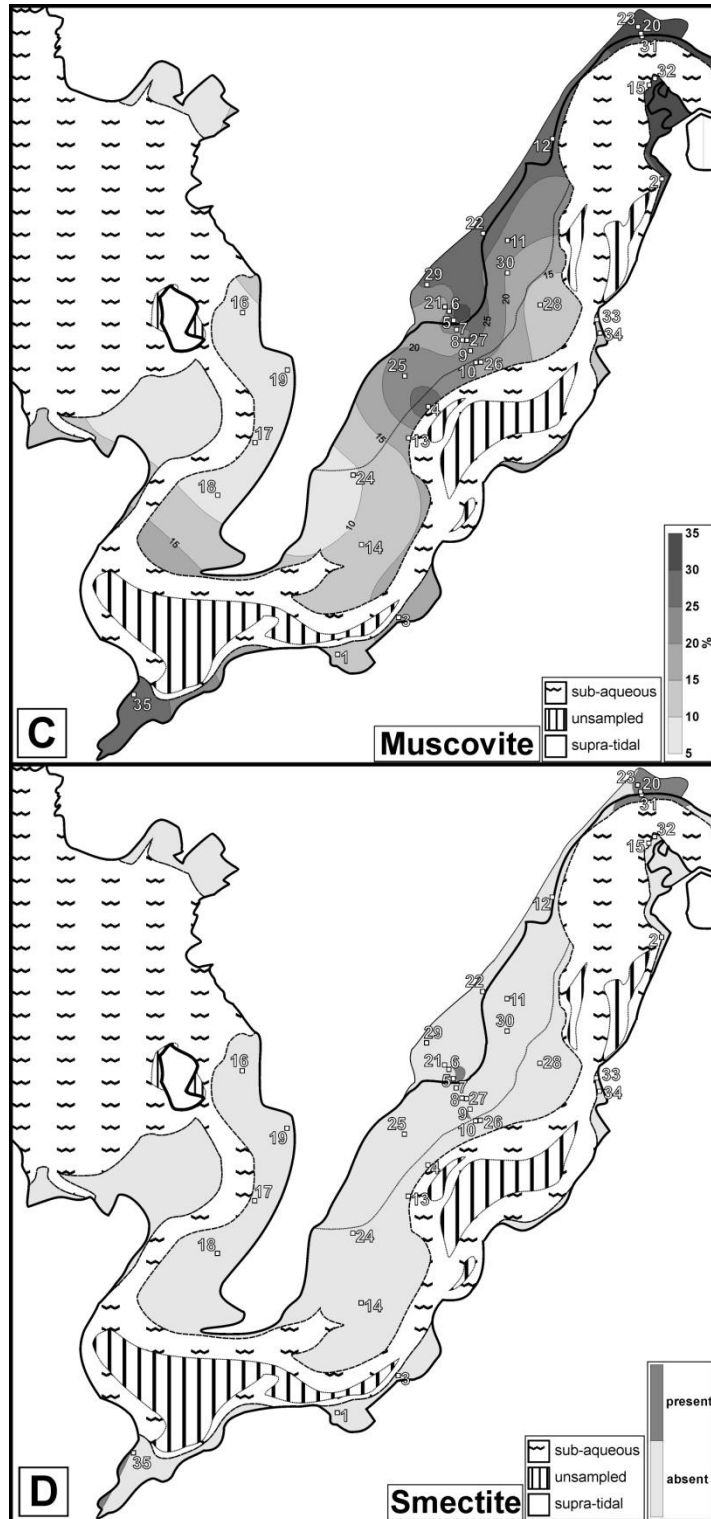


Figure 4.11 - Maps of clay mineral concentration in sediment fine fraction (C) Muscovite. (D) Smectite presence-absence map. Muscovite is in higher concentrations towards the low energy and fluvial-dominated parts of the estuary.

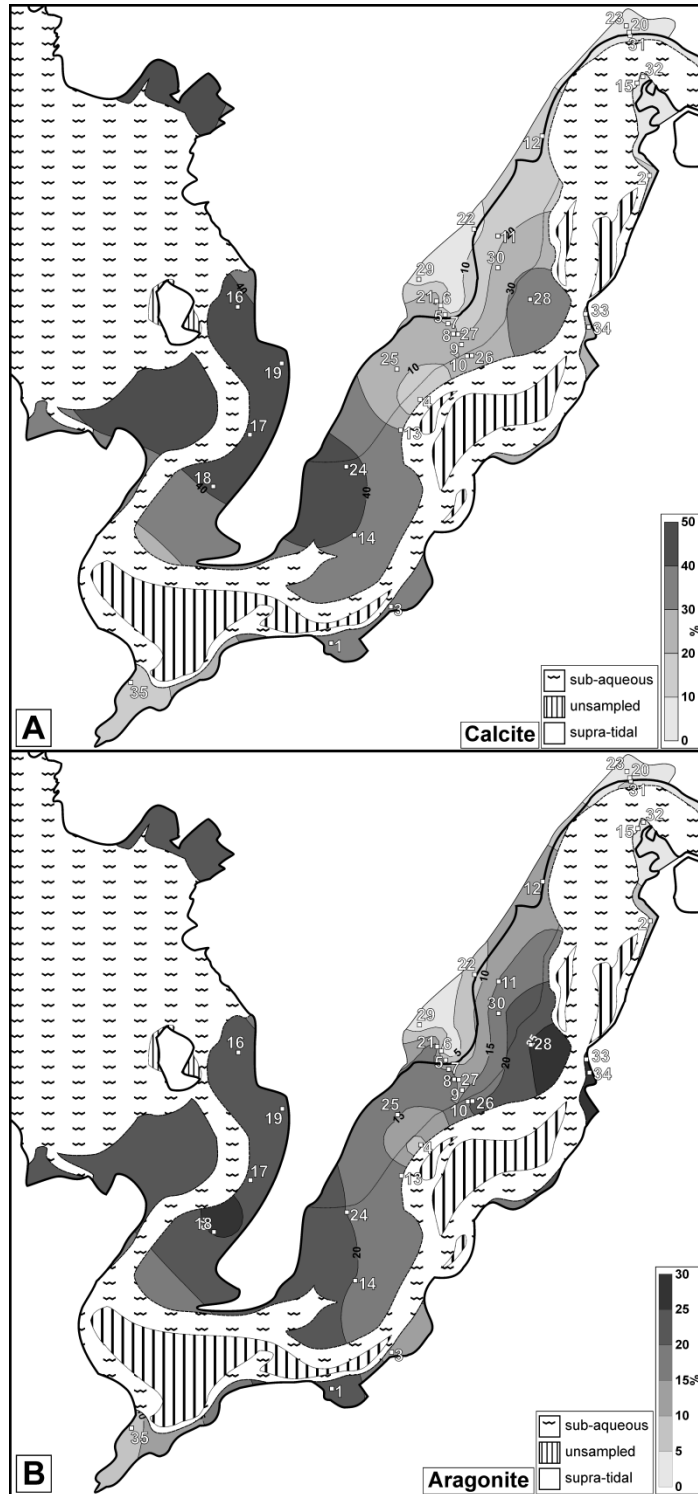
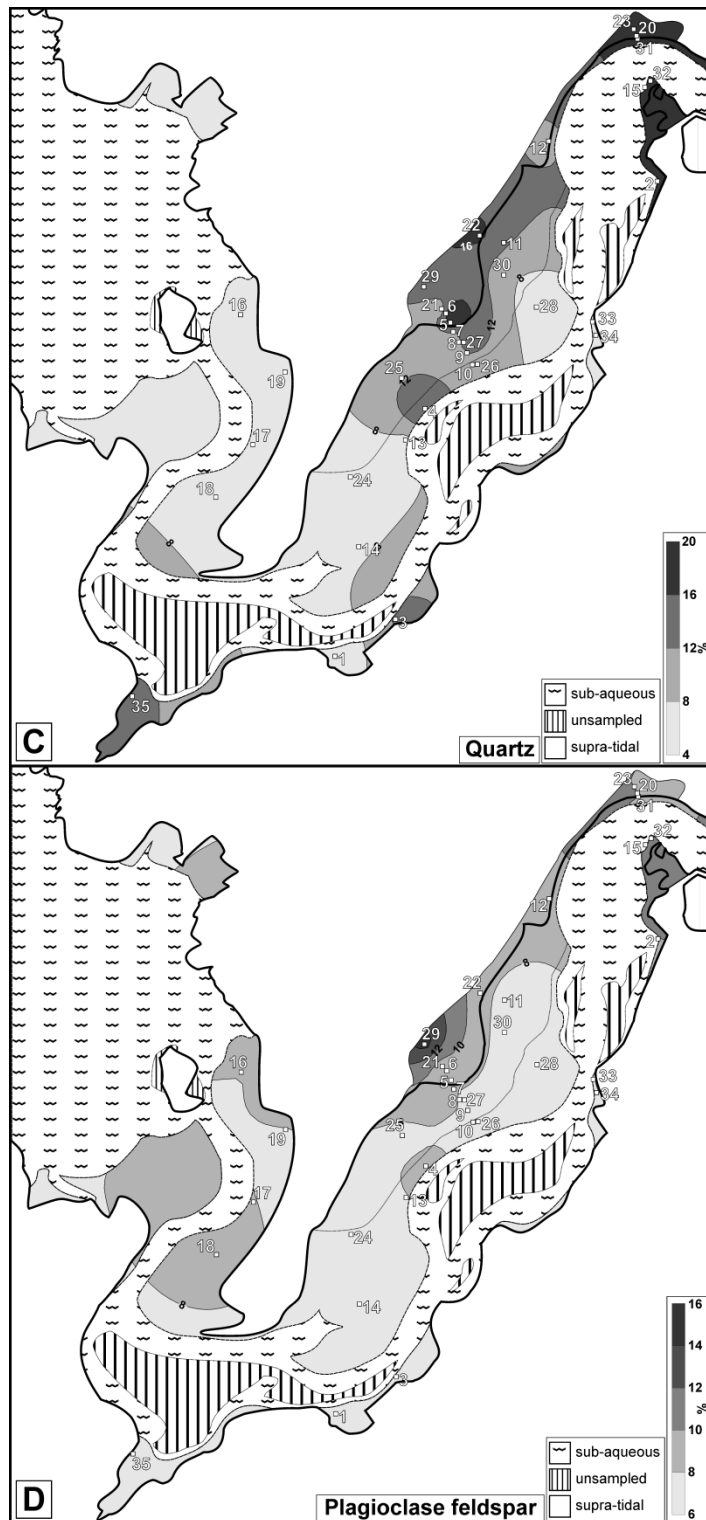


Figure 4.12 - Contoured maps of non-clay mineral concentration in sediment fine fraction. (A) Calcite. (B) Aragonite. Carbonate minerals (calcite and aragonite) are in higher concentrations towards marine-dominated areas of the estuary; siliciclastic minerals (quartz, plagioclase, K-feldspar and gibbsite) are in higher concentrations in low energy and fluvial-dominated parts of the estuary. Pyrite occurs in discrete locations on the inter-tidal flat.



**Figure 4.12 - Contoured maps of non-clay mineral concentration in sediment fine fraction. (C) Quartz. (D) Plagioclase. Carbonate minerals (calcite and aragonite) are in higher concentrations towards marine-dominated areas of the estuary; siliciclastic minerals (quartz, plagioclase, K-feldspar and gibbsite) are in higher concentrations in low energy and fluvial-dominated parts of the estuary. Pyrite occurs in discrete locations on the inter-tidal flat.**

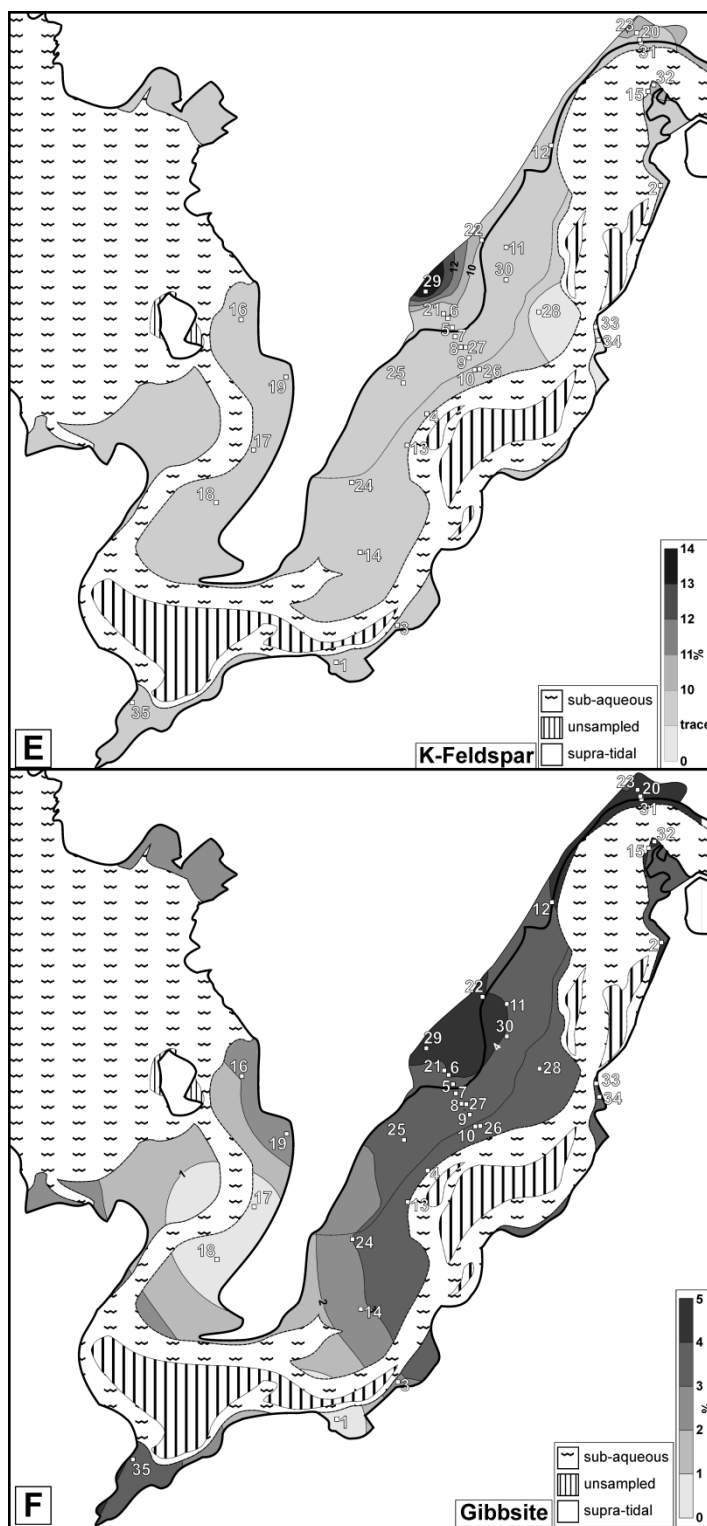
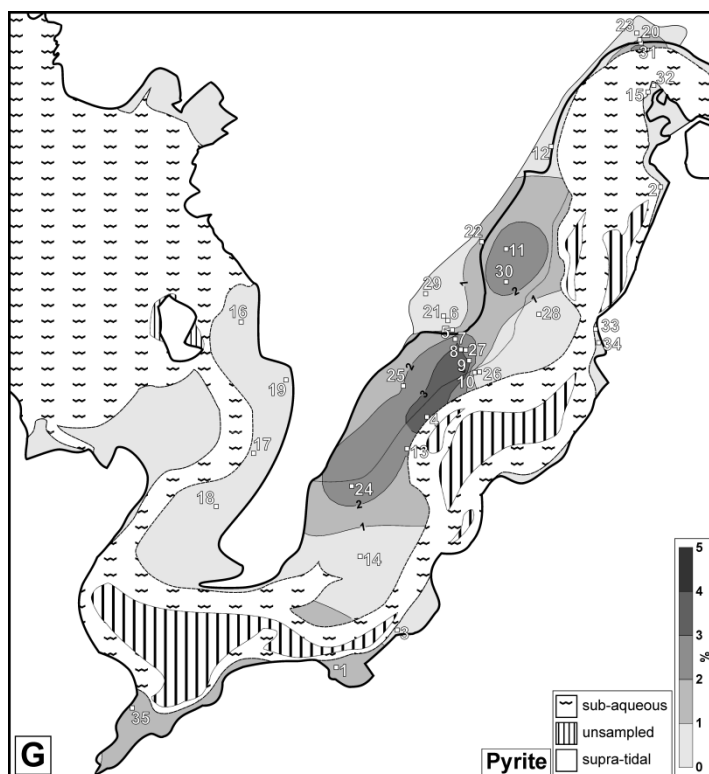


Figure 4.12 - Contoured maps of non-clay mineral concentration in sediment fine fraction. (E) K-feldspar. (F) Gibbsite. Carbonate minerals (calcite and aragonite) are in higher concentrations towards marine-dominated areas of the estuary; siliciclastic minerals (quartz, plagioclase, K-feldspar and gibbsite) are in higher concentrations in low energy and fluvial-dominated parts of the estuary. Pyrite occurs in discrete locations on the inter-tidal flat.



**Figure 4.12 - Contoured maps of non-clay mineral concentration in sediment fine fraction. (G) Pyrite. Carbonate minerals (calcite and aragonite) are in higher concentrations towards marine-dominated areas of the estuary; siliciclastic minerals (quartz, plagioclase, K-feldspar and gibbsite) are in higher concentrations in low energy and fluvial-dominated parts of the estuary. Pyrite occurs in discrete locations on the inter-tidal flat.**

Due to the relatively high detection limits for K-feldspar quantifying concentrations below ~10% is not feasible, and it therefore only appears to be present in at least trace quantities through most of the estuary (fig. 4.12E). The high detection limit for K-feldspar in this context is due to: (i) the presence of a range of K-feldspar polymorphs (triclinic, monoclinic), (ii) the variable composition of detrital alkali feldspars (variable sodium contents altering the crystallography), (iii) the low symmetry of these feldspars resulting in a large number of X-ray diffraction peaks, (iv) the large number of minerals in the sediment

resulting in a large number of overlapping peaks in the range just greater than  $27^\circ 2\theta$  where the K-feldspar peaks lie. Measurable concentrations only occur in saltmarsh sediments (10-14%).

Lowest gibbsite (fig. 4.12F) concentration (0-3%) occur on the shoreface and in areas close to the frontal spit, concentrations increase up the estuary proximal to river inputs and onto saltmarsh sediments (2-5%). Where pyrite is present, the highest concentrations generally occur in the muddy intertidal areas of the estuary. Pyrite is absent in some parts of the estuary (fig. 4.12G), principally on the shoreface and in areas close to the main estuary channel.

Mineral concentrations were also cross-plotted to assess mineral interrelationships. Visual assessment of relationships between two variables was supplemented with r-value calculations (Townend, 2003) and comparison to p-values ( $p=0.05$ ) for the sample number minus two degrees of freedom (Siegle, 2009). This gives a 95 percent confidence limit for correlations noted below. Cross-plots of sorting and mineral composition (fig. 4.13) show strong trends for the majority of minerals present in surface sediments. As sediment sorting decreases (fig. 4.13A) there is a decrease in the concentrations of calcite and aragonite and an increase in the concentrations of quartz, muscovite, kaolinite, and chlorite. When total carbonate (calcite plus aragonite) and total clay mineral (muscovite plus

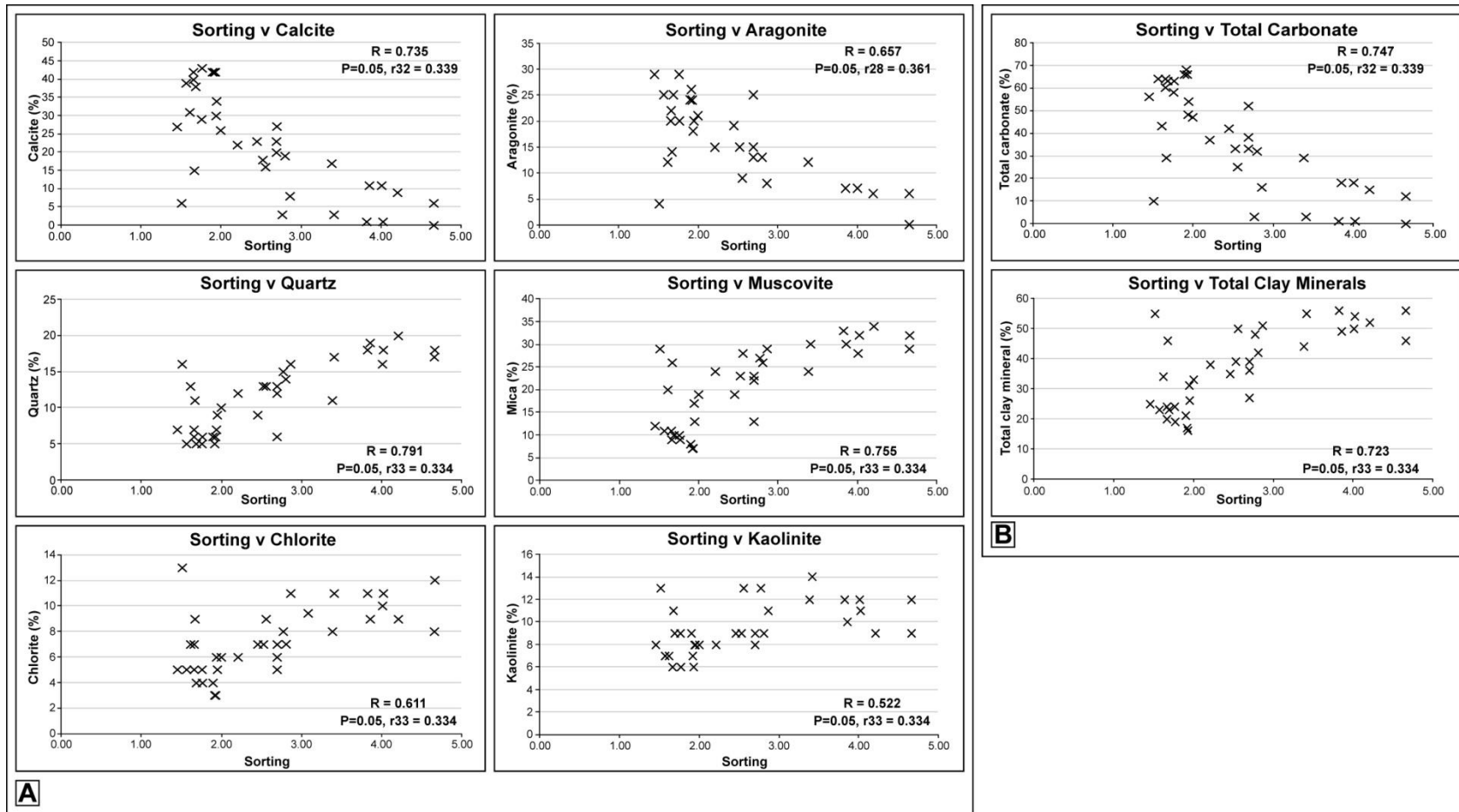
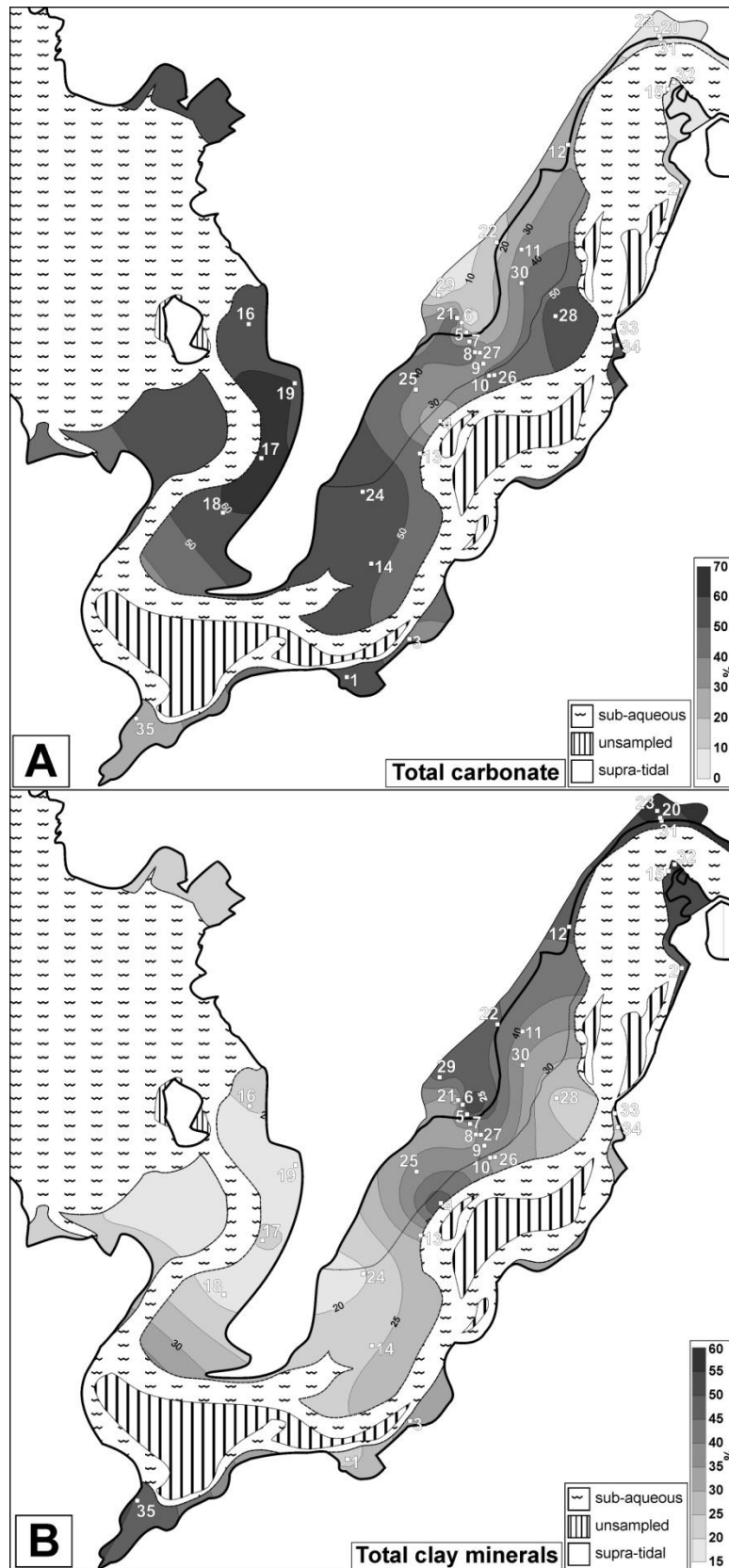


Figure 4.13 - Sorting versus mineral concentration cross-plots. (A) Individual minerals. (B) Summed total carbonate and total clay minerals. Where sorting is better, carbonate minerals are in higher concentrations indicate that marine processes effect sorting within the estuarine sediments. Conversely, siliciclastic sediments are in higher concentrations where sorting is poorer.



**Figure 4.14 - Total concentrations of carbonate and clay minerals in sediment fine fraction. (A) Total carbonate. (B) Total clay minerals. Total concentrations of carbonate and clay minerals show a distinct inverse relationship.**

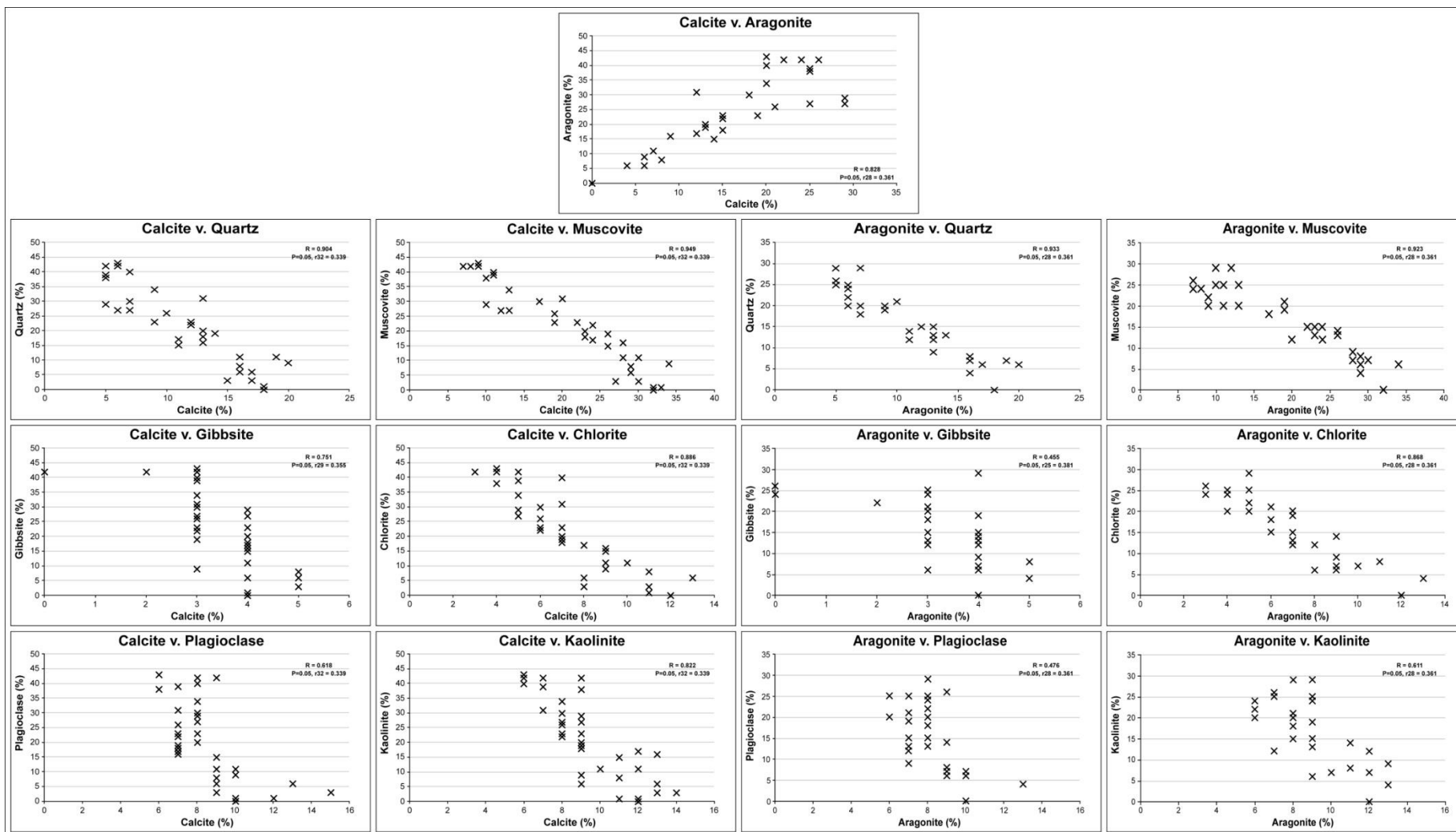


Figure 4.15 - Carbonate versus siliciclastic mineral concentration cross-plots. Carbonate and siliciclastic minerals display a strong inverse relationship.

kaolinite plus chlorite) concentrations are plotted against sorting (fig. 4.13A) the strong positive and negative correlations between sorting and mineral concentrations can be seen. Furthermore, when total carbonate and total clay mineral concentrations are mapped (fig. 4.14), there is a strong inverse spatial relationship between clay minerals and carbonate concentrations within the estuary.

Figure 4.15 is a cross-plot of calcite and aragonite against a selection of the other minerals present and against each other. This clearly shows that where calcite and aragonite are concentrated in the fine fraction of sediments it is at the expense of all other minerals. Similarly, cross-plots of clay minerals against a selection of other minerals (fig. 4.16A) shows; an inverse relationship, where there is an increase in the concentration of a particular clay mineral there is an increase in gibbsite, quartz and plagioclase, as well as the other clay minerals present.

#### **4.5.6 Relative estuary mineral data**

The relative (carbonate normalised) mineral concentrations for quantified clay minerals within the estuary are shown in figure 4.17. The relative chlorite concentrations (fig. 4.17A) are lowest (8-10%) in

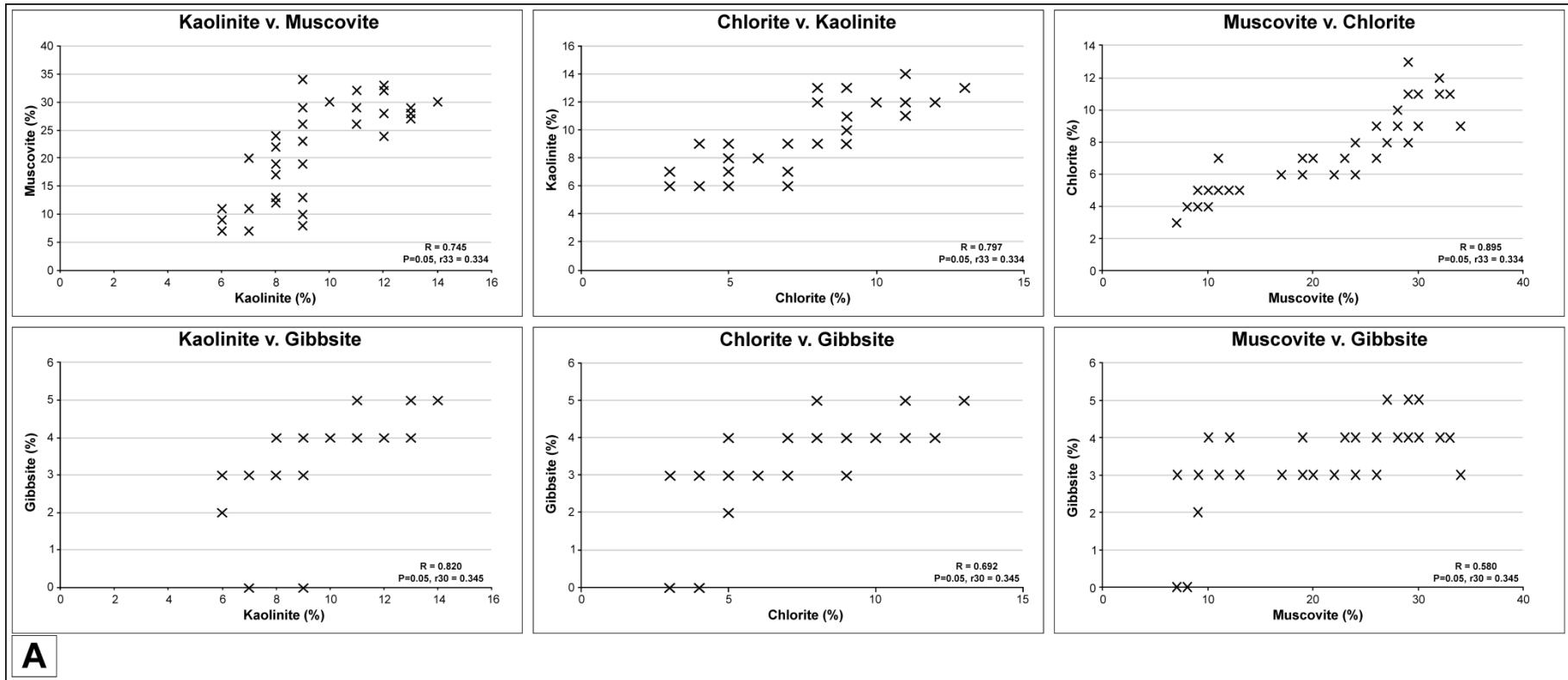


Figure 4.16A - Siliciclastic versus siliciclastic mineral concentration cross-plots. Gibbsite, quartz and plagioclase have a strong positive relationship with most clay minerals, similarly clay minerals are generally in higher concentrations where other clay minerals are in higher concentrations.

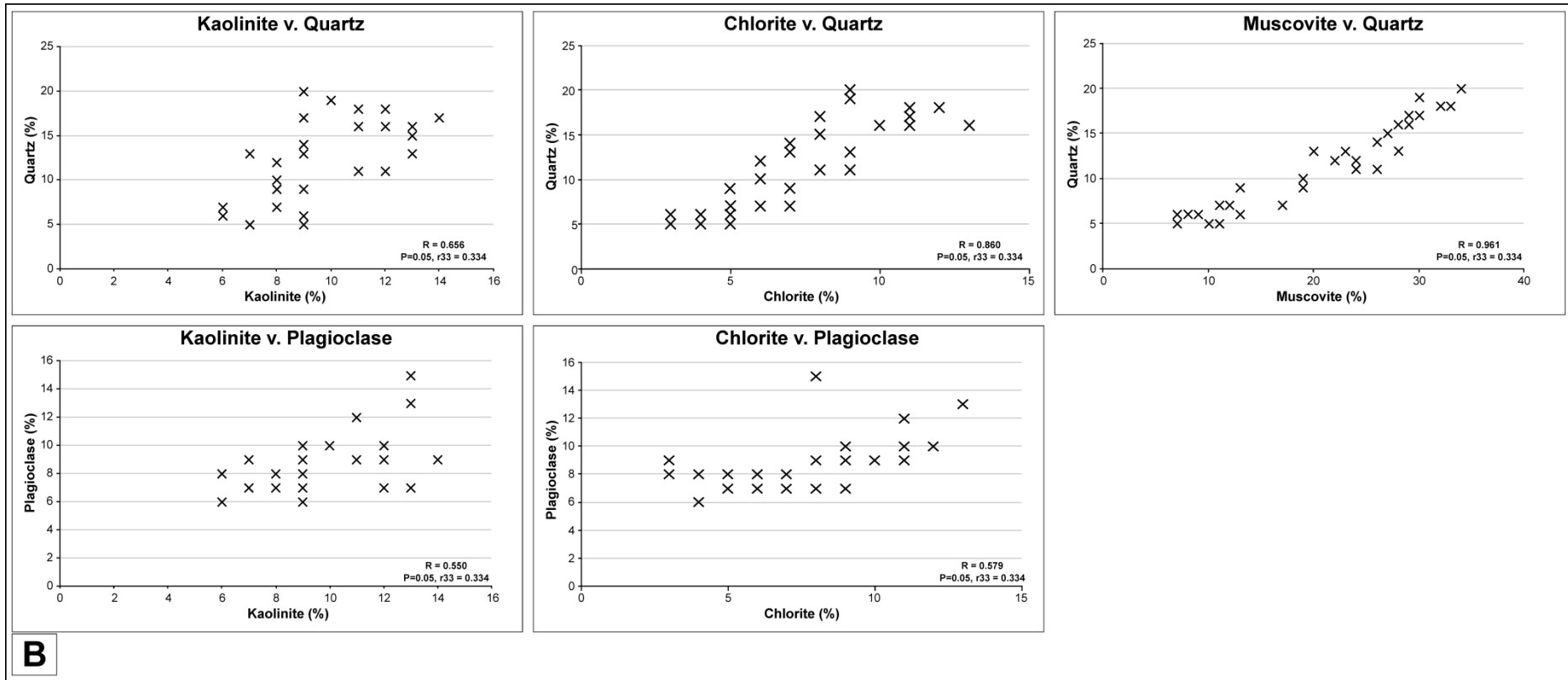


Figure 4.16B - Siliciclastic versus siliciclastic mineral concentration cross-plots. Gibbsite, quartz and plagioclase have a strong positive relationship with most clay minerals, similarly clay minerals are generally in higher concentrations where other clay minerals are in higher concentrations.

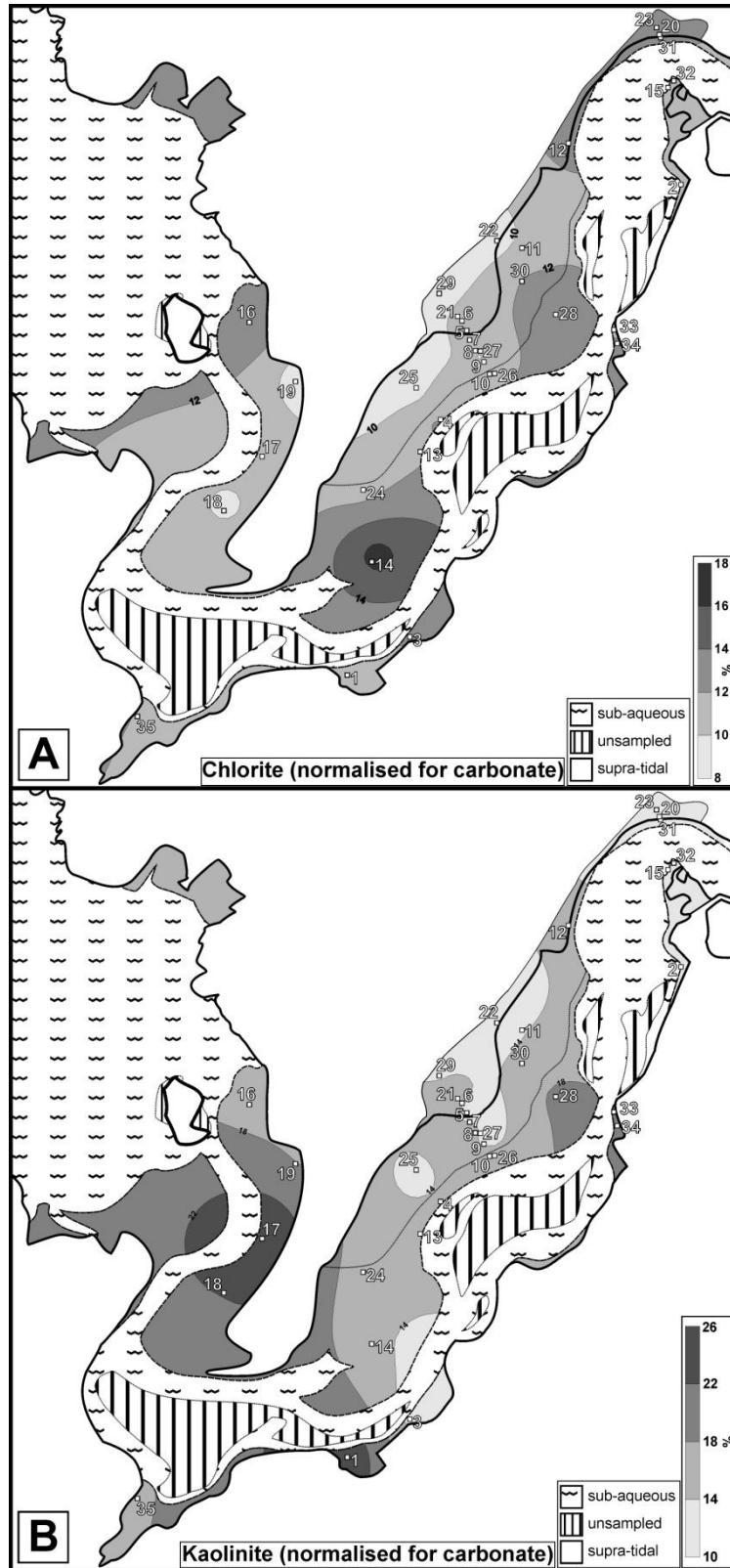


Figure 4.17 - Contoured maps of relative (carbonate normalised) clay mineral concentration in sediment fine fraction. (A) Chlorite. (B) Kaolinite. Carbonate-normalised kaolinite is generally in higher concentration towards the marine dominated part of the estuary. Carbonate-normalised chlorite varies considerably in concentration across the estuary, but does not display any noticeable trend.

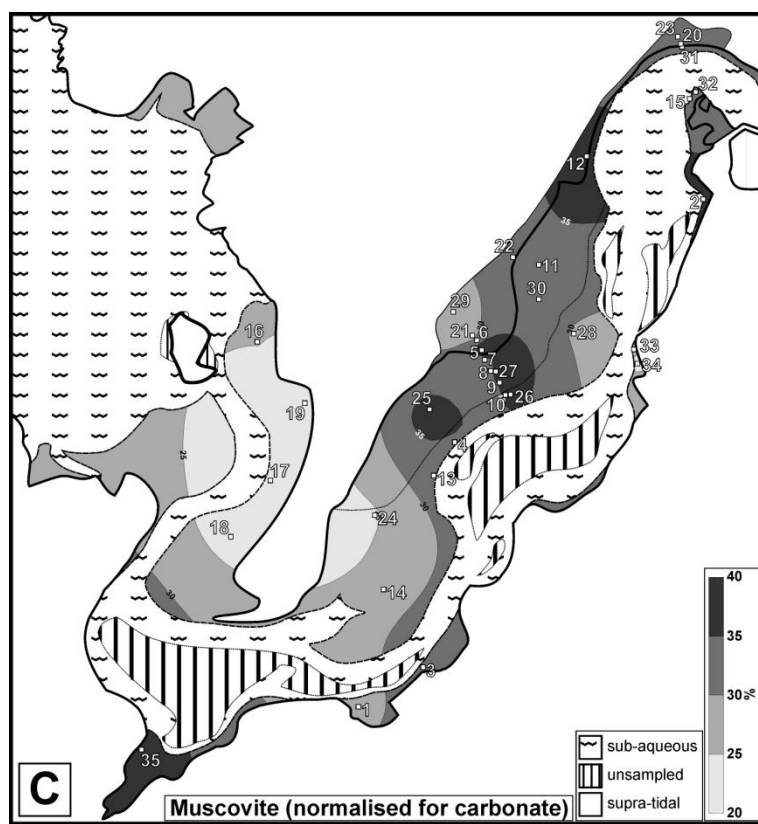
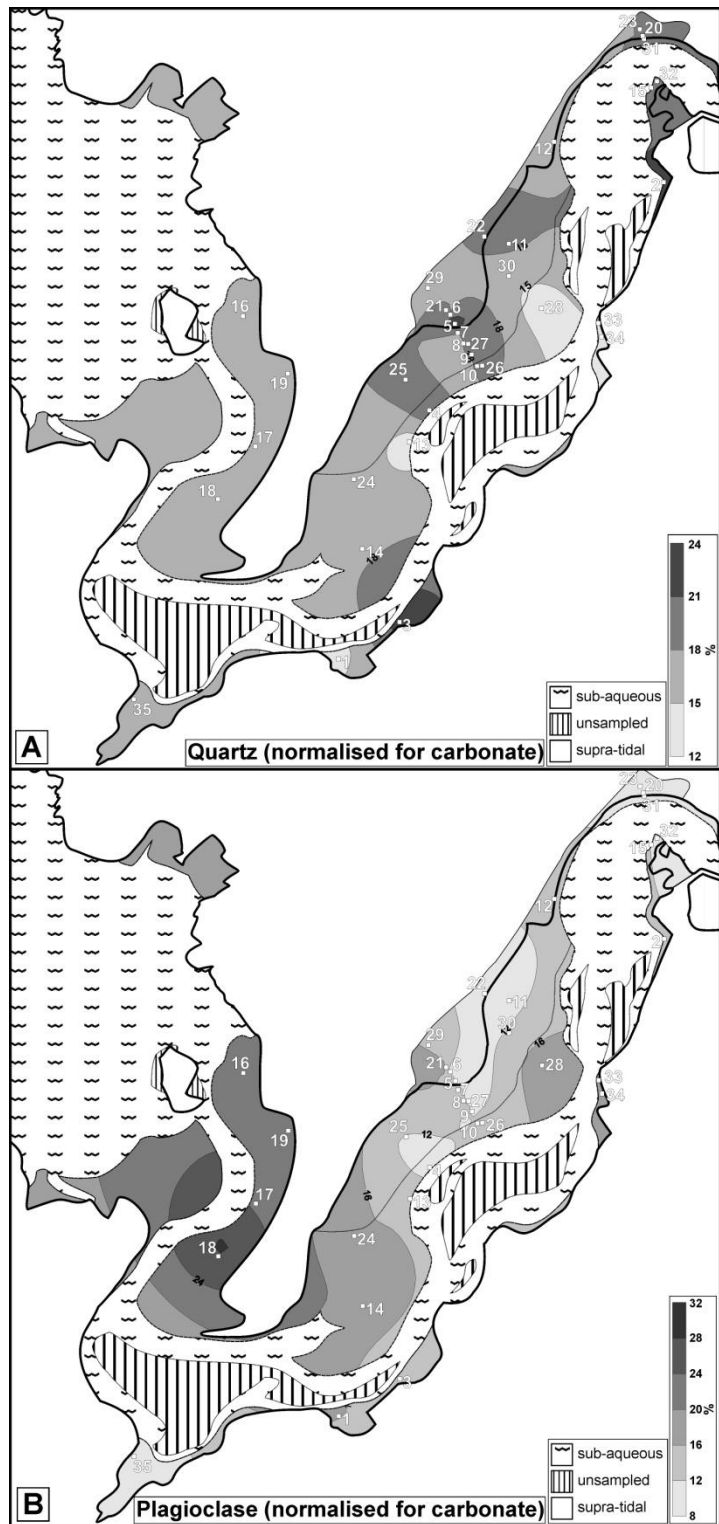
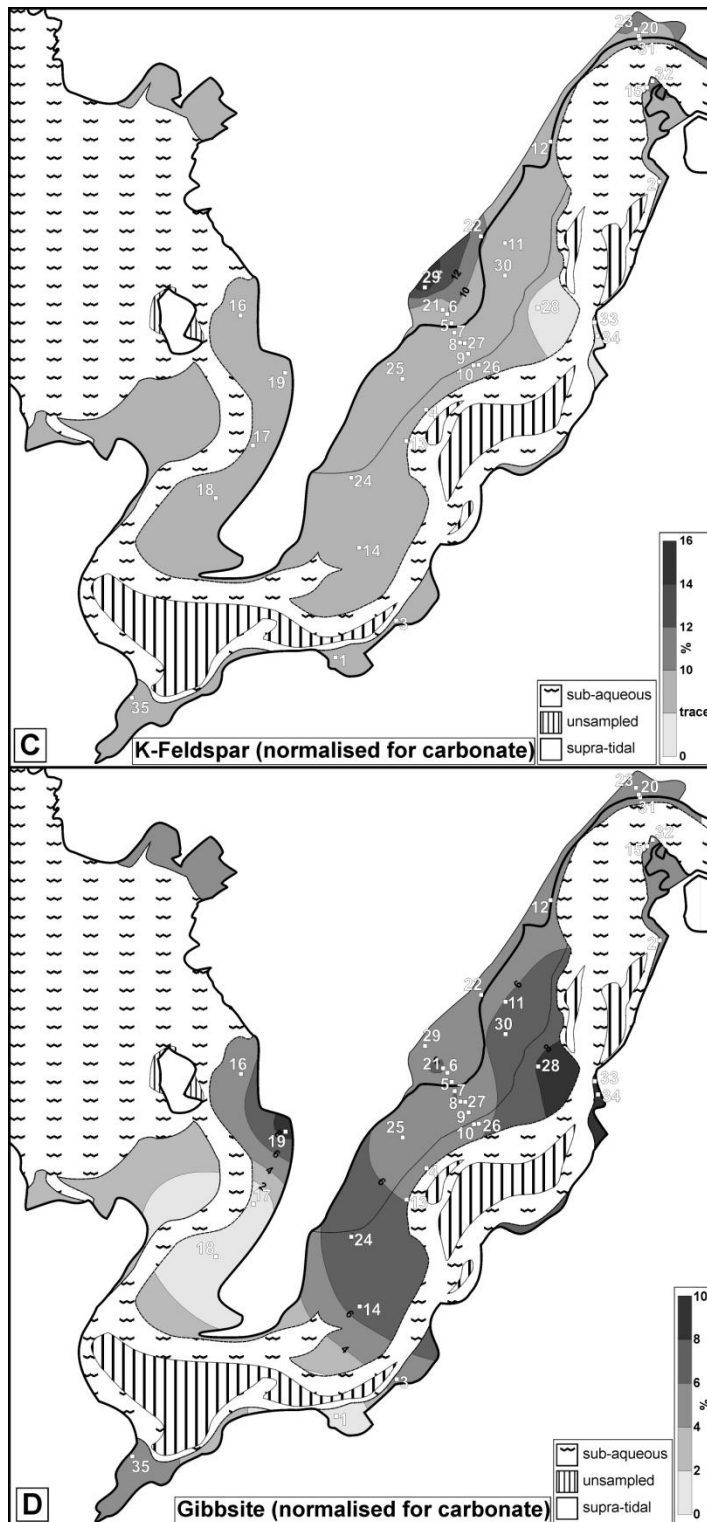


Figure 4.17 - Contoured maps of relative (carbonate normalised) clay mineral concentration in sediment fine fraction. (C) Muscovite. Carbonate-normalised muscovite is generally in higher concentrations in low energy, river-dominated parts of the estuary.



**Figure 4.18 - Contoured maps of relative (carbonate normalised) non-clay mineral concentration in sediment fine fraction. (A) Quartz. (B) Plagioclase. Carbonate-normalised quartz, K-feldspar and gibbsite are generally in higher concentration in low energy and river-dominated areas of the estuary. Carbonate-normalised plagioclase is generally in higher concentrations towards the marine-dominated section of the estuary. Pyrite is in higher concentrations on the inter-tidal flat.**



**Figure 4.18 - Contoured maps of relative (carbonate normalised) non-clay mineral concentration in sediment fine fraction. (C) K-feldspar. (D) Gibbsite** Carbonate-normalised quartz, K-feldspar and gibbsite are generally in higher concentration in low energy and river-dominated areas of the estuary. Carbonate-normalised plagioclase is generally in higher concentrations towards the marine-dominated section of the estuary. Pyrite is in higher concentrations on the inter-tidal flat.

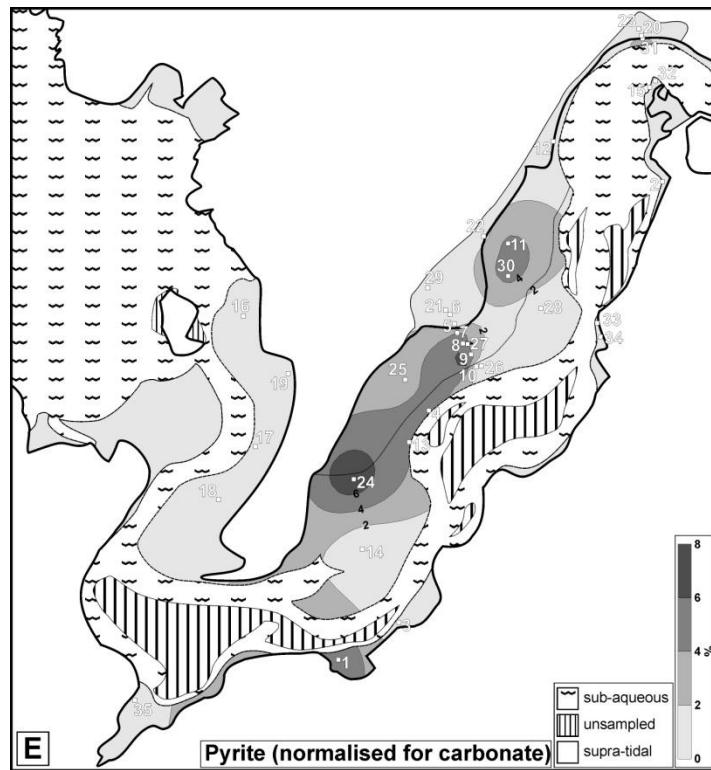


**Figure 4.18 - Contoured maps of relative (carbonate normalised) non-clay mineral concentration in sediment fine fraction. (E) Pyrite. Carbonate-normalised quartz, K-feldspar and gibbsite are generally in higher concentration in low energy and river-dominated areas of the estuary. Carbonate-normalised plagioclase is generally in higher concentrations towards the marine-dominated section of the estuary. Pyrite is in higher concentrations on the inter-tidal flat.**

saltmarsh sediments. Moderate concentrations (10-12%) occur at the front of the estuary and on the muddy intertidal flat, with highest concentrations (>12%) occurring in sediments proximal to the main estuary channel. Relative kaolinite concentrations (fig. 4.17B) are lowest in saltmarsh sediments (10-14%). On the muddy and sandy intertidal flat areas concentrations are generally intermediate (14-18%) or low. Highest relative kaolinite concentrations (18-26%) occur towards the front of the estuary and in shoreface sediments. Relative muscovite concentrations are much higher than either kaolinite or

chlorite (fig. 4.17C). Lowest concentrations are evident at the front of the estuary (20-30%); towards the middle of the estuary, concentrations increase (30-40%), particularly on the sandy and muddy intertidal flats areas and in the upper reaches of the saltmarsh.

The carbonate-normalised, relative non-clay mineral data are presented in figure 4.18. Relative quartz concentrations exhibit a high degree of local variability, particularly on the intertidal areas of the estuary. Quartz concentrations (fig. 4.18A) are generally within the range of 15-21%, with lower and higher concentrations only occurring at dispersed locations around the estuary. Relative plagioclase concentrations (fig. 4.18B) are generally lowest (8-16%) in saltmarsh sediments and muddy intertidal flat areas, concentrations generally increase towards the front of the lower estuary with intermediate (16-24%) and high (24-32%) concentrations in sandy intertidal and shoreface sediments. The low detection limits for quantifying K-feldspar using XRD mean that the relative concentrations (fig. 4.18C) show no real change from the raw data concentrations (fig. 4.12E). Gibbsite concentrations exhibit some variability (fig. 4.18D), although most concentrations within the estuary are broadly within the 4-8% range. Lowest concentrations are evident on the shoreface (0-4%), but there are two locations with higher concentrations (8-10%). Pyrite concentrations (fig. 4.18E) are generally low throughout much of the estuary (0-2%); higher concentrations appear to be associated with a

couple of sample locations within the muddy intertidal sand areas only.

Cross-plots of the relative concentrations of minerals (fig. 4.19), display some broad trends between different minerals. Minerals that show a positive correlation are; quartz and muscovite, plagioclase and kaolinite, gibbsite and kaolinite and plagioclase and gibbsite. Negative trends occur for: quartz and kaolinite, quartz and plagioclase, quartz and gibbsite, plagioclase and muscovite, kaolinite and muscovite, and gibbsite and muscovite.

#### **4.5.7 Estuary transects**

Figure 4.20 is a series of three transects down the length and across the width of the estuary, for both the raw mineral (fig. 4.20B) and the relative (carbonate normalised) concentrations (fig. 4.20C) in the fine fraction of samples. Figure 4.20B, shows that calcite and aragonite increase in concentrations towards both the marine-dominated sections and towards the main channel across the intertidal sections of the estuary. Although there is some variability the majority of the minerals remain at relatively similar concentrations at different locations across the estuary, particularly plagioclase, chlorite, gibbsite and kaolinite. K-feldspar only appears in measureable concentrations in the saltmarsh sediment. Muscovite and quartz concentrations decrease both down the estuary towards the marine-dominated sample locations, and towards the main channel across intertidal

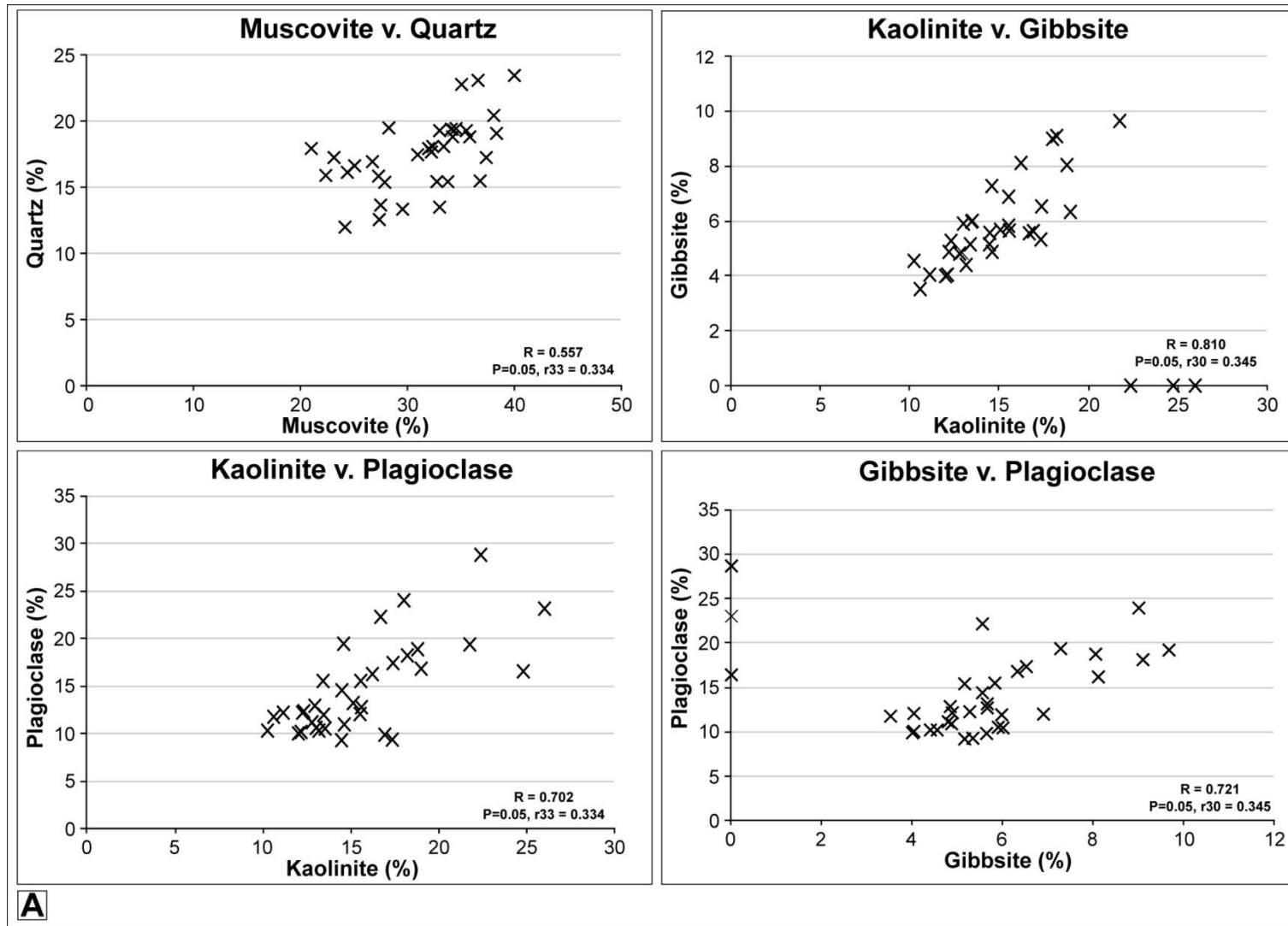


Figure 4.19 - Relative (carbonate normalised) siliciclastic versus siliclastic mineral concentration cross-plots. (A) Positive correlation. Carbonate-normalised concentrations show that there are distinct positive and negative correlations between some siliciclastic minerals.

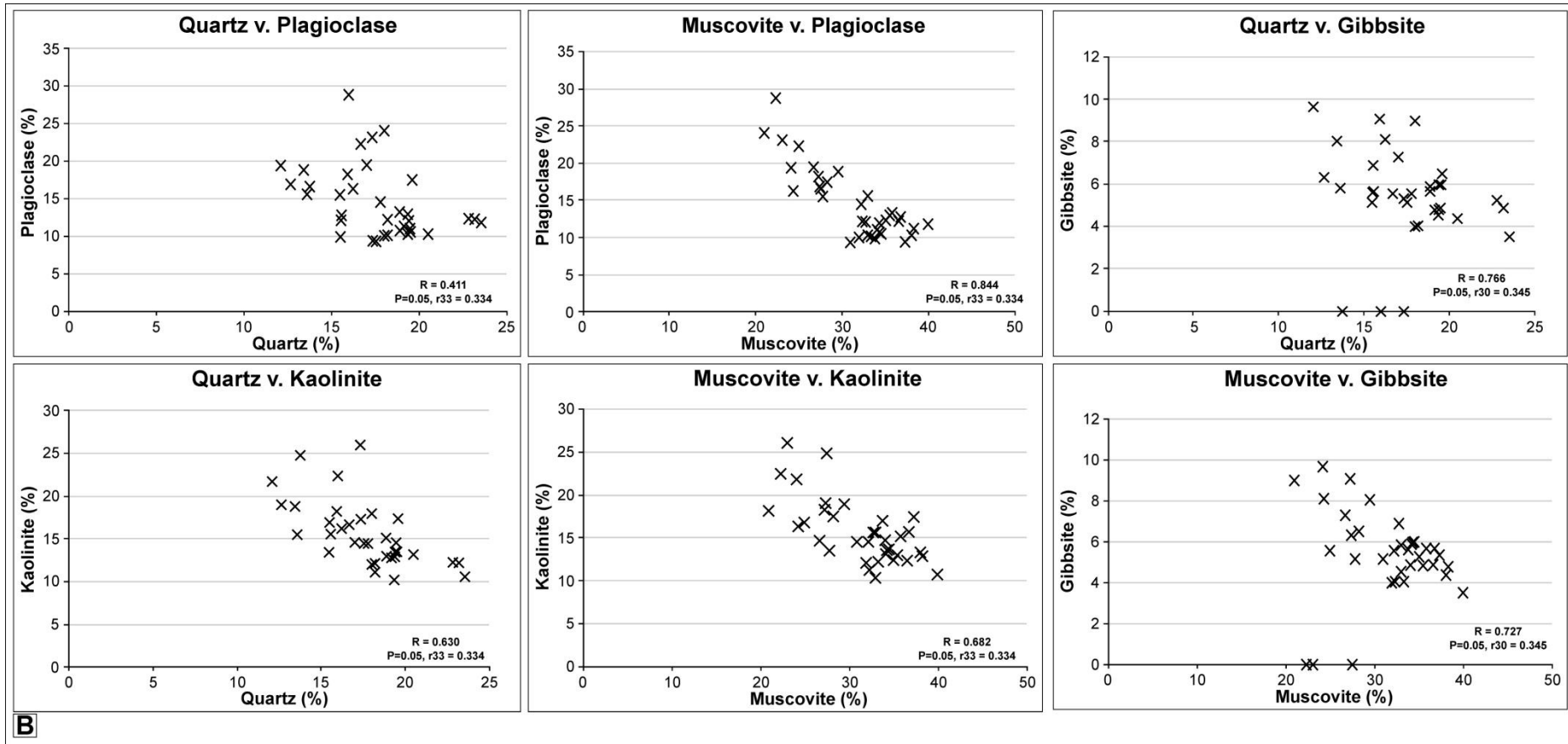


Figure 4.19 - Relative (carbonate normalised) siliciclastic versus siliclastic mineral concentration cross-plots. (B) Negative correlation. Carbonate-normalised concentrations show that there are distinct positive and negative correlations between some siliciclastic minerals.

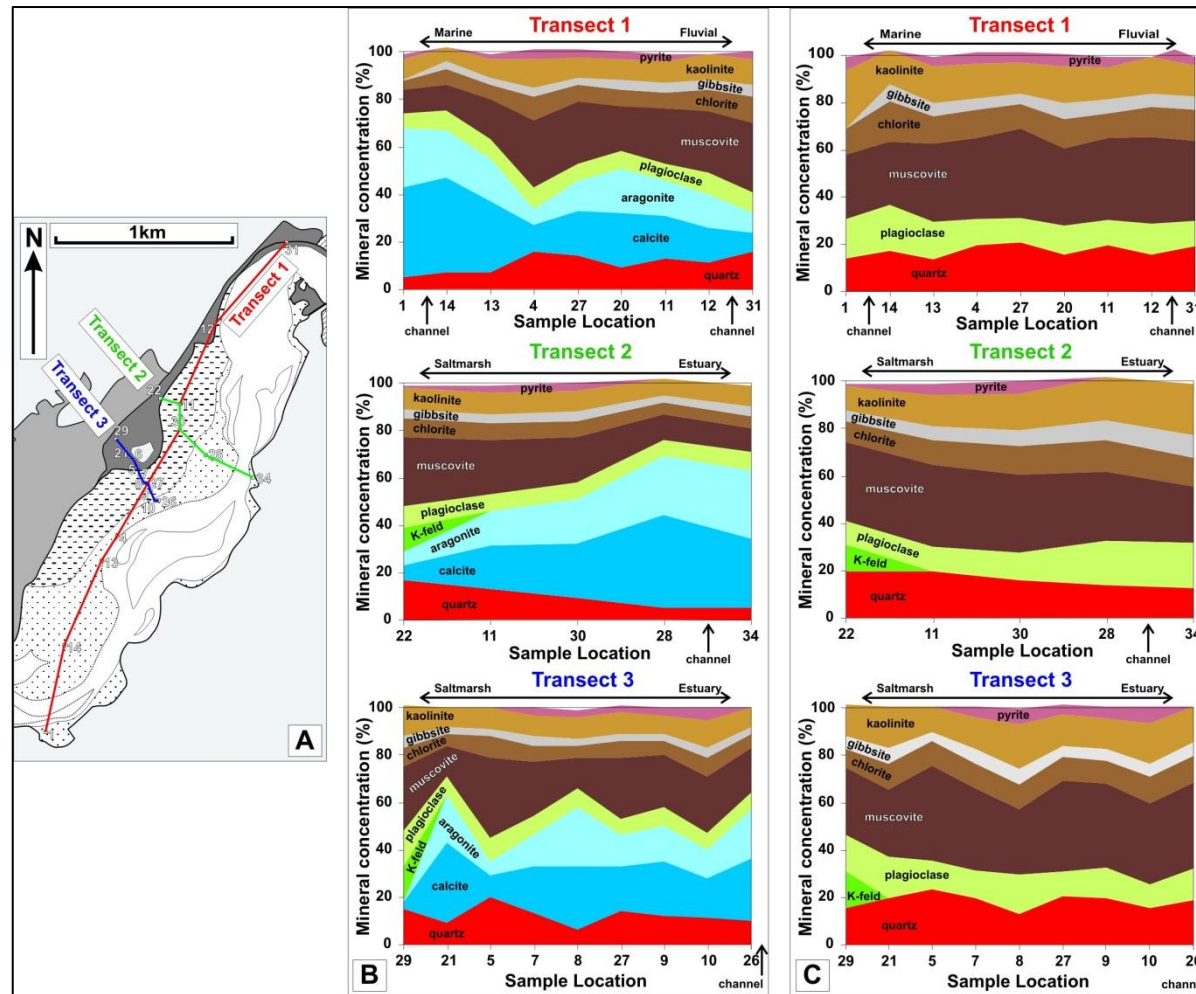


Figure 4.20 - Estuary mineral transects (A) Location map with transect points. (B) Mineral concentration transects. Transect indicates that carbonate minerals increase towards the marine-dominant parts of the estuary. (C) Relative (carbonate normalised) mineral concentration transect. Carbonate-normalised plagioclase and kaolinite increase in concentration towards the marine end of the estuary. Chlorite and muscovite show less of a decrease in concentration towards the marine end than in the raw data, while the decrease in quartz from the fluvial- to the marine-dominated end of the estuary is less pronounced. Gibbsite and pyrite show broadly

sections. Pyrite is variable, with measureable concentrations only occurring in the muddy intertidal flat areas, low and zero concentrations occur in saltmarsh and sandy intertidal environments close to the main channel.

The relative concentrations plotted in figure 4.20C, show a subtly different variability in mineral concentrations compared to the raw mineral data. In particular in the fluvial to marine transect, plagioclase and kaolinite increase in concentration towards the marine end of the estuary. Chlorite and muscovite show less of a decrease in concentration towards the marine end than in the raw data, while the decrease in quartz from the fluvial- to the marine-dominated end of the estuary is less pronounced. Gibbsite and pyrite show broadly similar concentrations down the estuary.

Of the two across-estuary transects (two and three), transect three has a higher degree of variability in mineral concentrations. Transect two has increases in plagioclase, chlorite, gibbsite and kaolinite across the intertidal flat towards the main estuary channel, with decreases in quartz and muscovite concentrations over the same profile. K-feldspar only occurs in saltmarsh sediments, while pyrite is only evident in intertidal sample sites, with particularly high concentrations in muddy intertidal flat areas. The variability in transect three makes it difficult to discern variations in mineral concentrations, however pyrite and K-feldspar display the same distributions as transect two, and

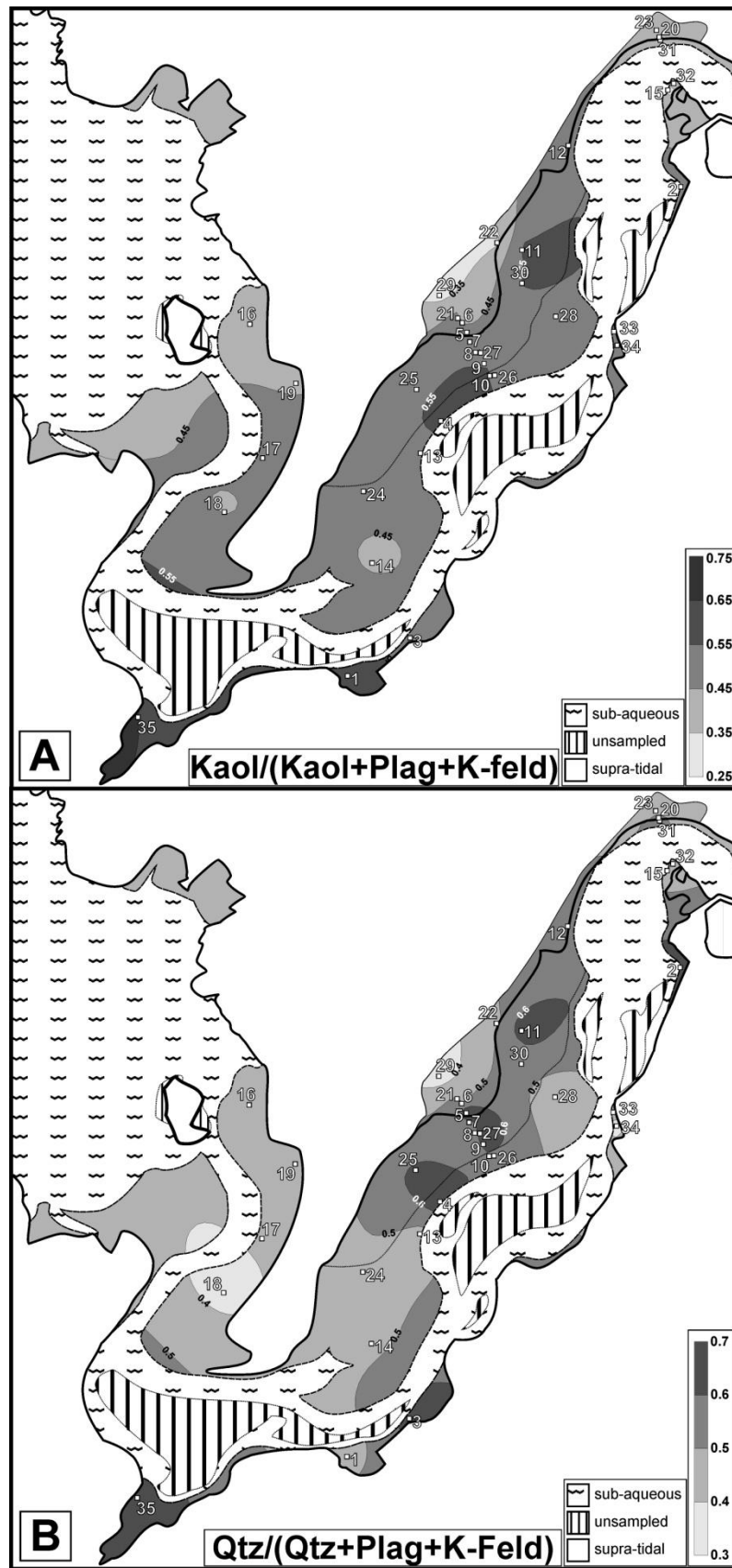


Figure 4.21 - Mineral indices maps. (A) Kaolinite-plagioclase-k-feldspar. (B) Quartz-plagioclase-k-feldspar. Kaol = kaolinite, plag = plagioclase feldspar, chlor = chlorite, musc = muscovite, qtz = quartz.

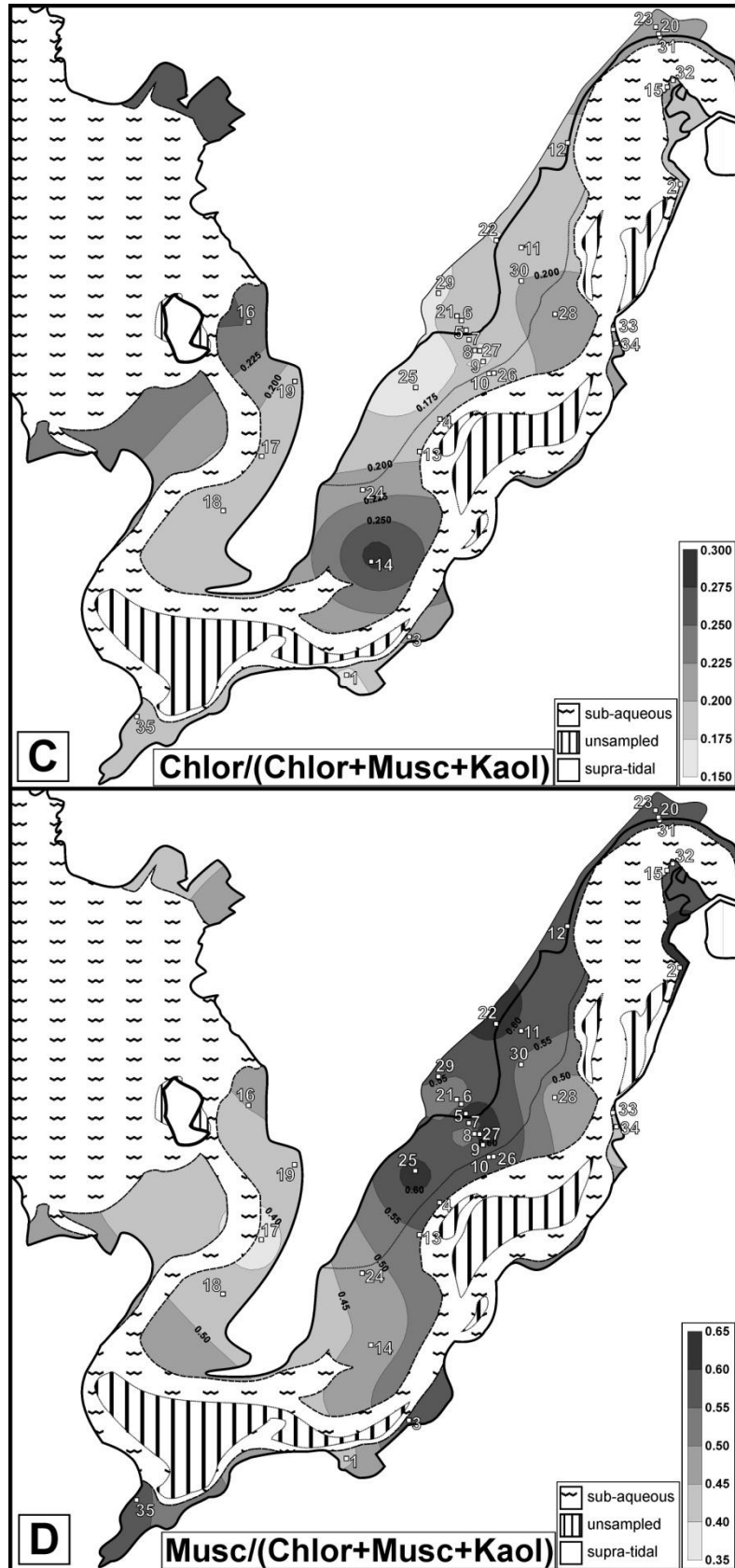


Figure 4.21 - Mineral indices maps. (C) Chlorite-muscovite-kaolinite. (D) Muscovite-chlorite-kaolinite. (E) Kaolinite chlorite-muscovite. Kaol = kaolinite, plag = plagioclase feldspar, chlor = chlorite, musc = muscovite, qtz = quartz.

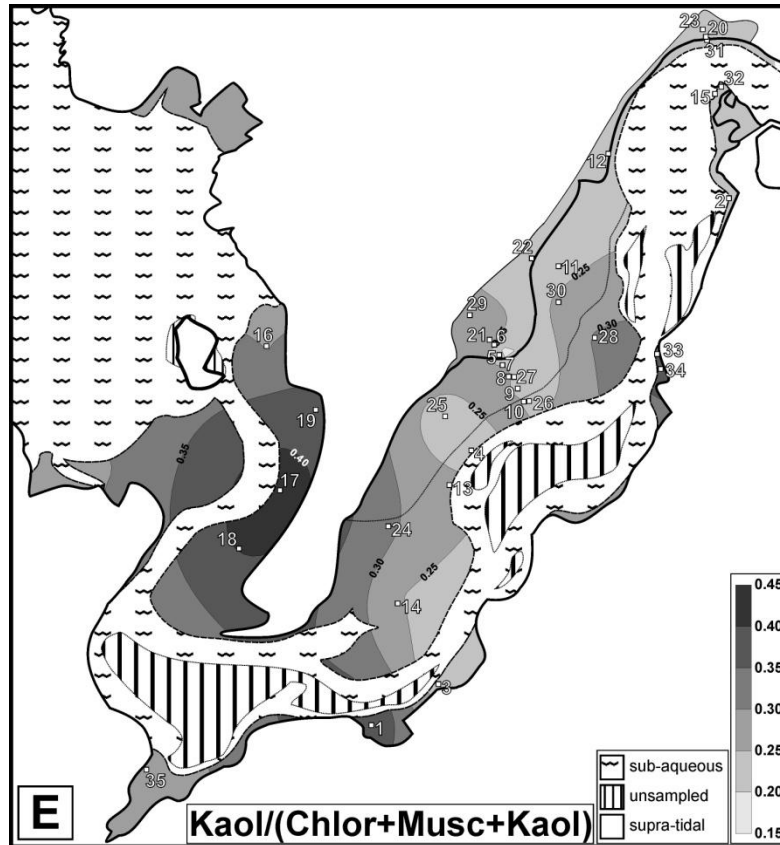


Figure 4.21 - Mineral indices maps. (E) Kaolinite chlorite-muscovite. Kaol = kaolinite, plag = plagioclase feldspar, chlor = chlorite, musc = muscovite, qtz = quartz.

most of the other minerals appear to have broadly the same concentrations, except for muscovite which appears to increase towards the estuary channel and plagioclase which displays a slight decrease in concentration over the same profile.

#### 4.5.8 Mineral indices

Maps of mineral indices (fig. 4.21) were generated for a range of different mineral relationships. Kaolinite weathering index was generated by dividing the kaolinite concentration at each location by the concentrations of kaolinite, plagioclase and K-feldspar (mimicking the chemical index of alteration used in geochemical

analysis of sedimentary materials; (Taylor and McLennan, 1985)). The kaolinite weathering index map (fig. 4.21A), indicates that lower weathering values (0.25-0.45) occur principally in saltmarsh areas, and at the front of the shoreface, intermediate values (0.45-0.55) occur over much of the rest of the estuary, with particularly high values on the south side of the estuary, close to the small river input and in areas proximal to the main estuary channel. The quartz-plagioclase-K-feldspar index (fig. 4.21B) has lowest values (0.3-0.5) at the front of the estuary, and in some sandy intertidal areas, as well as in upper saltmarsh environments. Highest values occur in muddy intertidal areas and proximal to the small river input on the south-side of the estuary.

A series of indices were also generated using the three clay minerals: chlorite, muscovite and kaolinite, the sum of the concentration at each location was used to divide each clay mineral concentration. These indices show a broadly similar distribution to the relative concentrations that are given in figure 4.18.

#### **4.5.9 Worm cast distribution & mineralogy**

Worm cast density was measured at six sites within the Anllóns estuary, while six surface and six worm cast sediment samples were collected from the same site. The average worm cast density map (fig. 4.22) shows that there is a high degree of variability in worm cast density

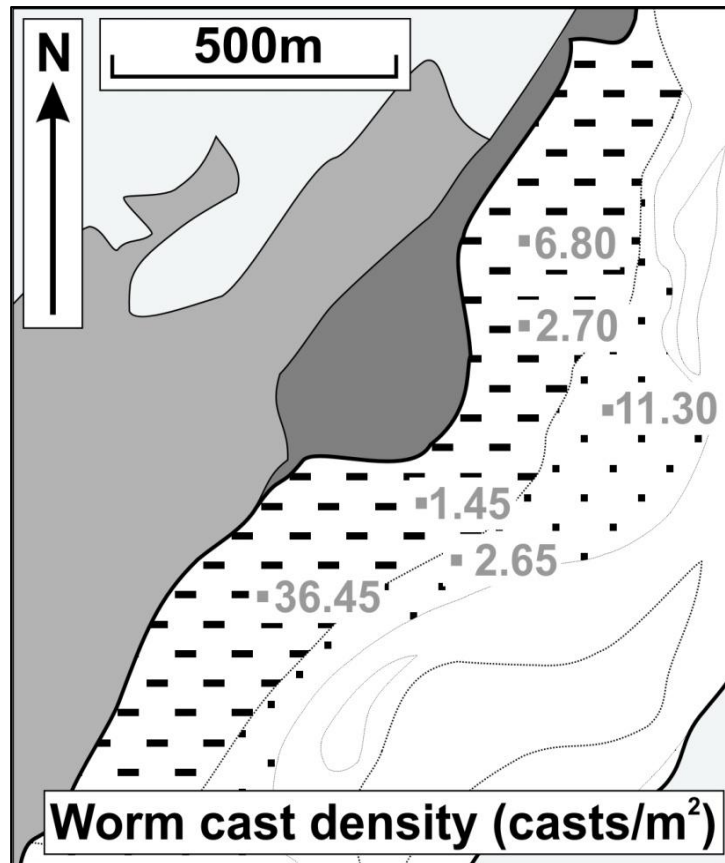


Figure 4.22 - Worm cast density map. Worm cast density varies considerably, but does not show any systematic variation, possibly due to subtle variation in different sub-environments.

over a relatively small area. Systematic variability in density between the muddy and sandy intertidal flat environments was not identified. However, there was a great deal of variability within the sub-environments themselves (e.g. topography, sea grass coverage, drainage creeks), which may not have been captured in this small-scale, low-density study.

Mineral concentrations for worm cast (fig. 4.23A), surface sample (fig. 4.23B), and mineral difference concentrations (generated by subtracting the relative worm cast mineral concentrations from the relative surface mineralogy concentration) (fig. 4.23C), were all

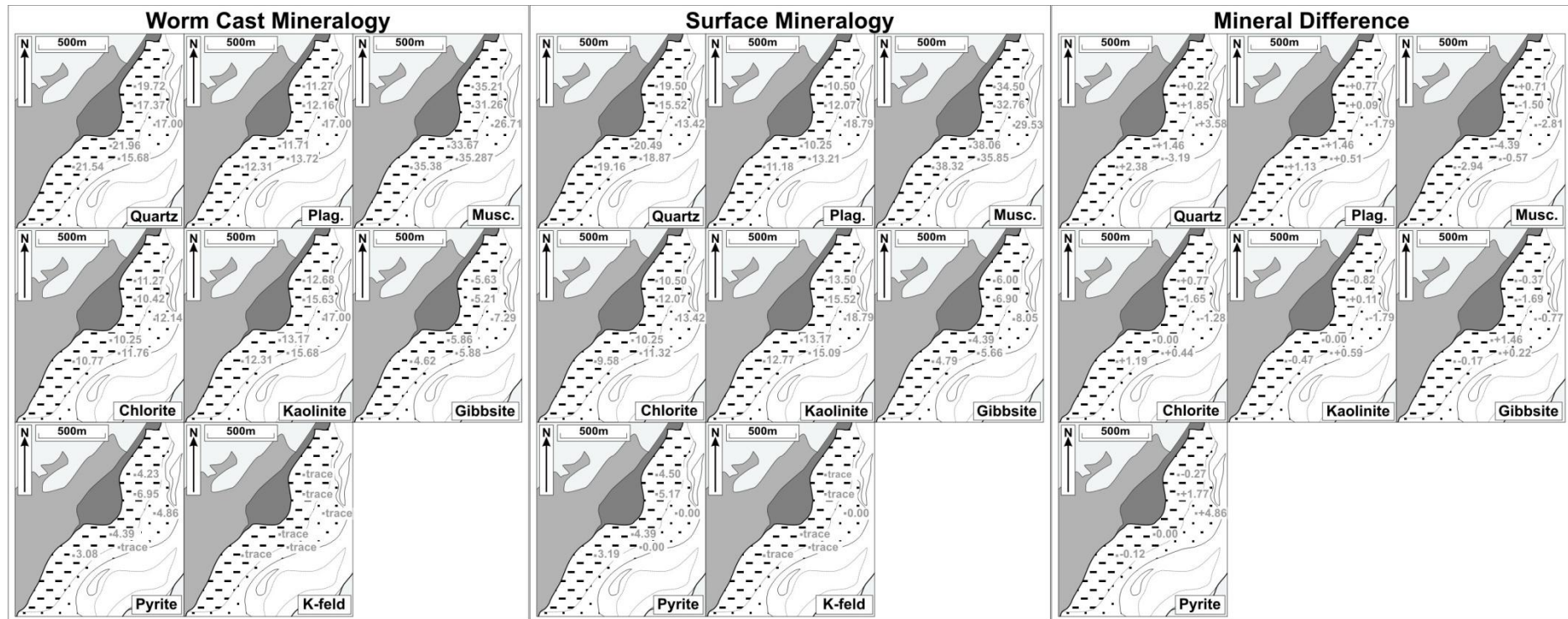


Figure 4.23 - Mapped relative (carbonate normalised) mineral concentrations in worm cast and estuary sediments. (A) Mineral concentration in worm cast sediment. (B) Mineral concentration in surface sediment. (C) Difference between worm cast and surface mineral concentrations in sediment location. The differences in mineral concentration are so small to likely to be within the analytical error of the measurement. Musc = muscovite, K-feld = potassium feldspar, plag = plagioclase feldspar

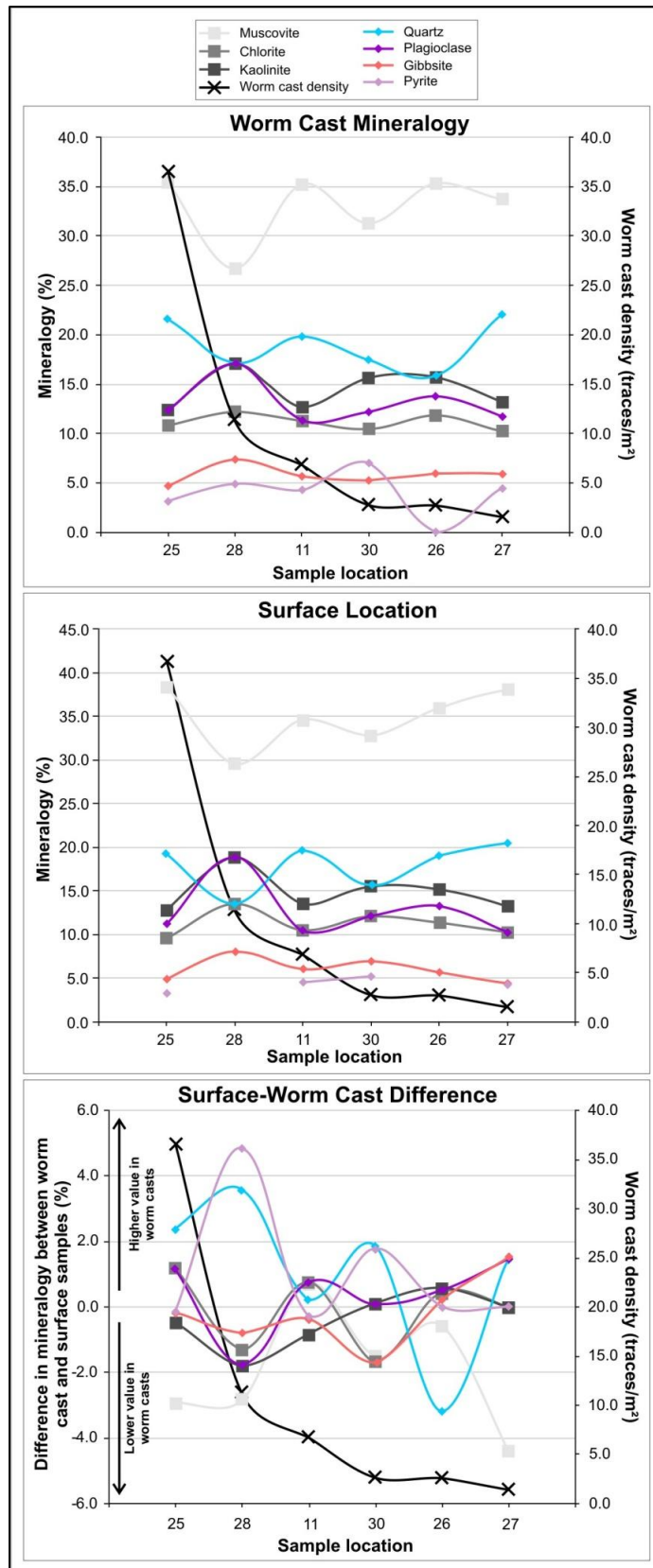


Figure 4.24 - Graphed relative (carbonate-normalised) mineral concentrations in worm cast and estuary sediments. (A) Mineral concentration in worm cast sediment. (B) Mineral concentration in surface sediment. (C) Difference between worm cast and surface mineral concentrations in sediment location. The differences in mineral concentration are so small to likely to be within the analytical error of the measurement.

mapped. The mineral concentrations for worm cast, surface and the difference between the two are also displayed graphically alongside the worm cast density for each sample location (fig. 4.24). The graphs do not appear to show any systematic variability in mineral concentration with increasing bioturbation by annelid worms. The mapped concentrations of the both the worm cast mineral and the difference mineral maps do not appear to show any systematic variation in mineral concentration between environments. Furthermore, the small variability that is seen between surface and worm cast samples is so small that it is within analytical error.

#### **4.5.10 Average concentrations comparison**

To ascertain distinct differences in mineral concentration between sample populations, the average value for worm cast, estuary surface and hinterland sediment sample were calculated using the relative (carbonate normalised) concentrations for worm cast and estuary surface samples. These were then plotted graphically alongside the error (one standard deviation) for each mineral (fig. 4.25). For most of the minerals the average concentrations are broadly similar for each sample population, although there is some variability in standard deviations, particularly with worm casts generally having a smaller error, and hinterland minerals having a larger error. K-feldspar has a zero value in the worm cast samples, and this is due to the high detection limits for K-feldspar in samples on the intertidal flat rather

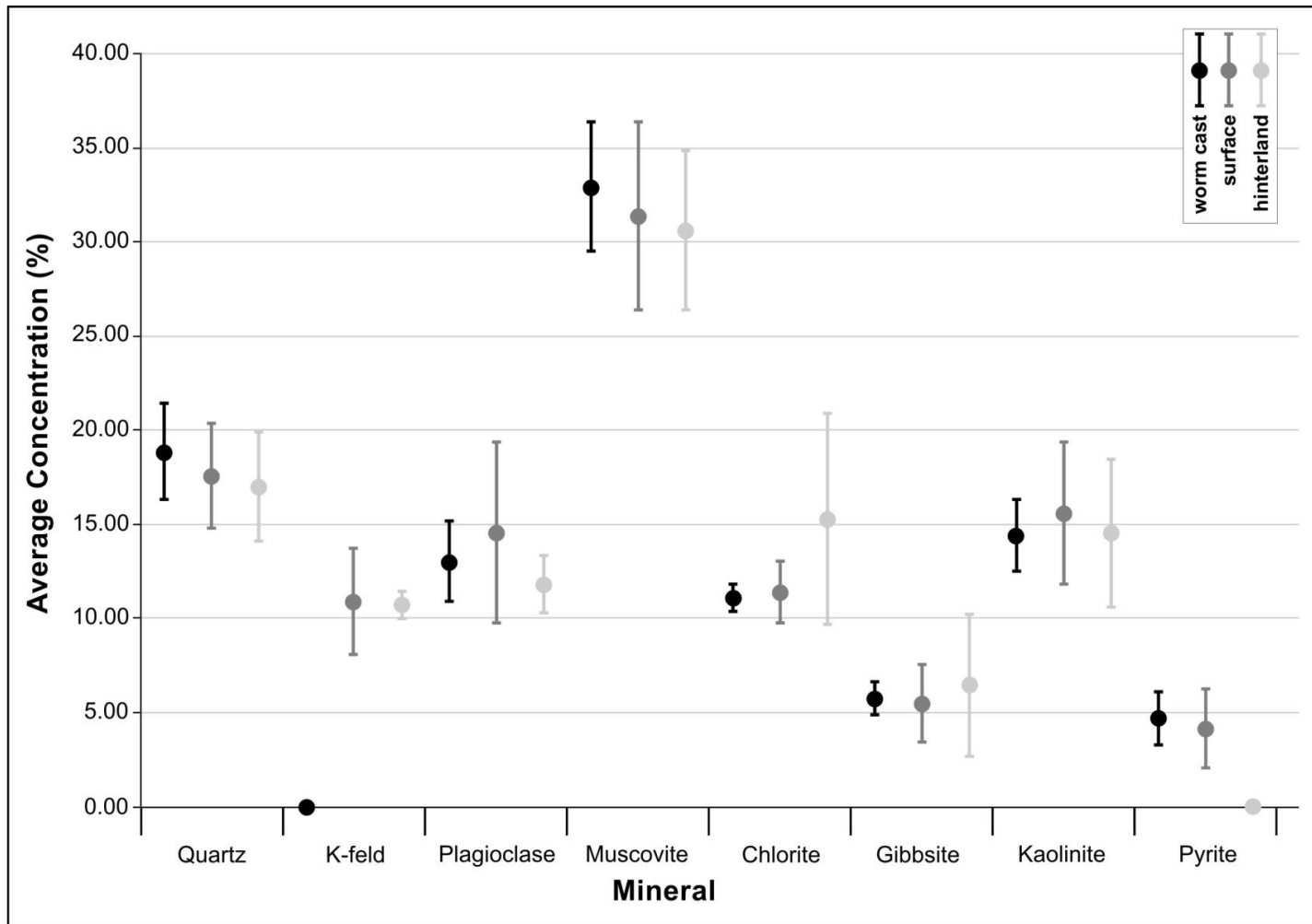


Figure 4.25 - Average relative (carbonate normalised) mineral percentages from worm cast, estuary and hinterland locations. K-feldspar has a zero value in the worm cast samples, and this is due to the high detection limits for K-feldspar in samples. Pyrite is typically only present in trace amounts in hinterland samples, whereas concentrations are approximately 4-5% within estuary sediments, chlorite also has distinctly high concentrations in hinterland samples. This may indicate that chlorite is altering to pyrite in the reducing conditions of the estuary. K-feld = potassium feldspar.

than a removal of K-feldspar from the sediment. Pyrite is typically only present in trace amounts in hinterland samples, whereas concentrations are approximately 4-5% within estuary sediments. Chlorite also has distinctly high concentrations in hinterland samples, and although the other concentrations are within error for hinterland samples the hinterland chlorite concentration is well outside the error of both the worm cast and surface samples.

## **4.6 Discussion**

### **4.6.1 Sediment texture**

The surface sediment of the Anllóns estuary is primarily composed of moderately to poorly sorted, medium sand (fig. 4.9). Coarser and moderately sorted sands with low fine fraction concentrations occur towards the lower part (marine end) of the estuary, particularly on the shoreface where wave reworking and the disaggregation of marine, biological carbonate grains has resulted in the suspension and export of fine grained sediment and the concentration of coarser shell debris. Behind the frontal spit wave energies are lower, sorting becomes increasingly poor and finer sediments are retained within the estuary system (fig. 4.10B).

Although medium sand is the dominant modal grain size on the muddy intertidal flat, sorting is poor, and there is an increase in the fine fraction concentration. The muddy intertidal environment is present approximately half-way up the estuary channel and is towards the

upper tidal limit. This appears to represent a zone of low velocity tidal motion probably resulting in the settling of fine grained minerals and biological particles during high tide slackwater. This is a zone of extensive sea grass development, which impedes tidal velocities and has a root system which binds the sediment together. Bioturbation by annelid worms is also extensive (but variable) in this area.

Saltmarsh sediments have variable texture with some areas dominated by medium, fine or very fine sands. Sorting in these sediments is generally poor or very poor and there are significant increases in fine fraction contents in these areas. Saltmarsh sediments are primarily sandy soils, with salt-tolerant plants covering the majority of the sediment surface. The saltmarsh area is only partially tidal with most of the saltmarsh in a zone beyond the mean high tide line. Tide lines and an extensive network of creeks mark the supra-tidal limit during spring high tides. The increase in fine fraction content is due to a combination of biological matter and the development of fine grained minerals in this area.

#### **4.6.2 Extra-estuarine controls on mineralogy**

The mineralogy of the fine fraction within the Anllóns estuary sediments appears to be predominantly sourced from both marine bioclastic debris and detrital bedrock sources within the river catchment. The high carbonate content (calcite and aragonite) in sediments towards the marine end of the estuary and the strongly inverse relationship

between carbonate minerals and non-carbonate minerals (figs. 4.12-4.15) imply that marine carbonate minerals are diluting the non-carbonate mineral components in the sediment fine fraction. The non-carbonate minerals in the fine fraction of estuarine and riverbank sediment samples appear to be derived from rocks in the hinterland, with all of the non-carbonate minerals present in the estuary found in the weathered bedrock samples in quantifiable concentrations. The dominance of granites and metamorphic schists (fig. 4.1) in the basin has resulted in generally high concentrations for quartz, plagioclase, chlorite and muscovite seen in sediment fine fraction (figs. 4.11 & 4.12).

Comparison of mineral types between hinterland riverbank soils and bedrock mineralogy (fig. 4.8 & Table 4.4) shows a broadly similar suite of minerals, indicating that there is relatively little variability in the suite of minerals present within this basin. Muscovite is absent in location 37, which is likely due to the presence of muscovite-free basic rocks underlying the sample location (Map location C; Fig. 1 & Table 4.4). Location 38 is formed on the same basic rock type, although muscovite is found in similar concentrations as in other locations suggesting that the soils in an area may not simply relate to the underlying bedrock type.

The comparison between mineral compositions in the fine fraction of estuary (figs. 4.11 & 4.12) and hinterland riverbank sediments (fig. 4.8) show that the minerals present are broadly the same. The data

presented in this study appear to support the contention of other authors in that there is a strong terrestrial supply of minerals found in coastal and marine environments around the Galician coastline (Bernárdez et al., 2012; Prego et al., 2012). In particular, studies in offshore settings found a strikingly similar suite of minerals to this study (Belzunce-Segarra et al., 2002).

Gibbsite is found in nearly all sediment samples and in one bedrock sample. Gibbsite generally develops through the intense weathering of feldspar or type 1:1 clay minerals such as kaolinite (Deer et al., 1992). Although commonly noted in tropical locations where intense weathering occurs, previously published work (Macias Vazquez, 1981; Calvo et al., 1983) indicates that the gibbsite present in northwest Iberia is likely to be the result of early weathering of plagioclase.

Clay minerals identified in the estuary sediments in this study are chlorite, muscovite, kaolinite and small trace quantities of smectite. Both chlorite and muscovite are present in bedrock and riverbank soil samples in the Anllóns catchment, and are considered to be primarily detrital. Kaolinite is present in significant quantities in both hinterland riverbank samples and in estuary sediments. Kaolinite is a common weathering product of feldspars, and particularly in the Galician region where large scale high grade kaolinite deposits are mined (Wilson, 1998; Fernández-Caliani et al., 2010); kaolinite was also noted in bedrock samples collected in this study. It therefore seem highly

likely that the majority of the kaolinite noted in the fine fraction of the hinterland and estuary samples was formed through the weathering of feldspars or muscovite in the bedrock and in soils (Deer et al., 1992).

Small quantities of smectite were also noted; smectite is a common clay mineral and can form from a variety of parent minerals in a through a variety of methods including terrestrial weathering (Deer et al., 1992) or authigenically in deep sea sediments (Belzunce-Segarra et al., 2002). Smectite within estuary sediments could potentially be sourced from either fluvial or marine sources. Smectite could develop in marine waters through the interaction of amorphous hydroxides and biogenic silica (Michalopoulos et al., 2000; Michalopoulos and Aller, 2004). A fluvial supply of smectite would necessitate the weathering of bedrock within the basin, and there is some evidence for the development of smectite from the weathering of muscovite inclusions in feldspar crystals in granite-derived saprolites in Galicia (Taboada and Garcia, 1999). That there is evidence for smectite forming in Galician rocks and smectite is evident in trace concentration within basin sediments (fig. 4.8) would suggest that a fluvial source may be more likely. If this is the case, a proportion of the smectite noted in the study (Belzunce-Segarra et al., 2002), particularly those in the Ria de Vigo, could be terrestrially- rather than marine-derived

### **4.6.3 Intra-estuarine controls on mineralogy**

The relative mineral concentrations within the Anllóns estuary display a non-uniform distribution (figs. 4.11, 4.12, 4.14, 4.17, 4.18 & 4.20). This variability is useful in developing estuarine dynamic and sediment budget models, and aids the understanding of early diagenetic mineral evolution in coastal settings. A discussion of the possible causes of the differences in mineral concentration is presented below.

#### 4.6.3.1 Local mineral source

The mineralogy of estuary sediments appears to be influenced by catchment area geology. Studies of sediments in northern Galician rias (Bernárdez et al., 2012; Prego et al., 2012) indicate that the mineralogy of coastal sediments can strongly reflect local geology particularly where rivers remain within the north-south grain of lithological units. The Anllóns river catchment drains across this lithological grain; it would therefore be expected to reflect the range of rock types and minerals within the basin. Small creeks and streams drain directly into the estuary and could locally influence mineral concentrations in parts of the estuary. However, the estuary is bounded by the four main lithological units: basic rocks, granite, schist and gneiss, so it should be expected that even if the majority of sediments are locally derived, the minerals still reflect regional geology, rather than local geology.

#### 4.6.3.2 Geochemical changes

Comparison of the average values of surface and hinterland sediment concentrations (fig. 4.25) indicates that for the majority of minerals, average concentrations in estuary locations are broadly similar to source sediments in the hinterland, with differences of around 1-3%. Pyrite is an exception and is present at ~4-5% in estuary surface and worm cast sediments, but is only present in trace quantities at hinterland locations. Pyrite in sediments forms in reducing conditions through the reaction of detrital iron-bearing minerals with sulphide, which is formed through the reduction of dissolved marine-sulphate in pore waters by bacteria (Berner, 1984). Un-compacted marine sediments flushed with sea water typically have low sulphide concentrations and pyrite tends to occur in anoxic offshore sediments. However pyrite can occur in organic-rich sediments where all  $\text{SO}_4^{2-}$  is removed by bacterial reduction to form sulphides (Tucker, 2001). Pyrite is generally absent in terrestrial settings due to the low concentrations of dissolved sulphate in sediments in these environments (Berner, 1984), and this probably explains its paucity in hinterland samples.

The possible sources of iron for the formation of pyrite are the in-situ weathering of iron-bearing chlorite, or the uptake of aqueous iron, or from suspended Fe-oxides, hydroxides and colloids from river-supplied estuary waters. In hinterland sediment, chlorite has a higher

concentration (~4%) which indicates that it may be the source of iron in the pyrite. This would also result in the release of aluminium and silica from the chlorite which could go on to produce kaolinite or muscovite, although there is no definitive increase in these minerals in estuary sediments. Alternatively these ions could be lost from the sediment.

Field observations indicate that reducing conditions are prevalent a few centimetres beneath the surface over the majority of the estuary. Pyrite is likely to develop from the breakdown of chlorite throughout large parts of the estuary, but without direct evidence of this process occurring uptake of aqueous iron from estuary waters is also still possible. Discrete locations where high concentrations of pyrite are found in estuary sediments (fig. 4.18E) may indicate that only these locations have particularly reducing conditions. Bioturbation by annelid worms may result in the pyrite being brought to the surface.

#### 4.6.3.3 Role of bioturbation

Worm cast density values from a small selection of sites within the estuary (fig. 4.22) indicate that there is no systematic variability of density on the scale of sample locations. Variations may have been expected between environments, with proximity to marine or terrestrial influence, or possibly down estuary, but density values do not change systematically with these variables. Field observations noted that worm cast density can vary considerably over the scale of

a few metres (fig. 4.4F), and a higher density study may capture this variability

Relative concentrations of minerals within worm cast sediments and the corresponding surface sediments in a location do not appear to show any systematic variation in concentrations either graphically or when mapped (figs. 4.23 & 4.24). Average concentrations for worm cast and estuary surface samples (fig. 4.25) have very similar concentrations indicating that there is no variation on the scale of the estuary. When the differences between the two concentrations at each site are mapped (fig. 4.23C) and presented graphically (fig. 4.24C) there is no systematic variation in mineralogy either positively or negatively. Differences in mineralogy are small enough to be within a measurement error. Bioturbation of the sediment therefore appears to have no overall effect on the local mineral concentrations in worm faecal casts. Comparison of the work from this study to experimentally derived clay minerals produced in the gut of annelid worms (McIlroy et al., 2003; Needham et al., 2004; Needham et al., 2005; Needham et al., 2006; Worden et al., 2006;) may underscore the difficulty in relating experimental works to modern environments. However the key difference is that the sediment used in those studies utilised unweathered Icelandic basalt, and the sediment found in the Anllóns estuary is composed of weathered, primarily felsic minerals. Unweathered basalt is likely to be more reactive than already

weathered minerals and component mafic minerals in basalt may also be more reactive than those derived from felsic source rocks. Minerals in estuary sediments, such as plagioclase and K-feldspar have the potential to weather to kaolinite or smectite, but do not appear to be effected by worm ingestion. This may suggest that both pre-weathered and felsic minerals may be less reactive in some real-world settings than in experiments, although bioturbation may still act to physically mix sediment within the estuary

#### **4.6.4 Estuarine dynamics**

In-situ geochemical changes to surface sediment mineralogy and the effects of biological interaction with sediment have been considered. It appears that within the estuary pyrite may be forming from the alteration of chlorite, and that the ingestion of sediment by annelid worms has no systematic effect on sediment composition within sediment fine fraction. With the effects of extra-estuarine controls on sediment composition already considered, particularly the effect of mixing marine carbonate and fluvial siliciclastic, it is pertinent to consider the role of intra-estuarine sediment dynamics on the distribution minerals within the fine fraction of sediments.

The focus of this work is concerned principally with the distribution of clay minerals and for this reason, relative clay mineral concentrations are treated separately to relative non-clay mineral concentrations.

#### 4.6.4.1 Clay minerals

Relative muscovite and kaolinite concentrations display the most striking distribution patterns. Relative muscovite concentrations within estuary sediments are lowest at the front of the estuary (fig. 4.7C), and concentrations tend to increase up the estuary. This is further demonstrated by the increase in relative muscovite concentrations in the estuary transect (fig. 4.20C), where highest concentrations occur on the muddy intertidal flat and in upper reaches of the estuary close to the river bend. Relative kaolinite concentrations display an inverse pattern to relative muscovite concentrations, with lowest concentrations in saltmarsh sediments and in the upper reaches of the estuary (fig. 4.17B). There is an increasing concentration of kaolinite towards the marine dominated end of the estuary (fig. 4.20C).

Relative chlorite concentrations are appear lower in saltmarsh and muddy intertidal environments (fig. 4.17A), as well as at the front of the estuary in shoreface sediments. Higher chlorite concentrations occur close to the main estuary channel (fig. 4,20C).

The inverse relationship between relative kaolinite and muscovite within estuary surface sediments indicates that there is some partitioning of clay minerals within the estuary. That the clay minerals all appear to be derived from terrestrial sources indicates that any partitioning is a result of internal estuarine controls rather than co-

dilution of marine and fluvially sourced siliciclastic sediments noted in some estuaries (Chamley, 1989; Feuillet and Fleischer, 1980).

The interaction of fluvial and marine waters is augmented by the cyclicity of a tidal prism (volume of water between mean high tide and mean low tide) moving up and down an estuary twice daily producing a uniquely complex set of depositional processes within each estuary. An increase in salinity causes flocculation processes resulting in the deposition of clay minerals and other flocculated material is coincident with higher flow velocities of the turbidity maximum. This potentially re-suspends and breaks apart flocculated material, as well as increasing particle drag, thus preventing settling. The balance between these two competing processes will vary considerably. Important factors include: estuary geometry and geomorphology, tidal range, position in the lunar and diurnal tidal cycles, local weather conditions, river discharge rate, concentration of biological matter, clay minerals types and their source (fluvial or marine) and concentration, clay mineral particle size and geometry, clay mineral specific gravity and clay mineral chemical composition and relative charges.

The movement of a saline turbidity maximum varies through time as the tide floods and then ebbs, and during spring-neap cycles. Taking this in to account, it is likely that clay minerals will occur in diffuse bands rather than at discreet points or lines. When considering the

distribution of relative clay mineral concentrations in estuary sediments (fig. 4.17), muscovite is concentrated in an upstream band, while kaolinite is concentrated in a downstream band. Taking salinity changes in isolation, muscovite seems to preferentially settle out of the water column where salinity is relatively low, while kaolinite may settle out at relatively higher estuarine salinities (fig. 4.26). Experimental works on the order clay mineral deposition due to flocculation with salinity have previously reported contrasting orders of clay flocculation (Whitehouse et al., 1960; Edzwald and O'Mella, 1975; Gibbs, 1983;). The present study of modern clay mineral distribution patterns in the Anllóns estuary would appear to partially support the order of deposition outlined by the works of Whitehouse et al. (1960) and Gibbs (1983). Both studies in static and turbulent water conditions suggested that illite (muscovite) may deposit before kaolinite. Important differences between the two published works and this present study are firstly, the likely differences in mineral types, particularly with respect to elemental chemistry, and particle characteristics including morphology, density and size. Secondly, the present study is in a modern environment and there may be issues with repeatability of such a dynamic environment in the laboratory. Another issue is that the chlorite distribution is not random, but also does not conform to any simple hydrodynamic or geological processes. Based on experimental work (Whitehouse et al., 1960), it may have been

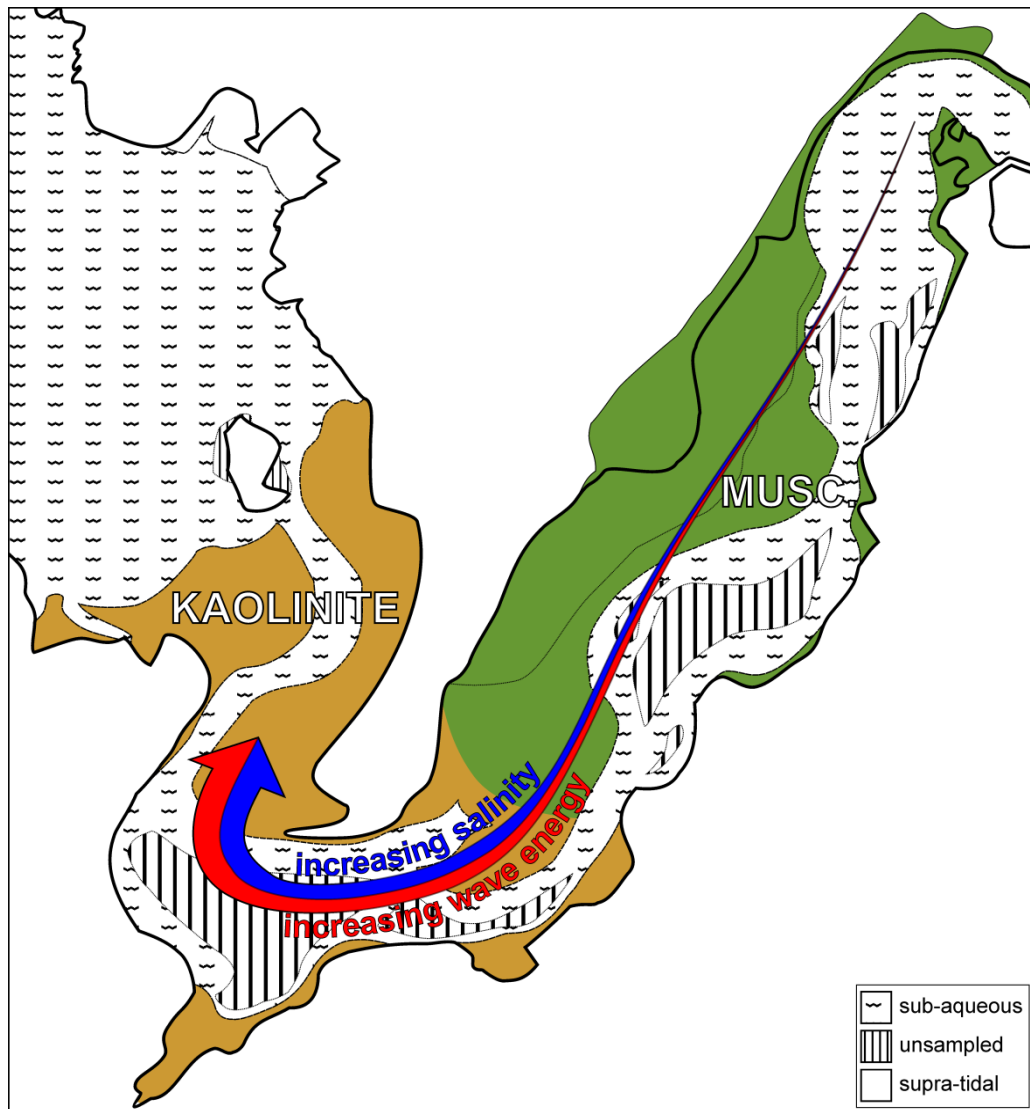


Figure 4.26 - Models for the distribution of muscovite and kaolinite in estuary sediment. Musc = muscovite

expected to flocculate and deposit last in the sequence, but this does not seem apparent from the present distribution.

If the distribution of relative concentrations of kaolinite and muscovite are considered in terms of estuarine energy conditions and the turbidity maximum, kaolinite is concentrated in a relatively higher energy environment while the muscovite settles out in particularly low-energy slackwater conditions (fig. 4.17). This conforms to the example from the Loire Estuary (Gallenne, 1974) where montmorillonite was

<b>Mineral</b>	<b>Shape</b>	<b>Size</b>	<b>Specific Gravity</b>	<b>Specific surface m<sup>2</sup>/g</b>
Kaolinite	6-sided flakes	long axis: 0.05-2um (Stack: 3000-4000um); short axis: 0.1-4um	2.60-2.68	10-20
Mica (illite)	flakes	long axis: up to 10um; short axis: 0.003-0.1um	2.60-3.0	65-100
Chlorite	flakes (similar to illite)	1um	2.6-2.96	65-100

**Table 4.5 - Characteristics of 3 main clay minerals in estuary fine fraction (from Mitchell & Soga 2005).**

reported to be suspended relative to illite in the turbidity maximum, only falling out of suspension in the slackwater periods.

Direct evidence for an estuarine hydrodynamic control on the distribution of clay minerals is lacking. The concentrations of clay minerals indicate that the physical parameters of the minerals themselves (table 4.5) may be extremely important in understanding their distribution. Both kaolinite and muscovite are generally flakes of varying size and shape; muscovite (especially illite) tends to form thin and long particles, while kaolinite has a variable size and long and short axes of similar dimensions of scale. Kaolinite can also form 'books' or stacks resulting in a much larger particle size. Due to its shape muscovite typically has a larger surface area than kaolinite. Specific gravities for the muscovite and kaolinite are of the same magnitude, but will vary depending on chemical composition of the clay minerals. In summary, specific gravity of individual clay mineral types may have an unknown effect on suspension and deposition of

clay minerals. However, muscovite may have a shape (thin and long flakes with large surface area) that is more likely to remain in suspension (or less likely to flocculate) or become suspended during turbulent flows than kaolinite may (possible stacking of rectangular flakes with relatively small surface area).

If muscovite is considered to be more easily suspendable than kaolinite, the high energy environment on the shoreface at the front of the estuary may either suspend or re-suspend muscovite leaving a relative concentration in kaolinite towards the marine end of the estuary. This may occur particularly during the initial stages of the flood tide and the later stages of the ebb tide as sediment velocities increase. During the slackwater phase of flood and ebb tides, flow velocities may decrease, giving muscovite an opportunity to deposit. The primary issue is that muscovite is found in all of the fine fraction sediments in significant quantities, and this interpretation would only account for a certain fraction of the fine fraction (possibly the smallest, lightest most 'suspendable' fraction). Furthermore, the data presented only accounts for the fine fraction of the sediment ( $<0.2 \mu\text{m}$ ), the coarsest clay mineral aggregates may be greater than  $0.2 \mu\text{m}$  (Table 4.5).

Smectite is only evident in a few samples in the estuary and is in such low quantities that it cannot be measured (Fig. 4.11D). Where it does occur it is in the upper reaches of the estuary and tends to be where

fine fraction contents are highest. This may suggest that smectite is only deposited in low energy environments when the during the high tide slackwater phase, similar to the distribution noted in the Loire Estuary (Gallenne, 1974).

In summary, estuarine dynamics may have an important role in concentrating some of the clay minerals evident within the estuary, and this could be related to physical parameters of the minerals. Distinguishing the processes which may control clay mineral concentrations within estuary sediments is a multi-faceted task, and may require further work on how clay minerals behave within hydrodynamic flows and how this relates to physical and chemical transport and deposition processes.

#### 4.6.4.2 Non-clay minerals

Of the non-clay minerals present in the fine fraction of estuary sediment pyrite appears to be forming within the estuary (Fig. 4.18E), while K-feldspar distribution analysis is impacted by detection limit issues (Fig. 4.18C). Quartz exhibits little variation (Fig. 4.18A) and is generally within the 15-18% range. Plagioclase has distinctly higher concentrations towards the front of the estuary (Fig. 4.18B); the cause for this could be either geochemical alteration or due to estuarine dynamics. As plagioclase weathers to form kaolinite, it is important to note that it has a broadly similar distribution to kaolinite. If plagioclase is altering to kaolinite it might be expected that it would vary with

respect to kaolinite and a higher concentration of kaolinite would be present where most alteration has occurred. However, more alteration may also take place in locations where plagioclase is concentrated. Therefore, the similar distribution of plagioclase and kaolinite may suggest that more kaolinite is generated where plagioclase is concentrated in the fine fraction or that there is little or no alteration of plagioclase to kaolinite occurring within estuary sediments. Gibbsite concentrations within the fine fraction of sediments (Fig. 4.18B) are generally lower at the front of the estuary, but only occur within a narrow range behind the spit. The lower concentrations at the front of the estuary may be because the gibbsite has a low specific gravity compared to other minerals evident in the fine fraction. The high energy regime at the front of the estuary may suspend fine gibbsite particles and move them offshore.

## **4.7 Conclusions**

Detailed quantitative clay mineral concentrations have been successfully mapped within an estuary for the first time. This study is important as it highlights the potential utility of large scale analyses of the composition of sediment fine fractions in order to understand controls on sediment supply, mineral alteration and sediment dynamics within modern and ancient estuarine and coastal systems.

The key findings of this study are:

1. Chlorite, muscovite and kaolinite are present in variable concentrations throughout the estuary. Smectite is also present in unquantifiable concentrations. Chlorite and muscovite are likely to be detritally derived from the hinterland geology, while kaolinite is a result of weathering in the drainage basin.
2. Within the fine fraction of sediments, clay minerals are generally concentrated in the upper reaches of the estuary and decrease in concentration towards the marine end of the estuary. Conversely, carbonate minerals increase in concentration towards the marine end of the estuary. Marine reworking of sediment is likely to be the cause for the distribution pattern of carbonate minerals, while clay mineral are concentrated in lower energy, areas towards the tidal limit and close to the river-dominated part of the estuary.
3. Within this, carbonate-normalised clay mineral distributions show that kaolinite and muscovite have an inverse concentration pattern, with kaolinite concentrated towards the marine-dominated front of the estuary, and muscovite concentrated towards the river-dominated and low energy areas close to the upper tidal limit. This distribution may be related to the physical characteristics of the clay minerals and how they behave in different hydrodynamic conditions. However this interpretation of process response needs further work.

4. Pyrite has higher concentrations where chlorite is slightly deficient, which is likely to indicate the alteration of chlorite to pyrite under reducing conditions.
5. Recently bioturbated sediment showed no variation in mineral concentrations compared to apparently non-bioturbated sediment samples collected in similar locations. This may be due to the un-reactive nature of pre-weathered felsic sediments (and thoroughly bioturbated sediment present)

## **5. Spatial and temporal variation in mineralogy and texture of sand grain-coatings from a modern estuary: Implications for subsurface investigations**

### **5.1 Abstract**

Detailed analyses of the texture and composition of grain-coatings on sand grains in modern estuary sedimentary environments in the Anllóns Estuary, Galicia, northwest Spain were determined utilising a combination of scanning electron and binocular microscopy, energy dispersive x-ray analysis, x-ray diffraction and infrared spectroscopy. This enabled the origin, development and distribution of sand grain-coatings within an estuarine setting to be discussed with respect to depositional environments and physical estuarine processes.

Sand grain-coatings in the Anllóns Estuary do not vary in texture and consist of poorly sorted mixtures of clay minerals, pyrite, lithic and bioclastic debris. The grain-coatings vary in average coat coverage and mineral composition between different depositional environments. The muddy intertidal flat (MIF) environment towards the top of the tidal limit hosts grains with the greatest average coat coverage (9.1 to 30.2%), while grains in the sandy intertidal flat (SIF) have the lowest average coat coverage (2.3 to 20.3%), and this may

be related to the higher energy conditions in this latter setting. Fine-grained sediment content within sands appears to control coat coverage with a small increase in fine fraction content (1-2%), enough to increase the coat coverage ranges in MIF and SIF sedimentary environments. Mineral concentrations in the fine fraction are controlled by marine influence and environment setting.

The possible causes of grain-coat formation are the co-deposition of fine-grained sediment with sands during high tide, mechanical infiltration/clay illuviation of fine grained material from tidal or formation fluids into underlying sands, and the ingestion and excretion of fine-grained and sandy sediment by lug worms, which may adhere coats to sand grains. On the basis of evidence from the Anllóns estuary, grain-coating in modern environments are dissimilar to ancient examples, and this is likely due to the diagenetic over printing of grain-coats during burial. Areas where grain-coatings may occur (improving or reducing reservoir quality) may be found in estuarine settings, close to the tidal limit where finer-grained sediment is concentrated through flow processes, and where bioturbation may occur.

## **5.2 Introduction**

Clay mineral coatings on sand grains can have a great effect on the pore volume characteristics within petroleum sandstones reservoirs (Dixon et al., 1989; Bloch et al., 2002; Størvoll et al., 2002; Geçer

Büyüktüku and Suat Bağcı, 2005; Berger et al., 2009), and can seriously affect recovery volumes where the coatings can restrict fluid flow (Glennie et al., 1978; Seemann, 1979; Kantorowicz, 1990; King, 1992). Alternatively, clay coats can restrict growth of pore-filling quartz cement and so lead to enhanced reservoir quality (Storvoll et al., 2002; Bloch et al., 2002; Dowey et al., 2012). Understanding the distribution of coatings from a regional to a facies scale within subsurface reservoirs is a key challenge in increasing recoverable volumes in both existing fields and discovering new prospects in maturing basins.

Geological models that attempt to forecast subsurface authigenic mineral evolution often rely on field or well analogues (Jahn et al., 2008). Refinement of models occurs through detailed knowledge of time-temperature histories enabling a better understanding of the effects of diagenesis on sandstone components (Ramm and Bjørlykke, 1994). However, knowledge of the geographic distribution of grain-size, initial textural characteristics and the starting mineralogy of sand sediment and its components can provide insight into subsequent stages of diagenetic development. An improved understanding of the texture and composition of sand coatings soon after deposition and during the earliest stages of diagenesis could help to enhance the subsurface capability for predicting where significant pore volumes are most likely to be preserved.

### **5.2.1 Ancient clay mineral cements in reservoirs**

Understanding the effect of clay mineral coatings in sandstones is of great importance, primarily because clay minerals in sandstone reservoirs tend to reduce porosity and permeability (Worden and Morad, 2003). Secondly, because some clay mineral coatings inhibit the formation of later mineral cements such as quartz and calcite (Moraes and De Ros, 1990) in reservoir sandstones which may result in porosity and permeability preservation at significant burial depths. Compiled helium porosity measurements from the Norwegian Continental Shelf reported up to 15% higher porosity for chlorite-coated sandstones at 4200m than would be expected from regional trends (Ehrenberg, 1993). Other factors important in the overall effect of authigenic clay mineral development on reservoir quality are the grain-size range and sorting characteristics of the sediment at the time of deposition, the mineralogy and chemistry of the sediment and composition and temperature of interacting pore waters (Bloch et al., 2002).

#### **5.2.1.1 The negative effects of clay mineral coats**

From a geological perspective, the negative effects of clay minerals in sandstone reservoirs are primarily due to the authigenic development of clay minerals and the deformation of ductile grains resulting in the loss of initial framework porosity and permeability (Dutton et al., 2012; Imam and Shaw, 1987). Authigenic clay minerals

are likely to develop if the initial composition of the sandstone is rich in detrital clay minerals, reactive lithics or feldspars (Jahren and Aagaard, 1989; Bloch et al., 2002; Karim et al., 2010). High temperatures and pressures within the deeply-buried sandstones result in the dissolution of some sandstone components and the precipitation of clay mineral coatings. In the Rotligend sandstones of the North Sea (Rossel, 1982), feldspars diagenetically alter to kaolinite, which with increasing burial, in turn develop into illite. The progressive alteration reduces permeability, with long thin illite threads impeding fluid flow through the pore volume. In the Clair Field, west of Shetland (Pay et al., 2000), high clay mineral contents (>15%) reduce permeability to less than 10mD, although the mineralogy of the coating appeared to have little effect on static reservoir quality.

#### 5.2.1.2 Positive effects of clay mineral coats

Clay minerals can also preserve porosity and permeability in deeply-buried sandstone reservoirs (Dowey et al., 2012) through inhibition of other authigenic cements such as quartz and calcite (Bloch et al., 2002). Experimental work suggests that the percentage of coat coverage on sand grains is the key factor in preventing the development of quartz overgrowths (Lander and Walderhaug, 1999; Lander et al., 2008). Chlorite grain-coatings are considered to limit the volume of growth space for incipient quartz overgrowths (Billault et al., 2003), thereby preventing large overgrowth development. Illite grain-

coatings have also been reported in one study to preserve porosity and permeability by preventing quartz overgrowths in the Garn Formation in the North Sea (Storvoll et al., 2002), but chlorite grain-coatings are generally considered to be more common (Pittman et al., 1992; Taylor et al., 2010).

A study of grain-coatings in a modern setting may enable a better understanding of the processes involved in producing subsurface authigenic grain-coats. The questions to be addressed by this paper are:

1. Do sand grain-coatings vary in character in a modern estuary?
2. What controls the coat coverage on sand grains in modern settings?
3. How do modern grain-coatings relate to subsurface coated sand grains in petroleum reservoirs?

### **5.3 Study area**

The Anllóns Estuary and surrounding study area are located in the province of Galicia on the northwest coast of Spain (fig. 5.1A). A summary of the geological history, geomorphology and mineralogy of the study area is presented below.

#### **5.3.1 Geology and tectonics**

The geological grain of the study area is dominated by a north-south trend resulting from the late Devonian to late Carboniferous Variscan

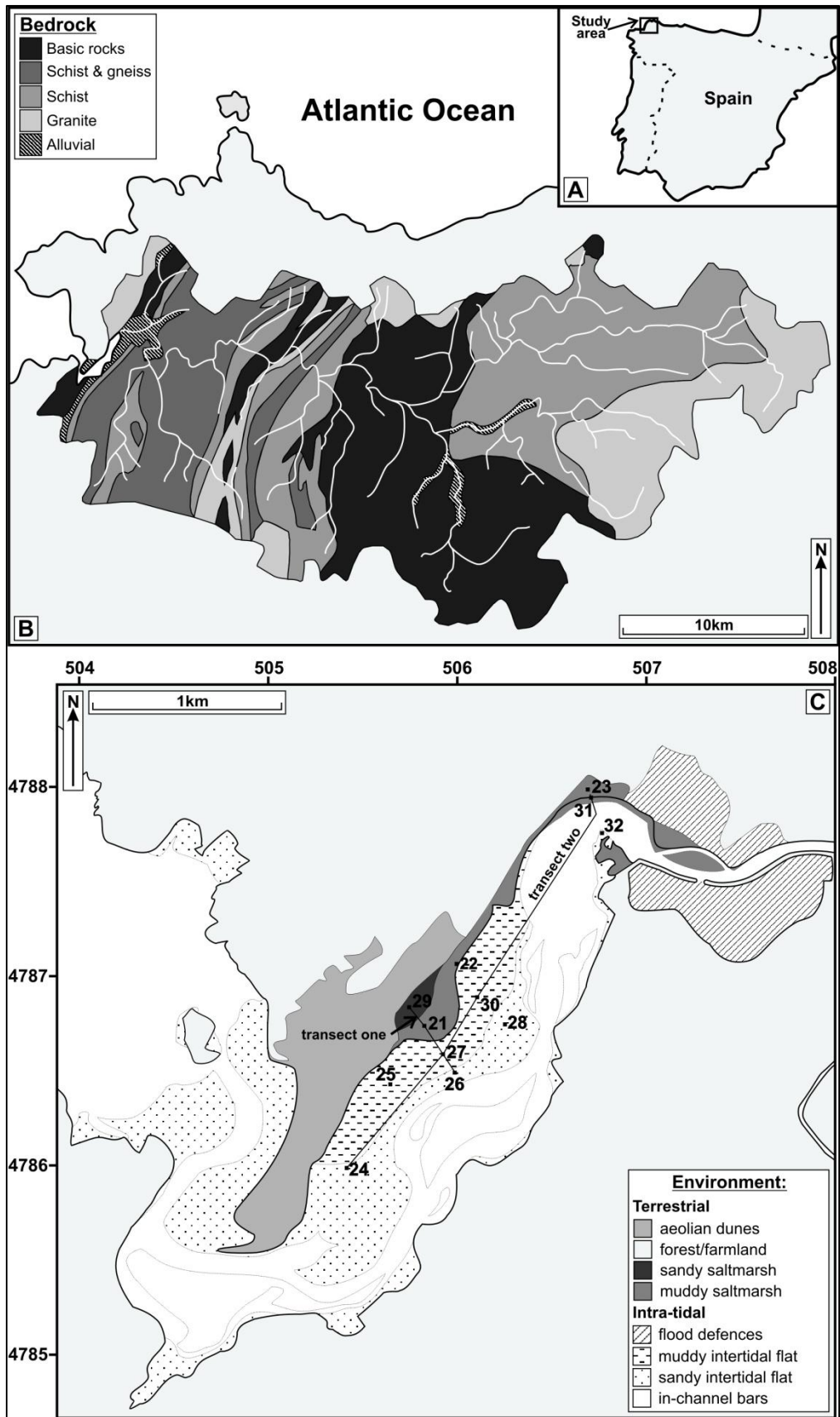


Figure 5.1 Spanish estuary setting. (A) Country location. (B) Geology of the Anllóns catchment. (C) Estuary geomorphology and core locations and position of correlation transects (fig. 5.6).

Orogen, which overthrust a series of allochthonous complexes on to the Gondwanan margin (fig. 5.1B). Two regional metamorphic events are associated with the Variscan orogen. The first during the early Variscan was a high pressure Barrovian-style metamorphic event related to Nappe emplacement. The grade of metamorphism and the types of minerals are variable and dependent on position within the orogen. The second high temperature metamorphic episode is locally associated with granite intrusions, these produced an inverted metamorphic gradient with underlying cold rocks (Dallmeyer et al., 1997).

Footwall units are primarily schistose meta-sediments and granites at outcrop. Hanging-wall rocks are more variable and include gabbroic and ultramafic ophiolitic and lower continental crust units plus basalt alkaline granitoids and low grade metamorphosed terrigenous sequences (Dallmeyer et al., 1997; Llana-Fúnez and Marcos, 2001). The mineralogy of bedrock in the Galician region is complicated due to the juxtaposition of various terranes associated with the Variscan event, and the related phases of metamorphism.

### **5.3.2 Relative sea level history**

A study of late Pleistocene raised marine and continental deposits preserved in embayments and rias along the north-west Galician coast (Alonso and Pages, 2007) provided insight into the relative sea level history of the area. Gravels and sands dated at 100-54 ka

deposited on a polycyclic abrasion surface 2-3 metres above present day sea level mark the last inter-glacial period (Eemian). Overlying this, soils, mass flow deposits and solifluction features are indicative of a cold, terrestrial, and periglacial environment during the earliest glacial stages and the beginning of sea level regression. As base level continued to fall, swamps developed depositing muds and peats. The final unit dated at 25-15 ka (contemporaneous with the last glacial maximum) is composed of breccias, gravels and conglomerates forming both stream channel-fills and debrites.

In the upper reaches of Ria de Vigo, the San Simón Bay forms an estuary at the confluence of three rivers (Pérez-Arlucea et al., 2007). Sediment cores from this estuary indicate an aggradational development from estuarine channels to abandonment and tidal flat development dated at 3.4-3.1 ka. This is followed by incision, and then another phase of channel development and tidal flat development dated at 0.98-0.78 ka. The authors interpreted this with respect to North Atlantic oscillations, with variations in climate controlling sediment supply to the basin. A colder (wetter) climate period supplies increased volumes of sediment resulting in the infill of channels and tidal flat development; with incision representing relative sediment starvation during warmer (drier) periods (Pérez-Arlucea et al., 2007).

### **5.3.3 Anllóns estuary catchment**

The Anllóns Estuary, Galicia (fig. 5.1C) is a relatively deeply incised, partially-filled valley with one large river draining from the east. The Anllóns river drains a 60 km long, 516 km<sup>2</sup> catchment (Varela et al., 2005) comprised principally of soils developed from granite and schist (fig. 5.1B); one small stream drains into the south side of the estuary southwest of the spit (fig. 4.2A). The area has an oceanic climate with a mean annual rainfall of 1000 to 2000 mm/yr (Arribas et al., 2010).

Anthropogenic effects on river and estuary environmental conditions are no more than moderate due to the lack of heavy industry in the area and along the catchment. Sections of the river downstream of the town of Ponteceso are managed defences (fig. 4.2B), which flood during high tide. The northern flood defence is an enclosed marshland partially filling through a network of channels (fig. 4.2C). The southern flood defence is open to the river and estuary channel and becomes completely covered at high tide (fig. 4.2D).

### **5.3.4 Anllóns estuary geomorphology**

The Anllóns Estuary is ~4km long, ~1km wide and has 4.0m maximum tidal range. Downstream of the managed flood defences the estuary channel turns 90 degrees toward the south-west (fig. 4.3A), possibly following the grain of the regional geological trend (fig. 5.1A). The estuary channel has a variable width with a series of in-channel bars (fig. 4.3B). A large frontal attached sandy spit (fig. 4.3C) protects the

inner portion of the estuary and forces the main estuary channel southward around its tip; the spit is mantled by an aeolian dune system (fig. 4.3D).

The tidally-influenced portions of the estuary have three components: intertidal to supra-tidal saltmarsh, muddy intertidal flat and sandy intertidal flat. The saltmarshes are principally developed in the middle and upper reaches of the estuary, with a large expanse on the northern western side of the estuary channel (fig. 4.4A). The saltmarsh has a terraced edge of variable height above the sandflat (fig. 4.4B). Surface sediment underlying the saltmarsh is composed of sand close to the dune system, and becomes increasingly mud-rich up the estuary. The saltmarsh is cut by small creeks and channels, which fill with water during high-tide (fig. 4.4C). Estuary-ward of the saltmarsh, the muddy intertidal flat is flat-lying and composed of a muddy sand veneer (<40 cm), (fig. 4.4D) that overlies relatively clean sand beneath. Plants, such as sea grass, also occur on the sediment surface (fig. 4.4E). Small meandering tidal streams draining the saltmarsh also cross the flat (fig. 4.4F).

Further towards the estuary channel, the sandy intertidal flat is low-lying and composed primarily of relatively clean sand with a low concentration of clay and silt grade sediment (fig. 4.5A). The sandy intertidal flat also has tidal streams, but these are straighter and drain into the main estuary channel at high tide (fig. 4.5B). The sandy

intertidal flat continues around the headland created by the spit and connects with the shoreface at the estuary mouth (fig. 4.5C). The sandy and muddy intertidal portion of the estuary exhibit variable intensities of bioturbation by annelid worms (fig. 4.5 D&E).

#### **5.4 Materials and methods**

Twelve sediment cores were collected along the Anllóns estuary to sample the texture and composition of the fine fraction within the sediment. Locations (Fig. 5.1C) were chosen to cover a range of environments and to form transects permitting the construction of correlation panels. Cores were collected with a jack-hammer driven window sampler (Van Walt Ltd., 2012). The window sampler drives a 50mm diameter core tube into the sediment, within the cutting head is a 'core-catcher', which keeps the collected core in place and prevents the sediment from being disturbed when the core tube is pulled from the sediment. The sediment core is collected whole within a plastic liner, enabling the core to be sealed within rigid plastic tubing and transported back to the laboratory for logging and sampling. Before logging the core is split into two, with one half re-wrapped in the liner and stored in a cool fridge. The remaining half is logged, split into sections and placed in a sample jar prior to sample preparation. A total of seventy-nine sub-samples were collected from the cores, with sample intervals defined by grainsize, composition, and colour where possible. All sub-samples were analysed using X-ray

diffraction. Grain-size analysis and coat coverage measurements were performed on sand sediments where possible. Sediment was also analysed and imaged using a binocular microscope to image the texture and composition of the sediment in the core sub-samples.

Sediment grain-size and sorting analysis are performed on core sub-samples and are based on laser granulometry utilising a Beckman Coulter LS200 (Beckman Coulter Incorporated, 2011). A slurry is made from a sediment sub-sample by adding calgon to de-flocculate sediment components. This is then added to the Coulter where the distributions of particles from 0.4  $\mu\text{m}$  to 2000  $\mu\text{m}$  are counted. Sixty-five grain size analyses were performed. Grain size data presented were analysed using Gradistat (version 6) software (Blott, 2008). All grain size and sorting values presented use the modified geometric (Folk and Ward, 1957) graphical measures.

Fine fractions ( $<2 \mu\text{m}$ ) and coarse fractions ( $>2 \mu\text{m}$ ) of the sediment were separated, with a fine fraction weight percentage (wt %) obtained for each sample location. Sediment sample preparation followed techniques outlined by Moore and Reynolds (1997) and Jackson (1969). Samples were homogenised, sub-sampled, and then air-dried at 60°C for 15-hours. Dry sub-samples were weighed then dispersed in tap water by means of four 5-minute cycles of ultrasonication and stirring. The supernatant liquid was decanted and the clay size fraction ( $<2\mu\text{m}$  e.s.d.) collected by centrifugation at 3500

rpm for 30-minutes. The clay size fraction was then dried at 60°C for 15-hours, ground and then weighed to obtain the clay size fraction percentage.

Random powders of each fine fraction sub-sample were scanned using a PANalytical X'Pert PRO X-ray diffractometer employing Ni filtered Cu k- $\alpha$  radiation, with a scanning range of 3.9-70.0°2 $\theta$  and using extended count times. PANalytical HighScore Plus software was used to semi-quantitatively ascertain the types of minerals in each sediment sub-sample from estuary sample locations. Samples were then glycolated for twenty-four hours and re-scanned over a range of 3.9 to 13.0 °2 $\theta$ , to assess the presence of expandable clay minerals (Moore and Reynolds, 1997).

An infrared spectral analysis on untreated sub-samples of the fine fraction was also performed on representative samples. 1.5mg of fine fraction sub-sample was mixed with 300mg of potassium bromide; this was hand-ground and then sintered at 10 tonnes in a press to produce a sample pellet of 0.5% concentration. The pellets were heated overnight at 150°C to remove any adsorbed water (Madejova, 2003). FTIR spectra were obtained with a Thermoelectron Nicolet 380 infrared spectrometer with an IR source, a germanium on KBr beamsplitter and a DTGS detector (Thermo Scientific, 2012).

Grain-coat coverage measurements were performed on 65 core sub-samples; sediment samples were analysed on polished grain-mount

section. Each sediment sample was sub-sampled and dried at room temperature in a covered petri dish overnight. Grains were mounted within in a plug of epoxy resin under vacuum to prevent spalling of the coat from the grain surface. The surface of the resin was polished and glued to a glass slide, from which excess material was cut and a final polish applied to reduce the size of the epoxy mounted sediment down to approximately 30 microns thick. Before analysis the thin section was covered with a thin veneer of carbon using a vacuum carbon coater.

The thin section was then analysed using backscattered electron (BSE) imaging on a Philips XL30 scanning-electron microscope (SEM) with an electron beam generated from a tungsten filament. A 5.5 spot size was used with a beam current of 20kv. Elemental analysis on samples was also performed with energy dispersive x-ray (EDX) spectroscopy. For each sample multiple images were taken of the sediment mounted on the thin section, with measurements of coat coverage on individual sand grains performed. The process involves measuring the outer perimeter of the grain that is coated in relation to the perimeter of the grain that is not coated to give a percentage coat coverage measurement for each grain. This means that coat coverage is independent of grain size. One hundred grains are counted per sample, with a total of 6500 coat coverage measurements performed in this dataset. Precision of the technique through repeated

measurement of the same sample during the sample run indicates an error of approximately two percent per sample analysed.

Samples were subject to further BSE textural analysis on stub mounts, this enabled a detailed analysis of the surface texture and extent of sand coatings. Sediment was adhered to an aluminium stub using a carbon-based sticker, and this involved dispersing a subsample of air dried sediment over the stub with the sticker attached. Care was taken to ensure that the subsample was from a representative range of grains within the sediment. The stub-mounted sediment was then covered with a thin veneer of gold-palladium (80%-20% ratio) using a vacuum sputter coater. Tests were also performed on blank stubs and the carbon sticker to reduce the effect of the mounting medium on EDX analysis.

## **5.5 Results**

### **5.5.1 Sedimentary environments**

Observations of modern sedimentary processes across tidal cycles were augmented by core descriptions, fine fraction percentages, coat coverage measurements, and textural and mineralogical analyses. From these observations five distinct environments of deposition were identified (figs 5.1C & 5.2). Mapped surface environments and their distributions were utilised as analogues to define the sedimentary environments within the cores. Two representative cores showing the full suite of data are in figure 5.3.

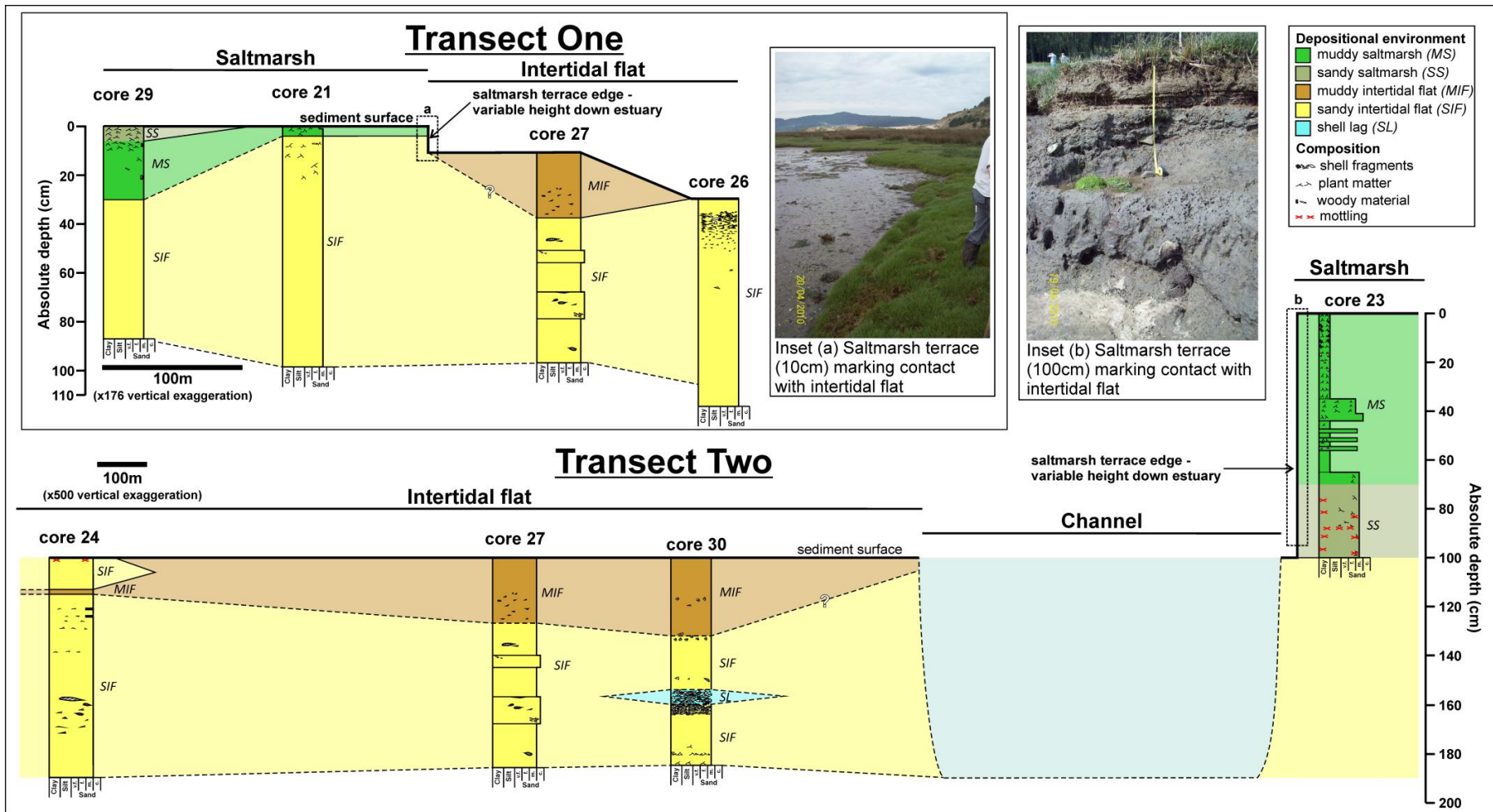
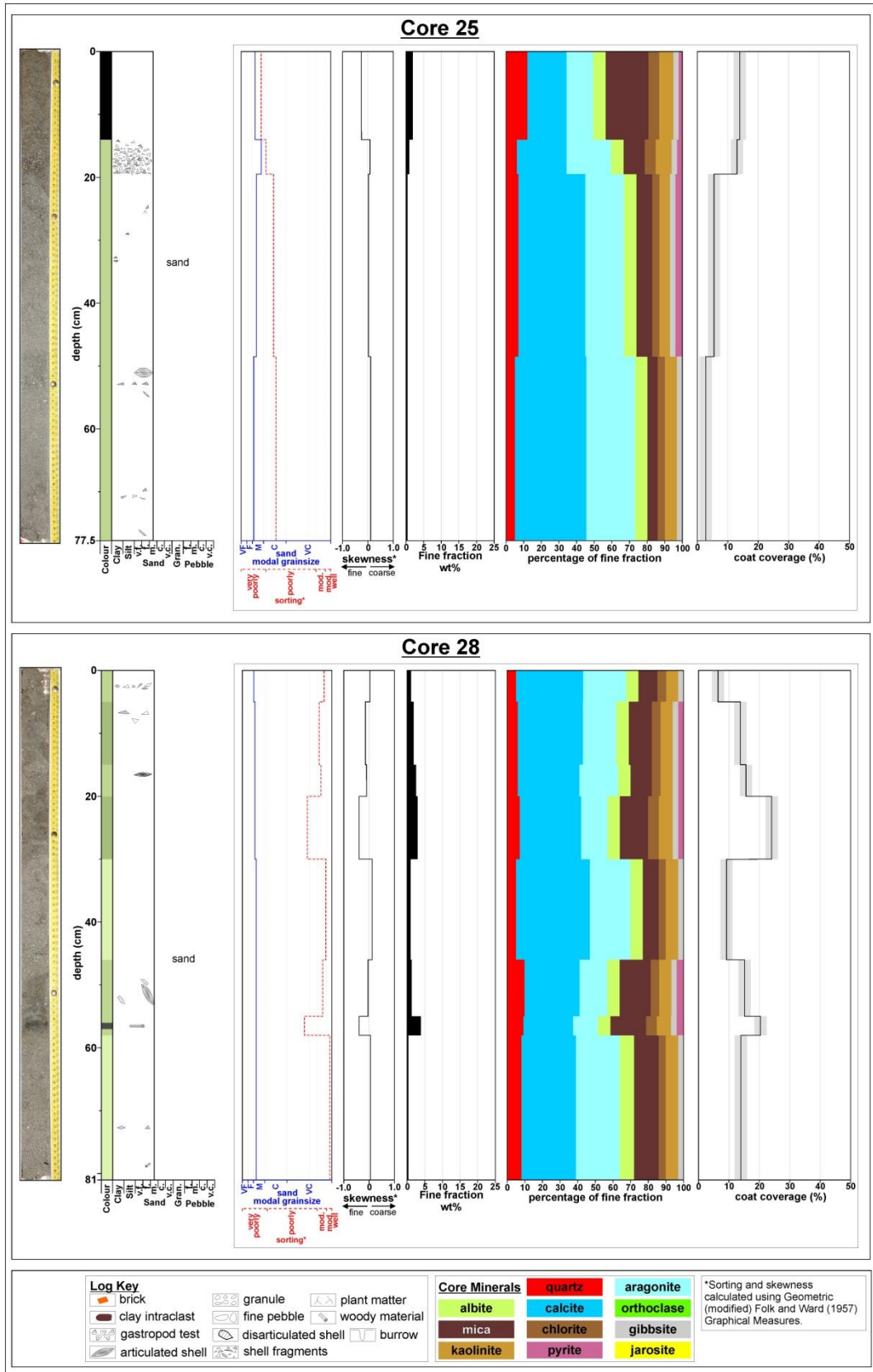


Figure 5.2 - Correlation panels along two estuary transects (locations marked in figure 5.1).



**Figure 5.3 - Core logs of two representative cores. Core logs contain the full suite of analyses performed on cores sections (The full set of core logs are available in appendix 4B).**

The remainder of the cores are available in Appendix 4B. Generally, sedimentary structures are not easily discernible in the cores except for rare clay lenses and localised worm burrows.

#### 5.5.1.1 Sedimentary environment SS: Sandy Saltmarsh

In the present day estuary, sandy salt marshes are not widespread and are primarily located on the western limit of the saltmarsh, close to the aeolian dunes. At the surface, this environment is partially influenced by tides. The sandy saltmarsh is composed of moderately to poorly sorted (average: poorly sorted) medium sand to silt with symmetrical to very fine skewness (average: fine). The fine fraction weight percentage is between 0.4 and 2.2% (average: 1.2%). Average sample coat coverage ranges from 7.5 to 15.6% (average: 10.3%). Plant roots, woody matter, shell material and sediment mottling are common. Calcite and aragonite in the fine fraction are in higher concentrations than all other minerals.

#### 5.5.1.2 Sedimentary environment MS: Muddy Saltmarsh

At the surface this environment covers most of the saltmarsh; it forms a strip on the channel bend closest to the tide defence which runs down the west side of the estuary as far as the southerly limit of the saltmarsh. Some areas closest to the intertidal flat are often partially covered by the tide, but the saltmarsh generally marks the margin of the tidal limit. Within the saltmarsh tidal creeks are filled by the tide as it reaches its higher limit. The muddy saltmarsh is moderately to poorly

sorted (average: poorly sorted) medium sands with fine to very fine skewness (average: very fine). The fine fraction weight percentage is between 1.2 and 22.5% (average: 5.6%). Average sample coat coverage ranges from 12.8 to 28.3% (average: 20.3%). Plant roots and woody matter, shell materials are common. Clay mineral contents are in higher concentrations compared to calcite and aragonite.

#### 5.5.1.3 Sedimentary environment MIF: Muddy Intertidal Flat

At the present day, the muddy intertidal flat is a 200-300m wide strip forming part of intertidal flat that runs parallel with the main channel and saltmarsh environment. This area is always covered at high tide. The muddy intertidal flat is composed of moderate to poorly sorted (average: poorly sorted) medium sands with fine to very fine skewness (average: very fine). The fine fraction weight percentage is between 1.9 and 3.9% (average: 2.6%). Average sample coat coverage ranges from 9.1 to 30.2% (average: 19.9%). Plant roots and shell material is common. Localised sediment mottling was observed in core. Clay minerals are in higher concentrations compared to calcite and aragonite.

#### 5.5.1.4 Sedimentary environment SIF: Sandy Intertidal Flat

The sandy intertidal flat occurs in a strip parallel to the main estuary channel. On the west side of the upper reaches of the estuary it is not apparent, but it develops where the estuary widens close to the southerly intersection of transect two with the main channel (Fig.

5.1C). Down the estuary from this location, the sandy intertidal flat widens becoming the only intertidal flat environment downstream of location 24. It is very well to poorly sorted (average: moderately sorted) fine to medium sands (average: medium) with coarse to fine skewness (average: symmetrical). The fine fraction weight percentage is between 0.2 and 1.8% (average: 0.8%). Average sample coat coverage ranges from 2.3 to 20.3% (average: 8.76%). Shell material is common. Occasional worm casts were observed in core. Calcite and aragonite occur in higher concentrations than other minerals in the fine fraction.

#### 5.5.1.5 Sedimentary environment SL: Shell Lag

This environment does not occur in the in the modern surface expression of the estuary. Composed of coarse to fine sand grade shell material and comprising disarticulated bivalve and gastropod shells plus shell fragments, the shell lag has a low fine-grained sediment concentration.

### **5.5.2 Estuary cross-sections**

Cross-sections down and across the estuary were constructed to indicate how individual cores relate to each other and the depositional environments within the estuary. Each transect is hung from the top of the saltmarsh surface, and the start of each core is based on field measurements.

#### 5.5.2.1 Transect one

Transect one (fig. 5.2) is aligned northwest to southeast (fig. 5.1C) and covers both saltmarsh and intertidal flat environments. The cores are primarily composed of medium sand, although finer grained sediment (silt-clay), shell material, roots, plant matter are all present in smaller concentrations. Core 26 is closest to the main estuary channel and is composed entirely of the sandy intertidal flat sedimentary environment. Core 27 is in a more landward position, and the lower 80cm is composed of sandy intertidal flat, sediments overlying this is a 20 cm wedge of muddy intertidal flat sediment, this contact was mapped out on the surface of the intertidal flat. Between cores 27 and 21 there is a small terrace (inset a, fig 5.2), which marks the surface exposure of the intertidal flat sediment; the surface of the terrace is composed of muddy intertidal flat sediment, which overhangs the sandy intertidal sediment. The lower 95cm of core 21 is composed of sandy intertidal flat sediment, with the upper 5cm composed of muddy saltmarsh sediment. To the northwest, core 24 is composed of sandy intertidal flat in the lower 55cm, above this is 25cm of muddy saltmarsh sediment, which is overlain by 5cm of sandy saltmarsh.

#### 5.5.2.2 Transect two

Transect two (fig. 5.2) is a down-estuary transect moving from the fluvial end of the estuary to a more marine-dominated position (fig.

5,1C). The cores are primarily composed of medium sand, although finer grained sediment (silt-clay), shell material, roots, plant matter are all present in smaller concentrations. The exception to this is core 23, which is composed entirely of sandy saltmarsh sediments with muddy saltmarsh inter-layers. Crossing into the estuary channel and down the estuary, the transect surface intersects muddy intertidal flat sediments overlying sandy intertidal flat sediments. In core 30, the lower part of the core is sandy intertidal flat sediment split by a shell lag layer composed primarily of disarticulated shells and shell fragments, this is the only occurrence of this sedimentary environment and therefore is here interpreted to be localised, and is overlain by 40cm of muddy intertidal flat sediment. Downstream, core 27 marks the intersection of the two transects. Between cores 30 and 27 the muddy intertidal flat environment thins to approximately 20 cm. Core 24 is the most marine core collected, and the muddy intertidal flat environment is not expressed on the surface of the sediment, although there is a thin lens of the muddy intertidal flat, which may link with the thicker section of muddy intertidal flat sediment at depth in core 27.

### **5.5.3 Textural characteristics of grain-coatings**

Textural analysis of grain-coatings was performed primarily with backscatter electron microscopy, and supplemented with binocular microscopy.

### 5.5.3.1 Sediment grain-coatings

Representative samples were collected from each section in the sediment cores and first analysed with a binocular microscope to assess the extent and nature of any grain-coatings (figs. 5.4). Backscatter electron microscopy (BSEM) enabled observation of the grain-coatings at a much higher resolution as well as elemental analysis of the components using EDX. Stub-mounted grains from representative samples were analysed that enabled an understanding of the grain-coatings in three dimensions (figs. 5.5). Thin section mounted grains enabled a view of the coat in cross-section (figs. 5.6).

Preliminary observations with the binocular microscope indicated that the majority of samples had few coatings, and those with the greatest coating came from sediment with higher fine-grained sediment content. Framework grains that hosted grain-coats were primarily round to sub-round, and the majority of grains were quartz, with subordinate amounts of plagioclase and potassium feldspar; calcite and aragonite bioclasts were also present in varying concentrations. Muscovite and chlorite were generally rare and not observable using the binocular microscope, possibly due to small grainsizes. Under low magnification (figs. 5.4 A&B) the coats appear as dark brown, fine-grained (clay-silt) material on the surface of grains and within the pore volume between framework grains. Coatings were initially wet, and

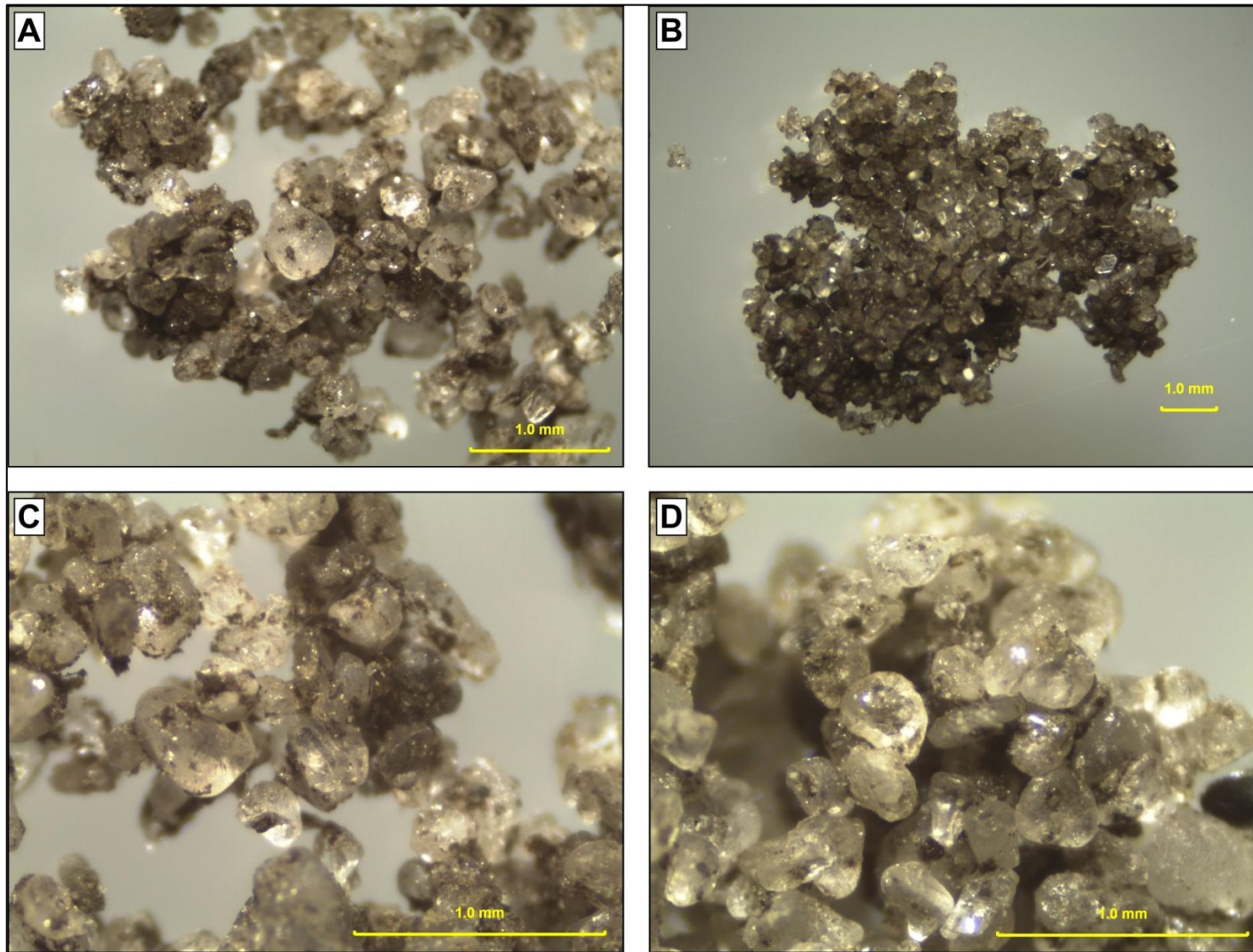


Figure 5.4 - Grain-coat images of sand grains using binocular microscope. (A) Low resolution images from sample B10 65-70cm. (B) Low resolution image from B20 0-12cm. (C) High resolution image from B10 65-70cm. (D) High resolution image from B20 0-12cm.

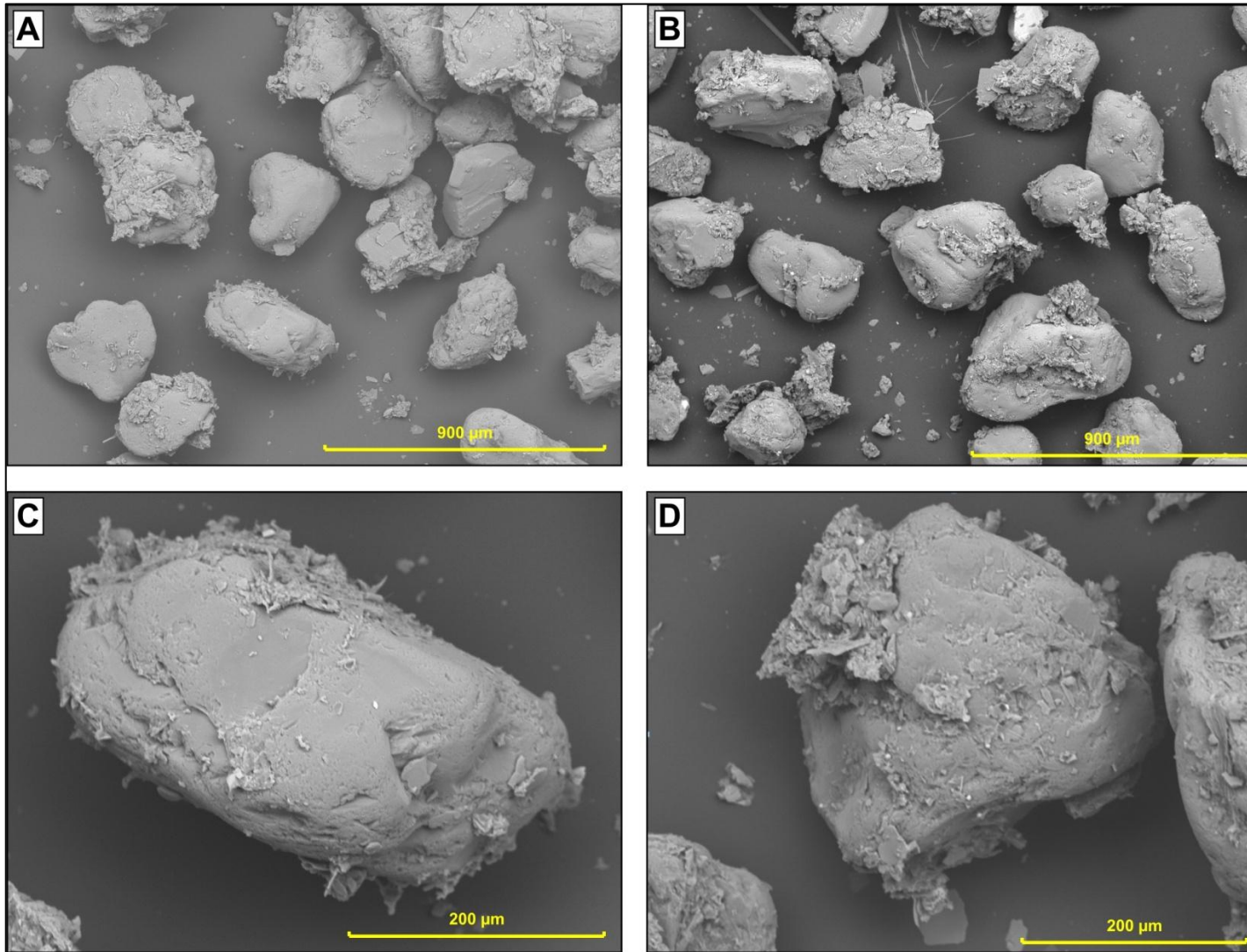


Figure 5.5 – BSE SEM image of stub-mounted, grain-coated sands grains. (A) Low resolution images from sample B10 65-70cm. (B) Low resolution image from B20 0-12cm. (C) High resolution image from B10 65-70cm. (D) High resolution image from B20 0-12cm.

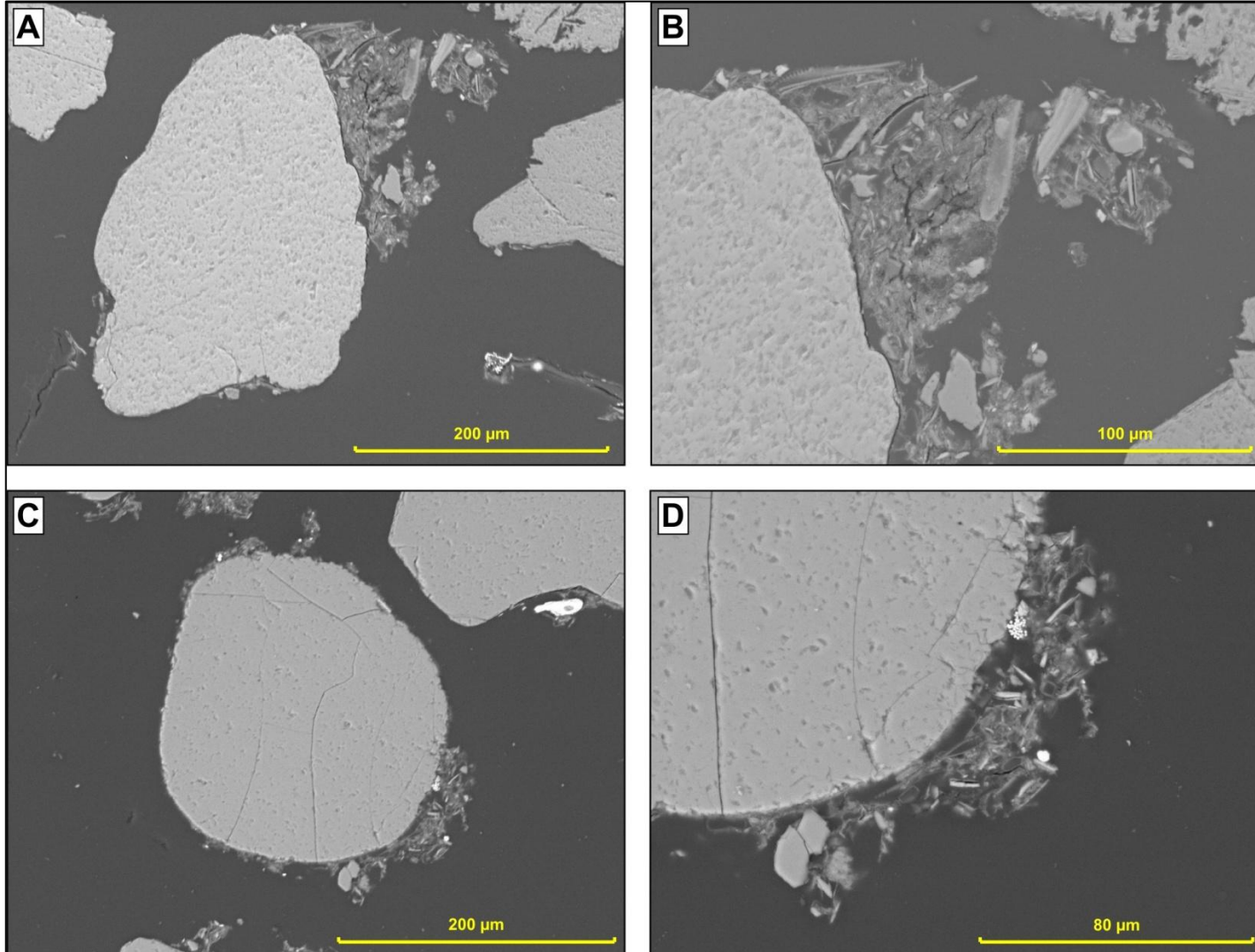


Figure 5.6 – BSE SEM image of thin section, grain-coated sands. (A) Low resolution images from sample B10 65-70cm. (B) Low resolution image from B20 0-12cm. (C) High resolution image from B10 65-70cm. (D) High resolution image from B20 0-12cm.

under the light of the microscope quickly dried out creating a hard but brittle mass of grains supported by the finer coating. At higher magnification (figs. 5.4 C&D) it was possible to view individual silt grains and plant matter within the fine grained clay-grade matrix.

The coatings identified using the binocular microscope are noted to be of varying completeness and thickness (figs. 5.4 A, C&D). Grain-coatings are only partially developed for the majority of grains, and constitute a small proportion of the overall coat surface. The remaining proportion of the coat area was a clean grain surface. The largest coatings can cover a significant proportion of the grain surface (figs. 5.5 A&B), but in the majority of samples average coat coverage rarely exceeds 25% of the grain perimeter. Coats did not form one singular mass, but were often composed of individual detrital lithic or carbonate fragments, with fine-grained clay mineral mass associated (figs. 5.5 C&D). The thickness of coatings varies considerably between 1-2 $\mu\text{m}$  up to 100-200  $\mu\text{m}$ . This variation results in an inconsistent coat thickness across a coat; accurate and quantitative description of coat thickness would have required coat thickness measurements at multiple points along the coat, greatly increasing the time needed to collect the dataset. Coatings observed in thin section displayed no internal texture or organisation (fig. 5.6B), and are composed of a fine clay matrix, plus silt size detrital

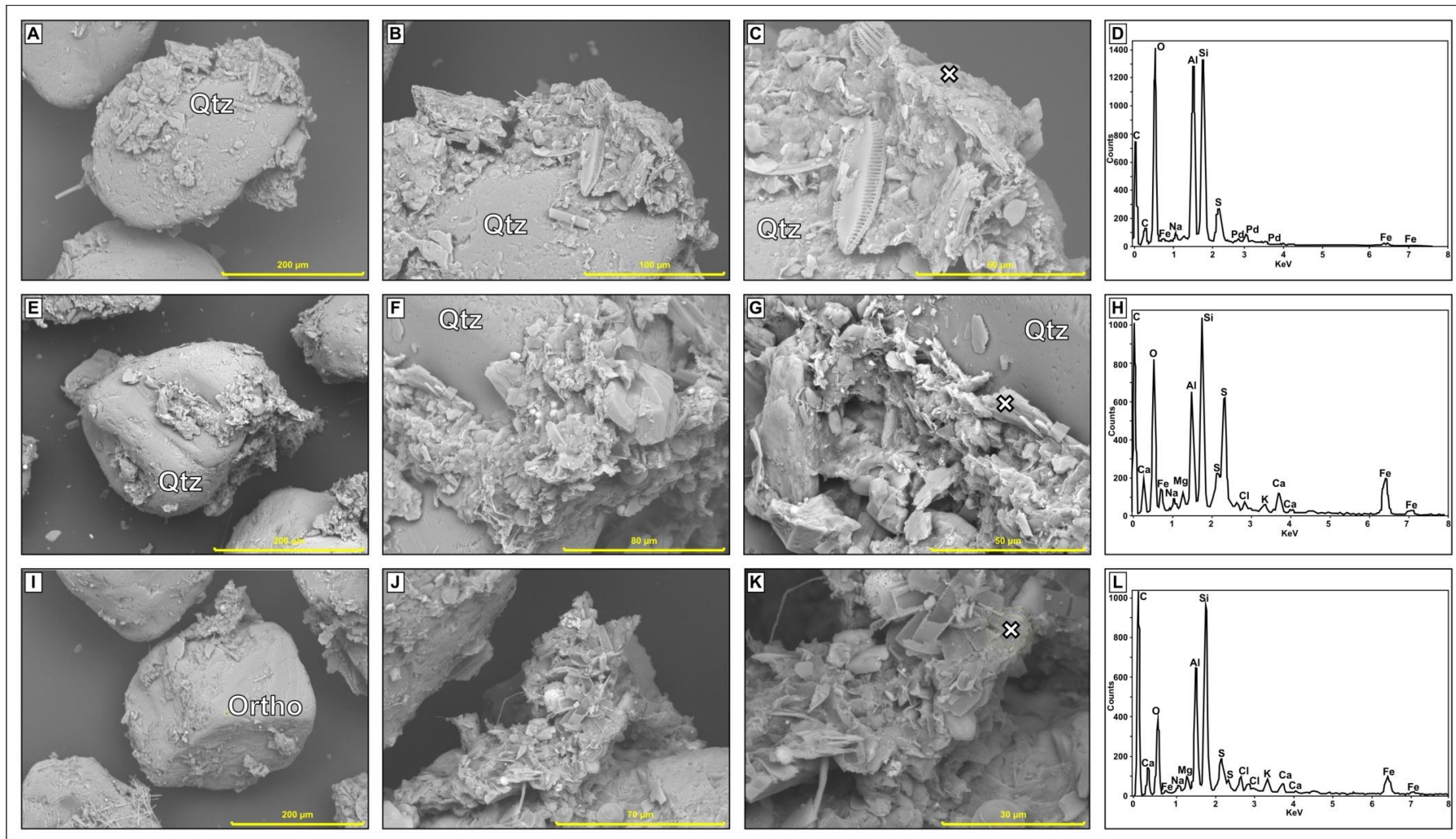


Figure 5.7 – BSE SEM images and energy dispersive x-ray (EDX) spectra (cross marks scan site) of stub-mounted grain-coat sand grains from core sample (Qtz: quartz; Ortho: orthoclase). (A, B & C) SEM images of coated sand grain from sample B10 65-70cm. (D) EDX spectra of coat indicating the presence of kaolinite and pyrite. (E, F & G) SEM images of coated sand grain from sample B20 0-12cm. (H) EDX spectra of coat indicating the presence of smectite or illite, and pyrite. (I, J & K) SEM images of coated sand grain from sample B20 0-12cm. (L) EDX spectra of coat indicating the presence of smectite or illite, and pyrite.

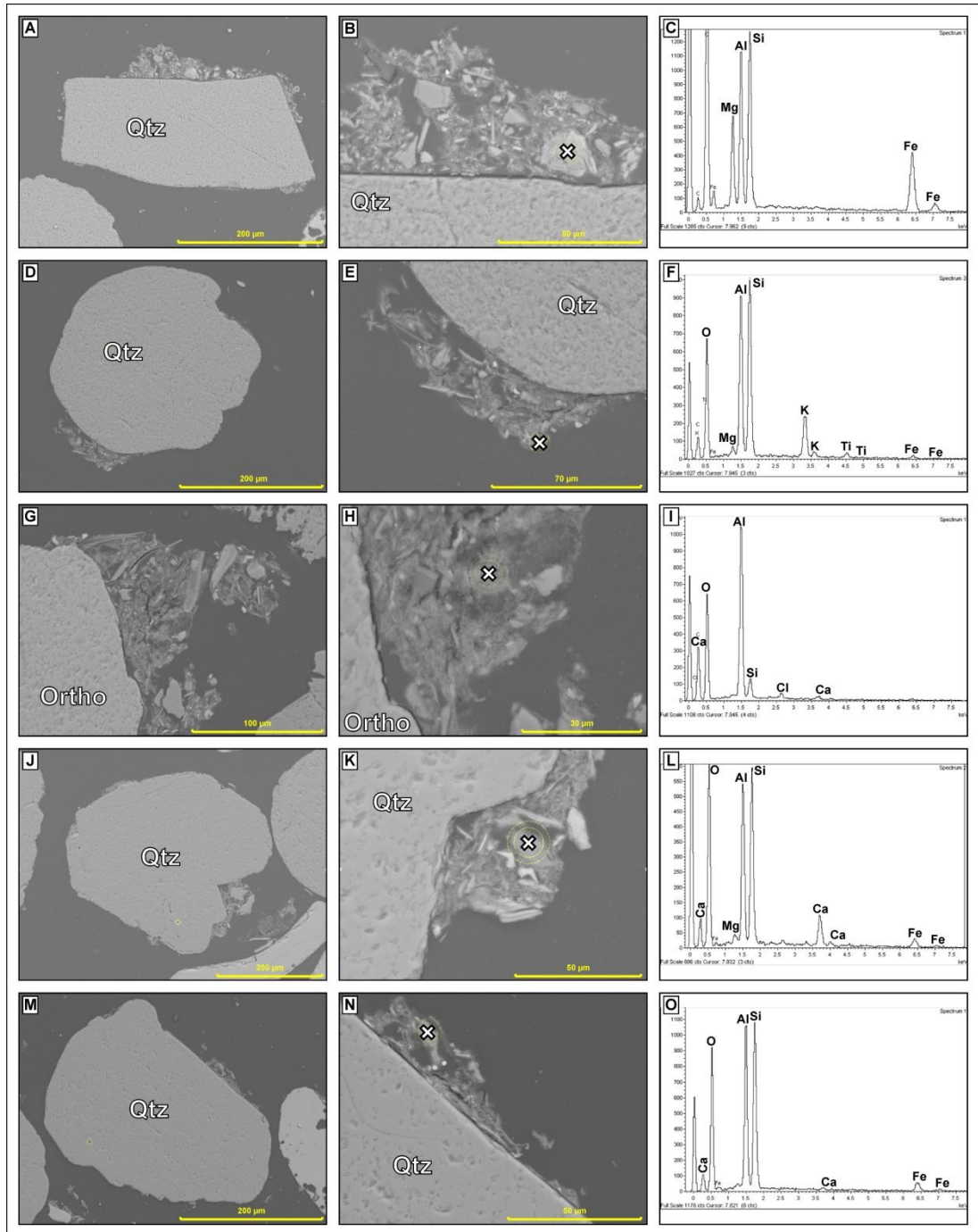


Figure 5.8 - SEM images and energy dispersive x-ray (EDX) spectra (cross marks scan site) of thin section grain-coat sand grains from core sample (Qtz: quartz). (A & B) SEM images of coated sand grain from sample B9 75-78cm. (C) EDX spectra of coat indicating the presence of chlorite. (D & E) SEM images of coated sand grain from sample B10 65-70cm. (F) EDX spectra of coat indicating the presence of smectite. (G & H) SEM images of coated sand grain from sample B10 65-70cm. (I) EDX spectra of coat indicating the presence of gibbsite. (J & K) SEM images of coated sand grain from sample B13 12.5-22cm. (L) EDX spectra of coat indicating the presence of smectite and possibly carbonate from a neighbouring grain. (M & N) SEM images of coated sand grain from sample B14 0-14cm. (O) EDX spectra of coat indicating the presence of kaolinite.

lithic grains, carbonate fragments and in many cases pyrite grains (Fig. 5.6).

Compositional analysis of coatings was undertaken using EDX on both stub and thin section mounted grains (figs. 5.7 & 5.8). Analysis of stub-mounted coatings proved difficult and most attempts to scan the grain-coatings could generally not be utilised due to the size and depth of the EDX interaction area and the small size of the target minerals.

High resolution stub mounted images of the fine grained matrix (figs. 5.7 C, G & K) show that it is largely composed of small plate-like minerals, which appear to be clay minerals. Scans of the elemental composition of the fine-grained matrix indicate that pyrite is a common component of the matrix, which makes it difficult to confirm the presence of iron-rich clay minerals. However, energy dispersive scans (figs. 5.7 D, H & L) indicate the presence of kaolinite and illite or smectite. Thin section mounted grains enabled better scans of coat composition, although these were still problematic. Scans on silt size lithic grains and on the fine-grained groundmass shows that clay minerals are chlorite smectite or illite and kaolinite, as well as gibbsite (Fig. 5.8).

#### 5.5.3.2 Sediment texture cross-plots

Grain size analysis of sandy sediment produced quantitative data on modal grain size, skewness and sorting of the whole sample.

Furthermore, fine fraction weight percentages were also measured for each sample during preparation for XRD analysis. Grain-coat coverage data were collected for sandy sediments where possible. These data were cross-plotted to try to understand how the textural features of the sediment, which may relate to sediment transport and deposition, and early diagenetic changes, could be used to predict initial coat coverage in sediments.

Cross-plots are presented in figure 5.9, and the colour code of the depositional environment of each sample was overlain (fig. 5.2). Visual assessment of relationships between two variables was supplemented with r-value calculations (Townend, 2003) and comparison to p-values ( $p=0.05$ ) for the sample number minus two degrees of freedom (Siegle, 2009). This gives a 95 percent confidence limit for correlations noted below. All of the cross-plots indicate that the sandy intertidal flat and sandy saltmarsh sediments tend to have the lowest average coat coverage, with muddy intertidal flat and muddy saltmarsh sediments tending to have higher concentrations. Grain size and coat coverage do not seem to have a particularly strong relationship (fig. 5.9A). Whereas fine fraction content, skewness and sorting all have strong trends with increasing coat coverage (fig. 5.9 B-D). The cross-plot of coat coverage with depth indicates that sediments with greatest average coat coverage are more likely to

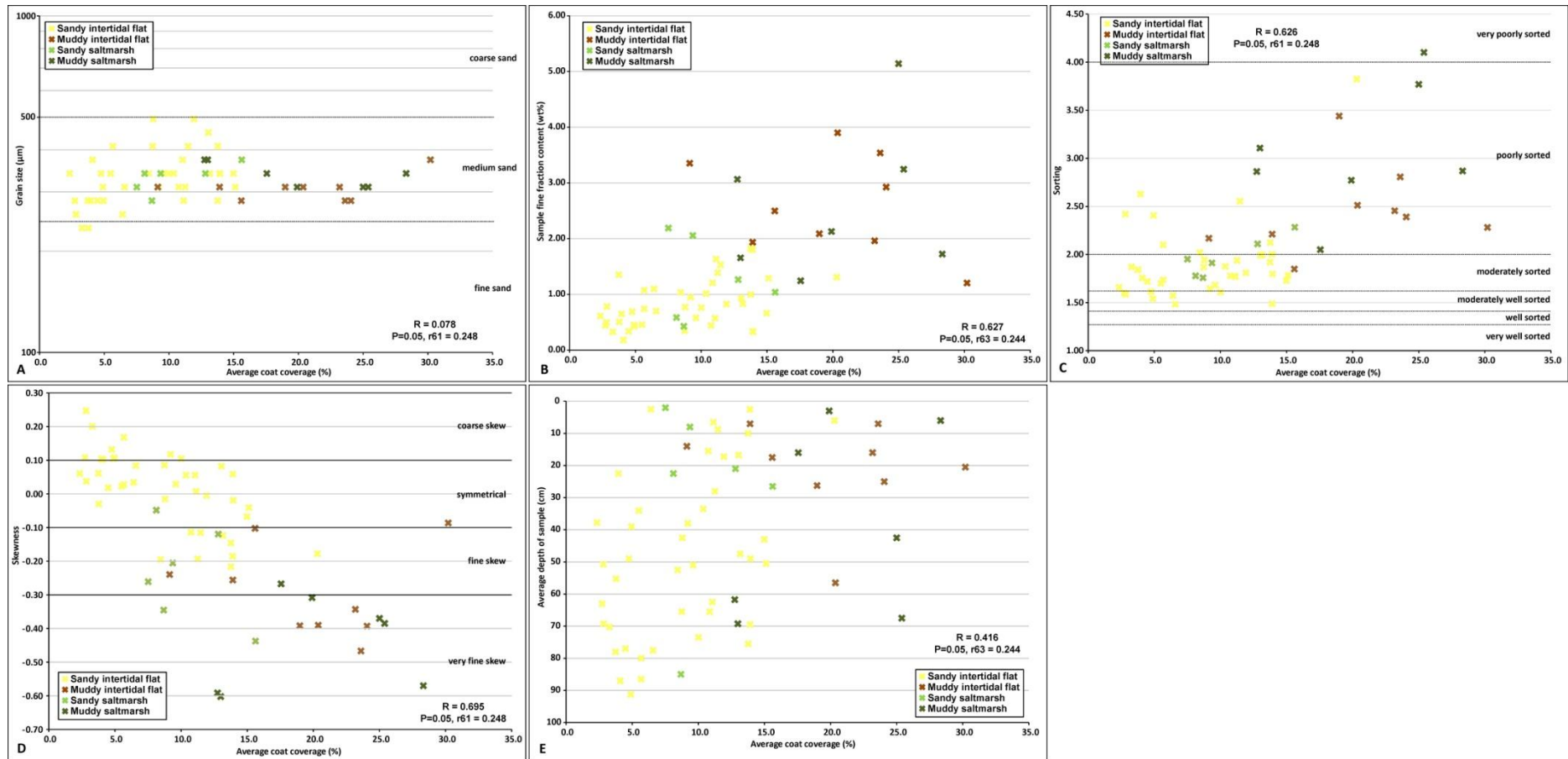


Figure 5.9 - Cross-plot of grain-coating versus measured particle size characteristics, depth and fine fraction content. Colours relate to facies designation (fig. 5.2).

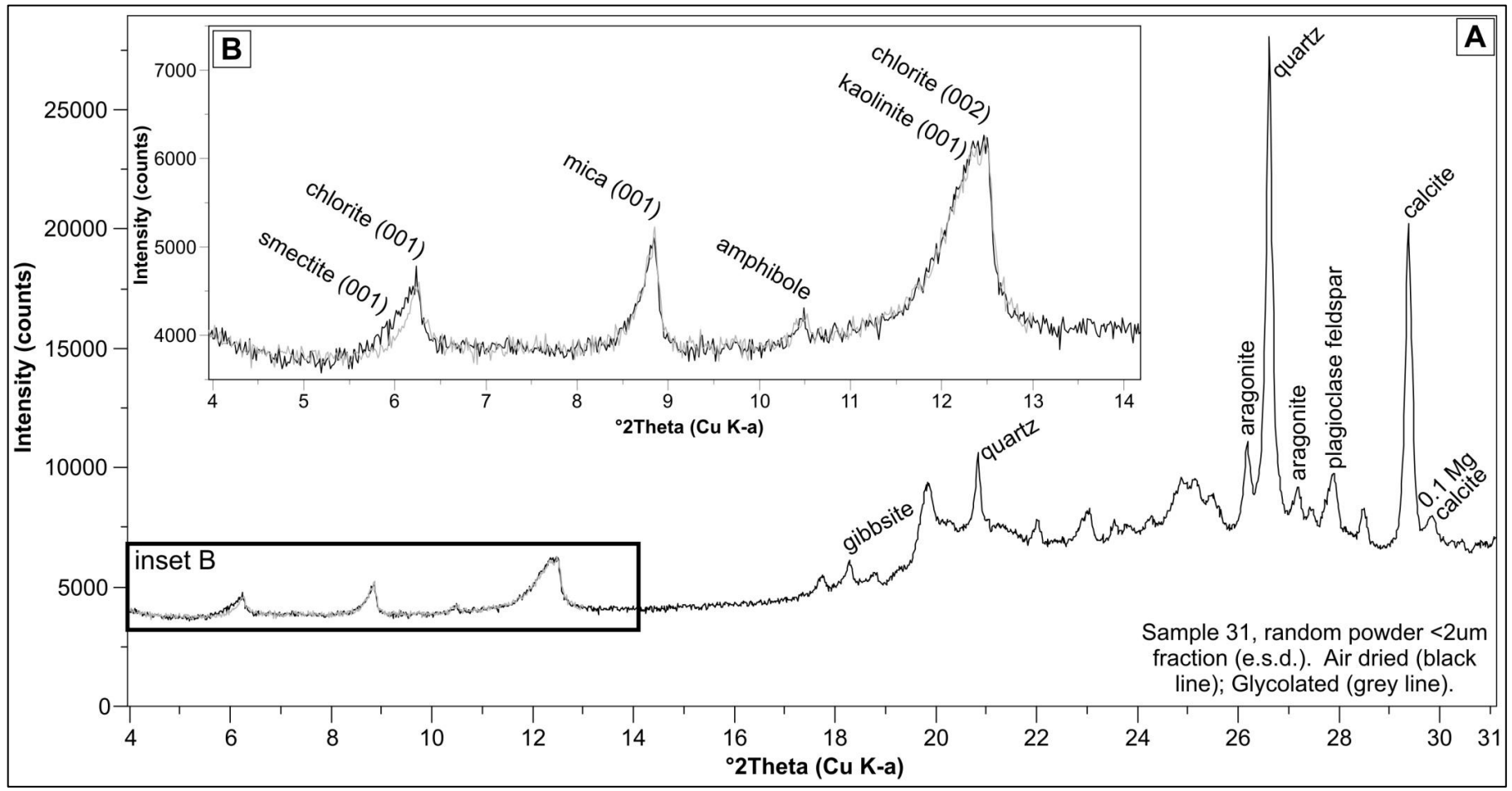


Figure 5.10 - Representative X-ray diffractogram of estuary fine fraction sub-sample. (A) Sample 2, low angle diffractogram with main peaks noted. (Inset B) close-up of (A), clay minerals in sample.

occur towards the top of the cores within muddy intertidal flat and muddy saltmarsh sediments (fig. 5.9E).

#### **5.5.4 Mineral identification**

Non-clay minerals of a quantifiable concentration identified in the fine fraction are gibbsite, quartz, albite, orthoclase, pyrite, gibbsite, calcite and aragonite, and peaks for most of these minerals are evident in figure 5.10A. The mineral jarrosite was also noted in some cores.

Clay minerals in the samples are evident in the low angle inset (fig. 5.10B): a broad peak at 14.1 Å, a sharp peak at 9.9 Å, a sharp peak at 7.1 Å and a broad peak at 7.2 Å. The 9.9 Å peak corresponds to an mica (001) peak, the sharp nature of this peak indicates that it has a well-ordered structure, and is likely to be dominated by detrital mica (such as muscovite). The two peaks at 7.1 Å and 7.2 Å indicate two clay mineral phases, corresponding to kaolinite (001) and chlorite (002) peaks (Moore and Reynolds, 1997). Chlorite is confirmed by the presence of the 14 Å peak (001); the sharp chlorite (002) peak also suggests that this is detrital. The broad nature of the kaolinite (001) peak is indicative of an authigenic mineral possibly formed from the weathering of other pre-existing minerals.

In summary, clay minerals identified in quantifiable concentrations within the Anllóns estuary core sediments are: (i) kaolinite, (ii) chlorite, (iii) muscovite.

#### 5.5.4.1 Sediment mineralogy bar chart

A large amount of quantitative mineral data was produced from the XRD analysis of the sediment fine fraction. The mineral data was also normalised to remove the carbonate proportion from these sediment analyses, this allows consideration of the non-carbonate mineral concentration to be considered. These datasets were both plotted for different attributes (fig. 5.11) allowing consideration of how the mineral concentrations may vary.

Figure 5.11A, is a plot of the original data organised for the carbonate concentration. The first point to note from this data is that the suite of minerals present in the fine fraction of samples is broadly the same for most (though not all) samples. This shows an increase in carbonate concentration from the origin along the x-axis. There is also trend of decreasing clay mineral content which is inverse to the carbonate trend; quartz also appears to have a similar trend. K-feldspar can be seen to be absent in samples with carbonate concentrations above 10%, and this is due to the issues outlined above (section 4.5.5.1, p.191). Albite appears to have a generally unclear trend with carbonate, as does pyrite and jarosite; gibbsite has the same concentration in most samples.

Figure 5.11B is a bar chart of the original data samples plotted for each core, with cores of greater geographic marine-dominance located further along the x-axis, cores are plotted from the surface to

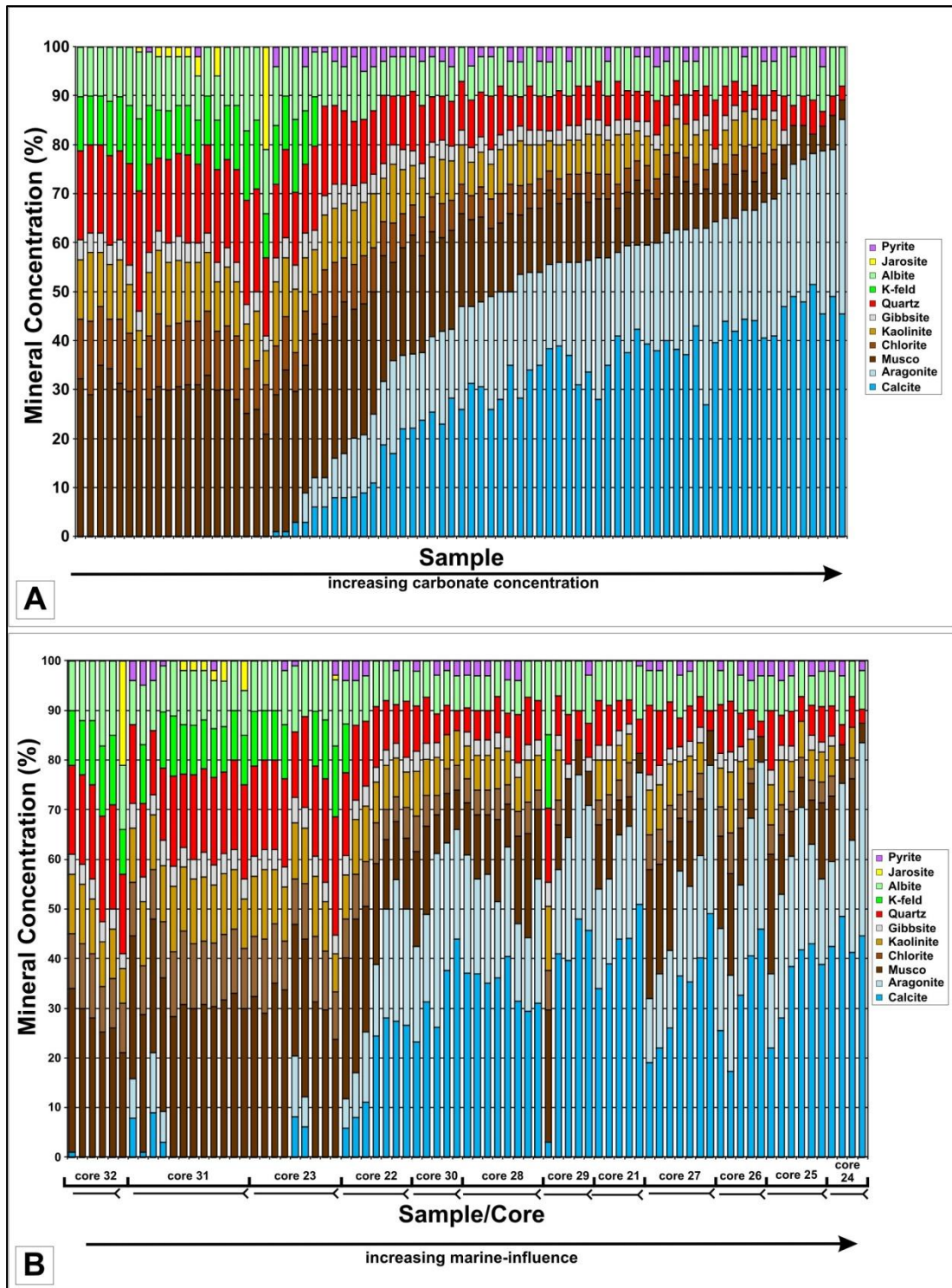


Figure 5.11 – Mineral bar chart. (A) All Samples with original mineral concentrations sorted for increasing carbonate content. (B) All Samples with original mineral concentrations sorted for increasing marine-influence, and depth within core. Cores closest to origin have less marine influence; samples from individual cores are plotted from deepest to shallowest (right to left). K-feldspar is absent from samples with greater than ~15% total carbonate concentration. This is likely to be due to the carbonate peaks over-lapping the k-feldspar peaks, the presence of K-feldspar polymorphs, the variable composition of alkali feldspar (variable sodium content alters crystallinity) and the low symmetry of these feldspars.

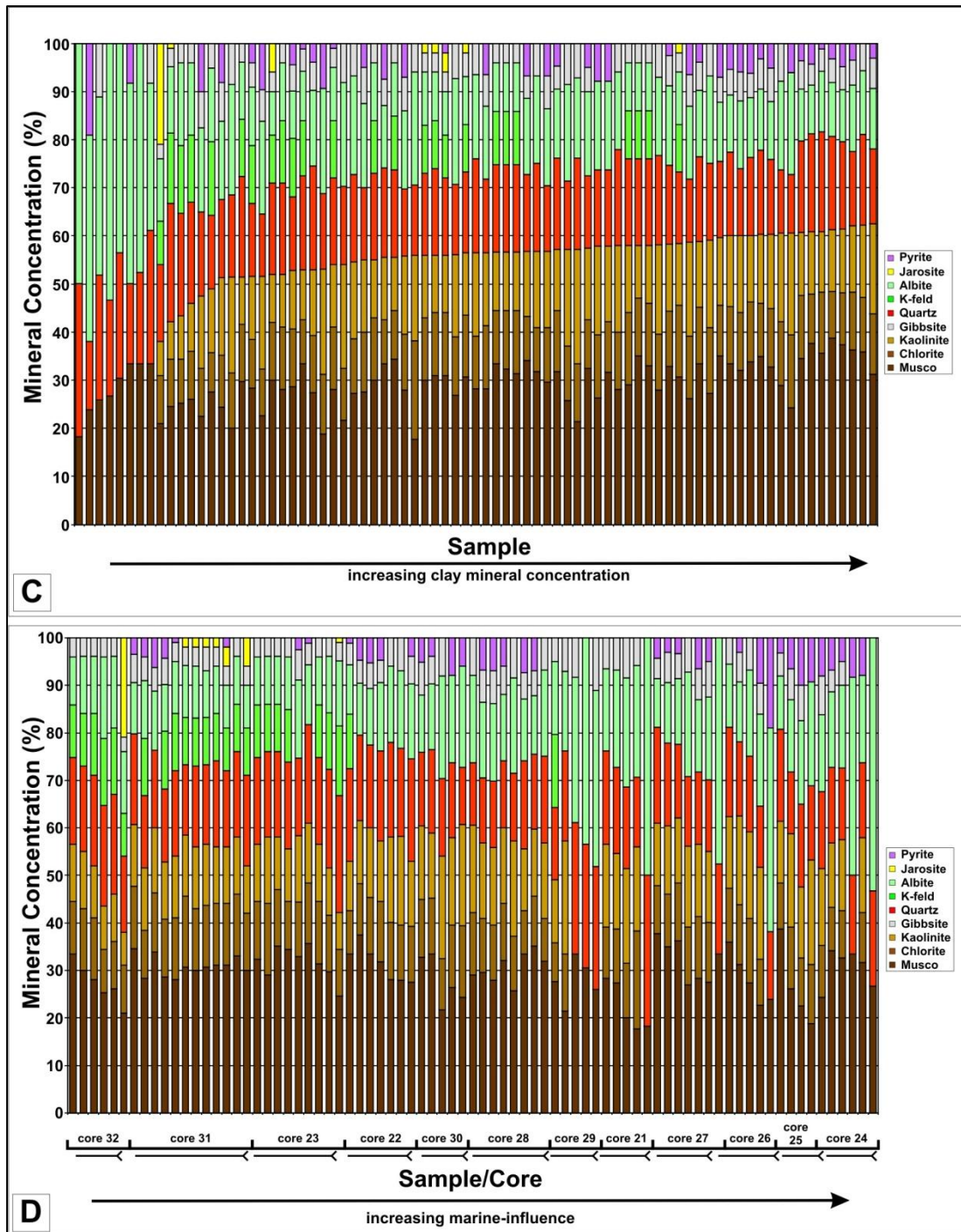


Figure 5.11 – Mineral bar chart. (C) All Samples from carbonate-normalised mineral concentrations sorted for increasing carbonate content. (D) All Samples from carbonate-normalised concentrations sorted for increasing marine-influence, and depth within core. Cores closest to origin have less marine influence; samples from individual cores are plotted from deepest to shallowest (right to left).

depth (left to right). This figure shows that the three river-dominated cores (cores 23, 31 and 32) generally have very low carbonate content, down the estuary from this point (fig. 1) the cores have a higher carbonate content which broadly increases down the estuary. The other pattern that can be observed from this data is that within individual cores, there is a general shallowing-upwards trend of decreasing marine-influence/increasing fluvial-influence indicated by the decreasing carbonate/increasing non-carbonate concentration.

Figure 5.11C is the carbonate-normalised mineral concentration for each sample, the samples are organised by ascending total clay mineral content, with higher total concentrations further along the x-axis. The main point is that the graph shows a similar concentration in minerals for a large number of sample locations. This bar chart shows that clay mineral concentration is approximately in the range of 50 to 60%, quartz concentration is normally between 10 to 20%, plagioclase is normally around 20% concentration, gibbsite is between 5 to 10% in concentration, pyrite rarely exceeds 10% concentration and jarosite has low concentrations and is generally rare. Figure 5.11D is the organised into cores in the same fashion as fig. 5.11B, the figure shows that clay mineral concentrations tend to increase towards the top of some cores (as in fig. 5.11B). The very low clay mineral concentration samples are typically in the deepest parts of the core.

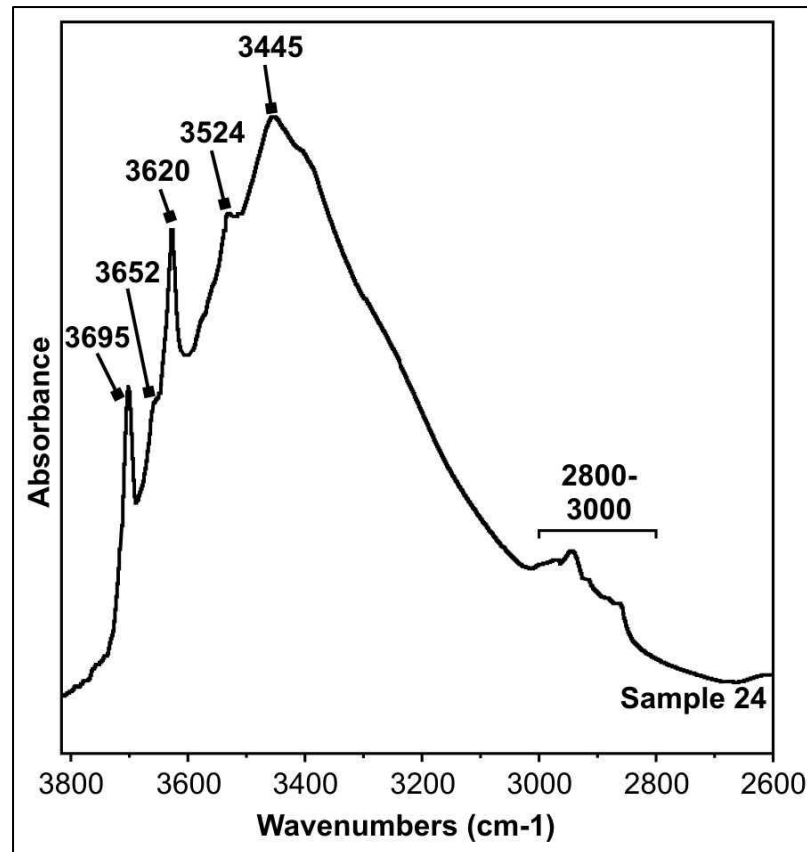


Figure 5.12 - Infrared spectra for representative estuary sample.

#### 5.5.4.2 Infrared spectroscopy

Infrared spectroscopy was performed on a selection of fine fraction samples and a representative trace is presented (fig. 5.12). In the OH-stretching region (3800-2500  $\text{cm}^{-1}$ ) there are several identifiable bands: 3695, 3652, 3620, 3524, and 3445  $\text{cm}^{-1}$ . The band at 2850-3000  $\text{cm}^{-1}$  is likely to be due to organics; the 3445  $\text{cm}^{-1}$  band is indicative of adsorbed water. Kaolinite is evidenced in the spectra by the distinct bands at 3695, 3652, 3620  $\text{cm}^{-1}$ . The 3620  $\text{cm}^{-1}$  band represents hydroxyls between tetrahedral and hydroxyl sheets, while the remaining bands represent OH groups at the octahedral surface

forming weak hydrogen bonds with oxygen molecules in the next tetrahedral sheet (Madejova, 2003). Where the  $3620\text{ cm}^{-1}$  band is larger than the  $3695\text{ cm}^{-1}$  band, this indicates the presence of an illite-type mica (Farmer, 1974) and this is present in the spectra. The band at  $3524\text{ cm}^{-1}$  indicates the presence of a magnesium-bearing chlorite (Farmer, 1974).

In summary, infrared analysis supports the presence of clay minerals identified using X-ray diffraction (chlorite, muscovite and kaolinite). It also suggests that the mica is illite or muscovite (as opposed to biotite), and that the chlorite is a magnesium-bearing variety.

## **5.6 Discussion**

### **5.6.1 Core interpretations & transects**

The sandy intertidal flat environment is the most common depositional environment noted in the Anllóns estuary cores. The surface expression of this environment is close to the main estuary channel and continues around the headland of the spit to form a continuous environment with the shoreface. The relatively clean nature of the sandy intertidal flat and the lack of internal sedimentary structures may indicate that this setting is subject to tidal and marine reworking thus removing much of the fine-grained sediment. The shell lag only occurs within one core and is spatially discrete. Therefore it is likely to be the localised infill of a scour with bioclasts, or the remnant of a more extensive storm event.

The muddy intertidal flat, sediments comprise finer-grained and less well sorted sands that occur in a strip running down the north western side of the estuary. The relationship between cores 24 and 27 indicates that the muddy intertidal flat may inter-finger with sandy intertidal flats in some areas. It appears from field observations, logged cores and sediment analyses that the muddy intertidal flat sediment forms a relatively lower energy setting compared to the sandy intertidal flats. This reflects an upper tidal zone within the estuary, when lower flow velocities during slackwater at high tide permit deposition of silt and clay sediment. During the subsequent falling stage of the tide, flow velocities are initially low, but ultimately reach a velocity capable of re-suspending finer grains at a point close to the intersection of the surficial contact between the muddy intertidal and intertidal flats. The muddy intertidal flat, therefore, marks a zone of net fine-grained sediment deposition in contrast to the sandy intertidal flat where fine-grained sediments have been re-suspended and transported. This process has been noted in the formation of tidal mudflats (Allen, 2000). This is enhanced by the colonisation of plants on the muddy intertidal flat (fig. 4.4 E & F), which help to bind the cohesive sediment together and may also reduce tidal velocities. Furthermore, areas of the muddy intertidal flat are prone to bioturbation by worms (fig. 4.5 D & E), which can result in the mixing of fine-grained sediment and underlying sand grade sediment (Volkenborn et al., 2007).

On the saltmarsh, sediment is composed of either muddy or sandy saltmarsh sediments. At the upstream end of the estuary (core 23), the saltmarsh cores have a sandy base that fines upwards with some inter-bedding of sandy and muddy dominated sections. It also has a high proportion of wood and plant matter. Towards the middle of the estuary the muddy saltmarsh occurs closest to the intertidal flat area and, although it is primarily composed of sand, it has a significant proportion of fine grained sediment and plant material (core 24). Cores 24 and 23 appear to reflect slightly different sub-environments within the estuary, with core 23 in a protected location proximal to the river sediment supply, while core 24 is closer to the marine end of the estuary, where fine grained sediment will be in lower concentrations.

Stratigraphically, the northern margin of the estuary shows an overall fining upwards trend. The clean sandy intertidal sediment underlies most parts of the estuary, which reflects high energy tidal and marine processes. Overlying this is the muddy intertidal flat, which appears to have encroached into areas that were formerly composed of sandy intertidal flat. Landward of this, saltmarsh development is also occurring on top of formerly sandy intertidal flat sediments. The saltmarsh and muddy intertidal flat may also be related with the muddy intertidal flat being the earliest stages of saltmarsh development (French, 1993; Allen, 2000).

The change in sedimentation patterns resulting in the fining upwards trend within the estuary may have a number of causes. Like most modern coastal sedimentary environments, the estuary has been subject to anthropogenic influence with the creation of flood defences further upstream (fig. 4.2 B & C). These flood defences fill during high tides, and are likely to impact estuarine dynamics causing an overall decrease in tidal velocities behind the tidal mixing zone, which could result in the deposition of fine grained sediments at the estuary margin and enhance the development of saltmarsh and muddy intertidal flat sediments.

The fining upward trend may also be due to estuarine infilling over time. As the narrowly incised valley gradually fills, the estuarine channel becomes more confined (Cooper, 1993) to the south eastern margin of the estuary. Areas on the intertidal flat are now no longer subject to channel avulsion where incision and reworking could cannibalise the saltmarsh and muddy intertidal sediments. This creates an energy- and sediment-differential with sandy environments becoming increasingly muddy away from the estuary channel.

The cause of the change from an entirely sand-dominated depositional environment to an increase in fine-grained sediment content at the margin of the estuary may also be a result of a change in calibre or volume of sediment within the estuary. Either an increase in fine sediment or a decrease in sand from either marine or fluvial

sources could produce the fining upward trend noted (Orton and Reading, 1993; Reading and Collinson, 1996). In the San Simón Bay estuary, changes in the overall volume of supply were reported to have an effect on the depositional environments (Pérez-Arlucea et al., 2007), with colder wetter climate resulting in increased sediment supply and the infilling of estuarine channels and the formation of estuarine flats. On this basis, climate change effecting sediment supply may be a possible explanation but this would require age-dating of the sediment in the Anllóns estuary to allow comparison to the climate record. Another potential cause of changes in sediment supply could come from further anthropogenic influences as the changes in land use and management within the Rio Anllóns itself, which could impact the calibre and volume of sediment (Walling, 1999; Walling, 2006).

### **5.6.2 Grain-coat locations & characteristics**

Average grain-coat coverage varies within the samples collected both within cores (fig. 5.3) and within depositional environments (Figs. 5.1 & 5.9), and particularly with depth (fig. 5.9E). The highest average coat coverage range occurs within the MIF (9.1-30.2%) and MS (12.8-28.3%) environments (Fig. 5.9), which preferentially occur in the upper sections of cores (Fig. 5.9E) in the upper-tidal margins of the estuary (Fig. 5.1). The lowest average grain-coat coverage range is within the SIF environment (2.3-20.3%; Fig. 5.9), which tends to occur closest to

the main estuary channel (Figs. 5.1, 5.2 & 5.9) and at depth in cores towards the upper-tidal area of the estuary (Fig. 5.9E). The SS have intermediate average coat coverage ranges of between 7.5% and 15.6% (Fig. 5.9). In the estuary, depositional environment and sample depth within cores are inter-related factors in the occurrence and coverage of sand grains by grain-coatings. Greater coat coverage occurs in shallower and surficial parts of the cores particularly in the muddy intertidal flat, and saltmarsh environments, and this may be related to the overall fining up trend noted within the estuary where fine fraction contents are increasing in marginal areas close to the upper tidal limit.

Average coat coverage variations within individual cores appear to be related to changes in fine fraction concentrations (figs. 5.3 & 5.9). Coat coverage is highest in samples that have the highest fine fraction contents, are the most poorly sorted and have a greater fine skew (fig. 5.9 B-D). Sample grain size appears to have less of an impact (fig. 5.9E), with no systematic variation with grain size. Images of grain-coats from all cores and in different sedimentary environments indicate that they lack any internal structure. The thickness of coatings varies considerably between 1-2 $\mu$ m up to 100-200  $\mu$ m, but as previously stated this was not measured on a grain by grain basis.

Grain-coats identified through EDX and XRD analysis in the Anllóns estuary are composed of the same suite of minerals and with very similar textures (figs. 5.5-5.7). Silt and clay size lithic fragments, bioclastic debris and pyrite occur as grains within matrix fine-grained clay minerals. XRD analysis of the fine fraction (<2µm) indicates that the clay minerals chlorite, illite and kaolinite are present (figs. 5.10 & 5.12); although some of these also occur as silt grade lithic grains (figs. 5.8 C, L & O).

The concentration of minerals within the fine fraction of samples can vary considerably in cores (figs. 5.3 & 5.11); and most samples contain a significant proportion of calcite and aragonite (fig 5.11 A & B). There are some clear trends of decreasing carbonate concentration and increasing clay mineral and other non-carbonate minerals up through the cores (fig. 5.3 & 5.11 A & B). This trend appears to indicate a decreasing marine-influence/increasing fluvial-influence up through the cores, with sandy intertidal flat sediment, overlain by muddy intertidal flat and saltmarsh environments.

Figure 5.11C indicates that the non-carbonate minerals in the fine fraction have similar ranges of concentrations in the majority of samples, however figure 5.11D indicates that there is a significant degree of variation within individual cores. This suggests that although the concentration of minerals in the fine fraction does not vary significantly on an estuary-wide scale there is some variation in mineral

concentrations within cores particularly in sub-environments where the cores show a shallowing-upwards trend.

### **5.6.3 Cause of grain-coatings**

On the basis of the observations above it can be seen that grain-coats have several characteristics and distribution patterns within the Anllóns estuary: 1) average grain-coat coverage is generally partial and rarely exceeds 25%, 2) highest coat coverage occurs in areas on the margins of the estuary, while lowest average grain-coat coverage occurs in areas close to the main estuary channel, 3) coat coverage is highest in muddy intertidal areas and lowest in sandy intertidal flat areas, 4) coat texture is a poorly-sorted mixture of silt and clay sized lithic and biogenic fragments, 5) the components of the grain-coats are carbonate and lithic grains (clay and silt grade plagioclase feldspar, quartz, etc.), clay minerals and pyrite. There are a number of potential processes which may result in the texture, composition and distribution of coatings noted above.

#### **5.6.3.1 Fine-grained sediment co-deposition and drying**

Sedimentary processes result in the sorting of sediment if processes of entrainment, transport and deposition are repeated or cyclical; particularly in coastal environments where waves and tides act upon sedimentary deposits to redistribute and sort sediment (Reading and Collinson, 1996; Edwards, 2001; Bird, 2011). In the Anllóns estuary, sediment is sorted and reworked on the sandy intertidal flat close to

the estuary channel to produce moderately sorted, medium sands with markedly low fine-grained sediment contents. Co-deposition of clay and silt grade material with sand grade sediment in the muddy intertidal flat appears to occur due to a deceleration in tidal flow velocities at high-tide turnaround periods as the tide reaches its landward limit close to the saltmarsh margin with the intertidal flat. Fine-grained silt and clay-sized sediment particles fall out of suspension and deposit in a zone between the relatively clean sandy intertidal flat and the saltmarsh.

The images of grain-coats (figs. 5.4-5.6) indicates that fine-grained sediment co-deposition is a possible coating method in the Anllóns estuary as the poorly sorted nature of the coat, with its mix of silt and clay sized detrital lithics, bioclastic debris and clay mineral components, lack any internal organisation and may have been deposited as dense, poorly sorted masses (Van der Lee, 2000; Fox et al., 2004) or as individual components.

This co-deposition of fine-grained sediment and sandy sediment requires a method of adhering the coat to the grain surface. One method, proposed by this study, is that fine-grained sediment deposited on the surface of sand grains could adhere through the drying out of the uppermost section of intertidal flat sediments, between tides. A possible scenario is that when the tide falls, exposing the intertidal flat, wind and sun may act upon the uppermost layer of

recently deposited sediment, drying its surface and resulting in silt and clay grade sediment particles adhering to the surface of sand grains. In this way the deposition of fine grained sediment at the upper tidal limit subsequently followed by repeated wetting and drying caused by the tidal cycle may act to form an incipient top-coat on intertidal sands soon after deposition. This may be evidenced by the muddy intertidal flat which occurs at the surface margins of the intertidal flat. As noted above, newly deposited sediment rapidly dried out under the intense heat of the binocular microscope stage, creating a hard and brittle mass of sand grains and sediment coat. A similar process, occurring with lower intensity may act to bind fine-grained sediment to the surface of sand grains.

An issue with this potential method of coating sand grains is that the coat itself may not adhere to the grain sufficiently to prevent the next strong tide stripping it off. Preservation of coat coverage in this way may be possible if sedimentation rates in an environment are rapid enough to prevent immediate entrainment and transport or during the waning tidal energy of a spring to neap tide. Silt and clay material coating the underside of sand grains or just beneath the surface of the sediment may also be protected from the removal by tides and wave action.

#### 5.6.3.2 Clay illuviation & mechanical infiltration

Another possible grain-coating process is the invasion of sediment-laden water through the sand body, resulting in the deposition of sediment on grain surfaces. Within the geological and soil science literature there has been debate as to how the process noted at the present day may relate to mechanical infiltration discussed in the ancient sediments.

Mechanical infiltration is the process of muddy water entering a sandbody and depositing fine clay size particles onto framework grain surfaces. Petrographic studies of ancient sandstone reservoirs have generally inferred that mechanical infiltration occurs in desert and river settings, but it may occur in most sandy environments where waters are prone to carry suspended loads. An ancient example of this process is reported in the fluvial Sergi Formation, Brazil (Moraes and De Ros, 1990; Moraes and De Ros, 1992). These authors split clay minerals into three types: i) 'depositional clays' which are eroded overbank clasts incorporated into sands, with subsequent compaction crushing the clasts, ii) 'mechanically-infiltrated clays' consisting of a range of textures including grain-bridges, geopetal fabrics, loose aggregates and coatings (cutans), iii) 'authigenic clays' which develop during diagenesis from detrital clay minerals and the dissolution-precipitation of detrital non-clay minerals. The mechanically-infiltrated clays are reported to have developed in a

semi-arid area with a lowered water table, where episodic run-off infiltrated coarse sands, and clays decreased in concentration further away from possible fluid entry points.

Clay illuviation is a process whereby clay grade sediment is moved from a surface or near surface soil layer down into an underlying soil layer where the sediment accumulates (illuviation). Eluviation is defined by Kuhn et al., (2010) as the vertical translocation of fine clay suspended in percolating soil water. This process occurs through three stages (Kuhn et al., 2010):

1. Dispersion – clay is dispersed into water, this is dependent upon the type of clay mineral, particle size, pH, cations present, organic matter content and electrolyte concentration in fluids.
2. Downward transport – clay particles in suspension percolate with the water through the pores volume and into underlying sediments.
3. Deposition – occurs when i) the flow of water is reduced or stopped, ii) a level with low macroporosity (barrier) is encountered or iii) electrolyte concentrations increase within pore waters resulting in flocculation.

Texturally, such coatings often occur in 'channels' within the soil pore volumes (Miedema et al., 1999). Although coarse coatings do occur (McKeague et al., 1971; Kemp et al., 1998), typically illuviated coats

tend to be fine grained, often with repeated coatings producing laminations (Miedema et al., 1999; Kuhn et al., 2010).

Mechanical infiltration and clay illuviation appear to be very similar (Buurman et al., 1998). The key difference is the source of the suspended material that adheres to grains. In ancient reservoir examples on the basis of environment, percolating sediment is believed to arrive in suspension with the fluid, typically as runoff or stream flow within a river system. In the process of clay illuviation, sediment is dispersed into the fluid from an overlying soil layer before percolating into an underlying layer. Although the local sources of the coating material are potentially different, the processes involved in transport through the pore space and deposition are considered in this study to be essentially the same.

In the Anllóns estuary, both clay illuviation and mechanical infiltration, as described in the literature (Kuhn et al., 2010; Moraes and De Ros, 1992; Moraes and De Ros, 1990), may occur. Sediment in suspension within the tidal prism (volume of water between mean high tide and mean low tide) will move over the estuary sediment twice a day. With a falling tide, areas of the estuary may be subject to tidal drawdown or tidal pumping (Horn, 2006; Santos et al., 2012) as silt and clay in suspension infiltrates into the sandy sediment with the falling water table. If the conditions for clay illuviation and eluviation outlined by Kuhn et al., (2010) occur within the sandbody - flow rate reduction,

encountering a barrier or the flocculation of particles - then fine-grained sediment may be deposited on grain surfaces. Fine-grained sediment may adhere to the grain surface through the drying mechanism noted in the section above (section 5.1), although this may not occur to the same extent at depth within the sediment. If sediment does not become fully adhered to a grain then the fine-grained sediment may be re-distributed within the sandbody during tide cycles.

Conversely a process more similar to clay illuviation (Kuhn et al., 2010), could also occur in the estuary where finer grained sediment overlies coarser grained sediment, for example beneath the muddy saltmarsh, or more likely, beneath the muddy intertidal flat sediments. In this instance, the sediment has been deposited on to the substrate in a previous tide forming a thin veneer over the sandy sediment. As the tide falls it may draw down the water table possibly entraining fine grained sediment as it moves, sediment may then become deposited (Kuhn et al., 2010) and adhere to grains as outlined above.

Grain-coats in the Anllóns estuary are composed of fine grained clay and silt sized detrital lithics, although commonly reported as being fine grained, coarse coatings formed through clay illuviation do occur (McKeague et al., 1971; Kemp et al., 1998). Coats formed through clay illuviation produce laminar coats through repeated cycles of sediment flow (Kuhn et al., 2010). In the Anllóns estuary, sediment

coats lack internal textures (figs. 5.6 & 5.8). The cyclical nature of the tide within the estuary would seem likely to produce fine grained laminar coatings. However, a soil is quite different to estuary intertidal flat, where large volumes of water flow rapidly through the sand body every day. The magnitude and repeated nature of the tidal process may be the cause of the lack of structure seen in the present coatings (figs. 5.6 & 5.8).

The interpretation of fine-grained sediment becoming concentrated in sandy sediment through tidal flow processes, would seem to support the contention of Matlack et al. (1989), who suggested that coatings were more likely to occur in environments with high suspended sediment concentrations, with fluctuating water levels and minimal sediment reworking, all of which seem to occur towards the margin of the estuary. Textures within the sediment reported here (Figs 5.6 & 5.7) are similar to structures reported in mechanical infiltration examples in ancient fluvial setting such as massive aggregates, grain bridges and pore-fillings (Moraes and De Ros, 1990; Moraes and De Ros, 1992; Dunn, 1992). Processes of clay illuviation are noted to occur down to tens of metres depth in marine-facing shoreface settings (Horn, 2006). It seems likely that in the lower energy environment of the Anllóns estuary that these processes may occur on a smaller scale and that may be why the maximum depth of muddy intertidal flat environment is approximately 40cm below the sediment surface.

#### 5.6.3.3 Bioturbation

Bioturbation of the intertidal flat sediment occurs on a large scale (fig 4.5 D & E). Experimental ingestion of interbedded sands and crushed slate by *Arenicola* worms (McIlroy et al., 2003; Needham et al., 2004; Needham et al., 2005; Worden et al., 2006; Needham et al., 2006) proved that bioturbation can lead to the formation of grain-coats. The experimentally-produced coats and those noted in the Anllóns estuary have a similar morphology, with no internal organisation. The experimental coatings created by the worms resulted in finer sediment adhering to the framework grain through a sticky mucus membrane; this is likely to produce stronger and more adherent grain-coats.

Worms were noted in great abundance in some sites of the muddy intertidal flat, where clay and silt grade sediment is most likely to be deposited. This may be due to the co-deposition of biological matter and finer sediment. In these locations, the veneer of clay and silt particles could be turned over resulting in the types of textures noted in the grain-coats within the sediment cores.

#### 5.6.3.4 Inherited grain-coatings

Inherited grain-coatings are defined as clay coats that form on framework grains prior to deposition (Wilson, 1992). Two modes of formation have been identified (Wilson, 1992): i) formation in aeolian sands through the infiltration of clay-bearing waters followed by mild re-working, ii) shelf deposits where clay coats form through

bioturbation, again with subsequent reworking. Coats produced through both mechanisms are reported to survive minor reworking, and this would indicate that most coated grains are likely to remain within the environment of deposition rather than be transported far from the site of formation. Survival of grain-coats prior to 'final' deposition will ultimately be the result of a balance in favour of coat adherence against the energy of sediment reworking, transport and deposition. The process of inherited coat formation outlined (Wilson, 1992) are essentially the same as the clay illuviation/mechanical infiltration and bioturbation processes outlined above.

#### 5.6.3.5 Cause of grain-coatings summary:

In summary, it seems likely that the processes of co-deposition fine-grained sediment, clay illuviation/mechanical infiltration and bioturbation could all potentially result in the grain-coating of sand grains. The processes of co-deposition of fine grained sediment and bioturbation are likely to work together to increase coat coverage in some depositional environments. Grain-coat formation through the processes of flow rate reduction, encountering a barrier or the flocculation of particles (Kuhn et al., 2010), which are known to occur in soils, may only result in weakly adhered coats which could become disaggregated through sediment reworking or be preserved through rapid sedimentation or adhere to the grain through drying out. Bioturbation has been noted to result in the adherence of fine-grained

material to sand grains with a mucus membrane (Worden et al., 2006) and this could produce grain-coatings that may be more likely to survive reworking. Where processes such as clay illuviation and mechanical infiltration occur to decimetre depths, then the sediment may be protected from surficial reworking.

Whether coats survive to be deeply buried and become diagenetically-altered within a sandstone depends on local tectonic and stratigraphic events. Whichever process(es) may create coated sand grains, it seems key that transport and deposition of fine-grained sediment in the muddy intertidal and saltmarsh areas allows this finest sediment to adhere to sand grains. In higher energy, more marine areas such as the shoreface, the coating of sand grains is not evidenced to the same extent probably due to low preservation potential. It may be possible with further work to repeat the observations noted in the Anllóns estuary through either further field or experimental studies to better understand the nature of the processes occurring.

#### **5.6.4 Implications for predicting coat coverings**

In the Anllóns estuary, sediment is sorted and reworked on the sandy intertidal flat close to the estuary channel to produce moderately-sorted, medium sands with a symmetrical skew, and an average fine fraction content of 0.8%. Landward of this, in a similar setting, the muddy intertidal flat has sediment that is composed of poorly-sorted,

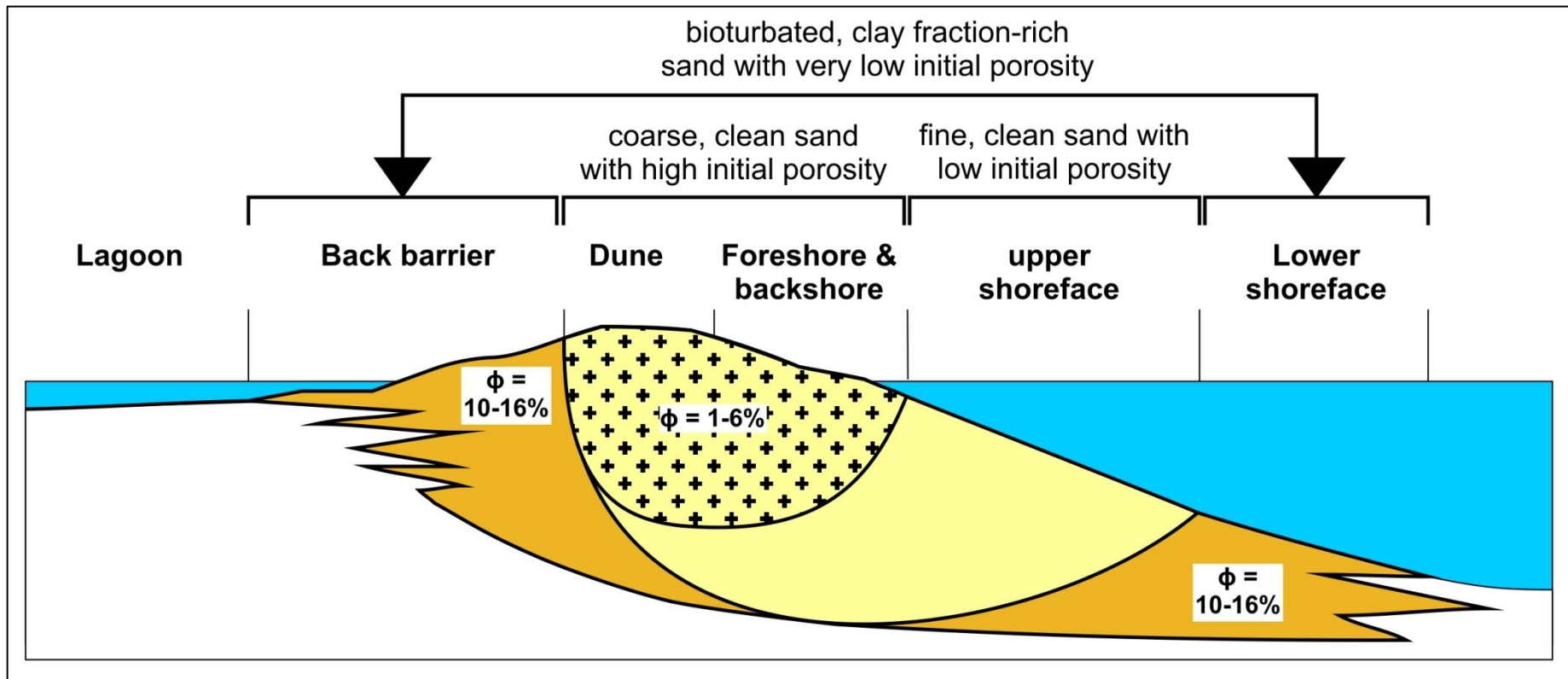


Figure 5.13 - Figure of generalised barrier island depositional model (after Westcott, 1983). Figure shows the depositional environment of facies and the porosity characteristics of facies types.  $\phi$  = porosity.

medium sands with a very fine skew and an average fine fraction concentration of 2.6%. This slight difference in fine fraction content produces a difference in average coat coverage values of approximately 11%. This observation shows that only a relatively small amount of fine grained sediment is required to produce a significant change in the coverage of grain-coats.

In an exploration scenario, on the basis of the analysis of grain-coats in the Anllóns estuary, a poorly sorted, bioturbated, medium sand facies, such as the muddy intertidal flat, may normally be interpreted as only a marginal quality reservoir. However, on the basis that this area has the greatest coat coverage it may be a more attractive exploration target. With the greater initial coat coverage the muddy intertidal flat may be more likely to preserve porosity and permeability by limiting cements such as quartz which can impact these characteristics. An example from the literature is that of the Cotton Valley sandstone, East Texas (Westcott, 1983). In this barrier island setting (fig. 5.13), high initial porosity and permeability occurs in well-sorted and clean

sandstones of the shoreface, more marginal areas of the lower shoreface and backbarrier consist of bioturbated sediments with a higher fine-grained sediment content than in the shoreface. During burial and diagenesis the shoreface sediments with the highest initial porosity and permeability become quickly cemented with authigenic calcite and quartz overgrowths because formation fluids are able to

freely move through these high permeability zones massively reducing the porosity and permeability of these reservoir zones to between 1-6%. In the lower shoreface and backbarrier environments, the interstitial fine-grained sediment between framework sand grains limited formation water movement preventing the development of authigenic calcite and quartz cements, in this zone porosity is preserved at between 10 and 16%.

High average grain-coat coverage only appears to occur in settings where there is significant fine-grained sediment content (figs. 5.9), in particular in areas where flow velocities are slightly reduced from those seen at the front of the estuary and proximal to the estuary channel. Using the Anllóns estuary and the widely cited Dalrymple et al. (1992) facies models, a schematic diagram is proposed to predict where greater fine-grained sediment content, and therefore grain-coats, in estuaries may be found (fig. 5.14). Following the Dalrymple et al. (1992) estuary classification scheme, the estuary is a hybrid wave- and tide-dominated estuary with a barrier separating the central basin from the sea behind which is a series of sandy and muddy intertidal flats dissected by channels and drainage creeks. Mean low tide is marked by the larger subaqueous channels and creeks. Mean high tide is the top surface of the saltmarsh, beyond which only spring tides may inundate parts of this area. The intertidal flat is split into two areas; the sandy intertidal flat close to the mouth of the barrier and

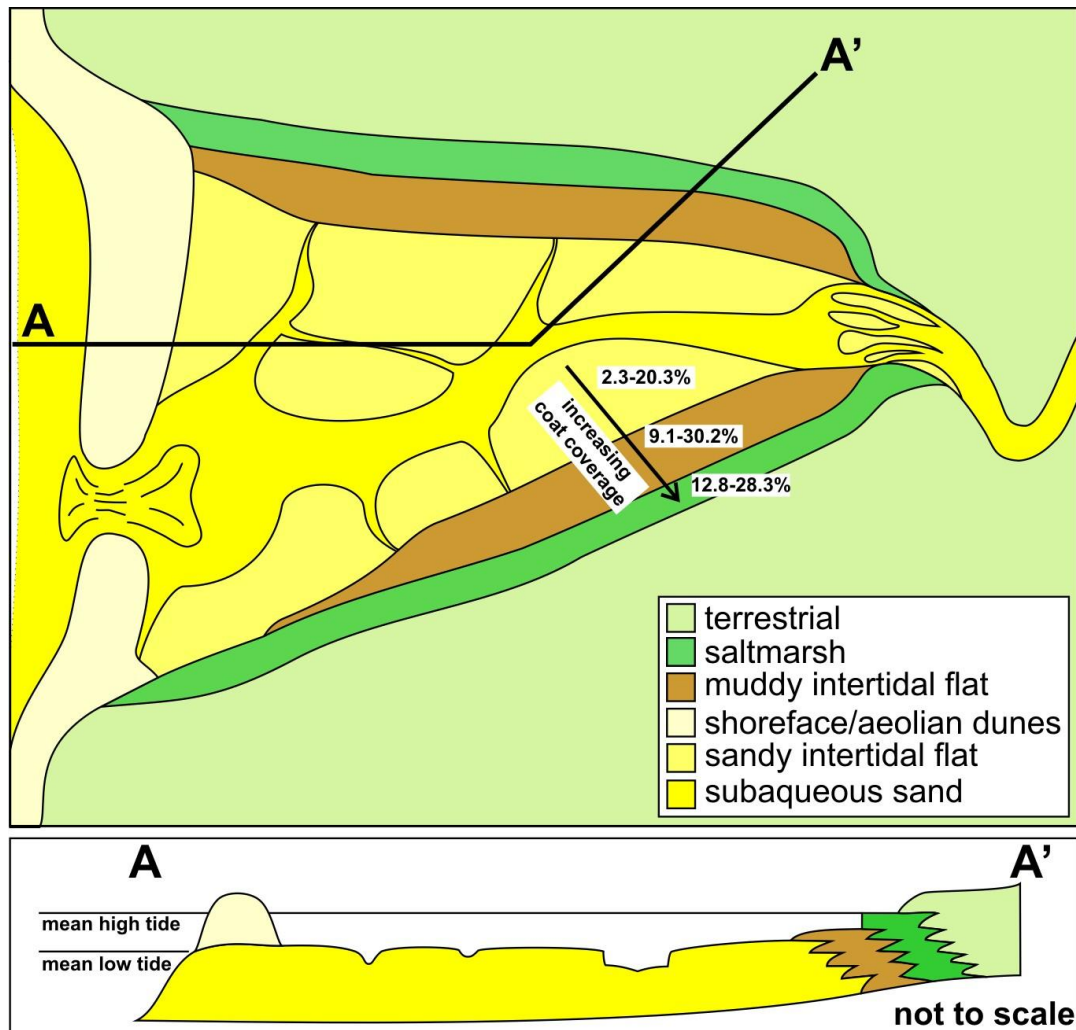


**Figure 5.14 - Schematic figure of the likely setting for high initial grain-coat coverage (after Dalrymple et al., 1992). Highest initial grain-coat coverage is likely to occur in the muddy intertidal flat environment around the margin of the intertidal portion of the estuary where fine-grained sediment is concentrated. Where energies are higher, marine reworking will reduce remove fine-grained sediment from the sandy portions of the intertidal flat.**

close to the larger estuary channels, in less energetic areas close to the mean high tide limit the muddy intertidal flat is developed.

Based on the evidence from the Anllóns estuary, areas that are subject to the greatest marine influence at the front of the estuary and proximal to the main estuary channel are likely to be extensively reworked by tides and waves resulting in the loss of fine grained sediment(fig. 5.14). Greater coverage of grain-coats within estuary

sands may be expected in the muddy intertidal flat zone, which consists predominantly of sand with slightly higher fine-grained sediment content than elsewhere. The fine-grained sediment is deposited during the highest stage of the high tide where flow velocities are at a low. The co-deposition of the fine-grained sediment, plus processes of mechanical infiltration/clay illuviation (Moraes and De Ros, 1990; Moraes and De Ros, 1992; Kuhn et al., 2010) through tidal processes and/or bioturbation from worms may result in fine-grained sediment adhering to grains within the sandy sediment (Needham et al., 2005).

A fining upwards trend is noted (fig. 5.14) resulting from a relative fall in sea level, a reduction in accommodation or a relative increase in fine-grained sediment supply. Where this occurs, the muddy intertidal flats may progressively overprint clean, sandy, intertidal areas generating more grain-coats. Similarly a coarsening upwards trend and a back-stepping of environments may occur when relative sea level rises, accommodation is created or when there is a relative increase in coarse-grained sediment supply. This would result in reworking of grain-coated sands, or a reduction in their formation. The alternation of these coat generation-destruction cycles will vary depending primarily on external factors such as relative sea level, sediment supply and climate.

The survivability of the coats during periods of reworking will be controlled by the strength of the coat versus the extent and nature of the reworking. Bioturbation of the sediment on the intertidal flat may adhere coats to grains with worm mucus (Needham et al., 2005), and these may be more likely to survive than those generated through mechanical infiltration/clay illuviation or co-deposition. Furthermore, coats on sands that have been subject to compaction or cementation during very early diagenesis may be more likely to survive than any other when subject to reworking (Wilson, 1992).

The modern coats consist of a range of silt and clay size detrital fragment plus bioclastic carbonate, pyrite and clay minerals. Authigenic grain cements have been subject to high temperatures and pressures, resulting in the alteration of primary mineralogy and the compaction of both framework grains and interstitial components. Authigenic mineral grain-coatings in reservoirs form from a variety of precursor minerals during diagenesis (Worden and Morad, 2003; Worden and Burley, 2003). With burial and alteration during diagenesis, many of the minerals noted in the Anllóns estuary coatings may subsequently develop into a range of different authigenic cements through dissolution and precipitation, possibly producing authigenic illite or chlorite (Worden and Morad, 2003).

Alternatively, the coats seen in the Anllóns estuary may not be the incipient stage of coat development seen in ancient settings. Textures

in the modern coating are markedly different from those in ancient examples where coats are composed of a series of different authigenic cements, rather than distinct detrital lithic fragments (Aagaard et al., 2000; Storvoll et al., 2002; Bloch et al., 2002; Worden and Morad, 2003). Also the coats in their current state do not seem strong enough to survive transport and re-deposition if the sands were reworked. Early cementation and compaction at shallow burial depths may adhere the coat more strongly, enabling coats to survive remobilisation internally within the estuary or externally to a marine setting (Wilson, 1992). Compaction of ductile material around framework grains with shallow burial may also result in greater coat coverage. Another potential method suggested for the formation of clay mineral coats in deposition environments is in tropical, offshore, high energy zones (Odin, 1988; Odin, 1990). Here sand grains are thought to be rolled repeatedly on clay substrate rich in chlorite precursor clay minerals such as odinite and berthierine this generate clay mineral coated sands and ooids which are noted in some ancient examples (Ehrenberg, 1993).

In summary, estuarine sandstones cemented with clay mineral coatings are more likely to develop in zones close to the limit of the tide where processes of co-deposition, bioturbation and mechanical infiltration/clay illuviation may incorporate fine grained sediment into sands. Although exact prediction of these types of zones still presents

a significant exploration challenge, it may be possible using well analogues to predict the presence of these types of facies during exploration, appraisal and development. The grain-coats in the modern Anllóns estuary are dissimilar to ancient examples of clay mineral cements, but this is likely to be due to the diagenetic overprinting of the initial depositional textures.

## **5.7 Conclusions**

1. Sand grain-coatings in the Anllóns estuary do not vary in texture and consist of poorly sorted mixtures of clay minerals, pyrite, detrital lithic and bioclastic debris. Grain-coatings do vary in average coat coverage and mineral composition between different sedimentary environments.
2. Average grain-coat coverage is generally partial and rarely exceeds 25% of the coat surface. The highest average coat coverage range occurs in the muddy intertidal flat environment (9.1 to 30.2%) and the muddy saltmarsh environments (12.8-28.3%) on the margins of the estuary. The lowest average grain-coat coverage range is within the SIF environment (2.3-20.3%), which tends to occur closest to the main estuary channel and at depth in cores towards the upper-tidal area of the estuary. The SS have intermediate average coat coverage ranges of between 7.5% and 15.6%.

3. The mineralogy of the coats appears to be influenced by marine processes and sedimentation as with increasing carbonate concentration, non-carbonate concentrations decrease. In the carbonate-normalised data, mineral concentrations do not seem to vary significantly on the scale of the estuary, but do vary within individual cores, due to differences in environment and deposition.
4. Coat coverage is controlled by overall fine-grained sediment concentration within sands. Greater coat coverage occurs in shallower and surficial parts of the cores particularly in the muddy intertidal flat, and saltmarsh environments, and this may be related to the overall fining up trend noted on the margins of the estuary. Likely processes which may coat fine-grained sediment on to grains are co-deposition of fine-grained sediment with sands, mechanical infiltration/clay illuviation of fine grained material into sands, possibly controlled by tidal processes, and the bioturbation of sediment which may adhere coats on to sand grains.
5. On the basis of evidence from the Anllóns estuary grain-coatings in modern environments are dissimilar to ancient examples, and this is likely due to the diagenetic over printing of grain-coats during burial.
6. Areas where grain-coatings may occur (improving or reducing reservoir quality) may be found in estuarine settings, close to the

tidal limit where finer-grained sediment is concentrated through flow processes, and where bioturbation may occur.

## 6. Summary and further work

### 6.1 Introduction

This chapter summarises and discusses the results of the preceding chapters, and outlines opportunities for further work in these areas. Summary figures are presented (figs. 6.1 & 6.2) to outline the nature of the research undertaken and how this varies in both temporal and geographic scale.

Figure 6.1, is a block diagram to illustrate the scale and context of the research completed for this thesis. It outlines the relationship between modern and ancient studies of sedimentary environments, sediments and mineralogy through time in a hypothetical drainage basin and sedimentary basin configuration. The block diagram shows a sedimentary sequence with varying environments through time. The cut-away represents chapter two and the common characteristics of chlorite-coats in a buried system identified in the meta-analysis of published literature undertaken in chapter two. Inset 6.1B, is a close-up of this cut away and highlights the varying scales over which this chapter assessed common chlorite-coat characteristics. The modern-day surface of the block diagram represents chapters three, four and five, with the detailed quantitative study of surface clay minerals in two modern day estuaries, and the grain-coat analysis performed on core sediments. The inset figure 6.1A outlines controls on the

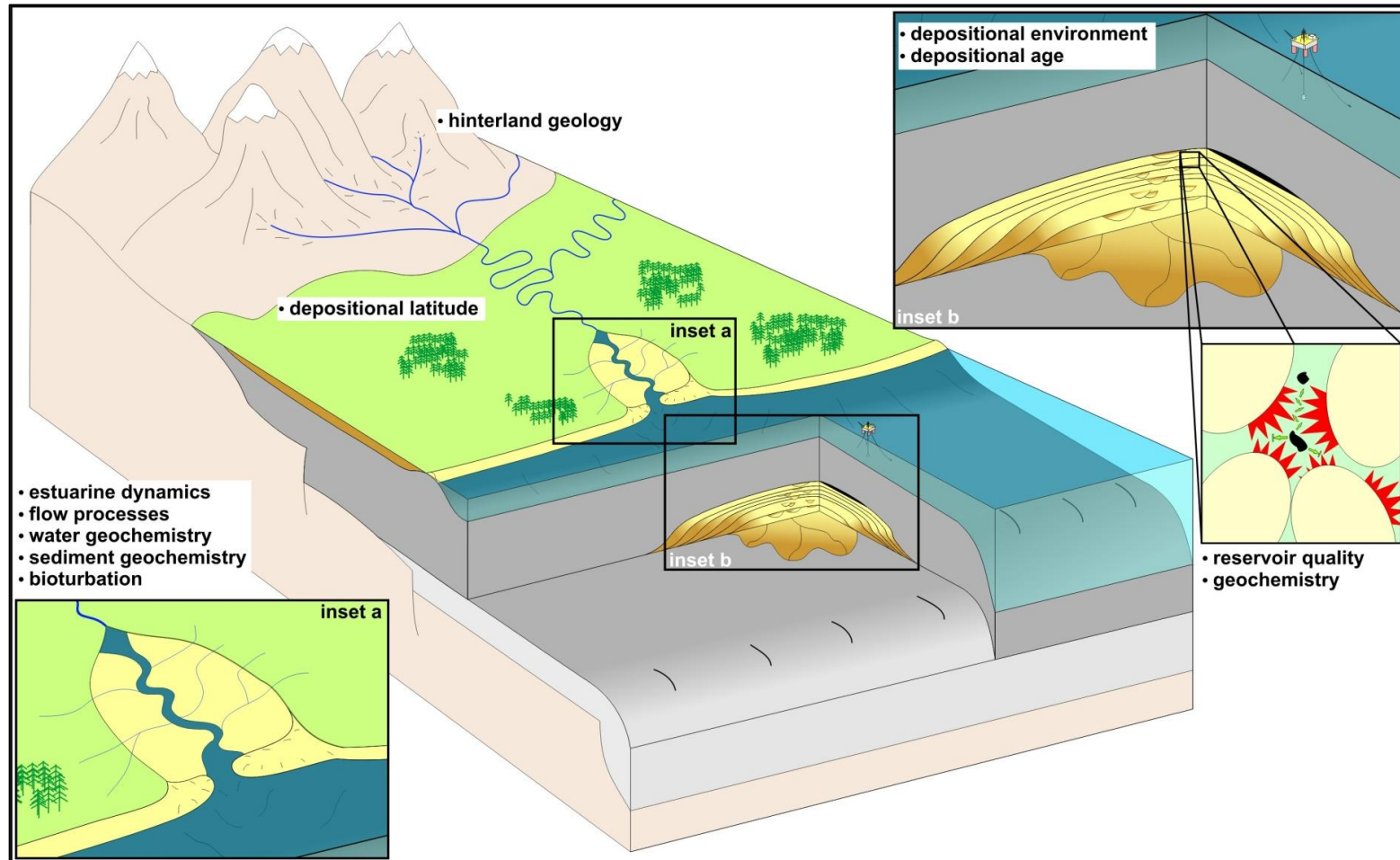


Figure 6.1 - Outline of the varying physical and temporal scales of the research questions addressed by this thesis and how these aspects are inter-related. The top surface and inset a of the block diagram represents the modern estuarine studies (chapters 3-5) and the processes and influences upon this aspect of the study. The cutaway and inset b, represent the ancient chlorite-coated reservoir study (chapter 2) and how this study varies in scale between addressing micrometer through to basin scale issues. The inter-related nature of the thesis is represented schematically by the temporal aspect, with the modern-day estuary influenced by modern day geochemistry, sedimentary processes, hinterland geology, climate and bioturbation. This stratigraphically overlies the ancient delta, which may have been influenced by many of the same sources and processes as the modern estuary.

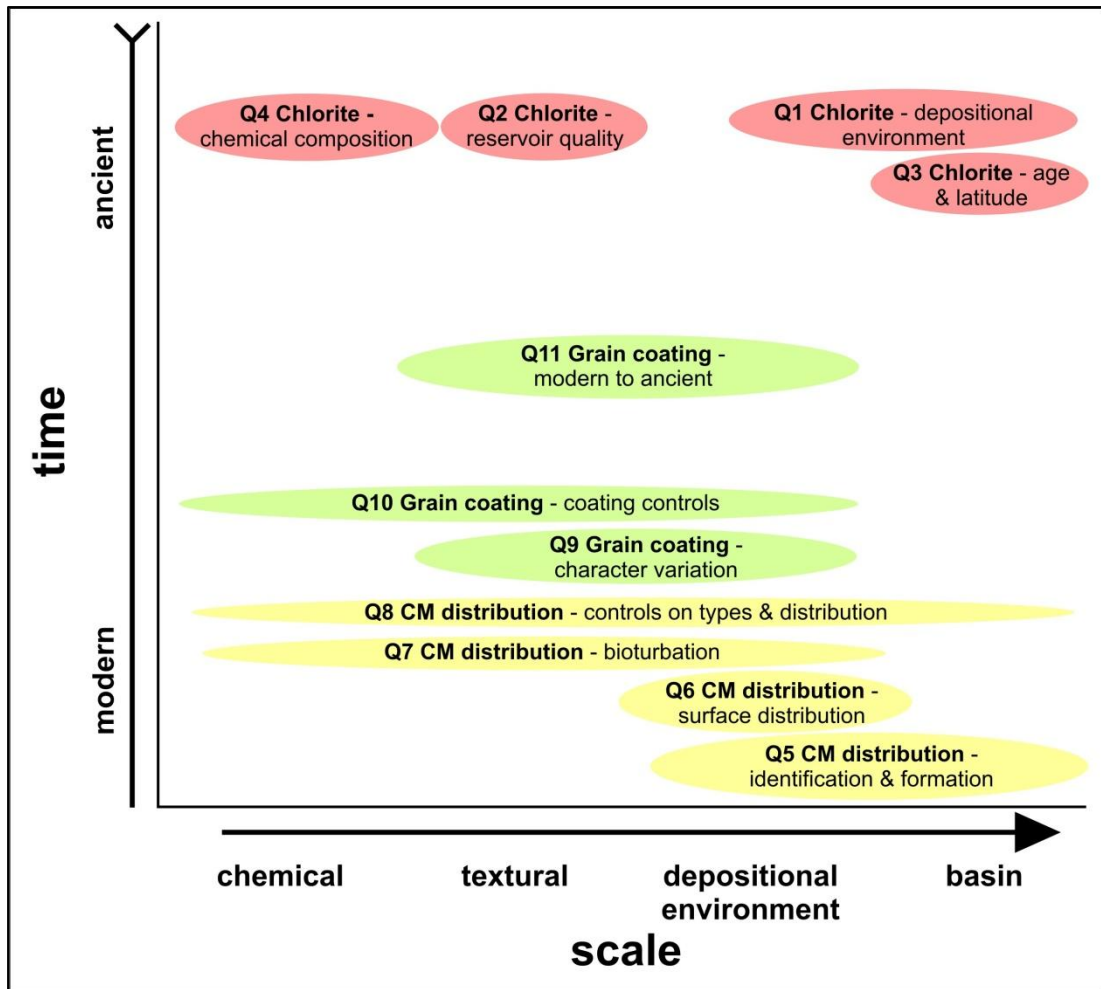


Figure 6.2 - Cross-plot of the key themes of the thesis. The figure outlines the key themes of the thesis: time and scale. Each of the research questions outlined in chapter one and discussed in this chapter are plotted in respect to these themes. For example question one is about the depositional environments that host chlorite-coated reservoir sandstones, and cover issues of a depositional environment to basin scale in ancient rocks. It therefore plots along the furthest points of these axes.

types and concentration of clay minerals both externally and internally to the estuary. The inset also outlines the study of grain-coat coverage, which assesses the environment of deposition of the grain-coats and how they may have developed.

Fig. 6.2 is a cross-plot of the relative spatial and temporal scale of the focus of different research questions addressed in this research. The reader can refer to this when considering the questions outlined in section two, below. The x-axis is where the question plots in terms of physical scale of the study, questions plotting close to the origin address issues on smaller textural or chemical scale. Those further along the x-axis address depositional- or basinal-scale issues. On the y-axis questions are plotted close to the origin if they address modern settings or environments. Further along the y-axis, questions address issues from ancient studies. The figure shows that the research undertaken in this thesis addresses questions of a wide range of physical and temporal scales. Although this approach covers a diverse range of topics in sedimentology and reservoir quality, it is hoped that it also demonstrates how employing diverse and under-used data sources could further the understanding of how sediments are formed and develop through time.

## **6.2 Summary of results and conclusions**

A series of eleven research questions were posed in Chapter 1. The questions were divided into three over-arching themes: 1) What

factors are common to the formation of chlorite-coated sandstone reservoirs; 2) How are clay minerals distributed in modern estuaries, and what processes and factors control their occurrence; and 3) Do grain-coats occur in modern estuarine environments and how do they form?

### **6.2.1 What factors are common to the formation of chlorite-coated sandstone reservoirs?**

Using a collection of published data in this chapter (section 2.4, appendix 1), it can be seen that there are a number of common factors in the formation of chlorite-coated sandstones. These factors include the depositional setting, the age and latitude of formation and the chemistry of the chlorite-coats (sections 2.5 & 2.6). These common factors of chlorite-coat formation were summarised in a figure form (fig. 2.6) describing the most likely and unlikely scenarios of formation. The utility of this is that it may be used by geoscientists in both frontier and mature exploration areas to compare the general characteristics of a basin setting to the likely and unlikely scenarios for chlorite-coat formation, possibly allowing plays and prospects to be de-risked.

Some potential issues with the data utilised in this research are that the scale of this study may not reflect smaller, facies scale variations in environment of deposition or texture of sediments, which may, in turn, have an impact on how the models created can be utilised. Also the

data have a strong North American and European bias, and a bias to the late Mesozoic and early Cenozoic (fig 2.2B & 2.5, section 2.5.2 & 2.6.2, appendices 1A-C), which may not reflect global scale factors in the formation of chlorite-coated sandstone reservoirs. Problems arising from using interpretations presented by other authors are also a factor, but by properly setting out the methodology (section 2.4) used in studies of this type and how decisions were arrived at makes this work stronger.

6.2.1.1 Question one - In which depositional environments did the chlorite-coating sandstone form?

Coastal settings and deltaic environments are the most common host for chlorite-coated sandstones, with 44% of all published examples occurring in the delta-related environments (fig. 2.2A; section 2.5.1 & 2.6.1). River environments also make up 19% of published examples, while other environment types only have a few examples (fig. 2.2A; section 2.6.1). Deltaic and other coastal environments make up a significant proportion of all reservoir sandstones (Ahlbrandt et al., 2005). Common features of coastal environments, such as high-energy conditions and the repeated reworking of sediment (Bird, 2011), are key processes in the formation of reservoir sandstones in general and not just the formation of reservoir sandstones with chlorite-coated grains. This may partly explain why these settings are frequently hosts for chlorite-coats.

The research indicates fluvial examples are also quite common, and deltaic environments are potentially heavily influenced by river-supplied waters and sediments and fluvial processes (section 2.6.1), suggesting proximity to a fluvial input is important. This link has been made before with studies suggesting that berthierine and odinite, which are chlorite precursor clay minerals, are more likely to be found in river-influenced coastal settings (Ehrenberg, 1993). The low numbers of other environment examples indicates that although the processes of chlorite-coat formation are not restricted to coastal and river environments entirely, the processes and features of these environments may allow chlorite-coats to have an impact on the reservoir quality of a sandstone.

The accurate description of a body of sedimentary rock prior to the drilling of an exploration or production wellbore is required to fully understand the pore volume characteristics of a reservoir. The nature of a rock body is primarily a function of the depositional environment (and its inherent controls on stratigraphy and sedimentary features), sediment components, and the effects of temperature, pressure and fluids during burial and diagenesis on the rock volume. Knowing in which environments chlorite-coats are mostly commonly found enables a greater understanding of which processes are essential to how the coatings develop, and whether these are a result of depositional or other factors. Deltaic and fluvial depositional

environments are more likely to host chlorite-coats so these reservoir types could be high graded when exploring for these types of reservoirs. Conversely, if a very deeply buried lacustrine reservoir sandstone is a potential lead it is unlikely to retain its porosity and permeability as chlorite-coats are less likely to occur in these settings.

6.2.1.2 Question two - What effect do diagenetic chlorite-coatings have on the reservoir quality of the sandstone?

Within the dataset compiled (fig. 2.2A; sections 2.5.1, 2.5.3 & 2.6.4) chlorite-coatings generally have a positive or mixed effect (positive and negative effect) on reservoir quality. A positive effect occurs when chlorite-coated sand grains preserve porosity and permeability at deeper levels than normally expected by preventing the development of other reservoir quality reducing cements (e.g. quartz) (Berger et al., 2009; Islam, 2009). A mixed-effect occurs when chlorite has a positive effect by preserving porosity and permeability to an extent, but by also reducing permeability through the creation of micro-pores between individual crystals or by the restriction of pore throats by the chlorite cement layer (Pay et al., 2000; Berger et al., 2009).

Knowing that the chlorite-coats generally have a positive or mixed effect on reservoir properties indicates that pore-filling chlorite, which would have a negative effect, is less common in petroleum reservoirs than pore-lining coats. The main issue with this data is that pore-filling

chlorite is likely to be under-reported in the studies used for the data than pore-lining as the former will reduce porosity and permeability to the point where a sandstone is no longer classed as reservoir. To fully understand this relationship, studies of intervals or units that are non-reservoir would be required. Accurately understanding the effects of chlorite-coats on the basis of published work is challenging and relies solely on the interpretation of other authors, and for the most part detailed quantitative data on the effect of chlorite is not supplied in published examples for proprietary reasons.

#### 6.2.1.3 Question three - At what age and latitude were the chlorite-coated sandstones deposited?

The age of the examples display a strong trend towards more recent reservoirs, which is likely to be a development and production bias, with older reservoirs generally less likely to be encountered due to being at a greater depth within a basin-fill (figs. 2.2B & 2.3; sections 2.5.1, 2.5.2, 2.6.2 & 2.6.3). Depositional latitude seems to play a role in the formation of chlorite-coated sandstones with all the examples deposited at between 60°N and 60°S. This is interpreted as being due to the effect of palaeo-weathering being greater at lower latitudes, with lower free water content and lower temperature inhibiting erosion (Bland and Rolls, 1998; Chamley, 1989) and possibly limiting the formation of chlorite precursor clay minerals, eroded lithic fragments and the generation of aqueous iron. While this is a factor

that will be common to the generation of all clay minerals it is still useful to consider this factor when assessing the lithic source regions for reservoir sediments.

The latitude of deposition of a reservoir is important particularly for understanding the types of chlorite precursor material that will be generated through weathering. The study has shown that reservoirs deposited at high latitudes are unlikely to produce the full range of material due to low weathering intensity that could enable the development of chlorite-coats during later diagenesis.

6.2.1.4 Question four - What is the range of chemical compositions of chlorite in the published examples?

Sections 2.4.5, 2.5.3 & 2.6.5 indicate that iron-rich chlorite examples are more likely to be found in coastal and deltaic environments than elsewhere (fig 2.4). This collation of published analyses supports the contention in this research and others (Ehrenberg, 1993; Bloch et al., 2002) that river-supplied iron is important to the generation of chlorite during authigenesis and its precursor iron-rich minerals formed at the time of deposition. Without a ready source of iron either as berthierine or odinite or as aqueous iron taken up as iron oxides it seems unlikely that iron-rich chlorite-coats would develop during diagenesis. The other elemental data collated in the meta-analysis contained generally mixed Fe-Mg-rich and Mg-rich reservoir examples which were formed in desert and deepwater environments.

Understanding the chemistry of chlorite-coated examples is essential to understanding how it formed at what the precursor material prior to diagenesis may have been. The chemistry of chlorite may also have an impact on the crystal structure and the morphology of the chlorite-coat. The main issue with this data is that elemental data is often unreported in studies of chlorite-coats. This means that the size of the dataset is quite small, with a lower number of analyses the data becomes less statistically significant compared to all chlorite-coated examples. Although the dataset appears large enough to be able to interpret trends, a fuller study of all the examples used would further confirm the interpretations of this research.

### **6.2.2 How are clay minerals distributed in modern estuaries, and what processes and factors control their occurrence?**

Chapters three and four are among the first attempts to quantitatively measure clay mineral distributions in the surface sediments of a modern estuarine setting. Furthermore, the clay mineral distributions are related to sediment transport and flow processes and mineral alteration processes in hinterland and estuary settings.

It appears from the results presented that clay mineral types are strongly controlled by the source mineralogy of the hinterland (sections 3.6.2, 3.6.4 & 4.6.2), with the same suite of minerals occurring in lithology, riverbank soil samples, and estuary samples. Within the estuary, physical processes appear to control the concentration of

clay minerals. Some clay minerals are concentrated preferentially in fluvially-dominated lower energy areas, while others are concentrated in higher energy more marine-dominated settings. This is the first time that such differences in clay mineralogy have been mapped on this scale. Related to this distribution, the distinct variation in concentrations of different clay minerals may suggest that the physical characteristics of the clay minerals may be important in controlling their distribution (sections 3.6.5.3 & 4.6.4.1, tables 3.5 & 4.5). Also within the estuary environment, the geochemical alteration of clay minerals is evidenced in sediments in both chapters two and three. Reducing conditions in sandy sediment at depth (<1m) and the bioturbation of sediment by worms both appear to be effecting the concentration of a different range of clay minerals within two different estuaries

6.2.2.1 Question five - What clay minerals are present and where did they form?

In chapter three, quantifiable clay minerals in the fine fraction of estuarine sediments are chlorite, smectite and inter-layer vermiculite. All three minerals are present in riverbank soil and glacial sediments sampled in the hinterland. Smectite is a common weathering product of basaltic rocks (Eggleton et al., 1987; Eggleton, 1975), while chlorite appears to have developed through the hydrothermal alteration of smectite during burial (Kristmannsdottir, 1979; Schiffman and

Friedleifsson, 1991; Sveinbjörnsdóttir, 1992) of the basalt (followed by weathering and release into the fluvial system). Inter-layer vermiculite may have formed from the alteration of either smectite or chlorite (Meunier, 2007; Wilson, 1999; Proust et al., 1986).

In chapter four, quantifiable clay minerals in the fine fractions of estuarine sediments are muscovite, chlorite and kaolinite. All three minerals are present in riverbank soil sediments sampled in the catchment. Chlorite and muscovite occurs in bedrock samples (Table. 4.4, Fig. 4.8) and are most likely detrital. Kaolinite is a common weathering product of feldspar and muscovite and it seems most likely that it formed through weathering (Wilson, 1998; Fernández-Caliani et al., 2010).

The clay mineralogy of both estuaries has a strong detrital control. All of the clay minerals in the studied estuaries are found in lithology and hinterland sediments (compare: sections 3.3.5, 3.3.6 & 3.5.3, Table: 3.5 & fig. 3.8; sections 4.3.1, 4.3.2 & 4.3.3, Tables 4.1 & 4.4 & fig. 4.11). This indicates that the processes of clay mineral development, inheritance, alteration or neoformation (Wilson, 1999) occur primarily outside of the estuarine environment. Large scale changes in the concentration of clay minerals in the estuary resulting from neoformation or alteration processes (which could potentially produce the same suite of clay minerals but alter their concentration) can also be attributed to physical transport processes so it is difficult to

ascertain if such reactions may be occurring at this stage. However localised alteration in clay mineral concentration appears to be occurring in both estuaries, and in one of the hinterland areas. In chapter three (section 3.5.3, fig. 3.13), alteration of either smectite or chlorite to inter-layer vermiculite appears to be occurring in riverbank soils. In Icelandic estuarine sediments, it is evidenced from the changes in concentration between bioturbated and surface sediments that the inter-layer spacing of smectite and inter-layer vermiculite may be partially filling (figs. 3.13, 3.14 & 3.15; sections 3.5.9 & 3.6.5.2). This observation supports earlier experimental work indicating clay mineral development can occur through sediment ingestion by annelid worms (McIlroy et al., 2003; Needham et al., 2005; Worden et al., 2006). The change in concentration of chlorite and pyrite in reducing estuarine conditions (chapter four; fig. 4.25; section 4.6.3.2 & 4.5.10) is evidence of the effects of early alteration of clay minerals post-deposition. This may have an important impact on the understanding of early chlorite alteration and pyrite formation in sandstone diagenesis, as pyrite can have an impact on the geochemistry within sandstone reservoirs (Ligthelm et al., 1991)

6.2.2.2 Question six - What is the surface sediment distribution of the clay minerals?

Despite the clay minerals being supplied *en masse* from the hinterland, the clay minerals in both the Leirárvogur and Anllóns

estuaries display variable (heterogeneous) concentrations in the fine fraction of sediments. In chapter four, the clay mineral concentrations in the fine fraction of sediments are lower in areas subject to strong marine-influence (sections 4.5.5.1 & 4.6.4; fig. 4.14), with carbonate content and clay mineral concentrations displaying a strongly inverse distribution (figs 4.15). The surface clay mineral distributions in both estuaries are represented schematically in figure 6.3. In chapter three (Iceland), smectite is the most common clay mineral and occurs in the highest relative concentrations in lower energy areas close to stream inputs. Conversely, inter-layer vermiculite occurs in higher concentrations in higher energy areas close to the marine-dominated parts of the estuary. In chapter four (Spain), the carbonate-normalised clay mineral concentration also have distinct distribution pattern between muscovite and kaolinite (sections 4.5.5.1 & 4.6.4; fig 4.17). The former occurs in higher concentration in low energy areas at the margins and close to the river-dominated parts of the estuary, while the latter occurs in higher concentrations towards the marine-dominated part of the estuary. Chlorite varies in concentration (sections 4.5.5.1 & 4.6.4; fig 4.17), but does not appear to have an easily interpretable distribution.

This distribution indicates that variations in concentration of clay minerals in estuarine surface sediments can be measured. It is possible, on the basis of the distribution outlined, that these clay

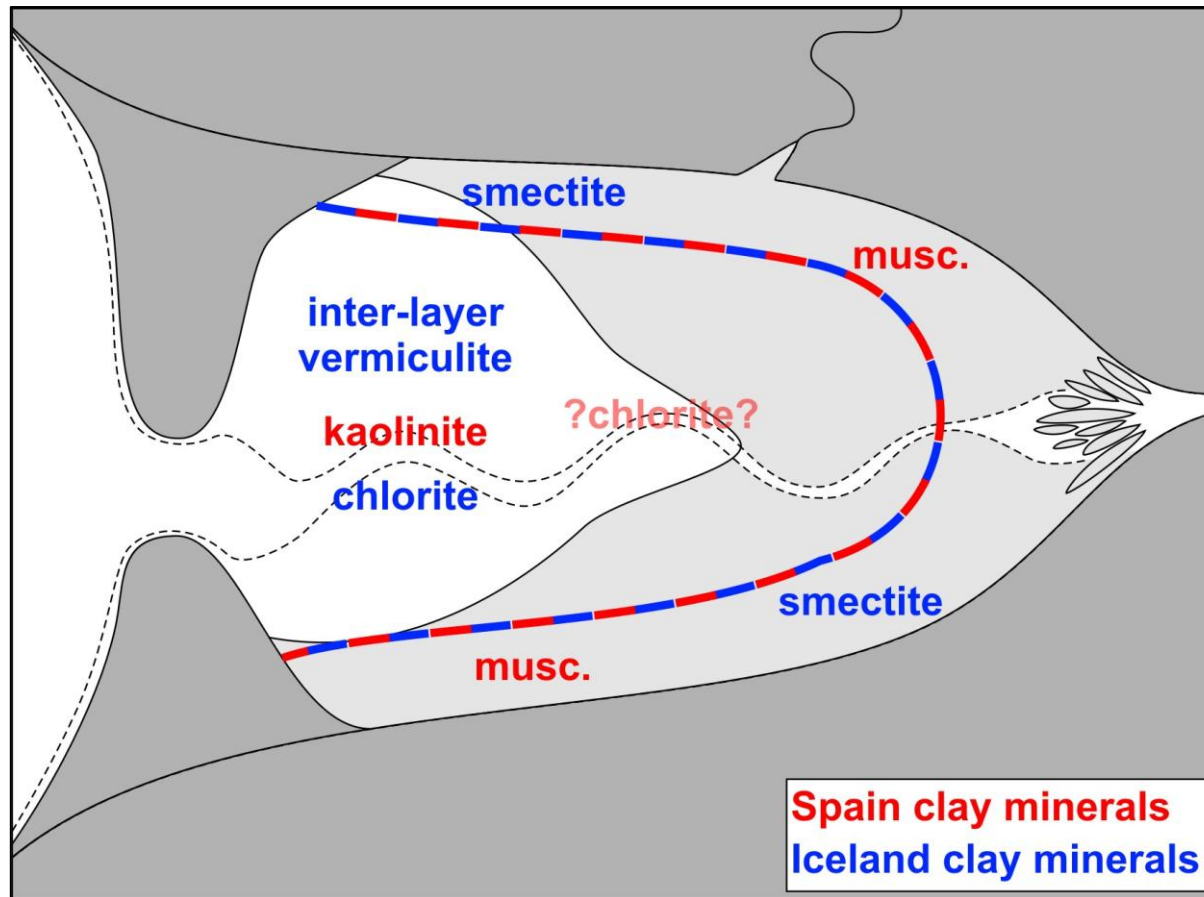


Figure 6.3 - Schematic illustration of concentrations of clay minerals in Icelandic and Spanish estuaries. Clay minerals in red are from the Spanish estuary, clay minerals in blue are from the Icelandic estuary. The figure demonstrates that in both estuaries there are varying concentrations of the minerals identified. In Spain, kaolinite is concentrated at the marine-dominated front of the estuary in higher energy conditions, while muscovite is concentrated in lower energy areas and close to river inputs at the margins of the estuary. Chlorite does vary in concentrations between locations in Spain but does not appear to have a readily interpretable distribution. In Iceland, inter-layer vermiculite and chlorite are in higher concentrations towards the marine-dominated front of the estuary, while smectite is in higher concentrations at the margins of the estuary and close to stream inputs. Collectively, due to the diverse range of clay minerals present the distribution is not contradictory, primarily because chlorite, the only clay mineral to occur in both estuaries, does not have an easily interpretable distribution in Spanish estuary. It is possible, therefore, that the distribution noted in both estuaries may occur for these clay mineral elsewhere.

mineral could occur in similar distributions elsewhere. Chlorite is the only clay mineral identified in quantifiable concentration to occur in both estuaries; that chlorites distribution in the Spanish estuary is not readily interpretable, neither supports or disproves the chlorite distribution identified in the Leirárvogur estuary. This observation may have implications for understanding the concentrations of this group of clay minerals in estuarine and other coastal settings. This is a distribution that could be testable in other estuaries.

#### 6.2.2.3 Question seven - Does bioturbation of sediment have any effect on clay mineral distribution in a modern setting

Sediment ingestion and excretion by worms appears to have an effect on clay mineral concentration in a modern estuary setting. In chapter three there is an increase in the relative concentration of chlorite and inter-layer vermiculite and a decrease in smectite in bioturbated Icelandic basaltic sands (fig. 3.13, 3.14 & 3.15). This supports experimental work (McIlroy et al., 2003; Needham et al., 2005; Worden et al., 2006), which indicated that the ingestion and excretion of unweathered basalt by worms can also produce clay minerals. However, within felsic and largely detrital-rich sediments in the Spain case study (chapter four) there is not a similar relationship (fig. 4.23 & 4.24) and the variations in muscovite, kaolinite and chlorite concentrations are so low as to be within measurement error. This may indicate is that the mineralogy of the sediment, and in particular

the clay minerals present, is the key factor in the development of clay minerals through bioturbation. In the mafic-rich sediment of the Icelandic estuary, unweathered primary minerals may be likely to alter to clay minerals through bioturbation. Similarly, minerals with expandable inter-layer spacing such as smectite and, to an extent, inter-layer vermiculite may also be likely to alter. In chapter four, the felsic-rich sediments have less reactive minerals, and the clay minerals present have a closed or limited inter-layer spacing potentially limiting the alteration of the clay minerals during bioturbation.

#### 6.2.2.4 Question eight – What are the controls on the types of clay minerals and their distribution pattern?

The controls on clay mineral distribution in both estuaries are summarised in the schematic estuary depicted in figure 6.4. The reader is asked to refer to this in the following section.

In chapter three and four, the controls on the types of clay minerals appear to be strongly influenced by the source geology of the sediment. In chapter three, smectite has formed as a result of primary weathering and chlorite is the result of hydrothermal alteration of basalt during burial (followed by exhumation and erosion), both of which are strongly controlled by the source lithology of the minerals in the primary rock type. The exception is inter-layer vermiculite, which appears to be an alteration product of either chlorite or smectite, and may have formed in soils or possibly in estuary sediments. In chapter

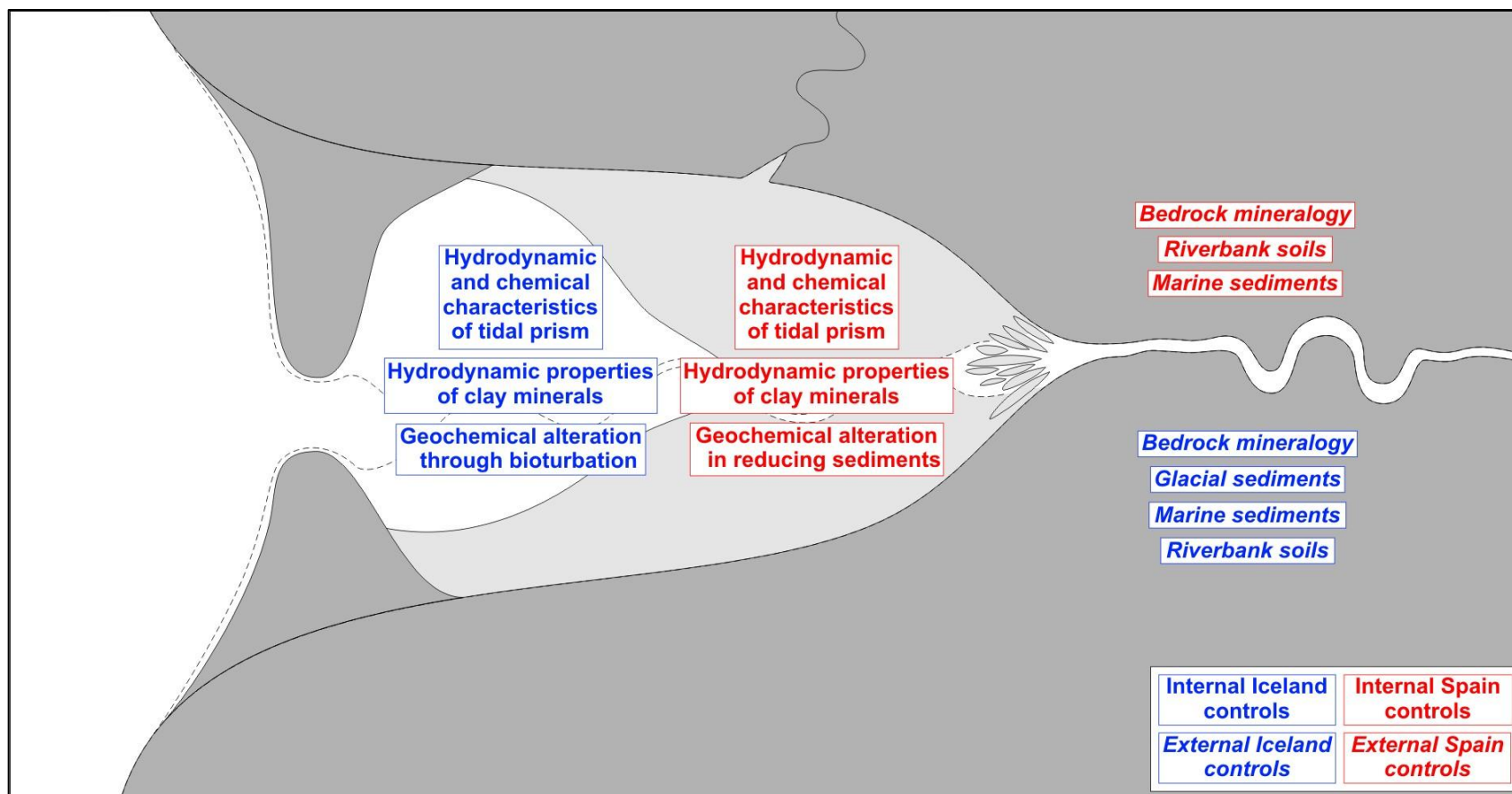


Figure 6.4 - Schematic illustration of the controls on clay mineral distribution in Icelandic and Spanish estuaries. Labels in red are from the Spanish estuary, labels in blue are from the Icelandic estuary; italic labels are external controls, non-italic labels are internal controls. The figure demonstrates that for both estuaries the external controls are broadly the same, with bedrock mineralogy, riverbank soils and marine sediments all affecting the distribution of clay minerals. The exception is the glacial sediments in Iceland, which may impact the mineralogy and distribution of clay minerals in estuary sediments. Internally the controls are also broadly the same with the hydrodynamic and chemical characteristics of the tidal prism and the hydrodynamic properties of clay mineral species possibly controlling the distribution of the clay mineral in both estuaries. In Iceland, an additional internal control is the geochemical alteration of clay minerals through bioturbation of the sediment. This process does not occur in the Spanish estuary, but the geochemical alteration of clay minerals does appear to be occurring due to the reducing conditions in the sediment. Other factors that are related to those outlined, but not identified in this study include: basin morphology, tidal range, internal estuarine geomorphology, sediment calibre and climate.

four both muscovite and chlorite appear to be detritally inherited from the predominately granitic and schistose geology in the hinterland, while kaolinite is a primary weathering product of muscovite or plagioclase.

Five out of six minerals identified and quantified in both study areas (chapters three and four) appear to be either directly detritally inherited or the result of the alteration of primary minerals in the bedrock. This confirms the role that source regions have in controlling the types of clay minerals generated in these sedimentary basins. Other factors such as climate and soil conditions impact the style and intensity of the weathering, but the suite of clay minerals are on the whole inherited from the source mineralogy moderated by hinterland sediments and soils (Chamley, 1989; Weaver, 1989; Wilson, 1999).

In both estuaries clay mineral concentrations and fine fraction percentages are lower where marine influence is high. This is most strongly evidenced in chapter four where total clay mineral and total carbonate concentration in the fine fraction of sediments display a strongly inverse relationship across the estuary (fig. 4.14). This relationship appears to be related to marine reworking by tides and waves, where clay minerals are suspended and either exported offshore or brought into the estuary and held in suspension before being deposited in lower energy zones. In the Spanish estuary,

sediment in these zones have a much higher fine fraction concentration and poorer sorting.

In both chapters three and four, there is systematic variation in relative clay mineral concentrations across the estuary for nearly all the clay minerals. In chapter three, smectite appears to be concentrated in lower energy zones, while chlorite and inter-layer vermiculite are in higher concentration in areas close to high-energy marine-dominated settings (fig 6.3). In chapter four, muscovite is concentrated in lower energy areas compared to kaolinite, which is concentrated in higher energy areas. The concentration of chlorite within estuary sediments does not appear to have a readily interpretable distribution (fig. 6.3). This distribution implies that there is a flow process control on clay minerals in these estuaries. Previous authors (Feuillet and Fleischer, 1980; Algan et al., 1994; Patchineelam and de Figueiredo, 2000; Sarma et al., 1993; Allen, 1991; Pandarinath and Narayana, 1992; Prego et al., 2012; Bernárdez et al., 2012) have explained clay mineral distributions in coastal areas in terms of salinity and hydrodynamic properties. Experimental work has attempted to recreate these types of distributions in the laboratory (Whitehouse et al., 1960; Edzwald and O'Mella, 1975; Gibbs, 1985), however the interpretation of much of this experimental research is contradictory and experiments do not appear to be readily repeatable. Typically, clay minerals have different physical properties depending on the chemistry and structure

of the mineral. These characteristics may result in individual clay minerals behaving (entrainment, transport and settling) differently to other clay minerals or even to clay minerals of the same species, in flowing bodies of water of varying salinity, but this assertion requires further work.

Processes of chemical alteration also appear to influence the concentration of clay minerals in both estuaries. In chapter three there is evidence (fig. 3.14 & 3.15) to suggest that ingestion by worms may be altering the mineralogy by partially infill of the inter-layer spacing of smectite and inter-layer vermiculite clay minerals. The reducing conditions in estuary sediments in chapter four appear to result in a decrease in chlorite concentration and a commensurate increase in pyrite concentration.

Overall, there are many controls on the types and concentrations of clay minerals (fig. 6.3), with the parent material having the strongest control over the types of mineral present; climate and weathering style also has an important role to play in mediating the types of clay minerals that are present. The concentration of clay minerals in the estuary appear to be controlled at an estuary- or basin-wide scale by alteration in hinterland soils, sedimentary transport and flow processes, as well as the type and structure of clay minerals generated from the parent lithology. On a local-scale chemically reducing sedimentary conditions and bioturbation can also alter the concentrations of clay

minerals in shallow surface sediments. Other factors that are related to those outlined, but not identified in this study include: basin morphology, tidal range, internal estuarine geomorphology and sediment calibre.

### **6.2.3 Do grain-coats occur in modern estuarine environments and how do they form?**

Grain-coatings are found in a modern estuarine environment, and occur in higher concentrations in low energy areas where fine-grained sediment is deposited. Formation of grain-coats seems to occur through the co-deposition of fine grained sediment, possibly along with bioturbation (sediment ingestion and excretion) and mechanical infiltration/clay illuviation. The coats noted in the Anllóns estuary are different to ancient grain-coatings, probably due to the effects of diagenesis altering the texture and composition of coats.

#### **6.2.3.1 Question nine - Do sand grain-coatings vary in character a modern estuary?**

Modern grain-coatings outlined in chapter five have variable average coat coverage and mineral composition between environments (sections 5.5.3, 5.5.4.1, 5.6.2; figs. 5.3, 5.9 & 5.11). Sediment in the muddy intertidal flat setting has higher coat coverage and this is due to the higher fine grained sediment concentration and poorer sorting of the sediment found in fluvial-dominated and lower energy intertidal areas, close to the upper tidal limit (section 5.3.4, 5.5.1 & 5.5.2; figs.

5.1, 5.2 & 5.3). In higher energy areas, around the marine-dominated section of the estuary and close to the main estuary channel, sands tend to be better sorted and have lower fine-grained sediment concentration resulting in cleaner coats (figs. 5.3 & 5.9). Mineralogical changes in sediment composition of the coats are also related to position in the estuary with areas close to the marine-dominated parts of the estuary containing more carbonate minerals in the fine fraction (fig. 5.11). In lower energy areas close to the fluvially-dominated end of the estuary and the upper tidal limit, clay mineral concentrations are generally higher (fig. 5.11). The coats are composed of poorly sorted mixtures of clay minerals, pyrite, lithic grains and bioclastic debris (figs. 5.4-5.8). Although average coat coverage varies between samples, the components of the coat remained the same. Variations in the mineralogy of the fine fraction of the coats were measured and show some significant differences in concentrations (fig. 5.11); however this dataset is still incomplete and has not been fully developed.

6.2.3.2 Question ten - What controls the coat coverage on sand grains in modern settings?

Coat coverage is controlled by the overall fine-grained sediment concentration within sands (section 5.6.2). This is evidenced by the strong relationships between average coat coverage percentage and fine-grained sediment concentration, sorting and skewness (fig.

5.9). This fine-grained sediment concentration appears to be related to depositional environment with lower energy areas having higher fine-grained sediment concentration and average coat coverage, while higher energy areas had a lower fine-grained sediment concentration and lower average coat coverage.

Other processes which may have coated sand grains in fine-grained sediment that was deposited at the surface (section 5.6.4) include mechanical infiltration/clay illuviation of fine grained material into sands (Buurman et al., 1998; Moraes and De Ros, 1990; Kuhn et al., 2010), possibly controlled by tidal processes (Horn, 2006; Santos et al., 2012), and the bioturbation of sediment which may result in coats adhering to sand grains (McIlroy et al., 2003; Needham et al., 2005; Worden et al., 2006). These processes have been observed to coat grain sand grains elsewhere and are likely to be occurring within the Spanish case study also.

6.2.3.3 Question eleven - How do modern grain-coatings relate to subsurface coated sand grains in petroleum reservoirs?

Grain-coats observed in this study appear different to those in ancient reservoirs (section 5.6.4). This observation is most likely to be a result of burial diagenesis resulting in the dissolution of grain-coat components and subsequent precipitation as other neoformed mineral cements, plus the alteration of clay minerals.

It may be possible to predict mineral grain-coating occurrence in estuarine sediments on the basis of this research. Initial coat coverage is highest closest to the estuary margins, where fine-grained sediment is concentrated. If the grain-coating observed in the Anllóns estuary is a precursor to ancient grain-coatings then these lower energy areas may be more likely to have better reservoir quality if chlorite-coats occur in an exploration area, or may have poor reservoir quality if kaolinite or illite occurs within the basin.

### **6.3 Further Work**

During this research a number of other research questions and ideas became apparent. These ideas are presented below and represent opportunities to expand on the research reported here and to further develop the research into related areas.

#### **6.3.1 Chlorite coat literature review**

##### 6.3.1.1 Further work on reservoir examples

Data quality issues from the published examples relating to depositional settings, environments and sedimentary facies as well as the effect chlorite-coats have on porosity are major obstacles in ensuring the accuracy of this work. Detailed comparison of sedimentary facies, grain size, composition, texture and the mineralogy and chemistry of chlorite cements in reservoir and non-reservoir examples would overcome many of these issues. A detailed study utilising slabbed cores, core plug measurements and detailed

analysis of thin sections of a selected subset of the examples in this study could provide useful information on chlorite genesis and development. Proprietary issues mean that collating these samples and collecting the data could be problematic.

#### 6.3.1.2 Meta-studies of other cement types and textures:

The results of the present study on chlorite-coated sandstones, indicates some common factors in chlorite development. Latitude of deposition, depositional environment and age all seem to factor in chlorite-coat formation. An assessment of other clay mineral cement types such as illite or kaolinite using the same methods could test if the factors outlined are common to all clay minerals or strictly to chlorite-coat development.

### **6.3.2 Estuarine surface sediment analysis**

#### 6.3.2.1 Further, more detailed, high density surface studies

A comparison of the research presented here to other estuaries and coastal settings would further improve the work. Although there may be similar controls on the distribution of clay minerals in both estuaries, studies of other estuarine types with different morphologies could show different relationships to those discussed above. Furthermore, studies of other coastal systems, for example deltas (common reservoir sandstone depositional settings), which have different physical and geochemical characteristics may provide further insight in to predicting clay mineral cement occurrences.

Sampling style and techniques could also be further improved. Sampling the sub-aqueous channel sections of estuaries and offshore areas would improve the spatial and environmental distribution of the dataset. Higher density studies would possibly highlight systematic local scale variations which appeared to occur in some locations of both estuaries. A more detailed and longer term worm cast density survey would also improve the quality of the data, with a larger scale study a higher degree of confidence could be given to the subtle changes in mineralogy, which were noted in worm cast sediments from Iceland.

Elemental and structural analyses of clay minerals could also be used to confirm if the subtle changes in inter-layer filling of 2:1 layer clay minerals interpreted in the Icelandic worm cast and riverbank soil sediments were occurring. Issues with separating the individual clay minerals within a sample may prove difficult, but a combination of transmission electron microscopy (TEM) and X-ray fluorescence (XRF) may enable these changes to be distinguished.

#### 6.3.2.2 Experimental studies

A lack of detailed information on the physical characteristics of clay minerals and published information on how clay minerals respond to different physical and chemical conditions in estuarine environments made interpretation of the concentrations of clay minerals that occurred in both estuaries problematic. A detailed study of the

morphology, structure and chemistry of real-world clay minerals occurring in either estuary using TEM or XRF, could enable an improved understanding of how they may behave within dynamic fluids of varying salinities. Furthermore, the postulated controls of turbidity maximum and salinity with respect to some clay minerals needs to be tested and this could be done using flume or tank experiments utilising either real-world clay minerals mixtures or laboratory standards. Different controlled experiments that vary parameters such as salinity, turbidity, shear stress, biological content and clay mineralogy could ascertain the order of deposition of clay minerals under different scenarios.

Further bioturbation experiments could also test whether the interpreted changes to the inter-layer spacing of smectite on bioturbation in Iceland can be repeated in more controlled laboratory conditions. The chlorite to pyrite alteration could also be repeated to test if this change was related to bioturbation, or the reducing conditions beneath the sediment surface. Other experiments on animal-sediment interaction looking at changes in felsic-dominated sediment versus mafic-dominated sediment could be used to quantify the optimum ratio of felsic-to-mafic components required to produce clay minerals within quartzo-feldspathic reservoir sand and on fresh and weathered sediment to see if this is an important factor in producing clay minerals.

### **6.3.3 Core coat coverage**

#### 6.3.3.1 Complete analysis of coat mineralogy

Analysis of the coat mineralogies from the Spain cores was not fully completed. A fuller analysis of the mineralogy in the cores with depth and average coat coverage percentage, will further aid an understanding of the post-depositional distribution of coats and their origin. In addition, the mineralogy of the coarse fraction of samples will also be quantified. Comparison of this data to the fine fraction concentrations of minerals will enable a fuller understanding of the mineralogical interactions of the sediment, and allow the complete mineralogy of a sample to be quantified.

#### 6.3.3.2 Deeper, higher density cores with improved sample preparation

Sediment cores down to tens of metres within an estuary, would greatly improve the temporal context of the study. Cores at this depth may begin to display the effects grain re-ordering and early diagenetic cements, characterisation of these features through time would provide important insights into mineral development and grain-coat formation. It would also allow estuarine development to be related to early estuarine stratigraphic development and post glacial relative sea level rise, allowing subsequent sediments to be placed within a sequence stratigraphic framework. Work on the Leirárvogur Estuary (fig. 6.5, appendix 5) showed that the stratigraphic history of

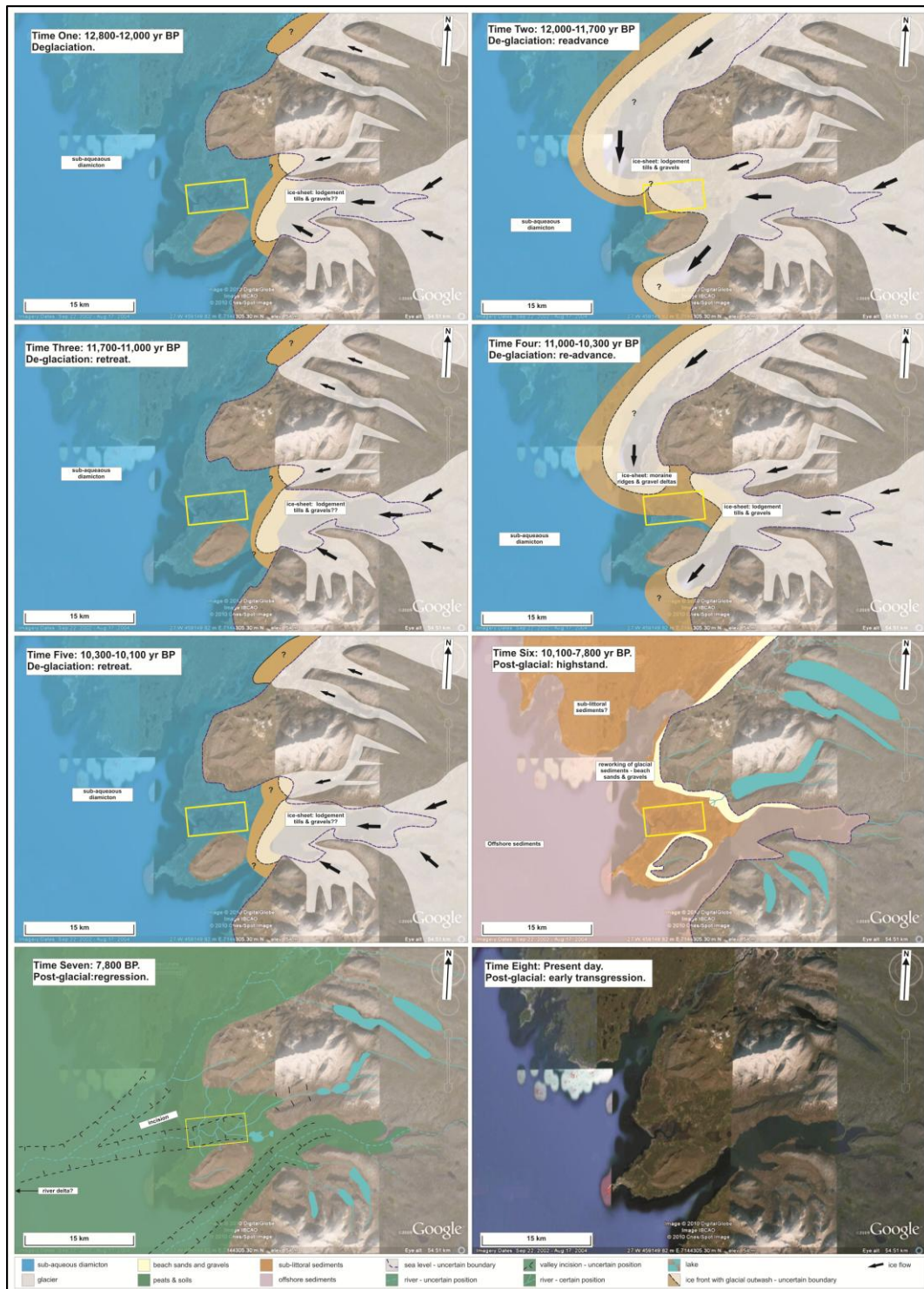


**Figure 6.5 - De-glaciation and post-glaciation of development of the Leirárvogur Estuary.** This work is developed from previous authors work (Ashwell 1975; Ingólfsson 1988; Le Breton et al. 2010) and on the basis of fieldwork and research undertaken by the author. Images from Google Earth. Dates are on the basis of radiocarbon ages from peats in the area (Ingólfsson 1988). Prior to Time one, during the last glacial maximum (20-17 ky BP) the Borgarfjörður region was covered by glaciers that extended up to 100-200 km seaward of the present day coast (Hubbard et al 2006). Between 12.8 and 10.1 ky BP (time steps one to five) the deglaciation of the region proceeded through a series of waning and waxing phases, with glaciers confined to valleys. During this period sea level was up to 60-90m higher than at the present day, and a series of glacially derived diamictons and sub-littoral sediments were deposited over the estuary. Cont'd overpage

**Figure 6.5 (cont'd) - At time six (10.1-7.8 ky BP) a relative highstand resulting resulted in the reworking of of sediments and the development of beach deposits and littoral terraces around 50-70m above present-day sea level (Ingólfsson 1988). Following the highstand at 10.1 ky BP, post-glacial uplift estimated at 120-170m (Le Breton et al. 2010) up until 7.8 ky BP, resulted in a regressive episode. On the basis of present day sounding maps (Icelandic Hydrographic Service 2009), it is likely that sea level could have been up to 30-40 km seaward of its present location. Intervening would have been a shallowly dipping terrestrial plain with soils and peats development (now present beneath the surface of the estuary), incised upstream river profiles are up to four metres below the present glacial sediments also support this interpretation. Between 7.8 ky BP and the present day (time eight) relative sea level has risen again up to 80-130m (10-17 mm/yr since 7.8ky BP) The cause of the transgression has been suggested as further ice loading resulting from the Little Ice Age (Geirsdóttir et al. 2009), rifting processes, or thermal contraction of the crust (Le Breton et al. 2010; Norddahl and Einarsson 2001).**

---

some estuaries can be very complex and need to be fully understood to enable other elements of the research to be placed in the correct context. Higher density core sampling would also further improve the understanding of stratigraphic development and potentially better characterise local variations in mineralogy and coat coverage noted in the study.

Measurement of coat coverage in this study resulted in slight disturbance to the sediment and potentially to grain-coatings. If the sediment within the cores could be set directly from the cores, either using a mounting medium or resin, this would ensure any delicate coat features that may be lost in preparation could be preserved.

#### 6.3.3.3 Measured and experimental assessment of fluid flow in sandy sediments

Clay illuviation or mechanical infiltration has been interpreted as potentially resulting in the formation of grain-coats through the effects of tidal pumping or flooding. To test this hypothesis a simple method

might be to bury flow meters at depth within the sand body and measure the flow velocities and flow direction of marine and fresh waters. At the same time grain size meshes could also be buried within the sediment to collect fine grained sediment as it was transported horizontally or vertically within the sandy sediment.

Fluid flow experiments simulating mechanical infiltration/clay illuviation in clean sands in a glass tank could measure the scale of fine-grained sediment movement through sands. A similar experiment could also test if clay and silt grade sediment is transported from a veneer of poorly sorted fine-grained sediment overlying clean sands, which would simulate the stratigraphy of sedimentary environments in the Anllóns estuary. Another experiment could simulate a turbid flood and ebb tide flowing through clean sands to test if fine-grained sediments are able to work through the sediment.

#### 6.3.3.4 Experimental diagenesis of modern grain-coatings

Another experiment could test how the grain-coats in the Anllóns estuary relate to subsurface ancient grain-coats. A previous experimental study of sandstones from shallow depths with berthierine coatings were able to synthesise chlorite-coats in a hydrothermal bomb (Aagaard et al., 2000). If the modern estuarine grain-coats were heated and pressurised to simulate diagenesis and reservoir conditions in simulated formation waters, it may be possible to create grain-coatings analogous to those in ancient reservoirs. Comparison

of these may give further insight into whether the modern grain-coats are potential precursor coats to ancient examples, and the mineralogy and chemistry of the coats produced could also provide further information about mineral development during diagenesis.

## 7. References

- Aagaard, P., Jahren, J.S., Harstad, A.O., and Nilsen, O., 2000, Formation of grain-coating chlorite in sandstones. Laboratory synthesized vs. natural occurrences: *Clay Minerals*, v. 25, p. 261–269.
- Ahlbrandt, T.S., Carpentier, R.R., Klett, T.R., Schmoker, J.W., Schenk, C.J., and Ulmishek, G.F., 2005, Global Resource Estimates from Total Petroleum Systems: AAPG Memoir, v. 86.
- Ajdukiewicz, J.M., Nicholson, P.H., and Esch, W.L., 2010, Prediction of deep reservoir quality using early diagenetic process models in the Jurassic Norphlet Formation, Gulf of Mexico: *AAPG Bulletin*, v. 94, no. 8, p. 1189–1227.
- AlDahan, A.A., and Morad, S., 1986, Chemistry of detrital biotites and their phyllosillicate intergrowths in sandstones: *Clays and Clay Minerals*, v. 34, no. 5, p. 539–548.
- Algan, O., Clayton, T., Tranter, M., and Collins, M.B., 1994, Estuarine mixing of clay minerals in the Solent region, southern England: *Sedimentary Geology*, v. 92, p. 241–255.
- Allen, J.R.L., 1991, Fine sediment and its sources, Severn Estuary and inner Bristol Channel, southwest Britain: *Sedimentary Geology*, v. 75, p. 57–65.
- Allen, J.R.L., 2000, Morphodynamics of Holocene salt marshes: A review sketch from the Atlantic and Southern North Sea coasts of Europe: *Quaternary Science Reviews*, v. 19, no. 12, p. 1155–1231.
- Allen, G.P., and Posamentier, H.W., 1993, Sequence stratigraphy and facies model of a incised valley; the Gironde Estuary, France: *Journal of Sedimentary Petrology*, v. 63, no. 3, p. 378–391.
- Allen, G.P., Salomon, J.C., Bassoullet, P., Du Penhoat, Y., and De Grandpre, C., 1980, Effects of tides on mixing and suspended sediment transport in macrotidal estuaries: *Sedimentary Petrology*, v. 26, p. 69–90.
- Alonso, A., and Pages, J.L., 2007, Stratigraphy of Late Pleistocene coastal deposits in Northern Spain: *Journal of Iberian Geology*, v. 33, no. 2, p. 207–220.

- Andrews, J.T., and Eberl, D.D., 2007, Quantitative mineralogy of surface sediments on the Iceland shelf, and application to down-core studies of Holocene ice-rafted sediments: *Journal of Sedimentary Research*, v. 77, p. 469–479.
- Anjos, S.M.C., De Ros, L.F., Schiffer de Souza, R., Assis Silva, C.M., and Sombra, C.L., 2000, Depositional and diagenetic controls on the reservoir quality of Lower Cretaceous Penedencia sandstones, Potiguar rift basin, Brazil: *AAPG Bulletin*, v. 84, no. 11, p. 1719–1742.
- Anjos, S.M.C., De Ros, L.F., and Silva, C.M.A., 2003, Chlorite authigenesis and porosity preservation in the Upper Cretaceous marine sandstones of the Santos Basin, offshore eastern Brazil, in Worden, R.H. and Morad, S. eds., *Clay Mineral Cements in Sandstones*, International Association of Sedimentologists, p. 291–316.
- Arnalds, O., 2004, Volcanic soils of Iceland: *Catena*, v. 56, p. 3–20.
- Arribas, J., Alonso, Á., Pagés, J.L., and González-Acebrón, L., 2010, Holocene transgression recorded by sand composition in the mesotidal Galician coastline (NW Spain): *The Holocene*, v. 20, no. 3, p. 375–393, doi: 10.1177/0959683609353429.
- Baas, J.H., Hailwood, E. a., McCaffrey, W.D., Kay, M., and Jones, R., 2007, Directional petrological characterisation of deep-marine sandstones using grain fabric and permeability anisotropy: Methodologies, theory, application and suggestions for integration: *Earth-Science Reviews*, v. 82, no. 1-2, p. 101–142, doi: 10.1016/j.earscirev.2007.02.003.
- Bailey, S.W., 1988, Odinite, a new dioctahedral-trioctahedral Fe<sup>3+</sup>-rich 1:1 clay mineral: *Clay Minerals*, v. 23, p. 237–247.
- Baker, J.C., Havord, P.J., Martin, K.R., and Ghori, K.A.R., 2000, Diagenesis and petrophysics of the Early Permian Moogooloo Sandstone, Southern Carnarvon basin, Western Australia: *AAPG Bulletin*, v. 84, no. 2, p. 250–265.
- Baugh, J. V, and Manning, A.J., 2007, An assessment of a new settling velocity parameterisation for cohesive sediment transport modeling: *Continental Shelf Research*, v. 27, no. 13, p. 1835–1855.
- Bayliss, P., 1975, Nomenclature of trioctahedral chlorites: *Canadian Mineralogist*, v. 13, p. 178–180.

Beckman Coulter Incorporated, 2011, Coulter LS Series - Product Manual:.

Belzunce-Segarra, M.J., Wilson, M.J., Fraser, A.R., Lachowski, E., and Duthie, D.M.L., 2002, Clay mineralogy of Galician coastal and oceanic surface sediments: contributions from terrigenous and authigenic sources: *Clay Minerals*, v. 37, no. 1, p. 23–37, doi: 10.1180/0009855023710015.

Berger, A., Gier, S., and Krois, P., 2009, Porosity-preserving chlorite cements in shallow marine volcanoclastic sandstones: Evidence from Cretaceous sandstones of the Sawan gas field, Pakistan: *AAPG Bulletin*, v. 93, no. 5, p. 595–615.

Bernárdez, P., Prego, R., Giralt, S., Esteve, J., Caetano, M., Parra, S., and Francés, G., 2012, Geochemical and mineralogical characterization of surficial sediments from the Northern Rias: Implications for sediment provenance and impact of the source rocks: *Marine Geology*, v. 291-294, p. 63–72.

Berner, R.A., 1984, Sedimentary pyrite formation: An update: *Geochimica et Cosmochimica Acta*, v. 48, no. 4, p. 605–615, doi: 10.1016/0016-7037(84)90089-9.

Billault, V., Beaufort, D., Barronnet, A., and Lacharpagne, J.-C., 2003, A nanopetrographic and textural study of grain-coating chlorites in sandstone reservoirs: *Clay Minerals*, v. 38, p. 315–328.

Bird, E., 2011, *Coastal Geomorphology: An Introduction*: John Wiley & Sons.

Blackbourn, G.A., and Thomson, M.E., 2000, Britannia Field, UK North Sea: petrographic constraints on Lower Cretaceous provenance, facies and the origin of slurry-flow deposits: *Petroleum Geoscience*, v. 6, no. 4, p. 329–343.

Bland, W., and Rolls, D., 1998, *Weathering: An introduction to the scientific principles*: Arnold, London.

Bloch, S., Lander, R.H., and Bonnell, L., 2002, Anomalously high porosity and permeability in deeply buried sandstone reservoirs: Origin and predictability: *AAPG Bulletin*, v. 86, no. 2, p. 301–328.

Blott, S.J., 2008, *Gradistat V. 7*:.

- Le Breton, E., Dauteuil, O., and Biessy, G., 2010, Post-glacial rebound of Iceland during the Holocene: *Journal of the Geological Society of London*, v. 167, p. 417–432.
- Brown, G., and Newman, A.C.D., 1973, The reactions of soluble aluminium with montmorillonite.: *Journal of Soil Science*, v. 24, no. 3, p. 339–354, doi: 10.1111/j.1365-2389.1973.tb00770.x.
- Burns, L.K., and Ethridge, F.G., 1979, Petrology and diagenetic effects of lithic sandstones: Paleocene and Eocene Umpqua Formation, southwest Oregon (P. A. Scholle & P. R. Schluger, Eds.): *Aspects of Diagenesis*. SEPM Special Publication 26,.
- Buurman, P., Jongmans, A.G., and PiPujol, M.D., 1998, Clay illuviation and mechanical clay infiltration - is there a difference?: *Quaternary International*, v. 51-52, p. 66–69.
- Cairncross, B., Stanistreet, I.G., McCarthy, T.S., Ellery, W.N., Ellery, K., and Grobicki, T.S.A., 1988, Palaeochannels (stone-rolls) in coal seams: Modern analogues from fluvial deposits of the Okavango Delta, Botswana, southern Africa: *Sedimentary Geology*, v. 57, no. 1-2, p. 107–118, doi: 10.1016/0037-0738(88)90020-6.
- Calvo, R.M., Garcia-Rodeja, E., and Macias, F., 1983, Mineralogical variability in weathering microsystems of a granitic outcrop of Galicia (Spain): *Catena*, v. 10, no. 3, p. 225–236, doi: 10.1016/0341-8162(83)90033-4.
- Chamley, H., 1989, *Clay Sedimentology*: Springer-Verlag.
- Chang, H.K., Mackenzie, F.T., and Schoonmaker, J., 1986, Comparisons between the diagenesis of dioctahedral and trioctahedral smectite, Brazilian offshore basins: *Clays and Clay Minerals*, v. 34, no. 4, p. 407–423.
- Cooper, J.A.G., 1993, Sedimentation in a river dominated estuary: *Sedimentology*, v. 40, p. 979–1017.
- Cressie, N.A.C., 1990, The Origins of Kriging: *Mathematical Geology*, v. 22, p. 239–252.
- Crump, B.C., Baross, J.A., and Simenstad, C.A., 1998, Dominance of particle-attached bacteria in the Columbia River estuary, USA: *Aquatic Microbial Ecology*, v. 14, no. 1, p. 7–18.

- Cummings, D.I., Kjarsgaard, B. a., Russell, H. a. J., and Sharpe, D.R., 2011, Eskers as mineral exploration tools: *Earth-Science Reviews*, v. 109, no. 1-2, p. 32–43, doi: 10.1016/j.earscirev.2011.08.001.
- Dallmeyer, R.D., Catalán, J.R.M., Arenas, R., Gil Ibarguchi, J.I., Gutiérrez, Alonso, G., Farias, P., Bastida, F., and Aller, J., 1997, Diachronous Variscan tectonothermal activity in the NW Iberian Massif: Evidence from <sup>40</sup>Ar/<sup>39</sup>Ar dating of regional fabrics: *Tectonophysics*, v. 277, no. 4, p. 307–337, doi: 10.1016/s0040-1951(97)00035-8.
- Dalrymple, R.W., Zaitlin, B.A., and Boyd, R., 1992, Estuarine facies models: conceptual basis and stratigraphic implications: *Journal of Sedimentary Petrology*, v. 62, no. 6, p. 1130–1146.
- Dapples, E.C., 1967, Diagenesis in sandstones, in Larsen, G. and Chilingar, G. V eds., *Diagenesis in sediments (Developments in Sedimentology 8)*,.
- Davies, N.S., and Gibling, M.R., 2010, Cambrian to Devonian evolution of alluvial systems: The sedimentological impact of the earliest land plants: *Earth-Science Reviews*, v. 98, no. 3-4, p. 171–200, doi: 10.1016/j.earscirev.2009.11.002.
- Deer, W.A., Howie, R.A., and Zussman, J., 1992, *An Introduction to the Rock-Forming Minerals*: Longman.
- Devesa-Rey, R., Paradelo, R., Díaz-Fierros, F., and Barral, M.T., 2008, Fractionation and bioavailability of arsenic in the bed sediments of the Anllóns River (NW Spain): *Water Air and Soil Pollution*, v. 195, p. 189–199.
- Dixon, S.A., Summers, D.M., and Surdham, R.C., 1989, Diagenesis and preservation of porosity in Norphlet Formation (Upper Jurassic), Southern Alabama: *AAPG Bulletin*, v. 73, no. 6, p. 707–728.
- Douglas, G.R., 1987, Manganese-rich rock coatings from Iceland: *Earth Surface Processes and Landforms*, v. 12, no. 3, p. 301–310, doi: 10.1002/esp.3290120308.
- Dowey, P.J., Hodgson, D.M., and Worden, R.H., 2012, Pre-requisites, processes, and prediction of chlorite grain coatings in petroleum reservoirs: A review of subsurface examples: *Marine and Petroleum Geology*, v. 32, no. 1, p. 63–75, doi: 10.1016/j.marpetgeo.2011.11.007.

- Duffin, M.E., Lee, M., De Vries Klein, G., and Hay, R.L., 1989, Potassic diagenesis of Cambrian sandstones and Precambrian granitic basement in UPH-3 deep hole, upper Mississippi Valley, U.S.A.: *Journal of Sedimentary Petrology*, v. 59, no. 5, p. 848–861.
- Dunn, T.L., 1992, Infiltrated materials in Cretaceous volcanogenic sandstones, San Jorge Basin, Argentina, *in* Houseknecht, D.W. and Pittman, E.D. eds., *Origin, diagenesis, and petrophysics of clay minerals in sandstones*, SEPM (Society for Petroleum Geology), Tulsa, Oklahoma, p. 159–174.
- Dutton, S.P., Loucks, R.G., and Day-Stirrat, R.J., 2012, Impact of regional variation in detrital mineral composition on reservoir quality in deep to ultradeep lower Miocene sandstones, western Gulf of Mexico: *Marine and Petroleum Geology*, v. 35, no. 1, p. 139–153, doi: 10.1016/j.marpetgeo.2012.01.006.
- Eckert, J.M., and Sholkovitz, E.R., 1976, The Flocculation of iron, aluminium and humates from river water by electrolytes: *Geochimica et Cosmochimica Acta*, v. 40, p. 147–148.
- Edwards, A.C., 2001, Grain size and sorting in modern beach sands: *Journal of Coastal Research*, v. 17, no. 1, p. 38–52.
- Edzwald, J.K., and O'Mella, C.R., 1975, Clay distributions in recent estuarine sediments: *Clays and Clay Minerals*, v. 23, p. 39–44.
- Egerton, R.F., 2005, *Physical Principles of Electron Microscopy: An Introduction to TEM, SEM, and AEM*: Springer.
- Eggleton, R.A., 1975, Nontronite topotaxial after hedenbergite: *American Mineralogist*, v. 60, p. 1063–1068.
- Eggleton, R.A., Foudoulis, C., and Varkevisser, D., 1987, Weathering of basalt: Changes in rock chemistry and mineralogy: *Clay and Clay Minerals*, v. 35, no. 3, p. 161–169.
- Ehrenberg, S.N., 1993, Preservation of anomalously high porosity in deeply buried sandstones by grain-coating chlorite; Examples from Norwegian Continental Shelf: *AAPG Bulletin*, v. 77, no. 7, p. 1260–1286.
- Eisma, D., 1986, Flocculation and de-flocculation of suspended matter in estuaries: *Netherlands Journal of Sea Research*, v. 20, no. 2, p. 183–199.

- Esterle, J.S., and Ferm, J.C., 1994, Spatial variability in modern tropical peat deposits from Sarawak, Malaysia and Sumatra, Indonesia: analogues for coal: *International Journal of Coal Geology*, v. 26, no. 1-2, p. 1–41, doi: 10.1016/0166-5162(94)90030-2.
- Eyles, N., and Kocsis, S., 1988, Sedimentology and clast fabric of subaerial debris flow facies in a glacially-influenced alluvial fan: *Sedimentary Geology*, v. 59, p. 15–28.
- Fagel, N., Robert, C., and Hillaire-Marcel, C., 1996, Clay mineral signature of the NW Atlantic Boundary Undercurrent: *Marine Geology*, v. 130, no. 1–2, p. 19–28, doi: 10.1016/0025-3227(95)00134-4.
- Fagel, N., Robert, C., Preda, M., and Thorez, J., 2001, Smectite composition as a tracer of deep circulation: the case of the Northern North Atlantic: *Marine Geology*, v. 172, no. 3-4, p. 309–330, doi: 10.1016/s0025-3227(00)00123-7.
- Farmer, V.C., 1974, *The Infrared Spectra of Minerals: Mineralogical Society Monograph 4*,.
- Fernandez Sanjurjo, M.J., Corti, G., and Ugolini, F.C., 2001, Chemical and mineralogical changes in a polygenetic soil of Galicia, NW Spain: *Catena*, v. 43, p. 251–265.
- Fernández-Caliani, J.C., Galán, E., Aparicio, P., Miras, A., and Márquez, M.G., 2010, Origin and geochemical evolution of the Nuevo Montecastelo kaolin deposit (Galicia, NW Spain): *Applied Clay Science*, v. 49, no. 3, p. 91–97, doi: 10.1016/j.clay.2010.06.006.
- Feuillet, J.-P., and Fleischer, P., 1980, Estuarine circulation; controlling factor of clay mineral distribution in James River Estuary, Virginia: *Journal of Sedimentary Petrology*, v. 50, no. 1, p. 267–279.
- Foix, N., Allard, J.O., Paredes, J.M., and Giacosa, R.E., 2012, Fluvial styles, palaeohydrology and modern analogues of an exhumed, Cretaceous fluvial system: Cerro Barcino Formation, Cañadón Asfalto Basin, Argentina: *Cretaceous Research*, v. 34, p. 298–307, doi: 10.1016/j.cretres.2011.11.010.
- Foley, S.F., Venturelli, G., Green, D.H., and Toscani, L., 1987, The ultrapotassic rocks: Characteristics, classification, and constraints for petrogenetic models: *Earth-Science Reviews*, v. 24, no. 2, p. 81–134, doi: 10.1016/0012-8252(87)90001-8.

- Folk, R.L., and Ward, W.C., 1957, Brazos river bar. A study in the significance of grain size parameters: *Journal of Sedimentary Petrology*, v. 27, no. 1, p. 3–26.
- Folkestad, A., Veselovsky, Z., and Roberts, P., 2012, Utilising borehole image logs to interpret delta to estuarine system: A case study of the subsurface Lower Jurassic Cook Formation in the Norwegian northern North Sea: *Marine and Petroleum Geology*, , no. 0, doi: 10.1016/j.marpetgeo.2011.07.008.
- Foster, M.D., 1962, Interpretation of the composition and a classification of the chlorites: Shorter contributions to General Geology, United State Geological Survey Professional paper, v. 314-A, p. 31.
- Fox, J.M., Hill, P.S., Milligan, T.G., and Boldrin, A., 2004, Flocculation and sedimentation on the Po River Delta: *Marine Geology*, v. 203, no. 1-2, p. 95–107.
- French, J.R., 1993, Numerical simulation of vertical marsh growth and adjustment to accelerated sea level rise, North Norfolk, UK: *Earth Surface Processes and Landforms*, v. 18, no. 1, p. 63–81, doi: 10.1002/esp.3290180105.
- Gallenne, B., 1974, Study of fine material in suspension in the estuary of the Loire and its dynamic grading: *Estuarine and Coastal Marine Science*, v. 2, no. 3, p. 261–272, doi: 10.1016/0302-3524(74)90016-4.
- Galler, J.J., and Allison, M.A., 2008, Estuarine controls on fine-grained sediment storage in the Lower Mississippi and Atchafalaya Rivers: *Bulletin of the Geological Society of America*, v. 120, no. 3-4, p. 386–398.
- Gaupp, R., Matter, A., Platt, J., Ramseyer, K., and Walzebeck, J., 1993, Diagenesis and fluid evolution of deeply buried Permian (Rotliegende) gas reservoirs, northwest Germany: *AAPG Bulletin*, v. 77, p. 1111–1128.
- Geçer Büyüktüku, A., and Suat Bağcı, A., 2005, Clay controls on reservoir properties in sandstone of Kuzgun formation and its relevance to hydrocarbon exploration, Adana basin, Southern Turkey: *Journal of Petroleum Science and Engineering*, v. 47, no. 3-4, p. 123–135, doi: 10.1016/j.petrol.2005.03.003.
- Gehrke, B., Lackschewitz, K.S., and Wallrabe-Adams, H.-J., 1996, Late Quaternary sedimentation on the Mid-Atlantic Reykjanes Ridge:

Clay mineral assemblages and depositional environment:  
*Geologische Rundschau*, v. 85, p. 525–535.

Geirsdóttir, Á., Miller, G.H., Axford, Y., and Ólafsdóttir, S., 2009, Holocene and latest Pleistocene climate and glacier fluctuations in Iceland: *Quaternary Science Reviews*, v. 28, p. 2107–2118.

Geyer, W., 1993, The importance of suppression of turbulence by stratification on the estuarine turbidity maximum: *Estuaries and Coasts*, v. 16, no. 1, p. 113–125, doi: 10.2307/1352769.

Gibbs, R.J., 1983, Coagulation rates of clay minerals and natural sediments: *Journal of Sedimentary Petrology*, v. 53, no. 4, p. 1193–1203.

Gibbs, R.J., 1985, Settling velocity, diameter and density for flocs of illite, kaolinite and montmorillonite: *Journal of Sedimentary Petrology*, v. 55, no. 1, p. 65–68.

Gibbs, R.J., 1967, The geochemistry of the Amazon River system: Part I. The factors that control the salinity and the composition and concentration of the suspended solids.: *Geological Society of America Bulletin*, v. 78, p. 1203–1232.

Gil Ibarra, J.I., and Ortega Gironés, E., 1985, Petrology, structure and geotectonic implications of glaucophane-bearing eclogites and related rocks from the Malpica—Tuy (MT) Unit, Galicia, northwest Spain: *Chemical Geology*, v. 50, no. 1-3, p. 145–162, doi: 10.1016/0009-2541(85)90117-2.

Girard, J.-P., and Barnes, D.A., 1995, Illitization and paleothermal regimes in the Middle Ordovician St. Peter sandstone, Central Michigan Basin: K-Ar, oxygen isotope, and fluid inclusion data: *AAPG Bulletin*, v. 79, no. 1, p. 49–89.

Gíslason, S.R., Arnórsson, S., and Ármannsson, H., 1996, Chemical weathering of basalt in southwest Iceland: effects of runoff age of rocks and vegetative/glacial cover: *American Journal of Science*, v. 296, p. 837–907.

Glennie, K.W., Mudd, G.C., and Nagtegaal, P.J.C., 1978, Depositional environment and diagenesis of Permian Rotliegendes sandstones in Leman Bank and Sole Pit areas of the UK southern North Sea: *Journal of the Geological Society of London*, v. 135, p. 25–34.

Golden Software, 2012, Surfer 7: v. 2012, no. 20th April 2012.

- Goldstein, J., Newbury, D.E., Joy, D.C., Lyman, C.E., Echlin, P., Lifshin, E., Sawyer, L.C., and Michael, J.R., 2007, *Scanning Electron Microscopy and X-ray Microanalysis*: Springer.
- Google, 2010, Aerial map of Iceland:.
- Griffin, G.M., 1962, Regional clay-mineral facies - Products of weathering intensity and current distribution on the northeastern Gulf of Mexico: *Geological Society of America Bulletin*, v. 73, p. 737–768.
- Grim, R.E., 1962, *Applied Clay Mineralogy*: McGraw-Hill, New York.
- Van Groos, A.F.K., and Guggenheim, S., 1986, Dehydration of K-exchanged montmorillonite at elevated temperatures and pressures: *Clays and Clay Minerals*, v. 34, no. 3, p. 281–286.
- Guggenheim, S., Bain, D.C., Bergaya, F., Brigatti, M.F., Drits, V.A., Eberl, D.D., Formoso, M.L.L., Galan, E., Merriman, R.J., Peacor, D.R., Stanjek, H., and Watanabe, T., 2002, Report of the Association Internationale pour l'Etude des Argiles (AIPEA) Nomenclature Committee for 2001: Order, disorder and crystallinity in phyllosilicates and the use of the "Crystallinity Index": *Clay Minerals*, v. 37, no. 2, p. 389–393, doi: 10.1180/0009855023720043.
- Habicht, J.K.A., 1979, Paleoclimate, Paleomagnetism, and Continental Drift: *AAPG Studies in Geology*, v. 9.
- Harward, M.E., and Brindley, G.W., 1965, Swelling properties of synthetic smectite in relation to lattice substitutions: *Clays and Clay Minerals*, v. 13, p. 209–222.
- Hathon, L.A., and Houseknecht, D.W., 1992, Origin and diagenesis of clay minerals in the Oligocenen Sespe Formation, Ventura Basin, in Houseknecht, D.W. and Pittman, E.D. eds., *Origin, diagenesis, and petrophysics of clay minerals in sandstones.*, SEPM (Society for Petroleum Geology), Tulsa, Oklahoma, p. 185–195.
- Hayward, A.B., 1985, Coastal alluvial fans (fan deltas) of the Gulf of Aqaba (Gulf of Eilat), Red Sea: *Sedimentary Geology*, v. 43, p. 241–260.
- Hillier, S., 1994, Pore-lining chlorites in siliclastic reservoir sandstones; electron microprobe, SEM and XRD data, and implications for their origin: *Clay Minerals*, v. 29, p. 665–679.

- Hillier, S., Fallick, A.E., and Matter, A., 1996, Origin of pore-lining chlorite in the aeolian Rotliegend of northern Germany: *Clay Minerals*, v. 31, p. 153–171.
- Hinckley, D.N., 1963, Variability in “crystallinity” values among the kaolin deposits of the coastal plane of Georgia and South Carolina: *Clays and Clay Minerals*, v. 11.
- Hirst, D.M., 1962, The geochemistry of modern sediments from the Gulf of Paria—I The relationship between the mineralogy and the distribution of major elements: *Geochimica et Cosmochimica Acta*, v. 26, no. 2, p. 309–334, doi: 10.1016/0016-7037(62)90017-0.
- Holdsworth, R.E., Woodcock, N.H., and Strachan, R.A., 2000, Geological Framework of Britain and Ireland, *in* Woodcock, N.H. and Strachan, R.A. eds., *Geological History of Britain and Ireland*, Blackwell Publishing.
- Horn, D.P., 2006, Measurements and modelling of beach groundwater flow in the swash-zone: a review: *Continental Shelf Research*, v. 26, no. 5, p. 622–652, doi: 10.1016/j.csr.2006.02.001.
- Hornibrook, E.R.C., and Longstaffe, F.J., 1996, Berthierine from the Lower Cretaceous Clearwater Formation, Alberta, Canada: *Clays and Clay Minerals*, v. 44, no. 1, p. 1–21.
- Van Houten, F.B., and Bhattacharyya, D.P., 1982, Phanerozoic oolitic ironstones--Geologic record and facies model: *Annual Review of Earth and Planetary Sciences*, v. 10, no. 1, p. 441–457, doi: doi:10.1146/annurev.ea.10.050182.002301.
- Hover, V.C., Walter, L.M., and Peacor, D.R., 2002, K Uptake by Modern Estuarine Sediments During Early Marine Diagenesis, Mississippi Delta Plain, Louisiana, U.S.A: *Journal of Sedimentary Research*, v. 72, no. 6, p. 775–792, doi: 10.1306/032502720775.
- Hubbard, A., Sugden, D., Dugmore, A., Norddahl, H., and Pétursson, G., 2006, A modelling insight into the Icelandic Last Glacial Maximum ice sheet: *Quaternary Science Reviews*, v. 25, p. 2283–2296.
- Humphreys, B., Smith, S.A., and Strong, G.E., 1989, Authigenic chlorite in Late Triassic sandstones from the Central Graben, North Sea: *Clay Minerals*, v. 24, p. 427–444.

- Hurst, A., Scott, A., and Vigorito, M., 2011, Physical characteristics of sand injectites: *Earth-Science Reviews*, v. 106, no. 3-4, p. 215–246, doi: 10.1016/j.earscirev.2011.02.004.
- Imam, M.B., and Shaw, H.F., 1987, Diagenetic controls on the reservoir properties of gas bearing Neogene Surma Group sandstones in the Bengal Basin, Bangladesh: *Marine and Petroleum Geology*, v. 4, p. 103–111.
- Ingólfsson, Ó., 1988, Glacial history of the Bogarfjörður area, western Iceland: *Geologiska Föreningens i Stokholm Förhandlingar*, v. 110, no. 4, p. 293–309.
- Islam, M.A., 2009, Diagenesis and reservoir quality of Bhuvan sandstones (Neogene), Titas Gas Field, Bengal Basin, Bangladesh: *Journal of Asian Earth Sciences*, v. 35, no. 1, p. 89–100, doi: 10.1016/j.jseaes.2009.01.006.
- Jackson, M.L.R., 1969, *Soil Chemical Analysis-Advanced Course*: Madison, Wis.
- Jahn, F., Cook, M., and Graham, M., 2008, *Hydrocarbon Exploration and Production Developments in Petroleum Science*: Elsevier.
- Jahren, J.S., and Aagaard, P., 1989, Compositional variations in diagenetic chlorites and illites, and relationship with formation water chemistry: *Clay Minerals*, v. 24, p. 157–170.
- Jenkins, R., and De Vries, J.L., 1996, *An introduction to x-ray powder diffractometry*: Wiley-Interscience.
- Jóhannesson, H., and Sæmundsson, K., 1999, *Geologic Map of Iceland. 1:500 000. Bedrock Geology*..
- Jónasson, K., 2007, Silicic volcanism in Iceland: Composition and distribution within the active volcanic zones: *Journal of Geodynamics*, v. 43, p. 101–117.
- Journel, A.G., 1989, Fundamentals of Geostatistics in Five Lessons, *in* Crawford, M.L. and Padovani, E. eds., *Shortcourse in Geology*, Washington D.C., American Geophysical Union.
- Kaiser, K., Eusterhues, K., Rumpel, C., Guggenberger, G., and Kögel-Knabner, I., 2002, Stabilization of organic matter by soil minerals - investigations of density and particle-size fractions from two acid forest soils: *Journal of Plant Nutrition and Soil Science*, v. 165, p. 451–459.

- Kantorowicz, J.D., 1990, The influence of variations in illite morphology on the permeability of M. Jurassic Brent Group, Cormorant Field, UK North Sea: *Marine & Petroleum Geology*, v. 7, p. 66–74.
- Karim, A., Pe-Piper, G., and Piper, D.J.W., 2010, Controls on diagenesis of Lower Cretaceous reservoir sandstones in the western Sable Subbasin, offshore Nova Scotia: *Sedimentary Geology*, v. 224, p. 65–83.
- Kemp, R.A., Mcdaniel, P.A., and Busacca, A.J., 1998, Genesis and relationship of macromorphology and micromorphology to contemporary hydrological conditions of a welded Argixeroll from the Palouse in Idaho: *Geoderma*, v. 83, no. 1 998, p. 309–329.
- Ketzer, J.M., Morad, S., and Amorosi, A., 2003, Predictive diagenetic clay-mineral distribution in siliciclastic rocks within a sequence stratigraphic framework, *in* Worden, R.H. and Morad, S. eds., *Clay Mineral Cements in Sandstones*. , Special Publication number 34 of the International Association of Sedimentologists, , p. 43–61.
- King, G.E., 1992, Formation clays: Are they really a problem in production?, *in* *Origin, diagenesis and petrophysics of clay minerals in sandstones: SEPM Special Publication 47*, p. 265–272.
- Kitazawa, T., 2007, Pleistocene macrotidal tide-dominated estuary–delta succession, along the Dong Nai River, southern Vietnam: *Sedimentary Geology*, v. 194, no. 1-2, p. 115–140, doi: 10.1016/j.sedgeo.2006.05.016.
- Kloprogge, J.T., Jansen, J.B.H., Schuiling, R.D., and Geus, J.W., 1992, The interlayer collapse during dehydration of synthetic Na0.7-beidellite: A <sup>23</sup>Na solid state Magic-Angle spinning NMR study: *Clays and Clay Minerals*, v. 40, no. 5, p. 561–566.
- Klug, H.P., and Alexander, L.E., 1974, *X-Ray Diffraction Procedures*: Wiley, New York.
- Krauskopf, K.B., and Bird, D.K., 1995, *Introduction to geochemistry*: McGraw-Hill.
- Kristmannsdottir, H., 1979, Alteration of Basaltic Rocks by Hydrothermal-Activity at 100-300°C, *in* Mortland, M.M. and Farmer, V.C. eds., *Developments in Sedimentology*, Elsevier, p. 359–367.
- Kugler, R.L., and McHugh, A., 1990, Regional diagenetic variation in Norphlet Sandstone: Implications for reservoir quality and the

origin of porosity: *Transactions of the Gulf Coast Association of Geological Societies*, v. 40, p. 411–423.

Kuhn, P., Aguilar, J., and Miedema, R., 2010, Textural Pedofeatures and Related Horizons, in Stoops, G., Marcelino, V., and Mees, F. eds., *Interpretation of Micromorphological Features of Soils and Regoliths*, Elsevier B.V., p. 217–250.

Lackschewitz, K.S., and Wallrabe-Adams, H.-J., 1991, Composition and origin of sediments on the mid-oceanic Kolbeinsey Ridge, north of Iceland: *Marine Geology*, v. 101, p. 71–82.

Lander, R.H., Larese, R.E., and Bonnell, L.M., 2008, Toward more accurate quartz cement models; The importance of euhedral versus noneuhedral growth rates.: *AAPG Bulletin*, v. 92, no. 11, p. 1537–1563.

Lander, R.H., and Walderhaug, O., 1999, Predicting Porosity through Simulating Sandstone Compaction and Quartz Cementation: *AAPG Bulletin*, v. B3, no. 3, p. 433–449.

Van der Lee, W.T.B., 2000, Temporal variation of floc size and settling velocity in the Dollard estuary: *Continental Shelf Research*, v. 20, no. 12-13, p. 1495–1511.

Ligthelm, D.J., De Boer, R.B., Brint, J.F., and Schulte, W.M., 1991, Reservoir Souring: An Analytical Model for H<sub>2</sub>S Generation and Transportation in an Oil Reservoir Owing to Bacterial Activity, in *Society of Petroleum Engineers*.

Llana-Fúnez, S., and Marcos, A., 2001, The Malpica–Lamego Line: a major crustal-scale shear zone in the Variscan belt of Iberia: *Journal of Structural Geology*, v. 23, no. 6-7, p. 1015–1030, doi: 10.1016/S0191-8141(00)00173-5.

Louvat, P., Gíslason, S.R., and Allègre, C.J., 2008, Chemical and mechanical erosion rates in Iceland as deduced from river dissolved and solid material: *American Journal of Science*, v. 308, p. 679–726.

Ltd., V.W., 2012, Van Walt Window Sampling Factsheet: , p. 1.

Luo, J.L., Morad, S., Salem, A., Ketzer, J.M., Lei, X.L., Guo, D.Y., and Hlal, O., 2009, Impact of diagenesis on reservoir-quality evolution in fluvial and lacustrine-deltaic sandstones: evidence from Jurassic and Triassic sandstones from the Ordos Basin China: *Journal of*

Petroleum Geology, v. 32, no. 1, p. 79–102, doi: 10.1111/j.1747-5457.2009.00436.x.

Macias Vazquez, F., 1981, Formation of gibbsite in soils and saprolites of temperate-humid zones: *Clay Minerals*, v. 16, p. 43–52.

MacQuarrie, K.T.B., and Mayer, K.U., 2005, Reactive transport modeling in fractured rock: A state-of-the-science review: *Earth-Science Reviews*, v. 72, no. 3-4, p. 189–227, doi: 10.1016/j.earscirev.2005.07.003.

Madejova, J., 2003, FTIR techniques in clay mineral studies: *Vibration Spectroscopy*, v. 31, p. 1–10.

Manning, A.J., Bass, S.J., and Dyer, K.R., 2006, Floc properties in the turbidity maximum of a mesotidal estuary during neap and spring tidal conditions: *Marine Geology*, v. 235, p. 198–211.

Markusson, S.H., and Stefánsson, A., 2011, Geothermal surface alteration of basalts, Krysuvik Iceland - Alteration mineralogy, water chemistry and the effects of acid supply on the alteration process: *Journal of Volcanology and Geothermal Research*, v. 206, p. 46–59.

Martin, K.R., Baker, J.C., Hamilton, P.J., and Thrasher, G.P., 1994, Diagenesis and reservoir quality of Palaeocene sandstones in the Kupe South Field, Taranaki Basin, New Zealand: *AAPG Bulletin*, v. 78, no. 4, p. 624–643.

Matlack, K.S., Housenknecht, D.W., and Applin, K.R., 1989, Emplacement of clay into sand by infiltration: *Journal of Sedimentary Petrology*, v. 59, no. 1, p. 77–87.

Matsunaga, K., Igarashi, K., Fukase, S., and Tsubota, H., 1984, Behavior of Organically-bound Iron in Seawater of Estuaries: *Estuarine, Coastal and Shelf Science*, v. 18, p. 615–622.

Mattsson, H.B., and Oskarsson, N., 2005, Petrogenesis of alkaline basalts at the tip of a propagating rift: Evidence from the Heimaey volcanic centre, south Iceland: *Journal of Volcanology and Geothermal Research*, v. 147, p. 245–267.

McIlroy, D., Worden, R.H., and Needham, S.J., 2003, Faeces, clay minerals and reservoir potential: *Journal of the Geological Society of London*, v. 160, p. 489–493.

- McKeague, J.A., Miles, N.M., Peters, T.W., and Hoffman, D.W., 1971, A comparison of luvisolic soils from three regions in Canada: *Catena*, v. 7, no. 1-2, p. 46–69.
- Meade, R.H., 1972, Transport and deposition of sediments in estuaries: *The Geological Society of America*, v. 133, p. 91–120.
- Mens, K., and Pirrus, E., 1986, Stratigraphical characteristics and development of Vendian-Cambrian boundary beds of the East European Platform: *Geological Magazine*, v. 123, no. 4, p. 357–360.
- Menzies, J., 2002, *Modern and Past Glacial Environments*: Butterworth-Heinemann.
- Meunier, A., 2005, Crystal Structure – Species – Crystallisation, *in Clays*, p. 470.
- Meunier, A., 2007, Soil hydroxide-interlayered minerals: A re-interpretation of their crystallochemical properties: *Clays and Clay Minerals*, v. 55, no. 4, p. 380–388.
- Michalopoulos, P., and Aller, R.C., 2004, Early diagenesis of biogenic silica in the Amazon delta: alteration, authigenic clay formation, and storage: *Geochimica et Cosmochimica Acta*, v. 68, no. 5, p. 1061–1085, doi: 10.1016/j.gca.2003.07.018.
- Michalopoulos, P., and Aller, R.C., 1995, Rapid Clay Mineral Formation in Amazon Delta Sediments; Reverse Weathering and Oceanic Elemental Cycles: *Science*, v. 270, no. 614-617.
- Michalopoulos, P., Aller, R.C., and Reeder, R.J., 2000, Conversion of diatoms to clays during early diagenesis in tropical, continental shelf muds: *Geology*, v. 28, no. 12, p. 1095–1098, doi: 10.1130/0091-7613(2000)28<1095:codtcd>2.0.co;2.
- Miedema, R., Koulechova, I., and Gerasimova, M., 1999, Soil formation in Greyzems in Moscow district: micromorphology, chemistry, clay mineralogy and particle size distribution: *Catena*, v. 34, no. 3-4, p. 315–347, doi: 10.1016/S0341-8162(98)00105-2.
- Millot, G., 1964, *Géologie des argiles*: Masson.
- Mitchell, J.K., and Soga, K., 2005, Soil Mineralogy 3.1, *in Fundamentals of Soil Behavior* (3rd Edition), John Wiley & Sons, p. 35–82.

- Moore, D.M., and Reynolds, R.C., 1997, *X-Ray Diffraction and the Identification and Analysis of Clay Minerals*: Oxford University Press, New York .
- Morad, S., Al-Ramadan, K.A., Ketzer, J.M., and De Ros, L.F., 2010, The impact of diagenesis on heterogeneity of sandstone reservoirs: A review of depositional facies and sequence stratigraphy: *AAPG Bulletin*, v. 94, no. 8, p. 1267–1309.
- Morad, S., Ketzer, J.M., and De Ros, L.F., 2000, Spatial and temporal distribution of diagenetic alterations in siliciclastic rocks: implications for mass transfer in sedimentary basins: *Sedimentology*, v. 47, no. (Suppl.1), p. 95–120.
- Moraes, M.A.S., and De Ros, L.F., 1992, Depositional, infiltrated and authigenic clays in fluvial sandstones of the Jurassic Sergi Formation, Reconcavo Basin, northeastern Brazil, *in* Origin, diagenesis and petrophysics of clay minerals in sandstones: *SEPM Special Publication 47*, p. 197–208.
- Moraes, M.A.S., and De Ros, L.F., 1990, Infiltrated clays in fluvial Jurassic sandstones of Recôncavo Basin, northeastern Brazil: *Journal of Sedimentary Petrology*, v. 60, no. 6, p. 809–819.
- Mosser-Ruck, R., Devineau, K., Charpentier, D., and Cathelineau, M., 2005, Effects of ethylene glycol saturation protocols on XRD patterns: A critical review and discussion: *Clays and Clay Minerals*, v. 53, no. 6, p. 631–638.
- Musial, G., Reynaud, J.-Y., Gingras, M.K., Féliès, H., Labourdette, R., and Parize, O., 2012, Subsurface and outcrop characterization of large tidally influenced point bars of the Cretaceous McMurray Formation (Alberta, Canada): *Sedimentary Geology*, v. 279, p. 156–172, doi: 10.1016/j.sedgeo.2011.04.020.
- Nadeau, P.H., 2000, The Sleipner Effect: A subtle relationship between the distribution of diagenetic clay reservoir porosity, permeability, and water saturation: *Clay Minerals*, v. 35, p. 185–200.
- Needham, S.J., Worden, R.H., and Cuadros, J., 2006, Sediment ingestion by worms and the production of bio-clays: a study of macrobiologically enhanced weathering and early diagenetic processes: *Sedimentology*, v. 53, p. 567–579.
- Needham, S.J., Worden, R.H., and McIlroy, D., 2004, Animal sediment interactions: the effect of ingestion and excretion by worms on mineralogy: *Biogeosciences Discussions*, v. 1, p. 533–559.

- Needham, S.J., Worden, R.H., and McIlroy, D., 2005, Experimental production of clay rims by macrobiotic sediment ingestion and excretion processes: *Journal of Sedimentary Research*, v. 75, p. 1028–1037.
- Norrdahl, H., and Einarsson, T., 2001, Concurrent changes of relative sea-level and glacier extent at the Weichselian-Holocene boundary in Berufjordur, Eastern Iceland: *Quaternary Science Reviews*, v. 20, p. 1607–1622.
- Odin, G.S., 1990, Clay mineral formation at the continent-ocean boundary: the verdine facies: *Clay Minerals*, v. 25, p. 477–483.
- Odin, G.S., 1988, The verdine facies: Introduction to the verdine facies, in Odin, G.S. ed., *Green Marine Clays: Oolitic Ironstone Facies, Verdine Facies, Glaucony Facies and celadonite-bearing Facies - A Comparative Study*, Elsevier, Amsterdam.
- Oliviera, A., Rocha, F., Rodrigues, A., Jouanneau, J., Dias, A., Weber, O., and Gomes, C., 2002, Clay minerals from the sedimentary cover from the Northwest Iberian shelf: *Progress in Oceanography*, v. 52, p. 233–247.
- Orton, G.J., and Reading, H.G., 1993, Variability of deltaic processes in terms of sediment supply, with particular emphasis on grain size: *Sedimentology*, v. 40, p. 475–512.
- Pandarínath, K., and Narayana, A.C., 1992, Clay minerals and trace metal association in the Gangolli estuarine Sediments, West Coast of India: *Estuarine, Coastal and Shelf Science*, v. 35, no. 4, p. 363–370, doi: 10.1016/s0272-7714(05)80033-2.
- Park, D., 1999, *Waves, Tides, and Shallow-water Processes*: Butterworth/Heinemann.
- Patchineelam, S.M., and De Figueiredo, A.G., 2000, Preferential settling of smectite on the Amazon continental shelf: *Geo-Marine Letters*, v. 20, no. 1, p. 37–42, doi: 10.1007/s003670000035.
- Pay, M.D., Astin, T.R., and Parker, A., 2000, Clay mineral distribution in the Devonian-Carboniferous sandstones of the Clair Field, west of Shetland, and its significance for reservoir quality: *Clay Minerals*, v. 35, p. 151–162.
- Pe-Piper, G., and Weir-Murphy, S., 2008, Early diagenesis of inner-shelf phosphorite and iron-silicate minerals, Lower Cretaceous Canada: *AAPG Bulletin*, v. 92, no. 9, p. 1153–1168.

- Pérez-Arlucea, M., Álvarez-Iglesias, P., and Rubio, B., 2007, Holocene evolution of estuarine and tidal-flat sediments in San Simón Bay, Galicia, NW Spain: *Journal of Coastal Research*, v. 50, p. 163–167.
- Pinet, P.R., and Morgan, W.P., 1979, Implications of clay-provenance studies in two Georgia estuaries: *Journal of Sedimentary Petrology*, v. 49, no. 2, p. 575–580.
- Piper, J.D.A., 1971, Ground magnetic studies of crustal growth in Iceland: *Earth and Planetary Science Letters*, v. 12, p. 199–207.
- Pittman, E.D., Goldhaber, M.B., and Spötl, C., 1997, Regional diagenetic patterns in the St. Peter sandstone: Implication for brine migration in the Illinois Basin: *U.S. Geological Survey Bulletin*, v. 2094-A.
- Pittman, E.D., Larese, R.E., and Heald, M.T., 1992, Clay coats: Occurrence and relevance to preservation of porosity in sandstones, *in* Houseknecht, D.W. and Pittman, E.D. eds., *Origin, diagenesis, and petrophysics of clay minerals in sandstones*, SEPM (Society for Petroleum Geology), Tulsa, Oklahoma, p. 241–255.
- Platt, J.D., 1994, Geochemical evolution of pore waters in the Rotliegend (Early Permian) of northern Germany: *Marine & Petroleum Geology*, v. 11, no. 1, p. 66–78.
- Porrenga, D.H., 1967, Glauconite and chamosite as depth indicators in the marine environment: *Marine Geology*, v. 5, p. 495–501.
- Porter, K.W., and Weimer, R.J., 1982, Diagenetic sequence related to structural history and petroleum accumulation: Spindle field, Colorado: *AAPG Bulletin*, v. 66, no. 12, p. 2543–2560.
- Postma, H., 1967, Sediment transport and sedimentation in the estuarine environment, *in* Lauff, G.H. ed., *Estuaries*, American Association for the Advancement of Science., Washington D.C.
- Prego, R., Caetano, M., Bernárdez, P., Brito, P., Ospina-Alvarez, N., and Vale, C., 2012, Rare earth elements in coastal sediments of the northern Galician shelf: Influence of geological features: *Continental Shelf Research*, v. 35, no. 0, p. 75–85, doi: 10.1016/j.csr.2011.12.010.
- Presti, M., and Michalopoulos, P., 2008, Estimating the contribution of the authigenic mineral component to the long-term reactive silica accumulation on the western shelf of the Mississippi River Delta:

Continental Shelf Research, v. 28, no. 6, p. 823–838, doi:  
10.1016/j.csr.2007.12.015.

Primmer, T.J., Cade, C.A., Evans, J., Gluyas, J.G., Hopkins, M.S., Oxtoby, N.H., Smalley, C., Warren, E.A., and Worden, R.H., 1997, Global patterns in sandstone diagenesis: Their application to reservoir quality prediction for petroleum exploration, *in* Kupecz, J.A., Gluyas, J.G., and Bloch, S. eds., AAPG Memoir 69: Reservoir Quality Prediction in Sandstones and Carbonates, p. 61–79.

Proust, D., Eyinery, J.P., and Beaufort, D., 1986, Supergene vermiculitization of a magnesium chlorite: iron and magnesium removal processes: *Clays and Clay Minerals*, v. 34, p. 572–580.

Ramm, M., and Bjørlykke, K., 1994, Porosity/depth trends in reservoir sandstones: assessing the quantitative effects of varying pore-pressure, temperature history and mineralogy, *Norwegian Shelf data: Clay Minerals*, v. 29, p. 475–490.

Ramm, M., and Ryseth, A.E., 1996, Reservoir quality and burial diagenesis in the Staffjord Formation, North Sea: *Petroleum Geoscience*, v. 2, no. 4, p. 313–324.

Ramussen, C., Dahlgren, R.A., and Southard, R.J., 2010, Basalt weathering and pedogenesis across an environmental gradient in the southern Cascade Range, California, USA: *Geoderma*, v. 154, p. 473–485.

Raven, J.A., and Edwards, D., 2001, Roots: Evolutionary origins and biogeochemical significance: *Journal of Experimental Botany*, v. 52, p. 381–401.

Reading, H.G., 1996, *Sedimentary Environments: Processes, Facies and Stratigraphy* (H. G. Reading, Ed.): Blackwell Science Ltd, Oxford.

Reading, H.G., and Collinson, J.D., 1996, Clastic coasts, *in* Reading, H.G. ed., *Sedimentary Environments: Processes, Facies and Stratigraphy*, Blackwell Science, Oxford.

Remy, R.R., 1994, Porosity reduction and major controls on diagenesis of Cretaceous-Paleocene volcanoclastic and arkosic sandstone, Middle Park Basin, Colorado: *Journal of Sedimentary Research*, v. A64, no. 4, p. 797–806.

Retallack, G.J., and Dilcher, D.L., 2012, Outcrop versus core and geophysical log interpretation of mid-Cretaceous paleosols from the Dakota Formation of Kansas: *Palaeogeography*,

Palaeoclimatology, Palaeoecology, v. 329-330, p. 47–63, doi: 10.1016/j.palaeo.2012.02.017.

Rich, C.I., 1968, Hydroxy interlayers in expansible layer silicates: *Clays and Clay Minerals*, v. 16, p. 15–30.

De Ros, L.F., Anjos, S.M.C., and Morad, S., 1994, Authigenesis of amphibole and its relationship to the diagenetic evolution of Lower Cretaceous sandstones of the Potiguar rift basin, northeastern Brazil: *Sedimentary Geology*, v. 88, p. 253–266.

Ross, G.J., and Kodama, H., 1976, Experimental alteration of chlorite into a regularly interstratified chlorite vermiculite by chemical oxidation: *Clays and Clay Minerals*, v. 24, p. 183–190.

Rossel, N.C., 1982, Clay Mineral Diagenesis in the Rotliegend aeolian sandstones of the southern North Sea: *Clay Minerals*, v. 17, p. 69–77.

Russell, K.L., 1970, Geochemistry and halmyrolysis of clay minerals, Rio Ameca, Mexico: *Geochimica et Cosmochimica Acta*, v. 34, no. 8, p. 893–907, doi: 10.1016/0016-7037(70)90127-4.

Ryan, P.C., and Reynolds, R.C., 1997, The chemical composition of serpentine/chlorite in the Tuscaloosa Formation, United States Gulf Coast: EDX vs XRD determinations, implications for mineralogic reactions and the origin of antase: *Clays and Clay Minerals*, v. 45, no. 3, p. 339–352.

Salem, A.M., Ketzer, J.M., Morad, S., Rizk, R.R., and Al-Aasm, I.S., 2005, Diagenesis and reservoir-quality evolution of incised-valley sandstone from the Abu Madi reservoirs (Upper Miocene), the Nile Delta Basin: *Journal of Sedimentary Research*, v. 75, p. 572–584.

Santos, I.R., Eyre, B.D., and Huettel, M., 2012, The driving forces of porewater and groundwater flow in permeable coastal sediments: A review: *Estuarine, Coastal and Shelf Science*, v. 98, p. 1–15, doi: 10.1016/j.ecss.2011.10.024.

Sarma, G.V.S., Satyakumar, P., Varma, K.U.M., Rao, E.N.D., and Rao, M.S., 1993, Clay Minerals of the Sarada-Varaha Estuary, East Coast of India: *Journal of Coastal Research*, v. 9, no. 4, p. 885–894.

Schiffman, P., and Friedleifsson, G.O., 1991, The smectite-chlorite transition in drillhole N 1-15, Nesjavellir geothermal field, Iceland: XRD, BSE and electron microprobe investigations: *Journal of Metamorphic Geology*, v. 9, p. 679–696.

- Schubel, J.R., 1972, Distribution and transportation of suspended sediment in upper Chesapeake Bay: *The Geological Society of America*, v. 133, p. 151–167.
- Seemann, U., 1979, Diagenetically formed interstitial clay minerals as a factor in the Rotliegend sandstone reservoir quality in the Dutch Sector of the North Sea: *Journal of Petroleum Geology*, v. 1, no. 3, p. 55–62.
- Service, I.H., 2009, South west Coast of Iceland: Selvogur-Hjörsey (I. H. Service, Ed.): *International Chart Series*, p. Mercator.
- Shi, Z., and Zhou, H.J., 2004, Controls on effective settling velocities of mud flocs in the Changjiang Estuary, China: *Hydrological Processes*, v. 18, no. 15, p. 2877–2892.
- Sholkovitz, E.R., Boyle, E.A., and Price, N.B., 1978, Removal of dissolved humic acids and iron during estuarine mixing: *Earth and Planetary Science Letters*, v. 40, p. 130–136.
- Siegle, D., 2009, Critical Values of the Pearson Product-Moment Correlation Coefficient:.
- Sigfusson, B., Gislason, S.R., and Paton, G.I., 2008, Pedogenesis and weathering rates of a histic andosol in Iceland: Field and experimental soil solution study: *Geoderma*, v. 144, p. 572–592.
- Sigfusson, B., Gislason, S.R., and Paton, G.I., 2006, The effect of soil solution chemistry on the weathering rate of a Histic Andosol: *Journal of Geochemical Exploration*, v. 88, no. 1-3, p. 321–324, doi: 10.1016/j.gexplo.2005.08.067.
- Sigmundsson, F., 2006, *Crustal Deformation and Divergent Plate Tectonics* : Praxis Publishing Ltd, Heidelberg.
- Sionneau, T., Bout-Roumazeilles, V., Biscaye, P.E., Van Vliet-Lanoe, B., and Bory, A., 2008, Clay mineral distributions in and around the Mississippi River watershed and Northern Gulf of Mexico: sources and transport patterns: *Quaternary Science Reviews*, v. 27, no. 17–18, p. 1740–1751, doi: 10.1016/j.quascirev.2008.07.001.
- Small, J.S., Hamilton, D.L., and Habesch, S., 1992, Experimental simulation of clay precipitation within reservoir sandstones; 1, Techniques and examples: *Journal of Sedimentary Research*, v. 62, no. 3, p. 508–519.

- Starkey, H.C., Blackmon, P.D., and Hauff, P.L., 1984, The routine mineralogical analysis of clay-bearing samples, in U.S. Geological Survey Bulletin 1563,.
- Stear, W.M., 1985, Comparison of the bedform distribution and dynamics of modern and ancient sandy ephemeral flood deposits in the southwestern Karoo region, South Africa: *Sedimentary Geology*, v. 45, p. 209–230.
- Stefánsson, A., and Gíslason, S.R., 2001, Chemical weathering of basalts, southwest Iceland: Effects of rock crystallinity and secondary minerals on chemical fluxes to the ocean: *American Journal of Science*, v. 501, p. 513–556.
- Stokkendal, J., Friis, H., Svendsen, J.B., Poulsen, M.L.K., and Hamberg, L., 2009, Predictive permeability variations in a Hermod sand reservoir, Stine Segments, Siri Field, Danish North Sea: *Marine and Petroleum Geology*, v. 26, no. 397-415.
- Storvoll, V., Bjorlykke, K., Karlsen, D., and Saigal, G., 2002, Porosity preservation in reservoir sandstones due to grain-coating illite: a study of the Jurassic Garn Formation from the Kristin and Lavrans fields, offshore Mid-Norway: *Marine and Petroleum Geology*, v. 19, no. 6, p. 767–781.
- Sveinbjörnsdóttir, A.E., 1992, Composition of geothermal minerals from saline and dilute fluids - Krafla and Reykjanes, Iceland: *Lithos*, v. 27, p. 301–315.
- Taboada, T., and Garcia, C., 1999, Smectite formation produced by the weathering in a coarse granite Saprolite in Galicia (NW Spain): *Catena*, v. 35, p. 281–290.
- Taboada, T., and García, C., 1999, Pseudomorphic transformation of plagioclases during the weathering of granitic rocks in Galicia (NW Spain): *Catena*, v. 35, no. 2-4, p. 291–302, doi: 10.1016/s0341-8162(98)00108-8.
- Taggart, M.S., and Kaiser, A.D., 1960, Clay mineralogy of Mississippi River deltaic sediments: *Geological society of America Bulletin*, v. 71, no. 5, p. 521–530, doi: 10.1130/0016-7606(1960)71[521:cmomrd]2.0.co;2.
- Taylor, J.C.M., 1978, Control of diagenesis by depositional environment within a fluvial sandstone sequence in the northern North Sea Basin: *Journal of the Geological Society of London*, v. 135, p. 83–91.

- Taylor, T.R., Giles, M.R., Hathon, L.A., Diggs, T.N., Braunsdorf, N.R., Birbiglia, G. V, Kittridge, M.G., Macaulay, C.I., and Espejo, I.S., 2010, Sandstone diagenesis and reservoir quality prediction: Models myths, and reality: AAPG Bulletin, v. 94, no. 8, p. 1093–1132.
- Taylor, S.R., and McLennan, S., 1985, The continental crust: its composition and evolution: an examination of the geochemical record preserved in sedimentary rocks.: Blackwell Scientific, Oxford.
- The International Centre for Diffraction Data, 2013,.
- Thermo Scientific, 2012, Thermo Scientific Nicolet 380 FT-IR Spectrometer - Product specifications:.
- Thomson, A., 1979, Preservation of porosity in the deep Woodbine/Tuscaloosa trend, Louisiana: Transactions of the Gulf Coast Association of Geological Societies, v. 29, p. 396–403.
- Thomson, A., and Stancliffe, R.J., 1990, Diagenetic controls on reservoir quality, eolian Norphlet Formation, South State Line field, Mississippi, in Barwis, J.H., McPherson, J.G., and Studlick, R.J. eds., Sandstone petroleum reservoirs, Springer-Verlag, New York, p. 205–224.
- Thordarson, T., and Hoskuldsson, A., 2002, Classic Geology in Europe 3: Iceland: Terra Publishing, Harpenden.
- Townend, J., 2003, Practical Statistics for Environmental and Biological Scientists: John Wiley & Sons, Chichester.
- Tucker, M.E., 2001, Sedimentary Petrology: Blackwell Science Ltd.
- Tucker, M.E., 1988, Techniques in Sedimentology (M. E. Tucker, Ed.):.
- Valloni, R., Lazzari, D., and Calzolari, M.A., 1991, Selective alteration of arkose framework in Oligo-Miocene turbidites of the Northern Apennines foreland: impact on sedimentary provenance analysis, in Morton, A.C., Todd, S.P., and Haughton, P.D.W. eds., Developments in Sedimentary Provenance Studies, The Geological Society, London, p. 125–136.
- Varela, M., Prego, R., Pazos, Y., and Moroño, Á., 2005, Influence of upwelling and river runoff interaction on phytoplankton assemblages in a Middle Galician Ria and Comparison with northern and southern rias (NW Iberian Peninsula): Estuarine,

Coastal and Shelf Science, v. 64, no. 4, p. 721–737, doi:  
10.1016/j.ecss.2005.03.023.

Volkenborn, N., Hedtkamp, S.I.C., Van Beusekom, J.E.E., and Reise, K., 2007, Effects of bioturbation and bioirrigation by lugworms (*Arenicola marina*) on physical and chemical sediment properties and implications for intertidal habitat succession: *Estuarine, Coastal and Shelf Science*, v. 74, p. 331–343.

Wada, K., Arnalds, O., Kakuto, Y., Wilding, L.P., and Hallmark, C.T., 1992, Clay minerals of four soils formed in eolian and tephra materials in Iceland: *Geoderma*, v. 52, p. 351–365.

Walling, D.E., 2006, Human impact on land–ocean sediment transfer by the world's rivers: *Geomorphology*, v. 79, no. 3-4, p. 192–216, doi: 10.1016/j.geomorph.2006.06.019.

Walling, D.E., 1999, Linking land use, erosion and sediment yields in river basins: *Hydrobiologia*, v. 410, p. 223–240.

Wallmann, K., Aloisi, G., Haeckel, M., Tishchenko, P., Pavlova, G., Greinert, J., Kutterolf, S., and Eisenhauer, A., 2008, Silicate weathering in anoxic marine sediments: *Geochimica et Cosmochimica Acta*, v. 72, no. 12, p. 2895–2918, doi: 10.1016/j.gca.2008.03.026.

Weaver, C.E., 1989, *Clays, Muds, and Shales*: Elsevier.

Weaver, C.E., 1960, Possible uses of clay minerals in the search for oil: *AAPG Bulletin*, v. 44, no. 9, p. 1505–1518.

Weisenberger, T., and Selbeckk, R.S., 2009, Multi-stage zeolite facies mineralization in Hvalfjörður area, Iceland: *International Journal of Earth Science*, v. 98, p. 985–999.

Welton, J.E., 2003, *Sem Petrology Atlas (Methods in Exploration Series)* (J. E. Welton, Ed.): The American Association of Petroleum Geologists, Tulsa, Oklahoma, U.S.A.

Westcott, W.A., 1983, Diagenesis of Cotton Valley Sandstone (Upper Jurassic), East Texas; Implications for Tight Gas Formation Pay Recognition: *AAPG Bulletin*, v. 67, no. 6, p. 1002–1013.

White, W.A., 1972, Deep Erosion by Continental Ice Sheets: *Geological society of America Bulletin*, v. 83, no. 4, p. 1037–1056, doi: 10.1130/0016-7606(1972)83[1037:debcis]2.0.co;2.

- White, W.A., 1988, More on deep glacial erosion by continental ice sheets and their tongues of distributary ice: *Quaternary Research*, v. 30, no. 2, p. 137–150, doi: 10.1016/0033-5894(88)90019-1.
- Whitehouse, U.G., Jeffrey, L.M., and Debbrecht, J.D., 1960, Differential settling tendencies of clay minerals in saline waters: *Clays and Clay Minerals*, v. 7, p. 1–79.
- Wilson, M.D., 1992, Inherited grain-rimming clays in sandstones from eolian and shelf environments: Their origin and control on reservoir properties, in *Origin, diagenesis and petrophysics of clay minerals in sandstones*: SEPM Special Publication 47, p. 208–225.
- Wilson, I.R., 1998, Kaolin deposits of western Iberia: *Geoscience in south-west England*, v. 9, p. 214–217.
- Wilson, M.J., 1999, The origin and formation of clay minerals in soils: past, present and future perspectives: *Clay Minerals*, v. 347, p. 7–25.
- Wilson, M.J., 2004, Weathering of the primary rock-forming minerals: processes, products and rates: *Clay Minerals*, v. 39, p. 233–266.
- Worden, R.H., and Burley, S.D., 2003, Sandstone Diagenesis: The Evolution of Sand to Stone, in *Sandstone Diagenesis*, Blackwell Publishing Ltd., p. 1–44.
- Worden, R.H., and Morad, S., 2003, Clay minerals in sandstones: Controls on formation, distribution and evolution, in Worden, R.H. and Morad, S. eds., *Clay Mineral Cements in Sandstones*, International Association of Sedimentologists, Special Publication vol. 34, p. 3–41.
- Worden, R.H., Needham, S.J., and Cuadros, J., 2006, The worm gut; a natural clay mineral factory and a possible cause of diagenetic grain coats in sandstones: *Journal of Geochemical Exploration*, v. 89, p. 428–431.
- Wu, J., Liu, J.T., and Wang, X., 2012, Sediment trapping of turbidity maxima in the Changjiang Estuary: *Marine Geology*, v. 303–306, no. 0, p. 14–25, doi: 10.1016/j.margeo.2012.02.011.
- De Zuane, J., 1997, *Handbook of Drinking Water Quality*: John Wiley & Sons.

## **8. Appendices (see associated data)**

### **8.1 Appendix 1 – Supplementary material to chapter two**

#### **8.1.1 Appendix 1A – USA database table**

#### **8.1.2 Appendix 1B – Europe database table**

#### **8.1.3 Appendix 1C – Rest of world database table**

#### **8.1.4 Appendix 1D – All chlorite compositional data**

#### **8.1.5 Appendix 1E – Average chlorite compositional data**

### **8.2 Appendix 2 –Supplementary material to chapter three**

#### **8.2.1 Appendix 2A – Sample location co-ordinate table**

### **8.3 Appendix 3 –Supplementary material to chapter four**

#### **8.3.1 Appendix 3A – Sample location co-ordinate table**

### **8.4 Appendix 4 –Supplementary material to chapter five**

#### **8.4.1 Appendix 4A – Sample location co-ordinate table**

**8.4.2 Appendix 4B – Core logs with all data**

**8.5 Appendix 5 –Supplementary material to chapter six**

**8.5.1 Appendix 5A - Iceland paleogeography talk (BSRG 2010)**